UNIVERSITY OF CALIFORNIA, SAN DIEGO

The Use of Fragment-Based Lead Discovery Towards the Design and Development of Metalloenzyme Inhibitors

A Dissertation submitted in partial satisfaction of the requirements for the degree Doctor of Philosophy

in

Chemistry

by

Jessica L. Sardo

Committee in Charge:

Professor Seth Cohen, Chair
Professor Joshua Figeroa
Professor Michael Gilson
Professor Tadeusz Molinski
Professor Yitzhak Tor

2013

The Dissertation of Jessica L. Sardo is approved, and it is acceptable in quality and form for publication on microfilm and electronically:

Chair

University of California, San Diego

2013

DEDICATION

For my best friend.

TABLE OF CONTENTS

SIGNATURE PAGE iii

DEDICATION iv

TABLE OF CONTENTS v

LIST OF SYMBOLS AND ABBREVIATIONS viii

LIST OF FIGURES xiii

LIST OF TABLES xvii

ACKNOWLEDGEMENTS xviii

VITA AND PUBLICATIONS xx

ABSTRACT OF THE DISSERTATION xxi

1 Introduction 1

1. A. Introduction 2

1. B. 1 Fragment Based Lead Discovery A Strategy for Inhibitor Design 2

1. B. 2 Library Screening Techniques 5

1. B. 3. Hit to Lead Development 8

1. B. 4. Zelboraf: A FBLD Clinical Success Story 13

1. C. 1. Metalloenzymes of Interest: Mononuclear Proteins 15

1. C. 1a. Matrix Metalloproteinases 16

1.C. 1b. Anthrax Lethal Factor 20

1. C. 1c. *Pseudomonas aeruginosa* Elastase 22

1. C. 1d. 5-Lipoxygenase 25

1. C. 2. Metalloenzymes of Interest: Dinuclear Proteins 28

1. C. 2a. Tyrosinase 28

1. C. 2b. Human Immunodeficiency Virus-1 Integrase 31

1. C. 2c. Methionine Aminopeptidase (MetAP) 35

1. D. Conclusions 38

1. E. References 39

2 Identifying Chelators for Metalloprotein Inhibitors Using a Fragment-Based Approach 47

2. A. Introduction 48

2. B. Design and Evaluation of CFL-1.1 51

2. C. 1. CFL-1.1 Results Against MMPs 54

2. C. 2. Hits Against Other Metalloenzymes 58

2. D. 1. 8-Hydroxyquinoline Sublibrary: Synthesis and Screening 60

2. D. 2. Docking Studies of Sublibrary Hits 65

2. E. Screening CFL-1.1 Against Different Metalloforms: Methionine Aminopeptidase (MetAP) 69

2. F. Conclusions 72

2. G. Experimental 74

2. H. Acknowledgements 94

2. I. References 95

3 Probing Chelation Motifs in HIV-1 Integrase Inhibitors 99

3. A. Introduction 100

3. B. 1. Design and Synthesis 102

3. B. 2. RCD Activity Screening 105

3. B. 3. Computational Docking Studies 108

3. C. 1. Unique Features of MBG Motifs 112

3. C. 2. MBG Scaffolds Novel to HIV-1 IN 121

3. D. Conclusions 126

3. E. Experimental 128

3. F. Acknowledgments 148

3. G. References 149

4 Antagonism of *P. aeruginosa* Elastase Using Unique Metal-Chelating Scaffolds 152

4. A. Introduction 153

4. B. Discovery and Design of LasB Inhibitors Via CFL-1.1 Screening 154

4. C. 1. 3-Hydroxy-1-alkyl-2-methylpyridine-4(1*H*)-thione Inhibitors 156

4. C. 2. 5-Amino-2-hydroxycyclohepta-2,4,6-trienone-based Inhibitors 160

4. D. Comparison of Small Molecule LasB Inhibitors: Cross-Inhibition Screen 169

4. E. Conclusions 172

4. F. Experimental 174

4. G. Acknowledgements 196

4. H. References 197

LIST OF SYMBOLS AND ABBREVIATIONS

3,4-HOPTO	3-hydroxy-1-alkyl-2-methylpyridine-4(1*H*)-thione
3P	3'-Processing
5-HPETE	5-Hydroperoxyeicosatetraenoic acid
5-LO	5-Lipoxygenase
Å	Ångström; 10^{-10} m
AA	Arachidonic acid
ADME	Absorption, distribution, metabolism, and excretion
AIDS	Acquired immunodeficiency syndrome
AMC	7-amido-4-metylcoumarin
amu	Atomic mass units
APCI-MS	Atmospheric pressure chemical ionization-mass spectrometry
ATP	Adenosine triphosphate
br	Broad peak (NMR)
CA	Carbonic anhydrase
CFL	Chelator fragment library
COPD	Chronic obstructive pulmonary disease
δ	Chemical shift; ppm
d	Doublet (NMR)
DCC	N,N'-dicyclohexylcarbodiimide
DCM	Dichloromethane
dd	Doublet of doublets (NMR)

DMAD	Dimethyl but-2-ynedioate
DMAP	4-Dimethylaminopyridine
DMF	Dimethylformamide
DMSO	Dimethylsulfoxide
DNA	Deoxyribonucleic acid
ε	Extinction coefficient
EDCI	1-Ethyl-3-(3-dimethylaminopropyl)carbodiimide
EF	Edema factor
ECM	Extracellular matrix
ESI-MS	Electrospray ionization mass spectrometry
EtOAc	Etheyl acetate
EtOH	Ethanol
FBLD	Fragment based lead design
FDA	Food and Drug Administration
FPMA	4-Fluorophenyl methanamine
FRET	Förster resonance energy transfer
H2DCFDA	2',7'-dichlorodihydrofluorescein diacetate
HAART	Highly active anti-retroviral therapy
HAC	Heavy atom count
HEPES	4-(2-hydroxyethyl)-1-piperazineethanesulfonic acid
HIV-1	Human immunodeficiency virus 1
HIV IN	HIV integrase
HMDO	Hexamethyldisiloxane

HMPO	5-hydroxy-3-methylpyrimidin-4(3*H*)-one
HOBt	Hydroxybenzotriazole
HPETE	5-Hydroperoxyeicosatetraenoic acid
HRMS	High resolution mass spectrometry
HSQC	Heteronuclear single quantum coherence
HTS	High throughput screening
IC_{50}	Inhibitor concentration leading to 50% enzyme activity
iNOS	Inducible nitric oxide synthase
J	Coupling constant (NMR)
K_d	Dissociation equilibrium constant
K_i	Inhibitor equilibrium constant
λ	Wavelength
LDH	Lactate dehydrogenase
L-DOPA	L-dopamine
LasB	Pseudomonas aeruginosa Elastase
LE	Ligand efficiency
LF	Lethal factor
m	Multiplet (NMR)
MAPKK	Mitogen-activated protein kinase kinase
MBG	Metal Binding Group
MetAP	Methionine aminopeptidase
MES	2-(*N*-morpholino)ethanesulfonic acid
MeOH	Methanol

MMP	Matrix metalloprotease
MMPi	Matrix metalloprotease inhibitor
MOPS	3-(N-morpholino)propanesulfonic acid
MTBE	Methyl tert-butyl ether
NA	Not applicable
NADPH	Nicotinamide adenine dinucleotide phosphate
ND	Not determined
NMR	Nuclear magnetic resonance
PA	Protective antigen
pK_a	Acid dissociation constant
π	Pi
PA	Protective antigen
PDB	Protein data bank
PFV	Prototype foamy virus
ppm	Parts per million
psi	Pound per square inch
RCD	Raltegravir chelating derivative
RMSD	Root-mean-square deviation
RT	Room temperature
s	Singlet (NMR)
SAR	Structure activity relationship
SPR	Surface plasmon resonance
ST	Strand transfer

t	Triplet (NMR)
TEA	Triethylamine
TFA	Trifluoroacetic acid
THF	Tetrahydrofuran
TIMP	Tissue inhibitors of metalloproteinases
TSB	Tryptic soy broth
TY	Tyrosinase
WHO	World health organization
ZBG	Zinc binding group

LIST OF FIGURES

Figure 1.1 Example of a FBLD versus HTS hit. The protein-binding pocket is shown in green. Yellow stars denote protein-ligand interactions. 5

Figure 1.2 Generic representation of the fragment merging strategy. Protein-binding pocket shown in green and stars denote protein-ligand interactions. a) Two fragments occupying the same binding site. b) A newly merged compound containing both functionalities. 9

Figure 1.3 Generic representation of the fragment linking strategy. Protein-binding pocket shown in green and stars denote protein-ligand interactions. a) Two fragments occupying nearby binding sites. b) A new compound that consists of the two fragments linked together. 10

Figure 1.4 Generic representation of the fragment growing strategy. a), A fragment is identified to bind to the protein. b) Additions are made to the fragment to optimizing interactions. c) A grown fragment now occupies multiple binding sites. 11

Figure 1.5 Representation of the fragment development strategy of in situ fragment assembly. Two fragments with complementary functional groups can react, forming a singular new molecule within the confines of the binding site. 12

Figure 1.6 Structures and IC_{50} values of selected compounds involved in the fragment-based discovery of FDA-approved Zelboraf (Vemurafenib). 14

Figure 1.7 a) Representative illustration of a MMP active site with the Zn(II) metal ion coordinated by three histidine residues and an axial water. b) Crystal structure of MMP-2 active site (PDB: 1QIB). 17

Figure 1.8 a) Structure of a hydroxamate-based MMP-3 inhibitor with the bidentate ZBG highlighted in red. b) Structure of MMP-3 active site with bound hydroxamte inhibitor (PDB: 1B3D). 19

Figure 1.9 a) Representative illustration of a LF active site with the Zn(II) metal ion coordinated by two histidine and one glutamic acid residues. b) Protein crystal structure of LF active site (PDB: 1YQY). 21

Figure 1.10 a) Representative illustration of LasB active site with Zn(II) metal ion coordinated by two histidine and one glutamic acid

residue. b) Structure of thermolysin Zn(II) ion shown in blue. c) Structure of LasB Zn(II) ion shown in blue 25

Figure 1.11 a) Representative illustration 5-LO active site, with the Fe(III) metal ion coordinated by three histidines. b) FDA-approved 5-LO inhibitor Zileuton, this compound utilizes a reverse hydroxamic MBG which chelates to the Fe(III) cofactor of 5-LO. c) Biosynthetic pathway for the formation of leukotrienes. 27

Figure 1.12 a) Representative illustration of TY active site with dinuclear Cu(II) metal ions coordinated by histidines b) Biosynthetic pathway used by TY to oxidize monophenols, and diphenols into quinines, like Dopaqunione. 29

Figure 1.13 Representative illustrations of the three isoforms of the TY active site with the copper ions coordinated to histidines (top). Protein crystal structure of the active site of the deoxy-tyrosinase isoform of TY (PDB: 2ZMX, bottom). 31

Figure 1.14 Crystal structure of PFV-IN (PDB 3OYA) complex with the FDA-approved HIV-1 IN inhibitor Raltegravir. 33

Figure 1.15 Structures of Raltegravir and other select potent HIV-1 IN inhibitors. 34

Figure 1.16 Structures and IC_{50} values of the metalloform specific inhibitors of *Ec*MetAP-1. From top to bottom selective scaffolds for Co(II), Mn(II) and Fe(II). 36

Figure 2.1 Structures of the compounds in the CFL-1.1 library organized by MBG. 50

Figure 2.2 Heat plot representing the results from the screens of CFL-1.1 against the listed metalloenzymes. 53

Figure 2.3 Synthesis of the 8-hydroxyquinoline sublibrary 61

Figure 2.4 Crystal structure of 4-fluoro-N-(8-hydroxyquinolin-2-yl)benzenesulfonamide **(72b).** 62

Figure 2.5 Results of 8-hydroxyquinoline sublibrary screening against MMP-2 at 25 μM 64

Figure 2.6 Docking results of **72b** (top) and **77b** (bottom) in the active site of MMP-2 (PDB: 1QIB). 67

Figure 2.7 Heatplot representing results of CFL-1.1 screened at 50 μM against Co(II) *Ec*MetAP-1 70

Figure 2.8 Heatplot representing results of CFL-1.1 screened at 50 μM against Mn(II) *Ec*MetAP-1. 71

Figure 3.1 Schematic representation of FDA-approved drug raltegravir bound to the Mg(II) metal ions of the HIV-1 IN (left). Structure of PFV-IN (PDB 3OYA) complex with Raltegravir (right). 101

Figure 3.2 Comparison of the structural similarities between raltegravir and two metalloenzyme inhibitors previously designed in our lab. 103

Figure 3.3 List of RCD compounds and parent compound raltegravir. 104

Figure 3.4 Comparison of the computational docking of **RCD-1** (pink) versus the reported crystal structure of raltegravir (green) bound in the PFV IN (blue) (PDB: 3OYA). 109

Figure 3.5 MBG numbering system and modes of metal binding for raltegravir and RCD compounds. The metal ions were labeled Mg_A and Mg_B; their respective chelate rings and size are colored blue and green..... 111

Figure 3.6 Computational docking results of atypical chelate ring patterns for RCD compounds. Compound **RCD-13** forms two 5-membered chelate rings, **RCD-18** forms two 6-membered chelate rings, and **RCD-15** is a case where only a single ring forms 113

Figure 3.7 Computational docking results of atypical chelate ring patterns for RCD compounds. Compounds **RCD-14** and **RCD-16** both form two 6-membered chelate rings. 114

Figure 3.8 Structures of Raltegravir and other select potent HIV-1 IN inhibitors. 115

Figure 3.9 Computational docking results of compounds **RCD-5** and **RCD-6**..... 116

Figure 3.10 Computational docking results of **RCD-4** in PVF (PDB: 3OYA). 117

Figure 3.11 Computational docking results of **RCD-12** (top) and **RCD-13** (bottom). 120

Figure 3.12 Structures and IC_{50} values of 2,3-dihydro-6,7-dihydroxy-1*H*-isoindol-1-one-based HIV-1 IN inhibitors..... 124

Figure 3.13 Structures of compound **RCD-8** analog sublibrary. 125

Figure 4.1 Structures and select in vitro IC_{50} values for hydroxamic acid containing small molecules against LasB. Percent inhibition when screened at 50 μM. 155

Figure 4.2 Fragment hits from screening of CFL-1.1 at 1 mM against LasB. Percent inhibition and select IC_{50} values are shown. 156

Figure 4.3 3,4-HOPTO sublibrary screened against LasB with select compounds IC_{50} values given. 157

Figure 4.4 Structures and corresponding IC_{50} values for analogs of 3,4-HOPTO hit **TM8/8b**..... 158

Figure 4.5 Swarming of *P. aeruginosa* strain PA14 in the presence of 25 μM of each of the following: a) DMSO; b) **TM8/8b** (left) **TM2/8a** (right). 160

Figure 4.6 List of tropolone and tropolone-like fragments with corresponding IC_{50} values against LasB..... 163

Figure 4.7 List of tropolone sublibrary compounds and controls. 165

Figure 4.8 Competitive inhibition curve to determine K_i of **4.a** to be 336 ± 24 nM. 167

Figure 4.9 Swarming of *P. aeruginosa* strain PA14 in the presence of 25 μM a) DMSO or b) **4.a** (left) **7** (right). 169

Figure 4.10 Cross-inhibition screening results of **TM8/8b** and **4.a** against MMPs -2, -9, hCAII and TY at 50 μM..... 171

LIST OF TABLES

Table 1.1 IC_{50} Values of Metalloform-Selective Inhibitors of *Ec*MetAP-1. 37

Table 2.1 Calculated IC_{50} values, heavy atom count, and ligand efficiency (LE) values for select hits from CFL-1.1. 57

Table 2.2 Crystal data and structure refinement for 4-fluoro-N-(8-hydroxyquinolin-2- yl)benzenesulfonamide **(72b)** crystal. 62

Table 2.3 IC_{50} values, heavy atom count (HAC), and ligand efficiency (LE) for **75a-d** and **77a-d** fragments. All LE values were calculated at 37 ºC. 64

Table 3.1 Results of RCD compounds against 3P and ST processes of HIV-1 IN. Also listed: inhibition of viral replication and the size of chelate rings. For clarity, the metal ions were arbitrarily labeled Mg_A and Mg_B. 106

Table 3.2 Assay results for **RCD-8** analog sublibrary against 3P and ST reactions of HIV-1 IN. The chelate ring sizes formed upon metal biding also included. 125

Table 4.1 Table of tropolone sublibrary IC_{50} values against LasB. 166

ACKNOWLEDGEMENTS

I would like to thank all of those who have helped and supported me through thick and thin during these last five years. I am infinitely grateful to have been blessed with such a truly amazing set of cheerleads, at by back. You have been there to share in the triumphs and in the tears and have always offered a shoulder to cry on or a swift kick in the rear (depending on what the circumstances required). To all my labmates past and present, thank you for all you have taught me, about science, life and myself. I have learned so much over the past five years working in the Cohen lab. Matthieu, thank for your unending patience and guidance and for showing me what it takes to be a good scientist. Noeris, thank you for the exposure into a field science I had never thought to explore or be so fascinated by. Joe, Min, and JP thank you for always making the time for me to bounce around ideas and lead me down the right path in problem solving. Amanda, you are incredibly talented researcher and I am grateful for our collaborations and knowledge you have shared with me. To those of you who openly shared your insecurities and fears in exchange for my own over innumerable coffees and beers, you are great, you know it, and thank you for making me feel the same. Last, but not least, Seth thank you for allowing me the opportunity to work and learn in your labs. I am grateful for all the experiences and opportunities that you have made possible for me. Truly, thank you, for all that you have invested in and done for me.

The text, schemes and figures of Chapters 2, 3, and 4 are in part reprints of the materials published in the following papers: Jessica L. Fullagar, Jennifer A. Jacobsen, Melissa T. Miller, and Seth M. Cohen. "Identifying Chelators for Metalloprotein

Inhibitors Using a Fragment-Based Approach" *J. Med. Chem*. **2011** *54*, 591-602; Arpita Agrawal, Jamie DeSoto, Jessica L. Fullagar, Kasthuraiah Maddali, Shahrzad Rostami, Douglas D. Richman, Yves Pommier, and Seth M. Cohen, "Probing Chelation Motifs in HIV Integrase Inhibitors" *Prod. Natl. Acad. Sci. USA* **2012** *109*, 2251-2256; Amanda L. Garner, Jessica L. Fullagar, Anjali K. Struss, Arpita Agrawal, Amira Y. Moreno, Seth M. Cohen, and Kim D. Janda, "3-Hydroxy-1-alkyl-2-methylpyridine-4(1*H*)-thiones: Inhibition of the *P. aeruginosa* Virulence Factor LasB" *ACS Med. Chem. Lett*. **2012** *3*, 668-672; Jessica L. Fullagar, Amanda L. Garner, Anjali K. Struss, Joshua A. Day, David P. Martin, Jing Yu, Xiaoqing Cai, Kim D. Janda, and Seth M. Cohen "Antagonism of a Zinc Metalloprotease Using a Unique Metal-Chelating Scaffold Tropolones as Inhibitors of *P. aeruginosa* Elastase" *Chem. Commun.* **2013** 49, 3197-3199. The dissertation author was a primary contributing author on the paper included. The co-authors listed in this publication also participated in the research. The permission to reproduce this paper was granted by the American Chemical Society, copyright 2011 and 2013, National Academy of the Sciences, copyright 2012, and Royal Society of Chemistry, copyright 2013.

VITA AND PUBLICATIONS

EDUCATION

University of California, San Diego 2013
Doctor of Philosophy, Chemistry
Advisor: Professor Seth M. Cohen

University of California, San Diego 2010
Masters of Science, Chemistry
Advisor: Professor Seth M. Cohen

Fairfield University 2008
Bachelor of Science, Chemistry

PUBLICATIONS

1. Jessica L. Fullagar*, Jennifer A. Jacobsen*, Melissa T. Miller , and Seth M. Cohen, "Identifying Chelators for Metalloprotein Inhibitors Using a Fragment-Based Approach" *J. Med. Chem.* **2011**, 54 (2), 591-602. *equal contributors

2 Arpita Agrawal, Jamie DeSoto, Jessica L. Fullagar, Kasthuraiah Maddali, Shahrzad Rostami, Douglas D. Richman, Yves Pommier and Seth M. Cohen, "Probing Chelation Motifs in HIV Integrase Inhibitors" *Proc. Natl. Acad. Sci. USA*. **2012**, 109 (7) *2*, 2251-2256.

3 Amanda L. Garner, Anjali K. Struss, Jessica L. Fullagar, Arpita Agrawal, Amira Y. Moreno, Seth M. Cohen, and Kim D. Janda, "3-Hydroxy-1-alkyl-2-methylpyridine-4(1H)-thiones: Inhibition of the *Pseudomonas aeruginosa* Virulence Factor LasB" *ACS Med. Chem. Lett*. **2012**, 3 (8), 668-672.

4 Jessica L. Fullagar, Amanda L. Garner, Anjali K. Struss, Joshua A. Day, David P. Martin, Xiaoqing Cai, Kim D. Janda, and Seth M. Cohen, "Antagonism of a Zinc Metalloprotease Using a Unique Metal-Chelating Scaffold: Tropolones as Inhibitors of *P. aeruginosa* Elastase" *Chem. Commun.* **2013** 49, 3197-3199.

5 Amanda L. Garner, Jessica L. Fullagar, Joshua A. Day, Seth M. Cohen, and Kim D. Janda, "Development of a High-Throughput Screen and Its Use in the Discovery of Streptococcus pneumoniae Immunoglobulin A1 Protease (IgA1P) Inhibitors" *J. Am. Chem. Soc*. **2013** (Accepted)

PATENTS

Jessica L. Fullagar, Amanda L. Garner, Kim D. Janda, and Seth M. Cohen, “Inhibitors of *Pseudomonas aeruginosa* Elastase (LasB) as Agents to Combat Antibiotic Resistance” provisional patent filed **2013** (Application No. SD2013-182).

ABSTRACT OF THE DISSERTATION

The Use of Fragment-Based Lead Discovery Towards the Design and Development of Metalloenzyme Inhibitors

by

Jessica L. Sardo

Doctor of Philosophy in Chemistry

University of California, San Diego, 2013

Professor Seth Cohen, Chair

The use of fragment-based lead discovery (FBLD) for the design and development of metalloenzyme inhibitors is examined. This thesis will first discuss the method of FBLD and compare it to more traditional drug discovery approaches, such as high-throughput screening (HTS). After establishing the concepts behind FBLD, the applications of utilizing a FBLD approach towards the development of inhibitors for select metalloenzymes is discussed.

A study into the use of a chelator fragment library (CFL) to identify new metal-binding groups (MBG) for metalloprotein inhibitors is discussed. The results of screening this library against a number of metalloenzymes identified important trends between

classes of chelators in addition to the identification of numerous metalloenzyme specific MBGs. Furthermore this study provides evidence that the CFL can be used as useful tool in metalloenzyme inhibitor design.

A second probes the types of key interactions a metal-binding inhibitor must posses to effectively inhibit the dinuclear metalloenzyme HIV-1 integrase (HIV-1 IN). A small library of compounds varying only in composition of their MBG was prepared. The activity of this series of compounds was also compared to a similar HIV-1 IN FDA-approved drug. Screening this library of compounds led to the identification of a potentially unique and more potent scaffold (hydroxypyrone-based compounds) for HIV-1 IN inhibitors. Additionally, a small sublibrary of compounds was developed to explore the effects of manipulating the pK_a of the chelator. The results of the systematic examination of the role the MBG contributes to HIV-1 IN inhibition are discussed.

Lastly, the discovery of two novel metal-binding scaffolds for the development *Pseudomonas aeruginosa* elastase (LasB) inhibitors is discussed. Further use of the above mentioned CFL, helped to identify the first nonpeptidic small molecule inhibitors of LasB. These compounds, in addition to displaying selective antagonism for LasB against a panel of similar metalloenzymes, also confirmed the role the enzyme plays in the swarming behavior of this organism.

1 Introduction

1. A. Introduction

A growing number of pathologies and an increased resistances to current therapeutics has lead to the need for new and innovative treatments. For new drug discovery to be successful, thoughtful choices must be made in the selection of therapeutic targets. One avenue that holds great potential is to target metalloenzymes. These metal containing proteins are ubiquitous, both in humans and in pathogens. A number of metalloenzymes are associated with various pathologies, including a variety of bacterial and viral infections. Additionally, a number of vital processes in the human body require close regulation of metalloenzymes to maintain homeostasis. As such, there is a need for investigative tools and therapeutics to study and regulate metalloenzymes. Efficient, rational design and understanding of how compounds interact with their target is essential for effective drugs to be discovered. To avoid promiscuity and off-target side effects a drug must be selective and tailored to its respective target. This chapter will explore emerging new routes for drug discovery and their relevance to the field of metalloenzyme inhibitor design. To this point, select metalloenzymes will be discussed for their potential as worthwhile targets for metalloenzyme drug discovery.

1. B. 1 Fragment Based Lead Discovery A Strategy for Inhibitor Design

At its most simplified level, drug discovery is a process by which novel and/or improved therapeutics are found, via targeting specific proteins or enzymatic pathways. The method by which this process occurs can vary and in many cases a blend of numerous strategies yields the best results. One such strategy, fragment-based lead discovery (FBLD), has grown in importance as a viable approach to drug design.[1,2] Drug discovery from a FBLD approach is an alternative to more established methods, such as

high-throughput screening (HTS). Drug development via FBLD begins with small fragment compounds. Typically compound libraries consist of a few hundred small (typically < 300 Da), low-affinity (10 μM-mM) fragments.[3] Fragment hits are assessed for how they interact with the target to guide further development and optimization of the most promising fragments into full-length inhibitors.[1,4] In contrast HTS requires the screening of enormous catalogs of large drug-like compounds to identify the most potent molecules. With such large screenings the hit rates for HTS investigations are usually quite low. For those that do advance, optimization can often diminish the initial drug-like characteristics of the compound, decreasing the potential for achieving a successful optimized drug candidate.

Some of the earliest FBLD ideas arose in the early 1980s. Jencks and coworkers proposed that drug-like compounds were merely the sum of their functional group parts.[5] Therapeutics could be thought of as the combination of two or more individual binding fragments. Utilizing these concepts FBLD began in earnest with studies conducted by Fesik and coworkers at the Abbott laboratories in the mid 1990s.[6] Coining the phrase "SAR by NMR," researchers developed the method of using heteronuclear single quantum coherence (HSQC) NMR to monitor and measure fragment molecules binding to proteins. With advancements in techniques and technology, it became possible to conduct a type of high throughput NMR screening. Numerous fragments could be screened simultaneously for their binding to a target of interest.[7] The driving principal of this approach was to identify small molecule fragments that have specific affinities to different areas within a protein. These fragments could then be connected or integrated into a single larger drug-like molecule.

FBLD is a more efficient method of drug discovery when compared with HTS approaches. Smaller fragments have a better probability of fitting into a cleft of a target protein-binding site than full-sized, drug-like compounds. Additionally, functional groups on fragments are not constrained to a predetermined size and shape like those in a drug-like compound (Figure 1.1).[8] FBLD has advantages over to HTS particularly when it comes to exploration of chemical space. If rationally designed, a library consisting of a relatively small number of fragments can cover a larger amount of chemical space than a HTS library comprised of many more compounds.[2,9] Since the number of possible molecules increases exponentially with molecular weight, a HTS library with drug-sized molecules will, by necessity, be larger than a small library of low molecular weight fragments that can represent a higher proportion of the available chemical space.[10] In principle, fragments are quite sufficiently simple and can be obtained commercially or require minimal synthetic efforts. When compared to FBLD, the larger and more complex HTS molecules have a greater synthetic requirement, even prior to optimization. In FBLD, synthetic labor focused after an initial hit is identified towards the desired target. Likewise, the larger, more elaborate compounds found in HTS libraries have a greater potential to encounter steric hindrance within the protein-binding site.[8] The smaller fragments have more free range of motion, which allows for binding to occur in the most energetically favorable arrangement. Therefore binding is free from any possible strain caused by an unaccommodating, pre-formed scaffold, as shown to occur in HTS.[8,11]

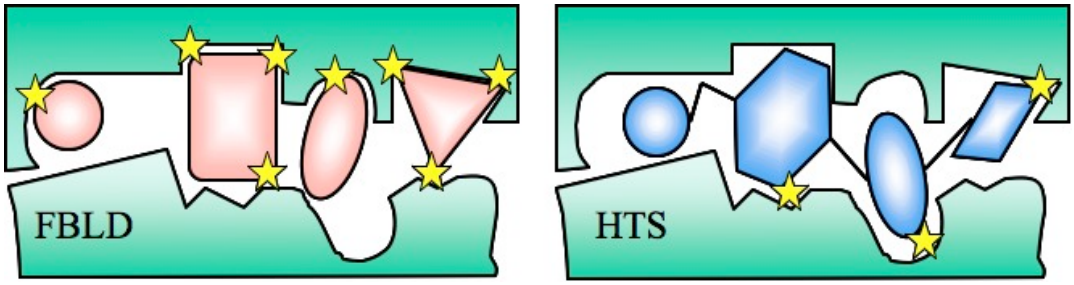

Figure 1.1 Example of a FBLD versus HTS hit. Protein-binding pocket shown in green and yellow stars denote protein-ligand interactions. The red fragments have free range of motion, allowing for the highest number interactions with the protein. The constrained full-length inhibitor in blue is limited in number of functional groups as well as linker space between each group.

1. B. 2 Library Screening Techniques

Hits rates of fragment screenings are typically higher than those observed in HTS investigations.[8] These fragment hits are generally very efficient with high relative binding affinity per atom; however, compared to a HTS hit the absolute potency of fragments are still quite low.[6,12] There are a number of techniques that can be used to identify weak binding fragments.[2] The methods must be sensitive enough to detect low affinity binders with K_d values in the in the high millimolar to micromolar range. NMR, first employed for FBLD by Fesik, is just one of many techniques that can be used to screen fragment libraries.[6,13,14] Additionally, the use of X-ray crystallography,[7,15] in vitro bioassays,[16] surface plasmon resonance (SPR), and virtual screening can be utilized to screen fragment libraries.[17]

Each of the aforementioned methods has its own strengths and shortcomings.[18]. Through NMR screening, information pertaining to the affinity and binding modes of fragments can be gained. This is achieved through monitoring the shifts associated with a

fragment binding to different sites in the ^{15}N-labled target protein.[14] Relatively small amounts of materials are required for these screenings and numerous fragments can be screened simultaneously.[6,13]

X-ray crystallography can be used as a method of fragment screening in which the identification of hits as well as important structural information can be gained.[7,15] This technique allow for multiple fragments to be soaked into a crystal into a protein simultaneously, providing for relatively rapid screening. However, crystallography can also have significant drawbacks. A crystal structure is a static snapshot of a protein and therefore cannot account for the dynamics of a protein in solution. Crystallography often requires large amounts of protein, which can be quite laborious and time-consuming to obtain. Furthermore, not every protein target readily crystallizes or is amenable to fragment soaking.[7]

In contrast, in silico docking is a completely virtual screenings method. It requires no physical material, protein, or fragments. The labor and resource requirements are significantly less; and can provide critical structural information.[17] A virtual screening can identify hits as well as predict the mode of binding of the fragments; However the predictive capabilities can be limiting. Docking programs have made significant advancements and can usually be quite accurate in predicting possible protein-ligand interactions. However, calculating metal-ligand interactions, necessary to predict the binding of metal-chelating inhibitors, is still an underdeveloped area.[19-21]

The biosensor screening technique known as Surface Plasmon Resonance (SPR) can yield important data about fragments binding to target proteins. This binding data (K_d, K_{on}, K_{off}) is obtained by immobilizing the target protein on the surface of an optical

sensor and passing solutions of the fragments over the thin layer of the stationary protein. As accumulation of the fragment occurs, due to protein-ligand binding, shifts in the refractive index of the surface sensor are measured.[22,23] Competition assays like this are helpful in reducing the number of false positives due to off-target effects. Similar to NMR, low concentrations of materials are required to achieve detection of low affinity binders.[24] SPR is limited by the ability to immobilize the protein on the surface sensor with out compromising enzymatic function in a way that will change the measured binding constants.[22]

In vitro biological assays can be used to measure inhibitory activity against a protein target.[16] In general, the types of resources and equipment required to perform biological assays are less expensive and more available than other screening methods such as X-ray crystallography. Unlike NMR and other biophysical techniques, in which the screening is typically conducted on a truncated enzyme (usually only containing the catalytic or active domain) and not in the presence of substrate or other important macromolecules, bioassays offer a more physiologically relevant environment.[25] These assays have limitations as well; biological assays are not as sensitive as other techniques discussed, therefore the assays must be adapted to perform with high concentrations of the fragments (up to 1 mM) in order to elicit an observable response from low affinity fragments.[26] Such high concentrations can limit fragment solubility and fragment aggregation can occur leading to false positives through non-selective inhibition.[27] Additionally, no structural information is obtained from these types of assays.[18]

1. B. 3. Hit to Lead Development

Unlike HTS, fragment hits are generally of very low molecular weight and far from a lead compound. The process to take a fragment hit to a full-length drug candidate can be intensive. Once a target is selected, hit generation begins with an initial screen of fragment libraries to identify hits. To generate a general scaffold for the compound, hits are assessed and sometimes grouped based on structural similarities before being developed. These larger drug-like leads are then further optimized; typically a lead is designed to mimic the profile of other successful clinical candidates. Criteria include activity, selectivity and the absorption/administration, distribution, metabolism and excretion (ADME) characteristics of the compound.[1,18,28] Lead optimization is performed with the goal of creating a compound that can be moved into clinical trials as a drug candidate.

Fragment development typically utilizes one (or a combination of) the following strategies: merging, growing, linking and in situ assembly.[1,2,5,18,29] For example, a merging approach would be implemented in a scenario where two fragments are capable of occupying the same space within the active site. One possible option would be to merge the potent functional groups of two compounds into a new single fragment. Ideally, contributions from both parent fragments have a constructive effect and the newly merged compound will have increased potency (Figure 1.2).[2]

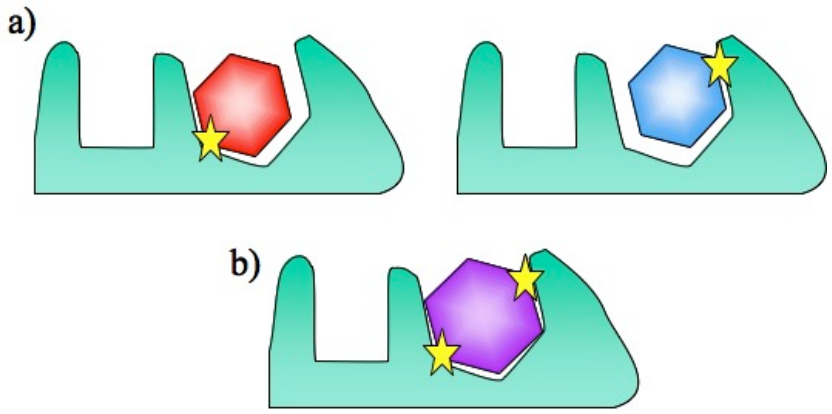

Figure 1.2 Generic representation of the fragment merging strategy. Protein-binding pocket shown in green and yellow stars denote protein-ligand interactions. a) Two fragments capable of occupying the same binding site but contribute two different protein-ligand interactions. b) A newly merged fragment containing both functionalities.

A linking strategy would be employed in a case where data indicates that two fragments bind to a protein in separate areas within an active site (Figure 1.3). A synthetic linker is designed to bridge the two fragments forming a new compound. As such, a linking strategy can turn two small fragments into one larger compound with multiple functional groups capable of making several binding interactions simultaneously.[1,5]

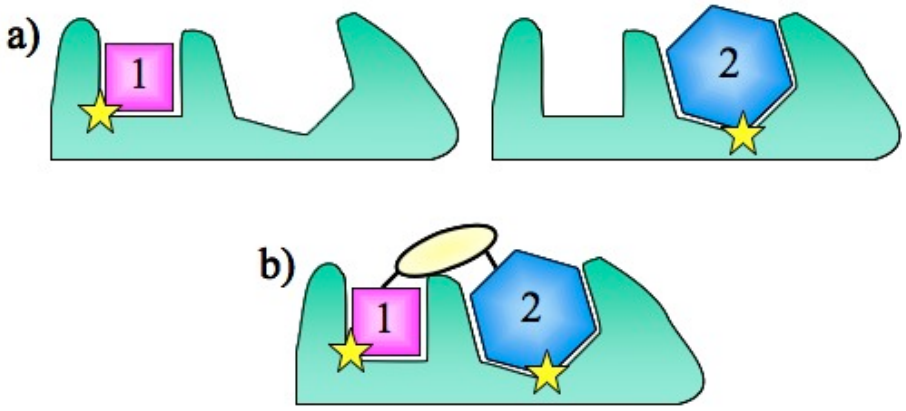

Figure 1.3 Generic representation of the fragment linking strategy. Protein-binding pocket shown in green and yellow stars denote protein-ligand interactions. a) Two fragments occupying nearby binding sites. b) A new compound that consists of the two fragments linked together.

In a situation where only a single binding fragment is identified, a more classical SAR medicinal chemistry strategy may be implemented in hopes of growing the small molecule to further exploit the active site of the target (Figure 1.4). Step-wise exploration of the biding site occurs by slightly changing the original binding fragment via chemical synthesis in order to probe the active site for more potent ligand-protein interactions. These elaborations of the binding fragment are then re-screened. Those which are most potent are further advanced to improve compound potency.[1,30]

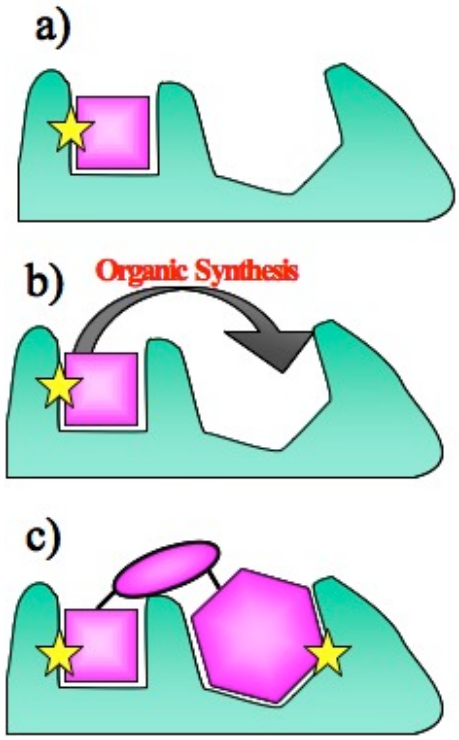

Figure 1.4 Generic representation of the fragment growing strategy. In a), a single fragment is identified to bind to the protein active site. b) Additions are made to the fragment in a step-wise fashion to determine optimal interactions, which yield c) a grown fragment of a) that now occupies multiple binding sites.

The above methods of fragment optimization discussed require additional chemical synthesis such as 1) merging two fragments into one, 2) linking nearby fragment hits together, and 3) growing a fragment to increase interactions in a protein-binding site. In situ fragment assembly is a creative alternative to these methods. As illustrated in Figure 1.5, two smaller fragments with complementary appendages can react, forming a potent molecule within the confines of the binding site. This approach integrates two fragments in adjacent binding pockets by its own self-formed linker. For

this method, structural knowledge regarding the positioning and binding modes of the fragments involved is essential to identifying the appropriate complementary functional groups.[30]

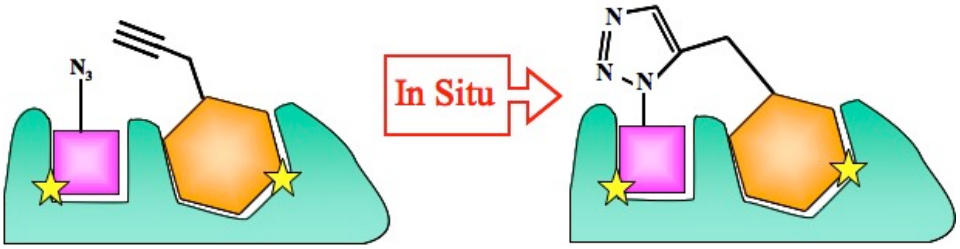

Figure 1.5 Representation of the fragment development strategy of in situ fragment assembly. Two fragments with complementary functional groups (for example an azide and alkyne) can react, forming a singular new molecule within the confines of the binding site.

Often fragment progression requires at least one fragment to remain constant in its mode of binding, throughout the evolution of the compound. This point of binding is consistent while other protein-ligand interactions are explored, allowing hits to develop, evolve, and increase in affinity specific to the target.[1,2,30] The ability of each fragment to bind and interact with a protein at differing areas can lead to a more potent and tailored lead compound. In the cases of linking and merging strategies structural data (i.e. crystallographic, virtual, or NMR) is necessary for efficient fragment development. Growing can be a more forgiving approach. Specifically, this strategy has the ability to probe the site around the bound fragment with small step-wise synthetic advancements.

This allows for subtle discovery about the different types of interactions capable in the protein.[2]

1. B. 4. Zelboraf: A FBLD Clinical Success Story

FBLD is still considered a newer approach for drug discovery, having only been actively pursued since the 1990s. Due to its infancy, FBLD received its first significant validation as a drug discovery approach when the drug Zelboraf was approved in 2011.[31] Remarkably, the time span from the first fragment investigations to approval was only six years. Zelboraf, also known as Vemurafenib or PLX4032 (Figure 1.6) is a kinase inhibitor for the V600E allele of B-Raf. The V600E allele is known to have activity that is linked with decreased response to chemotherapy in human tumors particularly associated with malignant melonoma.[32,33] In what is described as a "structure-guided discovery approach," 20,000 fragments were screened against a panel of kinases and approximately 200 fragment hits were selected for crystallization structure studies. Based off the resulting structural data, 7-azaindole was revealed to be a promising fragment hit. This starting fragment had an IC_{50} value of approximately 200 μM against a generic screening kinase, Pim-1. Through the use of a growing strategy, a 3-aminophenyl group, which further increased kinase inhibition, was introduced. Subsequent hit-to-lead development identified that substituents appended to the 3- and 5-positons of the azaindole provided the most potent compounds.[32,33] After numerous iterations, the original 7-azaindole fragment was finally optimized to include a difluoro-containing sulfonamide (3-positon) and a chlorophenyl group at the 5-postion. The final compound PLX4032 was found to have an IC_{50} value of ~30 nM against the B-Raf^{V600E} target (Figure 1.6).[31-33]

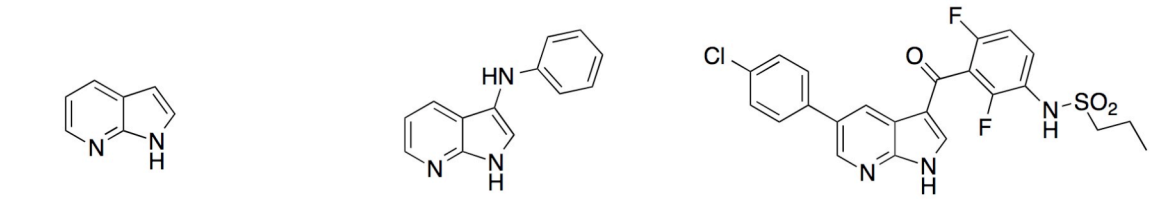

Figure 1.6 Structures and IC_{50} values of selected compounds involved in the fragment-based discovery of FDA-approved Zelboraf (Vemurafenib).

Zelboraf is an extraordinary compound shown to block proliferation and cause tumor regression in patients by exhibiting potency and selectivity achieved through the development of a simple 7-azaindole fragment. Moreover, the success of this drug goes beyond a new treatment for malignant melanoma; it marks the first successful FBLD drug candidate. In the past decade, approximately ten FBLD-based leads have been introduced into clinical phase trials.[31]

Drug discovery for inhibitors of metalloenzymes holds a unique opportunity for utilizing FBLD. The metal itself becomes the ideal candidate to direct initial binding efforts. Basic metal binders, or chelators, are fragments that represent the fundamental motif necessary to result in a covalent interaction with a metal.[12,34-36] The mode of binding for many chelators are either historically documented or can be modeled when applying basic principles of inorganic chemistry. Furthermore, the metal ions in these proteins are typically associated with catalytic activity and therefore fragments and/or developed lead compounds bound at the metal will likely lead to competitive inhibitors.[37-40]

High concentration biological assays were used to screen fragment libraries against metalloenzymes in the studies described in Chapters 2, 3 and 4. With this technique a few educated assumptions are being made to facilitate the hit identification process. These assays will not yield structural data, but with appropriate controls to minimize false positives, a hit generated from a chelator fragment library against a metalloenzyme can be biased as binding to the metal ion. Initial studies focused primarily on mononuclear metalloenzymes, these proteins contain only one catalytic metal ion in their active site. Many of the enzymes chosen for these studies were based on factors such as active site metal identity, availability of structural data, and clinical/therapeutic interest.

1. C. 1. Metalloenzymes of Interest: Mononuclear Proteins

Metalloenzymes comprise more than a third of all known proteins. These metalloproteins, containing an essential metal ion cofactor, are vital to many life processes.[41,42] Metal cofactors serve roles in electron transport, and the catalysis of essential enzymatic processes, and can also contribute to structural integrity and stability of some proteins. The most abundant of these metals in the human body are iron and zinc.[43] Iron is well known for its role in respiration (hemoglobin, myoglobin) but it is also associated with nearly all homeostatic functions in the body including electron transport, immune response and inflammation.[43,44] Zinc is also essential in many fundamental processes, such as cell life cycle regulation, metabolism, pH balances, and inflammation.[35,45] Metals are not only essential to humans', bacterial and viral organisms who require metals to catalyze vital functions.

1. C. 1a. Matrix Metalloproteinases

Matrix metalloproteinases (MMPs), are a Zn(II) dependent class of proteolytic enzymes.[39] The different isoforms of this family can be classified and divided into sub-groups based on their substrate specificity dictated by the pockets surrounding the active site. These include collagenases, gelatinases, stromelysins, and membrane-type enzymes.[46,47] All MMPs contain a catalytic Zn(II) ion in the active site of the enzyme. This Zn(II) ion is coordinated to three histidine residues, along with an additional fourth bond to a labile water molecule (Figure 1.7). The majority of MMP inhibitors (MMPi) are designed with a zinc-binding group (ZBG) to chelate the catalytic metal ion and have backbones that can interact with the amino acids in the pockets. Targeting for the S1' pocket has provided the foundation of selectivity for numerous MMPi.[47,48] This pocket can be classified based on size to provide a way to make isoform-specific MMPis. Generally, it is thought that the S1' pockets of MMP-1 and MMP-7 are shallow compared to the deep pockets of MMPs -3, -8, and -12. Lastly, the S1’ pocket of MMP-2, -9, and -13 are typically considered to be intermediate in size.[46,49]

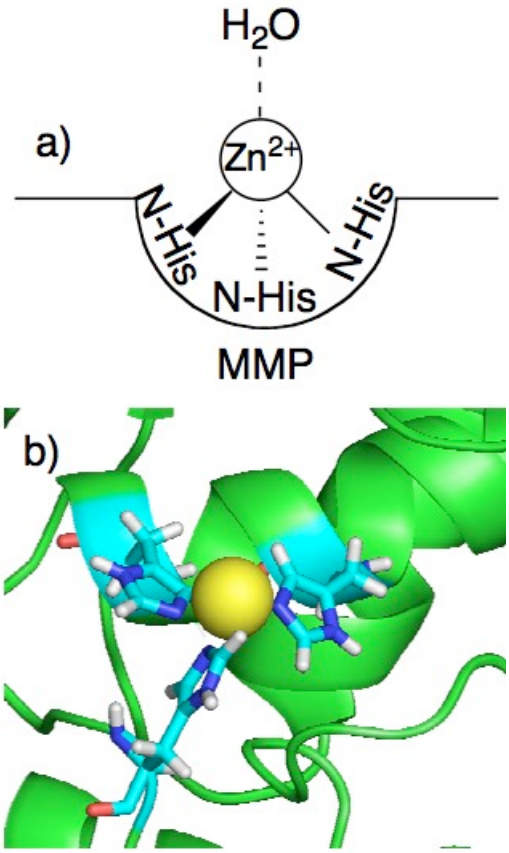

Figure 1.7 a) Representative illustration of a MMP active site with the Zn(II) metal ion coordinated by three histidine residues and an axial water. b) Crystal structure of MMP-2 active site (PDB: 1QIB). A yellow sphere represents the Zn(II) ion and coordinating histidine residues are shown in blue.

This family of over 20 endopeptidases is involved in numerous physiological and pathogenic processes. MMPs are responsible for the degradation and remodeling of the extracellular matrixes (ECM) for the purpose of angiogenesis, immune response, apoptosis, cell proliferation and signaling.[49,50] Due to such a wide variety of roles within the body, regulation of MMP activity must be strictly regulated. In healthy systems, MMPs are closely kept in balance by four endogenous proteins called tissue inhibitors of

MMPs (TIMPS). Additionally, MMPs are secreted in their pro-enzyme form. These regulations require the upregulation and activation of MMPs to occur prior to function; typically it is a TIMP that will inhibit an activated MMP in order to halt degradation processes.[51] Misregulation and over expression of MMPs has been associated with numerous health issues and diseases.[52,53] A loss of balance between MMPs and TIMPs has been implicated in cancer, arthritis, cardiovascular disease, osteoarthritis (MMP-13), chronic obstructive pulmonary disease (COPD, MMP-12), and destruction of the blood brain barrier in the wake of ischemia after strokes (MMPs -2 and -9).[54] Due to the association with such a wide variety of pathologies MMPs have become a prominent therapeutic target in drug design. There are two proposed routes to the inhibition of MMPs: downregulation by controlling TIMPs within a system or the creation of small-molecule inhibitors of MMPs.

Historically many MMPi have fallen short of their potential, and in clinical trials, numerous pharmaceutical companies have suffered significant losses due to late stage attrition in the clinic.[50,55] As should be expected with a class of ubiquitous enzymes, broad-range MMPi yielded undesirable side effects, most likely due to non-specific MMP inhibition.[50] As a result, renewed efforts were directed towards the development of MMP isoform specific MMPi. This has proven to be a more daunting task than initially proposed. In order to be considered a significantly selective inhibitor, there should be at least a factor of 10^3 difference in potency between the targeted MMP and others, especially those that share the same substrate sub-group.[55]

Hydroxamic acids have classically been the most widely used ZGB for MMPi development. This ZBG has been closely related to MMPs from when the enzyme was

first discovered.[35,36] The hydroxamate moiety is a bidentate ligand to the Zn(II) ion, utilizing both oxygen donor atoms (Figure 1.8).[55,56] Despite some hydroxamate-based MMPis achieving potency in the low nanomolar range, all inevitably fell short in clinical trials. Metabolic instability of this ZBG and promiscuity are two probable contributors to the failure of this set of inhibitors to achieve clinical success.[57]

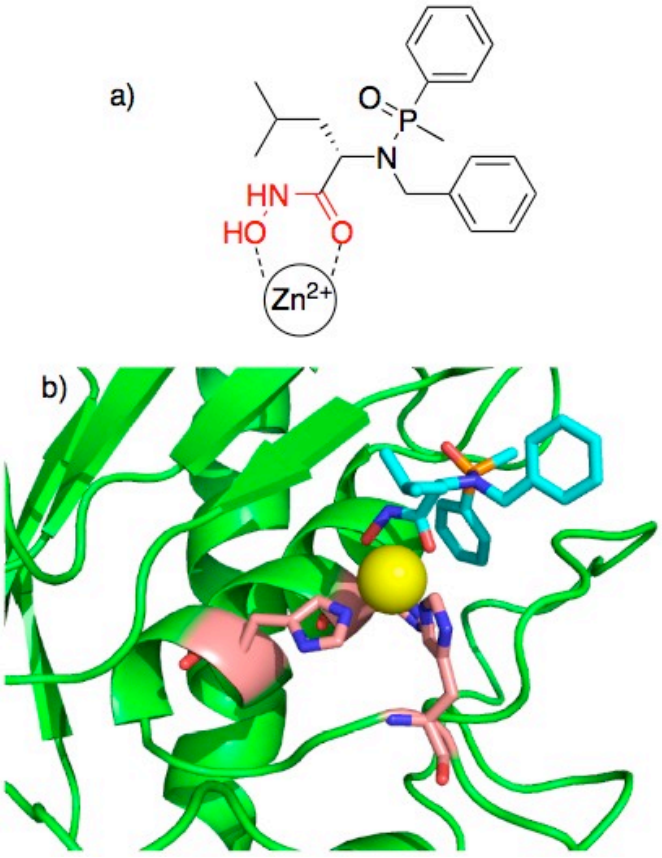

Figure 1.8 a) The structure of hydroxamate-based MMP-3 inhibitor with bidentate ZBG highlighted in red. b) Structure of MMP-3 active site with bound hydroxamte inhibitor (PDB: 1B3D).[58] A yellow sphere represents the Zn(II) ion, coordinating histidine residues in red and bound inhibitor shown in blue.

1.C. 1b. Anthrax Lethal Factor

Another mononuclear Zn(II) dependent metalloenzyme is the endopeptidase lethal factor (LF). There are some structural similarities between LF and MMPs beyond the use of the same metal ion cofactor. Two histidines (instead of three as in MMPs), as well as a glutamic acid, comprise the zinc-binding motif of LF. Additionally, similar to MMPs, a catalytic water coordinates axially to the zinc and plays a crucial role in the hydrolysis of peptides (Figure 1.9).[59,60] While MMPs are inherently vital for healthy biological processes, LF is part of a virulence factor of a foreign invading metalloenzyme that preys upon cell-signaling pathways in order to protect bacteria from the immune response of the host.[61] LF is one of three constituents comprising the exotoxin known as anthrax toxin, secreted by *Bacillus anthracis*, which causes anthrax.[61,62] Drawing national attention in 2001, anthrax toxin was responsible for the widespread panic and subsequent deaths of five people as a result of coming in contact with letters containing active anthrax spores that were distributed to members of the media and U.S. Senate.[61]

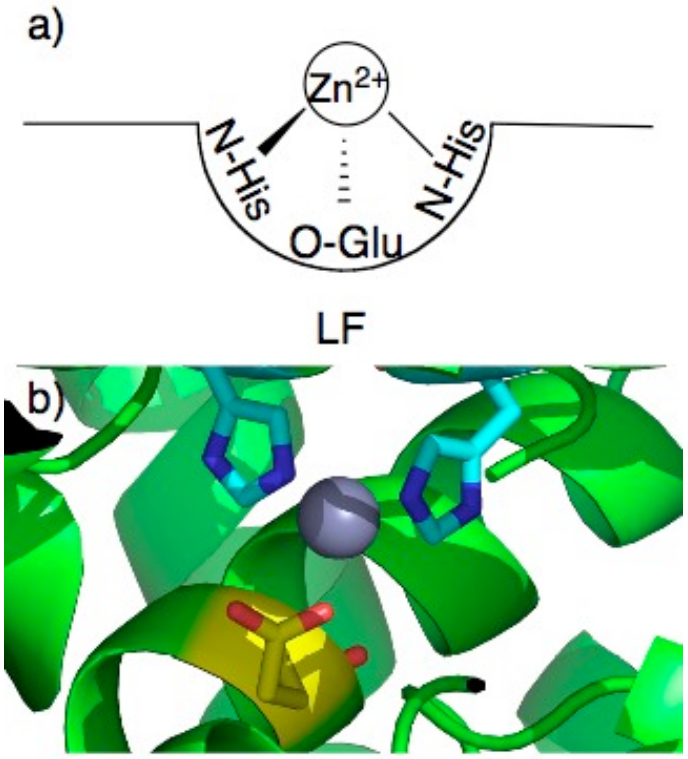

Figure 1.9 a) Representative illustration of a LF active site with the Zn(II) metal ion coordinated by two histidine and one glutamic acid residues. b) Protein crystal structure of LF active site (PDB: 1YQY). A grey sphere represents the Zn(II) ion, coordinating histidine residues are shown in blue and glutamic acid in yellow.

Anthrax toxin consists of three proteins: a cell-binding component called protective antigen (PA), and two other proteins called edema factor (EF) and LF.[63] The host typically contracts anthrax toxin through physical contact, by inhalation and/or ingestion of *B. anthracis* spores.[62] Unlike spores of fungi, these bacterial spores are a survival mechanism of the organism when conditions are too harsh to support propagation. The dormant bacterium can survive for decades prior to resuscitation, a reaction triggered by introduction to a more auspicious environment.[59] The individual

portions of the complex are not toxic. Thus, neither PA, EF, or LF will cause damage, but when combined these enzymes cause the dangerous effects of anthrax that culminate in cell death.[62,63] Upon entering a host, PA will bind to the surface of a macrophage and is then cleaved by the host proteases. This cleavage initiates the activation of the protein, which oligimerizes to form the beginnings of a pore for the insertion of either EF or LF. Again facilitated by the host, PA undergoes endocytosis causing a cascade of reactions resulting in a fully formed membrane insertion canal.[64] EF and LF are then transported via the newly formed pore into the cytosol, where they begin forming their respective toxins. EF releases a toxin causing general edema, hindering immune response and aiding in further promotion of the bacteria. LF cleaves mitogen-activated kinase kinases (MAPKK), via a Zn(II) catalyzed process at the N-terminal, disrupting cell signaling, and resulting in cell death.[59,62,63]

LF inhibitor design has mirrored MMPi and typically contain hydroxamic acid ZBGs. A number of LF inhibitors have been reported, but few have reached submicromolar potencies, and many lack the necessary cell and animal studies necessary to pursue the compounds as drug candidates.[65-67] Current treatment for anthrax rely heavily on the use of antibiotics, but the toxins and their effects can persist even after the eradication of the bacteria.[65] These factors make LF a desirable therapeutic target with a need for selective and potent inhibitors.

1. C. 1c. *Pseudomonas aeruginosa* Elastase

Pseudomonas aeruginosa is a Gram-negative bacterium found in many damp environments including soil, plants, and animal tissue. This bacterium is considered to be very versatile and adaptive and has become one of the top sources of opportunistic human

infections.[68] *P. aeruginosa* is a leading cause of hospital-acquired pneumonia as well as bacteraemia in burn victims. Antibiotic resistance has become a hallmark of this bacterium. The versatility of P. *aeruginosa* is attributed to its large genome, containing genes for many virulence factors.[68,69] To further promote infection in the host, *P. aeruginosa* secretes a number of virulence factors, which help the pathogen to adapt and change to specific environments. Similar to anthrax LF, these virulence factors are crucial in the invasion of the host as well as in evading and suppressing the immune response of the host. Such adaptability is believed to be a contributing factor to mounting resistance to conventional antibiotic treatments by *P. aeruginosa*.[69,70]

P. aeruginosa is a triple threat because of high incidence rates, severe infections and growing resistance. As such there is a dire need for new and alternative strategies to treat these infections.[69] One vein of interest is to target the pathogenic virulence factors. Of particular relevance is the third metalloenzyme investigated, *P. aeruginosa* elastase (LasB). LasB is a metalloproteinase thought to be responsible for the tissue damaging effects during infection.[71] In addition to the ability of this enzyme to degrade elastin and collagen, LasB can demonstrate cytotoxic effects like damaging cell membranes. This Zn(II) dependent metalloenzyme is also thought to contribute to the formation of biofilms which are associated with swarming and antibiotic resistance via impermeability.[72,73] Infection models in which LasB has been knocked out presented less severe infections.[74] As such, LasB presents an opportunity to explore not only the development of new inhibitors but also investigate the validity of targeting virulence factors as treatments in infection. This relatively new target has had little success with investigations into the application of non-peptidic inhibitors that exhibit antagonism against secreted LasB.[75,76]

Inhibition of LasB activity by various proteinase inhibitors including plasma $\propto_2$-macroglobulin and phosphoamidone has been reported.[77-80] The crystal structure of LasB, elucidated by Thayer and coworkers in 1991 depicts an active site very similar to the well-studied enzyme thermolysin.[81] The single catalytic Zn(II) is coordinated by two histidines and a glutamic acid (Figure 1.10). The "active site cleft" in the hinge region of LasB is drastically wider and more open than the thermolysin counterpart. Implications of such a variation could include differences in preference and binding constants of inhibitors (Figure 1.10). This would suggest that with proper inhibitor design, selectivity for LasB over thermolysin could be achieved despite both enzymes having remarkably similar overall tertiary structures.[81]

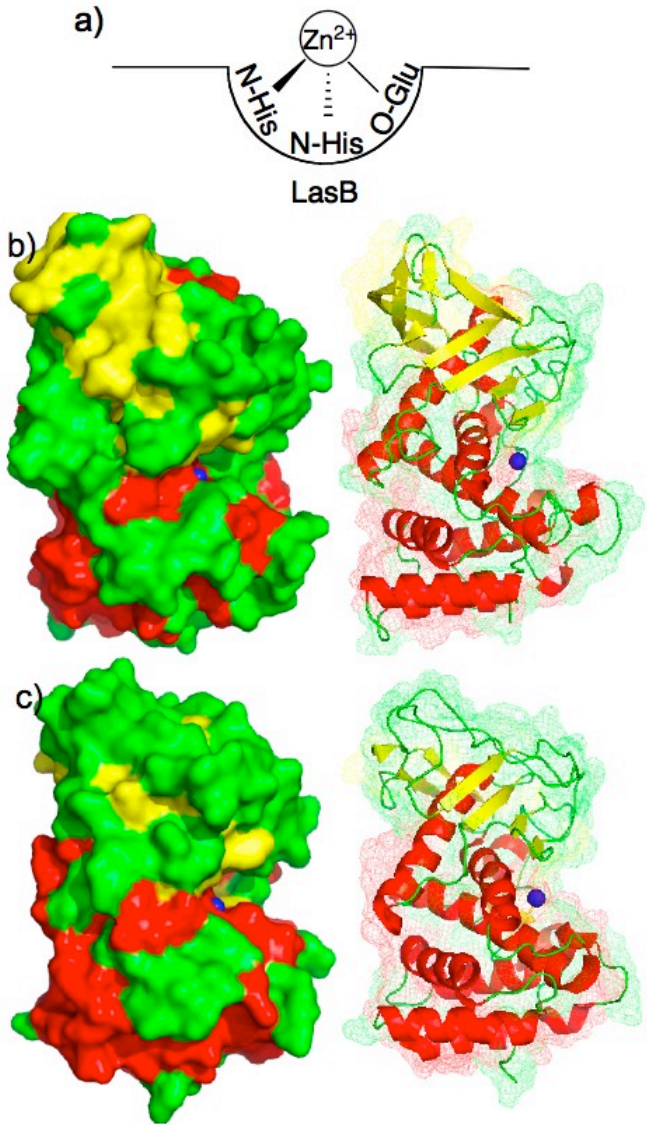

Figure 1.10 a) Representative illustration of LasB active site with Zn(II) metal ion coordinated by two histidine and one glutamic acid residue. b) Structure of thermolysin Zn(II) ion shown in blue. c) Structure of LasB Zn(II) ion shown in blue. [81]

1. C. 1d. 5-Lipoxygenase

5-Lipoxygenase (5-LO) is a non-heme iron metalloenzyme implicated in the inflammatory response.[82] All enzymes in the lipoxygenase family contain iron cofactors,

typically bound to their respective active sites by histidine residues (Figure 1.11). Various lipoxygenases differ in what role during the process of dioxygenation they play. In mammals, 5-LO is essential for the synthesis of leukotrienes.[83] Leukotrienes are a class of inflammatory regulators associated with immune response.[84] The primary steps in the process of changing arachidonic acid (AA) into subsequent leukotiens are mediated by 5-LO (Figure 1.11). AA is first converted into hydroperoxyeicosatetraenoic acid (HPETE) and further evolved into leukotriene A_4. The resulting epoxide in leukotrine A_4 is unstable and will rapidly undergo additional conversion by either leukotrine-specific hydrolase or synthases. Many of the resulting molecules are known as cysteinyl leukotrines, which promote the stimulation of mucosal secretions and participate as bronchoconstrictors.[82]

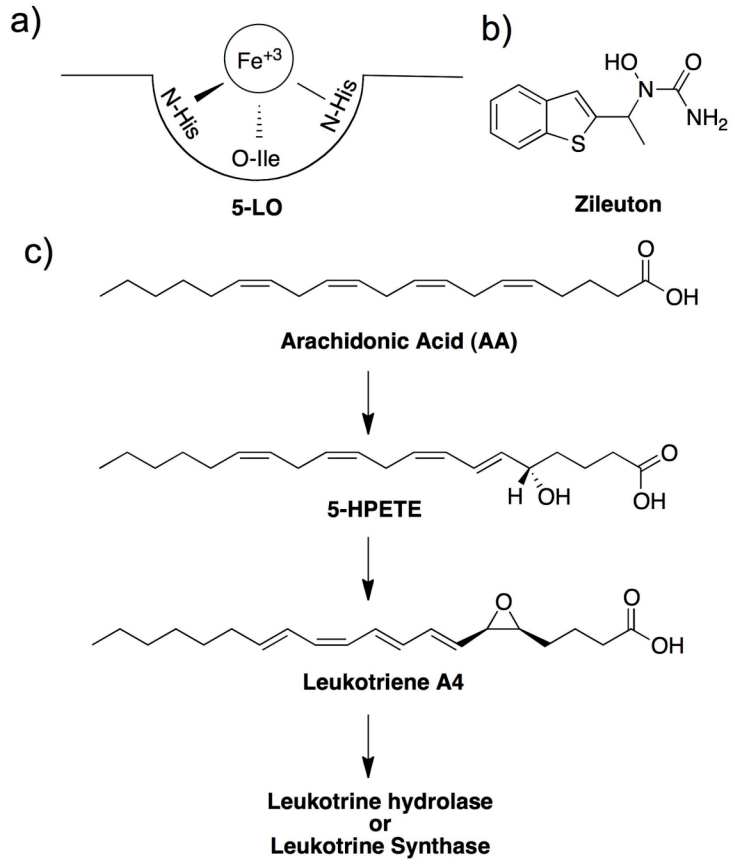

Figure 1.11 a) Representative illustration 5-LO active site, activated with the Fe(III) metal ion coordinated by three histidines. b) FDA approved 5-LO inhibitor Zileuton, this compound utilizes a reverse hydroxamic MBG which chelates to the iron cofactor of 5-LO. c) Biosynthetic pathway for the formation of leukotrienes.[82]

As with many iron-containing enzymes, the cofactor in 5-LO is utilized in electron transport. The entire process is catalyzed by hydroperoxides, oxidizing the iron from Fe(II) to Fe(III). The resulting redox chemistry acts as an electron shuttle during the reaction.[82] These lipid mediators of inflammation are typically associated with numerous cardiovascular and respiratory pathologies; as such, leukotrienes and the enzymes associated with their regulation and synthesis are of great therapeutic interest. Much

attention has been given to 5-LO inhibitors as treatments for asthma, COPD, and allergic reactions associated with inflammation.[85] Currently, the most widely known inhibitor of 5-LO is Zileuton, which is used in the treatment of asthma related inflammation (Figure 1.11). This compound inhibits 5-LO activity by chelating to the iron cofactor and thus hinders the electron transport processes.[86] Unlike Zileuton, inhibitors designed to disrupt the redox process in 5-LO have been shown to have numerous detrimental off target-effects. Most notably would be the negative interactions with another abundant iron-containing enzyme in the human body, hemoglobin. Many of these inhibitors can oxidize the hemoglobin iron to Fe(III) resulting in toxicity.[87] With few successes in 5-LO inhibitors (achieving both potency as well as non-toxicity), investigations into molecules that interact with the enzyme's metal ion cofactor may lead to advancements in 5-LO inhibitor design.

1. C. 2. Metalloenzymes of Interest: Dinuclear Proteins

Another class of metalloenzymes contain two metal ion cofactors. These enzymes present a new dynamic to explore when designing and screening MBG fragments. The presence of two metals offers multiple sites of chelation. The binding environments between the two metals may differ, altering the type of metal-binding interactions preferred.

1. C. 2a. Tyrosinase

Tyrosinase (TY) is a dinuclear metalloenzyme often linked with pigmentation, due to its role in the melanin biosynthetic pathway. This Cu(II)-containing enzyme is the rate limiting step for two oxidation processes in the formation of melanin.[88,89] This pigment is found in most living organisms and mutations in the TY gene can cause

albinism in humans and animals.[90] TY oxidizes phenols like tyrosine with O_2 to form diphenols (Figure 1.12). Subsequent conversions of these diphenols result in various forms of melanin.[91] The process is frequently observed in the browning of fruit, such as bananas or the production of melanin in the tanning of human skin. In humans substrate specificity is quite pronounced, and only the L-form of the monophenol dopamine (L-DOPA) is used in melanogenesis.[89]

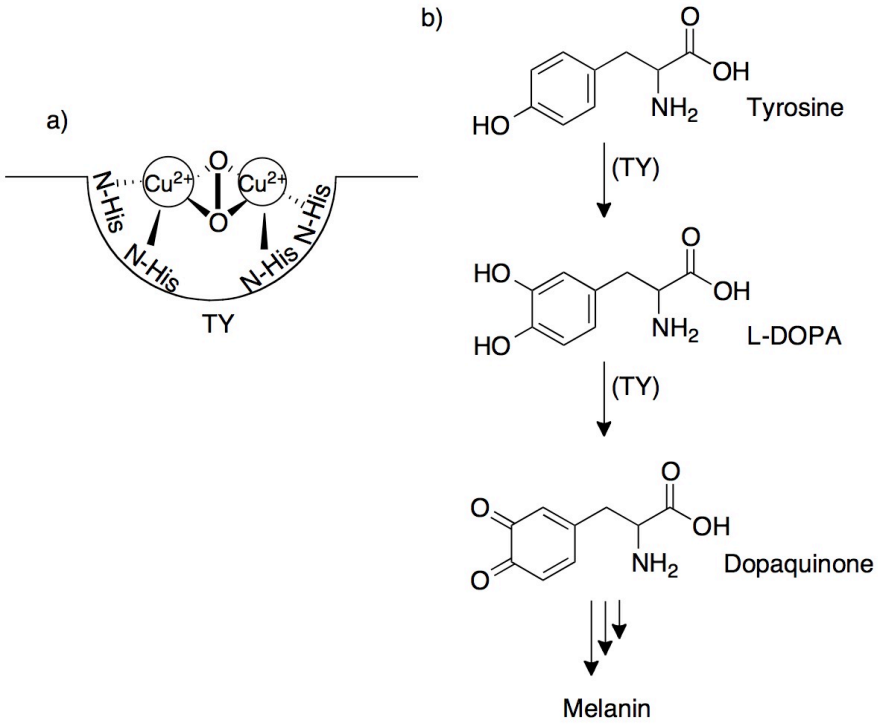

Figure 1.12 a) Representative illustration of TY active site with dinuclear Cu(II) metal ions coordinated by histidines (*Oxy*-tyrosinase form). b) Biosynthetic pathway of TY used to oxidize monophenols, like tyrosine, into L-DOPA and subsequently oxidize the formed diphenols into quinines, like Dopaqunione.

The structure of TY varies greatly between forms; to date there has been no observation of a universal TY structure. Even with such a wide variety of shapes the tertiary structure of TY can possess, all forms of TY have one aspect in common the dinuclear copper active site.[92] The two Cu(II) metal ions in the active site of TY are categorized as a type-3 copper center.[93] Due to the reactivity and proximity of the two copper ions, TY can exist as three different isoforms (Figure 1.13).[94] The inactive form, *met*-tyrosinase consists of a singular oxygen bridging the two Cu(II) ions. Both the deoxy- and *oxy*-tyrosinase forms are involved in enzyme activity with mono and diphenols.[95] It is important to note that only the *oxy*-tyrosinase isoform (in which the two Cu(II) ions are bound to a bridging dioxygen) interacts with the potent inhibitor tropolone (IC_{50} value = ~400nm).[95,96] Because this enzyme is involved in such a ubiquitous process, inhibitors of TY have applications in a wide variety fields including agriculture, cosmetics, and therapeutics. One advantage to the different forms of TY having no common overall structure is the potential to develop inhibitors that will only be specific to the target isoform of TY. This could be particularly beneficial to the application of TY inhibitors as food preservative, where selective TY inhibition between human and plant TY would be vital.

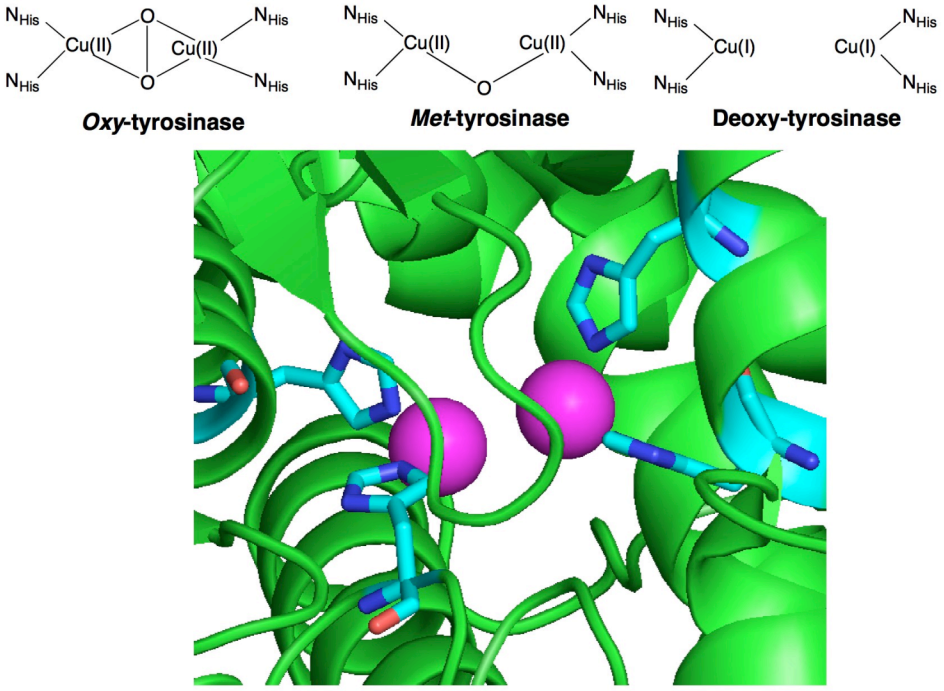

Figure 1.13 Representative illustrations of the three isoforms of the TY active site with the copper ions coordinated to histidines (top). Protein crystal structure of the active site is of the deoxy-tyrosinase isoform of TY (PDB: 2ZMX). Purple spheres represent the copper metal ions and the coordinating histidine residues are shown in blue (bottom).

1. C. 2b. Human Immunodeficiency Virus-1 Integrase

Human Immunodeficiency Virus (HIV) is a retrovirus that causes the disease known as acquired immunodeficiency syndrome (AIDS). Currently there is no cure for AIDS, although advancements in therapeutic treatments have drastically improved quality of life.[97-99] These powerful antiretroviral drugs, when administered early in pregnancy, have even helped to reduce the potential to pass the virus from mother to child.[100] HIV-1 integrase (HIV-1 IN) is one of three essential enzymes for HIV-1 replication (along with HIV-1 reverse transcriptase and protease). The metalloenzyme

performs two functions, the first is known as 3'-processing (3P). HIV-1 IN generates reactive CpA 3′- hydroxyl ends (cytosine–adenosine overhangs) by specifically cleaving two nucleotides from the viral cDNA. The second function, known as strand transfer (ST) occurs upon translocation to the nucleus where HIV-1 IN uses the hydroxyl ends to integrate the viral DNA into the host genome.[101,102] Due to the above functions, HIV-1 IN is the 'point of no return' in infection of a host cell.[103]

The active site of HIV-1 IN contains a dinuclear magnesium center, in which the metal ions are coordinated by the carboxylate ligands of two aspartic acids and one glutamic acid (Figure 1.14). The catalytic Mg(II) ions are essential to HIV-1 IN function. Additionally, substitution of any of the three metal-binding residues (DDE) abolishes HIV-1 IN activity, suggesting that metal-binding is necessary for HIV-1 IN function.[104]

Due to solubility issues crystallization of full length HIV-1 IN has been very difficult. Recently however, a crystal structure of an integrase from the prototype foamy virus (PFV) bound to its cognate DNA was successfully characterized (Figure 1.14). Complex crystal structures with known inhibitors of HIV-1 IN, including the FDA-approved Raltegravir were also obtained. It has been proposed that the mode of action for Raltegravir is to inhibit via binding to both Mg(II) (Figure 1.15).[105] Raltegravir consists of a 5-hydroxy-3-methylpyrimidin-4(3*H*)-one (HMPO) MBG, effective at binding to the binuclear metal site in HIV-1 IN. The HMPO chelating group was discovered by HTS efforts and was found to possess suitable metal-binding activity and pharmacokinetics.

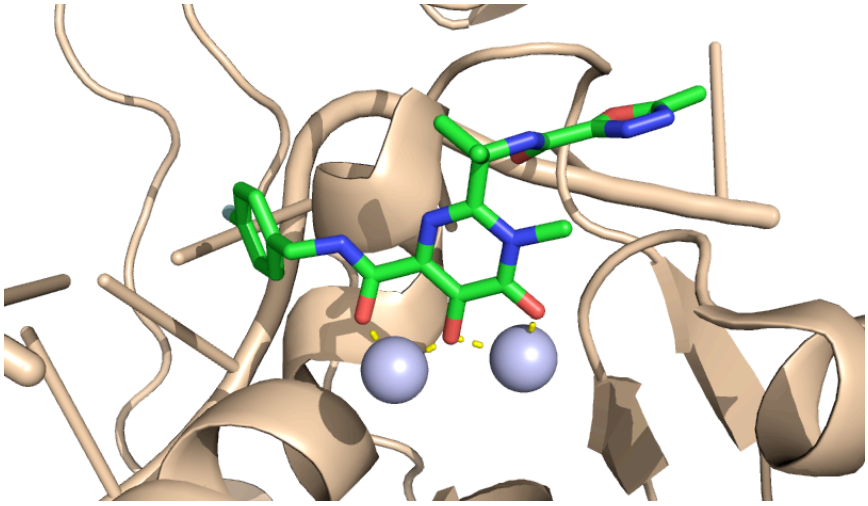

Figure 1.14 Crystal structure of PFV-IN (PDB 3OYA) complex with the FDA-approved HIV-1 IN inhibitor raltegravir. The tan ribbon represents the protein and viral DNA, grey spheres represent the Mg(II) ions and Raltegravir is shown as the green rods.

As illustrated in figure 1.15, the MBG of raltegravir (the HMPO chelator) consists of a three-oxygen donor atom triad. Shown in figure 1.14, this triad aligns in a coplanar fashion to bind and bridge between the two Mg(II) metal ions in HIV-1 IN. Other promising HIV-1 IN inhibitors such as Elvitegravir and GSK364735 also depend on donor atom triads to effectively inhibit the enzyme. It is important to note however, that the metal-binding atom triad in each of these inhibitors is unique. Unlike raltegravir, GSK364735 has a pyridyl-nitrogen atom forming a N,O,O donor set. Elvitegravir has an O,O,O donor atom similar to raltegravir yet the combination of carbonyl and phenolic oxygen atoms is different.[106,107] Due to these adjustments and variations in the donor atom sets these compounds do not share identical binding modes or bond angles between the donor atoms. This potential for a variety of different types of successful inhibitors implies that different MBGs capable of forming a number of different chelating

orientations have the capacity to inhibit HIV-1 IN at the same active site.[108] However, very few studies have conducted the necessary systematic studies to examine the various features of these MBGs.[109]

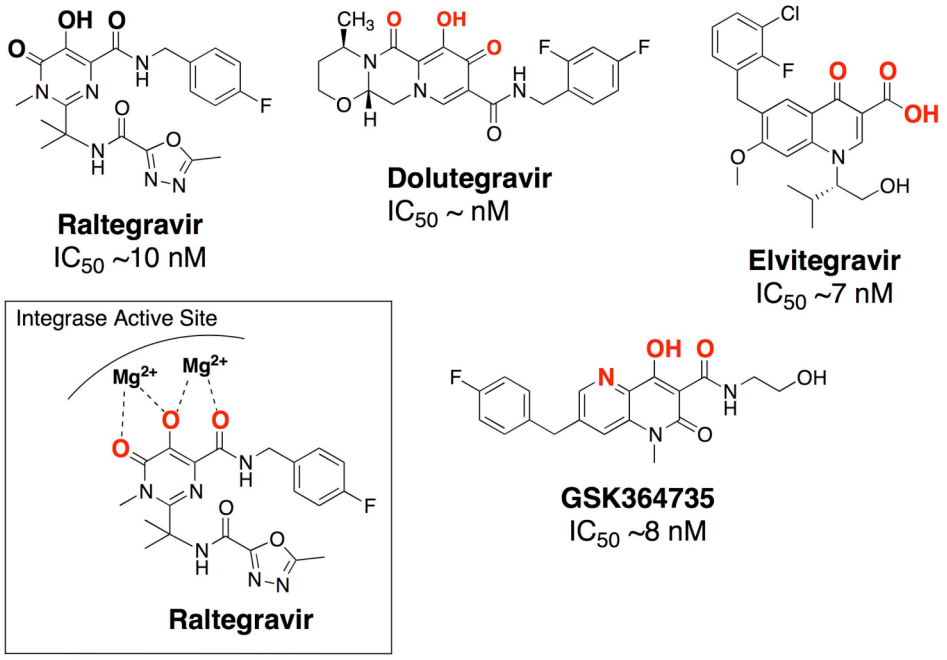

Figure 1.15 Structures of Raltegravir and other select potent HIV-1 IN inhibitors. The donor atoms highlighted in red comprised the MBG of each compound. Boxed off is an illustration of Raltegravir bound to the Mg(II) metal ions in the HIV-1 IN active site.

To date there is only one HIV-1 IN inhibitor approved by the FDA. This compound, Raltegravir (Figure 1.15), was only introduce in 2007 and there is already an emergence of resistant HIV-1 strains. HIV-1 is notorious for its ability to rapidly mutate and adapt to new drugs. One way to combat resistance is to use combinational cocktails of drugs targeting various portions of the virus known as highly active anti-retroviral therapy (HAART). Another method for developing treatments resilient to resistance is to

target essential functions or areas that the virus cannot afford to mutate. As mentioned before the catalytic Mg(II) metals ions are essential to the enzyme for activity and as such cannot be occluded or removed. Importantly, of the Raltegravir-resistant mutants characterized thus far, none appear to alter the metals or the binding motif.[110] It would stand to reason that if a very potent metal binder of HIV-1 IN were to be discovered, the efficacy achieved by the MBG could outweigh any potential new mutations of the enzyme.

1. C. 2c. Methionine Aminopeptidase (MetAP)

Methionine aminopeptidase (MetAP) is a dinuclear metalloenzyme capable of being reconstituted in an active form by a number of metal ions.[111] MetAPs serve to remove the N-terminal methionine residue from proteins and peptides of at least three residues in length.[112] The removal of this methionine residue is crucial to the maturation of proteins allowing for proper function in all forms of life.[113] Two types of MetAP exist, Type I and Type II, they vary in the addition of an extra catalytic domain in MetAP2. In bacteria, eukaryotes contain both types of MetAP, where as eubacteria and archaea only have one, MetAP1 and MetAP2, respectively. In mammals, homologs of both classes are necessary for cell proliferation.[112,113] All forms of the MetAP possess a dinuclear active site with two metal ions that catalyze activity.[111] Inhibitors of this enzyme are of interest for their potential as anticancer and antibacterial agents. MetAP in bacteria is encoded by a single gene and is essential for bacterial survival; deletion of this gene in *Escherichia coli* and *Salmonella typhimurium* have shown to be lethal.[112,113] It is proposed that a majority of bacteria rely on MetAP to modify nascent proteins and thus the development of inhibitors could produce novel broad-spectrum antibiotics.

MetAP can be activated by numerous metals including: Cu(II), Co(II) Ni(II), Mn(II) and Fe(II). With such a range of metals there has been much debate in regards to which metal ion(s) is/are physiologically relevant in bacteria.[111,112] Traditionally, Co(II) has been used for in vitro studies as this metal has proven to highly activate purified apo-MetAP. Recently it has been suggested that using Co(II) for inhibitor discovery assays may be the wrong choice. Many instances have occurred in which potent in vitro inhibitors (in the presence of Co(II)), show little to no efficacy when evaluated in cell-based assays.[114,115] The work of Ye and coworkers strongly suggest that Fe(II) may be the physiologically relevant metal in *E.coli* MetAP-I.[115] Using a HTS approach Ye was able to identify metalloform specific scaffolds exclusive to either Co(II), Mn(II) or Fe(II) forms.

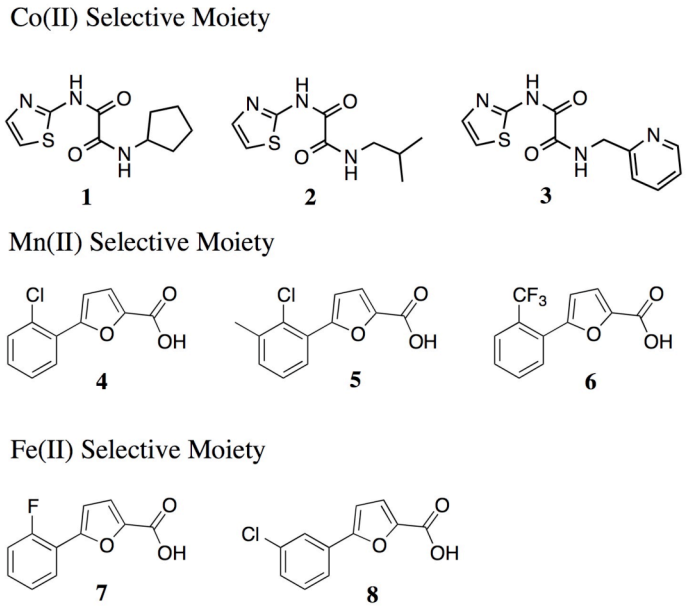

Figure 1.16 Structures and IC_{50} values of the metalloform specific inhibitors of *Ec*MetAP-1. From top to bottom selective scaffolds for Co(II), Mn(II) and Fe(II).[115]

Table 1.1 IC_{50} Values of Metalloform-Selective Inhibitors of *Ec*MetAP-1.[115]

Inhibitor	IC_{50} Values (μM)		
	Co(II)	Mn(II)	Fe(II)
1	0.067	53	46
2	0.28	108	118
3	0.073	54	65
4	154	0.24	182
5	69	0.96	>200
6	73	0.063	195
7	198	14	>200
8	193	19	>200

As illustrated in Figure 1.16 and Table 1.1, the three unique metal-binding scaffolds are selective for different metalloforms of *Ec*MetAP-1, allowing researchers to pinpoint which form(s) are found in the naturally occurring bacteria. The selective scaffolds were introduced to *E.coli* systems and bacterial growth was monitored. It was observed that only bacteria grown in the presence of the Fe(II) specific scaffolds demonstrated a loss in bacterial growth.[114-116] Such results indicate that the physiologically relevant metal of this enzyme is the Fe(II) form. As suspected, this may be the root cause of many failed attempts to create potent in vivo MetAP inhibitors, particularly when those studied in vitro were conducted on the Co(II) form.[118] This HTS approach led to the discovery of both potent and selective inhibitors of MetAP. Additionally, work by the Ye group illustrates the structural similarities between two of the metalloforms (Co(II) and Mn(II)). Even though the two metalloforms have near identical active site environments, compound **4** is >600-fold more potent towards the Mn(II), while compound **1** is ~800-fold more selective for the Co(II) form. Further studies will need to be conducted to fully comprehend the basis for the selectivity of

these compounds. It is quite apparent though, that the metal ion cofactor plays an important role in dictating the types of potent inhibitors.

1. D. Conclusions

This Chapter sought to introduce the concepts and processes by which FBLD can be employed to develop new drugs. While this strategy is relatively new and does not compete with the volume of successful compounds to come out of more traditional drug discovery methods such as HTS, there are distinct advantages to FBLD. Better use of chemical space, more efficient screening compounds and the ability to be adapted to research labs of all sizes (in respect to capacity and resources) are just a few of the advantages of FBLD. The screening methods and fragment development techniques utilized in a FBLD approach were also discussed. A synopsis of a FBLD clinical success story helped to validate the claims that this approach is a viable method to drug discovery. The properties that make metalloenzymes ideal for FBLD targets were also presented. The metal ion cofactors in these enzymes are essential to enzymatic activity and present an ideal tethering point for fragments. Lastly, a number of metalloenzymes, which can be used to investigate potential fragments for inhibitor design were presented. The function, structure, current inhibitors and potential applications for the design of new inhibitors were discussed.

1. E. References

(1) Congreve, M.; Chessari, G.; Tisi, D.; Woodhead, A. J. *J. Med. Chem.* **2008**, *51*, 3661-3680.

(2) Leach, A. R.; Hann, M. M.; Burrows, J. N.; Griffen, E. J. *Mol. Biosyst.* **2006**, *2*, 429-446.

(3) Carr, R. A. E.; Congreve, M.; Murray, C. W.; Rees, D. C. *Drug Discov. Today* **2005**, *10*, 987-992.

(4) Maly, D. J.; Choong, I. C.; Ellman, J. A. *Proc. Natl. Acad. Sci. USA* **2000**, *97*, 2419-2424.

(5) Lipinski, C. A. *Drug Discov. Today Technol.* **2004**, *1*, 337-341.

(6) Lipinski, C. A.; Lombardo, F.; Dominy, B. W.; Feeney, P. J. *Adv. Drug Deliv. Rev.* **2001**, *46*, 3-26.

(7) Veber, D. F.; Johnson, S. R.; Cheng, H.-Y.; Smith, B. R.; Ward, K. W.; Kopple, K. D. *J. Med. Chem.* **2002**, *45*, 2615-2623.

(8) Oprea, T. I.; Davis, A. M.; Teague, S. J.; Leeson, P. D. *J. Chem. Inf. Comput. Sci.* **2001**, *41*, 1308-1315.

(9) Jencks, W. P. *Proc. Natl. Acad. Sci. USA* **1981**, *78*, 4046-4050.

(10) Hajduk, P. J.; Sheppard, G.; Nettesheim, D. G.; Olejniczak, E. T.; Shuker, S. B.; Meadows, R. P.; Steinman, D. H.; Carrera Jr., G. M.; Marcotte, P. A.; J, S.; Walter, K.; Smith, H.; Gubbins, E.; Simmer, R.; Holzman, T. F.; Morgan, D. W.; Davidsen, S. K.; Summers, J. B.; Fesik, S. W. *J. Am. Chem. Soc.* **1997**, *119*, 5818-5827.

(11) Blundell, T. L.; Jhoti, H.; Abell, C. *Nat. Rev. Drug Disocv.* **2002**, *1*, 45-54.

(12) Hann, M. M.; Leach, A. R.; Harper, G. *J. Chem. Inf. Comput. Sci.* **2001**, *41*, 856-864.

(13) Carr, R.; Jhoti, H. *Drug Discov. Today* **2002**, *7*, 522-527.

(14) Lipinski, C.; Hopkins, A. *Nature* **2004**, *432*, 855-861.

(15) Teague, S. J.; Davis, A. M.; Leeson, P. D.; Oprea, T. *Angew. Chem. Int. Ed.* **1999**, *38*, 3743-3748.

(16) Agrawal, A.; Johnson, S. L.; Jacobsen, J. A.; Miller, M. T.; Chen, L.-H.; Pellecchia, M.; Cohen, S. M. *ChemMedChem* **2010**, *5*, 195-199.

(17) Pellecchia, M.; Bertini, I.; Cowburn, D.; Dalvit, C.; Giralt, E.; Jahnke, W.; James, T. L.; Homans, S. W.; Kessler, H.; Luchinat, C.; Meyer, B.; Oschkinat, H.; Peng, J.; Schwalbe, H.; Siegal, G. *Nat. Rev. Drug Disocv.* **2008**, *7*, 738-745.

(18) Shuker, S. B.; Hajduk, P. J.; Meadows, R. P.; Fesik, S. W. *Science* **1996**, *274*, 1531-1534.

(19) Kuhn, P.; Wilson, K.; Patch, M. G.; Stevens, R. C. *Curr. Opin. Chem. Biol.* **2002**, *6*, 704-710.

(20) Nakamura, C. E.; Abeles, R. H. *Biochemistry* **1985**, *24*, 1364-1376.

(21) Lewell, X. Q.; Judd, D. B.; Watson, S. P.; Hann, M. M. *J. Chem. Inf. Comput. Sci.* **1998**, *38*, 511-522.

(22) Erlanson, D. A.; McDowell, R. S.; O'Brien, T. *J. Med. Chem.* **2004**, *47*, 3463-3482.

(23) Esposito, E. X.; Baran, K.; Kelly, K.; Madura, J. D. *J. Mol. Graphics Modell.* **2000**, *18*, 283-289.

(24) Irwin, J. J.; Raushel, F. M.; Shoichet, B. K. *Biochemistry* **2005**, *44*, 12316-12328.

(25) Menikarachchi, L. C.; Gasicn, J. A. *Curr. Top. Med. Chem.* **2009**, *10*, 46-54.

(26) Perspicace, S.; Banner, D.; Benz, J. r.; M√ºller, F.; Schlatter, D.; Huber, W. *J. Biomol. Screen.* **2009**, *14*, 337-349.

(27) Nordstroàm, H.; Gossas, T.; Haàmaàlaàinen, M.; Kaàllblad, P.; Nystroàm, S.; Wallberg, H.; Danielson, U. H. *J. Med. Chem.* **2008**, *51*, 3449-3459.

(28) Neumann, T.; Junker, H.; Schmidt, K.; Sekul, R. *Curr. Top. Med. Chem.* **2007**, *7*, 1630-1642.

(29) Schade, M.; Oschkinat, H. *Curr. Opin. Drug Discov. Devel.* **2005**, *8*, 365.

(30) Leach, A. R.; Hann, M. M.; Burrows, J. N.; Griffen, E. J. *Mol. Biosyst.* **2006**, *2*, 429-446.

(31) McGovern, S. L.; Helfand, B. T.; Feng, B.; Shoichet, B. K. *J. Med. Chem.* **2003**, *46*, 4265-4272.

(32) Bleicher, K. H.; Buhm, H.-J.; Muller, K.; Alanine, A. I. *Nat. Rev. Drug Disocv.* **2003**, *2*, 369-378.

(33) Ramstradm, O.; Lehn, J.-M. *Nat. Rev. Drug Disocv.* **2002**, *1*, 26-36.

(34) Rees, D. C.; Congreve, M.; Murray, C. W.; Carr, R. *Nat. Rev. Drug Disocv.* **2004**, *3*, 660-672.

(35) Baker, M. *Nat. Rev. Drug Disocv.* **2013**, *12*, 5-7.

(36) Bollag, G.; Hirth, P.; Tsai, J.; Zhang, J.; Ibrahim, P. N.; Cho, H.; Spevak, W.; Zhang, C.; Zhang, Y.; Habets, G.; Burton, E. A.; Wong, B.; Tsang, G.; West, B. L.; Powell, B.; Shellooe, R.; Marimuthu, A.; Nguyen, H.; Zhang, K. Y. J.; Artis, D. R.; Schlessinger, J.; Su, F.; Higgins, B.; Iyer, R.; D/'Andrea, K.; Koehler, A.; Stumm, M.; Lin, P. S.; Lee, R. J.; Grippo, J.; Puzanov, I.; Kim, K. B.; Ribas, A.; McArthur, G. A.; Sosman, J. A.; Chapman, P. B.; Flaherty, K. T.; Xu, X.; Nathanson, K. L.; Nolop, K. *Nature* **2010**, *467*, 596-599.

(37) Tsai, J.; Lee, J. T.; Wang, W.; Zhang, J.; Cho, H.; Mamo, S.; Bremer, R.; Gillette, S.; Kong, J.; Haass, N. K.; Sproesser, K.; Li, L.; Smalley, K. S. M.; Fong, D.; Zhu, Y.-L.; Marimuthu, A.; Nguyen, H.; Lam, B.; Liu, J.; Cheung, I.; Rice, J.; Suzuki, Y.; Luu, C.; Settachatgul, C.; Shellooe, R.; Cantwell, J.; Kim, S.-H.; Schlessinger, J.; Zhang, K. Y. J.; West, B. L.; Powell, B.; Habets, G.; Zhang, C.; Ibrahim, P. N.; Hirth, P.; Artis, D. R.; Herlyn, M.; Bollag, G. *Proc. Natl. Acad. Sci. USA* **2008**, *105*, 3041-3046.

(38) Jacobsen, F. E.; Lewis, J. A.; Cohen, S. M. *J. Am. Chem. Soc.* **2006**, *128*, 3156-3157.

(39) Jacobsen, J. A.; Jourden, J. L. M.; Miller, M. T.; Cohen, S. M. *Biochim. Biophys. Acta* **2010**, *1803*, 72-94.

(40) Muri, E. M. F.; Nieto, M. J.; Sindelar, R. D.; Williamson, J. S. *Curr. Med. Chem.* **2002**, *9*, 1631-1653.

(41) Puerta, D. T.; Cohen, S. M. *Inorg. Chem.* **2002**, *41*, 5075-5082.

(42) Puerta, D. T.; Cohen, S. M. *Inorg. Chem.* **2003**, *42*, 3423-3430.

(43) Puerta, D. T.; Lewis, J. A.; Cohen, S. M. *J. Am. Chem. Soc.* **2004**, *126*, 8388-8389.

(44) Puerta, D. T.; Schames, J. R.; Henchman, R. H.; McCammon, J. A.; Cohen, S. M. *Angew. Chem. Int. Ed.* **2003**, *42*, 3772-3774.

(45) Lu, Y. *Inorg. Chem.* **2006**, *45*, 9930-9940.

(46) McRae, R.; Bagchi, P.; Sumalekshmy, S.; Fahrni, C. J. *Chem. Rev.* **2009**, *109*, 4780-4827.

(47) Jarcho, S. *Am. J. Cardiol.* **1958**, *2*, 507-508.

(48) Ludwiczek, S.; Theurl, I.; Bahram, S.; Schümann, K.; Weiss, G. *J. Cell. Physiol.* **2005**, *204*, 489-499.

(49) Dive, V.; Chang, C.-F.; Yiotakis, A.; Sturrock, E. D. *Curr. Pharm. Des.* **2009**, *15*, 3606-3621.

(50) Agrawal, A.; Romero-Perez, D.; Jacobsen, J. A.; Villarreal, F. J.; Cohen, S. M. *ChemMedChem* **2008**, *3*, 812-820.

(51) Rao, B. G. *Curr. Pharm. Des.* **2005**, *11*, 295-322.

(52) Cuniasse, P.; Devel, L.; Makaritis, A.; Beau, F.; Georgiadis, D.; Matziari, M.; Yiotakis, A.; Dive, V. *Biochimie* **2005**, *87*, 393-402.

(53) Overall, C. M.; Kleifeld, O. *Br. J. Cancer* **2006**, *94*, 941-946.

(54) Coussens, L. M.; Fingleton, B.; Matrisian, L. M. *Science* **2002**, *295*, 2387-2392.

(55) Uchida, M.; Shima, M.; Shimoaka, T.; Fujieda, A.; Obara, K.; Suzuki, H.; Nagai, Y.; Ikeda, T.; Yamato, H.; Kawaguchi, H. *J. Cell. Physiol.* **2000**, *185*, 207-214.

(56) Nagase, H.; Visse, R.; Murphy, G. *Cardiovasc. Res.* **2006**, *69*, 562-573.

(57) Nuti, E.; Tuccinardi, T.; Rossello, A. *Curr. Pharm. Des.* **2007**, *13*, 2087-2100.

(58) Dollery, C. M.; McEwan, J. R.; Henney, A. M. *Circ. Res.* **1995**, *77*, 863-868.

(59) Hidalgo, M.; Eckhardt, S. G. *J. Natl. Cancer Inst.* **2001**, *93*, 178-193.

(60) Brown, P.; Giavazzi, R. *Ann. Oncol.* **1995**, *6*, 967-974.

(61) Flipo, M.; Charton, J.; Hocine, A.; Dassonneville, S.; Deprez, B.; Deprez-Poulain, R. *J. Med. Chem.* **2009**, *52*, 6790-6802.

(62) Chen, L.; Rydel, T. J.; Gu, F.; Dunaway, C. M.; Pikul, S.; Dunham, K. M.; Barnett, B. L. *J. Mol. Biol.* **1999**, *293*, 545-557.

(63) Tonello, F.; Montecucco, C. *Mol. Aspects Med.* **2009**, *30*, 431-438.

(64) Hammond, S.; Hanna, P. *Infect. Immun.* **1998**, *66*, 2374-2378.

(65) Burnett, J. C.; Henchal, E. A.; Schmaljohn, A. L.; Bavari, S. *Nat. Rev. Drug Discov.* **2005**, *4*, 281-297.

(66) Moayeri, M.; Leppla, S. H. *Curr. Opin. Microbiol.* **2004**, *7*, 19-24.

(67) Collier, R. J.; Young, J. A. *Annu. Rev. Cell Dev. Biol.* **2003**, *19*, 45-70.

(68) Abrami, L.; Reig, N.; van der Goot, F. G. *Trends Microbiol.* **2005**, *13*, 72-78.

(69) Agrawal, A.; de Oliveira, C. A. F.; Cheng, Y.; Jacobsen, J. A.; McCammon, J. A.; Cohen, S. M. *J. Med. Chem.* **2009**, *52*, 1063-1074.

(70) Johnson, S. L.; Chen, L.-H.; Barile, E.; Emdadi, A.; Sabet, M.; Yuan, H.; Wei, J.; Guiney, D.; Pellecchia, M. *Bioorg. Med. Chem.* **2009**, *17*, 3352-3368.

(71) Lewis, J. A.; Mongan, J.; McCammon, J. A.; Cohen, S. M. *ChemMedChem* **2006**, *1*, 694-697.

(72) Stover, C.; Pham, X.; Erwin, A.; Mizoguchi, S.; Warrener, P.; Hickey, M.; Brinkman, F.; Hufnagle, W.; Kowalik, D.; Lagrou, M. *Nature* **2000**, *406*, 959-964.

(73) Mesaros, N.; Nordmann, P.; Plesiat, P.; Roussel-Delvallez, M.; Van Eldere, J.; Glupczynski, Y.; Van Laethem, Y.; Lebecque, P.; Malfroot, A.; Tulkens, P. M.; Van Bambeke, F. *Clin. Microbiol. Infect.* **2007**, *13*, 560-578.

(74) Breidenstein, E. B. M.; de la Fuente-Nunez, C.; Hancock, R. E. W. *Trends Microbiol.* **2011**, *19*, 419-426.

(75) Wretlind, B.; Pavlovskis, O. R. *Rev. Infect. Dis.* **1983**, *5*, S998-S1004.

(76) Kamath, S.; Kapatral, V.; Chakrabarty, A. M. *Mol. Microbiol.* **1998**, *30*, 933-941.

(77) Overhage, J.; Bains, M.; Brazas, M. D.; Hancock, R. E. W. *J. Bacteriol.* **2008**, *190*, 2671-2679.

(78) Woods, D. E.; Cryz, S. J.; Friedman, R. L.; Iglewski, B. H. *Infect. Immun.* **1982**, *36*, 1223-1228.

(79) Felise, H. B.; Nguyen, H. V.; Pfuetzner, R. A.; Barry, K. C.; Jackson, S. R.; Blanc, M.-P.; Bronstein, P. A.; Kline, T.; Miller, S. I. *Cell Host Microbe* **2008**, *4*, 325-336.

(80) Grobelny, D.; Poncz, L.; Galardy, R. E. *Biochemistry* **1992**, *31*, 7152-7154.

(81) Cathcart, G. R.; Gilmore, B. F.; Greer, B.; Harriott, P.; Walker, B. *Bioorg. Med. Chem. Lett.* **2009**, *19*, 6230-6232.

(82) Cathcart, G. R.; Quinn, D.; Greer, B.; Harriott, P.; Lynas, J. F.; Gilmore, B. F.; Walker, B. *Antimicrob. Agents Chemother.* **2011**, *55*, 2670-2678.

(83) Kessler, E.; Israel, M.; Landshman, N.; Chechick, A.; Blumberg, S. *Infect. Immun.* **1982**, *38*, 716-723.

(84) Nishino, N.; Powers, J. C. *J. Biol. Chem.* **1980**, *255*, 3482-3486.

(85) Thayer, M. M.; Flaherty, K. M.; McKay, D. B. *J. Biol. Chem.* **1991**, *266*, 2864-2871.

(86) Werz, O.; Steinhilber, D. *Pharmacol. Ther.* **2006**, *112*, 701-718.

(87) Samuelsson, B.; Dahlen, S. E.; Lindgren, J. A.; Rouzer, C. A.; Serhan, C. N. *Science* **1987**, *237*, 1171-1176.

(88) Peters-Golden, M.; Canetti, C.; Mancuso, P.; Coffey, M. J. *J. Immunol.* **2005**, *174*, 589-594.

(89) Hite, G. A.; Mihelich, E. D.; Suarez, T.; Google Patents: 1991.

(90) Israel, E.; Cohn, J.; Dubum, L.; Drazen, J. M.; Ratner, P.; Pleskow, W.; DeGraff Jr, A.; Chervinsky, P.; Wasserman, S.; Nelson, H. *J. Am. Med. Assoc.* **1996**, *275*, 931-936.

(91) Young, R. N. *Eur. J. Med. Chem.* **1999**, *34*, 671-685.

(92) Kim, Y.-J.; Uyama, H. *Cell. Mol. Life Sci.* **2005**, *62*, 1707-1723.

(93) Sanchez-Ferrer, A.; Rodreguez-Lopez, J. N.; Garcia-Cnovas, F.; Garcia-Carmona, F. *Biochim. Biophys. Acta* **1995**, *1247*, 1-11.

(94) Kaplan, J.; De Domenico, I.; Ward, D. M. *Curr. Opin. Hematol.* **2008**, *15*, 22-29

(95) Hearing, V.; Ekel, T. *Biochem. J* **1976**, *157*, 549.

(96) Jaenicke, E.; Decker, H. *Biochem. J.* **2003**, *371*, 515-523.

(97) Lewis, E. A.; Tolman, W. B. *Chem. Rev.* **2004**, *104*, 1047-1076.

(98) Seo, S.-Y.; Sharma, V. K.; Sharma, N. *J. Agric. Food. Chem.* **2003**, *51*, 2837-2853.

(99) Espin, J. C.; Wichers, H. J. *J. Agric. Food. Chem.* **1999**, *47*, 2638-2644.

(100) Liu, J.; Yi, W.; Wan, Y.; Ma, L.; Song, H. *Bioorg. Med. Chem.* **2008**, *16*, 1096-1102.

(101) Mangili, A.; Murman, D.; Zampini, A.; Wanke, C.; Mayer, K. H. *Clin. Infect. Dis.* **2006**, *42*, 836-842.

(102) Paterson, D. L.; Swindells, S.; Mohr, J.; Brester, M.; Vergis, E. N.; Squier, C.; Wagener, M. M.; Singh, N. *Ann. Intern. Med.* **2000**, *133*, 21-30.

(103) Friedland, G. H.; Williams, A. *AIDS* **1999**, *13*, S61-S72.

(104) De Cock, K. M.; Fowler, M. G.; Mercier, E.; de Vincenzi, I.; Saba, J.; Hoff, E.; Alnwick, D. J.; Rogers, M.; Shaffer, N. *J. Am/ Med. Assoc.* **2000**, *283*, 1175-1182.

(105) Hazuda, D. J.; Felock, P.; Witmer, M.; Wolfe, A.; Stillmock, K.; Grobler, J. A.; Espeseth, A.; Gabryelski, L.; Schleif, W.; Blau, C. *Science* **2000**, *287*, 646-650.

(106) Craigie, R. *J. Biol. Chem.* **2001**, *276*, 23213-23216.

(107) Chiu, T. K.; Davies, D. R. *Curr. Top. Med. Chem.* **2004**, *4*, 965-977.

(108) Leavitt, A.; Shiue, L.; Varmus, H. *J. Biol. Chem.* **1993**, *268*, 2113-2119.

(109) Hare, S.; Vos, A. M.; Clayton, R. F.; Thuring, J. W.; Cummings, M. D.; Cherepanov, P. *Proc. Natl. Acad. Sci. USA s* **2010**, *107*, 20057-20062.

(110) Grobler, J. A.; Stillmock, K.; Hu, B.; Witmer, M.; Felock, P.; Espeseth, A. S.; Wolfe, A.; Egbertson, M.; Bourgeois, M.; Melamed, J. *Proc. Natl. Acad. Sci. USA* **2002**, *99*, 6661-6666.

(111) Pommier, Y.; Johnson, A. A.; Marchand, C. *Nat. Rev. Drug Discov.* **2005**, *4*, 236-248.

(112) Marchand, C.; Maddali, K.; Métifiot, M.; Pommier, Y. *Curr. Top. Med. Chem.* **2009**, *9*, 1016-1037.

(113) Christ, F.; Voet, A.; Marchand, A.; Nicolet, S.; Desimmie, B. A.; Marchand, D.; Bardiot, D. e.; Van der Veken, N. J.; Van Remoortel, B.; Strelkov, S. V. *Nat. Chem. Biol.* ***2007***, *6*, 442-448.

(114) Metifiot, M.; Maddali, K.; Naumova, A.; Zhang, X. M.; Marchand, C.; Pommier, Y. *Biochemistry* **2010**, *49*, 3715-3722.

(115) Lowther, W. T.; Matthews, B. W. *Biochim. Biophys. Acta* **2000**, *1477*, 157-167.

(116) Vaughan, M. D.; Sampson, P. B.; Honek, J. F. *Curr. Med. Chem.* **2002**, *9*, 385-409.

(117) Bradshaw, R. A.; Brickey, W. W.; Walker, K. W. *Trends Biochem. Sci.* **1998**, *23*, 263-267.

(118) Li, J.-Y.; Chen, L.-L.; Cui, Y.-M.; Luo, Q.-L.; Li, J.; Nan, F.-J.; Ye, Q.-Z. *Biochem. Biophys. Res. Commun.* **2003**, *307*, 172-179.

(119) Wang, W.-L.; Chai, S. C.; Huang, M.; He, H.-Z.; Hurley, T. D.; Ye, Q.-Z. *J. Med. Chem.* **2008**, *51*, 6110-6120.

(120) Chai, S. C.; Ye, Q.-Z. *Bioorg. Med. Chem. Lett.* **2009**, *19*, 6862-6864.

2 Identifying Chelators for Metalloprotein Inhibitors Using a Fragment-Based Approach

2. A. Introduction

As described in Chapter 1, metalloenzymes makeup at least one-third of all proteins and utilize a wide variety of metal ion cofactors for many critical roles.[41] Inhibitors of these enzymes are useful for mechanistic studies, pesticides, preservatives, cosmetics, as well as a wide range of therapeutics.[117-121] Pathogenic metalloenzyme activity has been linked to a number of disease states including cancer, inflammatory, infectious, cardiovascular, and neurodegenerative diseases.[45,50,61,122-130] The presence of a metal ion cofactor in these enzymes has frequently been exploited for the development of synthetic inhibitors, typically as a point to anchor compounds to the active site and thereby block catalytic activity.[34] Metalloenzyme inhibitor discovery has resulted in the identification of metal-binding groups (MBGs) for these inhibitors. The ultimate goal of fragment studies of MBGs is to explore how the MBGs can influence potency, selectivity and stability in inhibitors to better utilize these functional groups in drug design.[34,46,131,132] The work presented in this chapter describes the first steps in the identification of MBGs for use as metalloenzyme chelating inhibitors.

Fragment-based lead discovery (FBLD) is a drug design approach where low molecular weight compounds (fragments) are evaluated against drug targets of interest. Binding fragments are further developed to generate potent leads, these leads should have good ligand efficiencies (LE); a measurement used to compare compound potency as a function of molecular size. LE is defined by the formula: $LE = -RT(\ln[IC_{50}])/HAC$, in which IC_{50} is the fragment concentration at which enzyme activity is reduced 50% and HAC is the heavy atom (or non-hydrogen atom) count.[12,133] Several studies have applied

FBLD to the development of metalloenzyme inhibitors; however, variations in the MBG scaffold have rarely been the focus of such investigations.[134,135]

Simple metal chelators are well suited to be employed as fragments for FBLD. Several have known binding affinities to a number of metal ions, (typically with K_d values in the micro- to milli-molar range), and are commercial available and/or easy to synthesize. Fragments that have micromolar binding constants would be readily detected using bioassays, making chelator fragments more easily screened then other fragments that have been used in FBLD.[1] Furthermore, the binding mode of chelators may be modeled by synthetic complexes that mimic metalloenzyme active sites or may be inferred from available crystallographic data of the chelator bound to the metal of interest.[37,38,40,136] Because of the availably of such structural data, other structural analysis (e.g. macromolecular cyrstallography or NMR), may not be as essential when developing inhibitors from a chelator fragment. In this Chapter, the use of FBLD to identify new MBGs for metalloenzyme inhibitors will be described. An initial chelator fragment library (CFL-1.1) of 96 metal chelators (Figure 2.1) was assembled and screened against a panel of metalloenzymes in order to probe its use as a tool to generate new MBGs for a wide range of metalloenzymes. This Chapter also demonstrates the advancement of a hit from the library to produce focused libraries against MMP-2 based on an 8-hydroxyquinoline-fragment scaffold. Lastly, Chapter 1 introduces the study of CFL-1.1 against the dinuclear metalloenzyme, methionine aminopeptidase (MetAP), an enzyme that will allow for numerous metal ion cofactors to be explored in the same enzymatic environment. The findings presented show that chelator fragment libraries are a viable approach to the discovery of metalloprotein inhibitors.

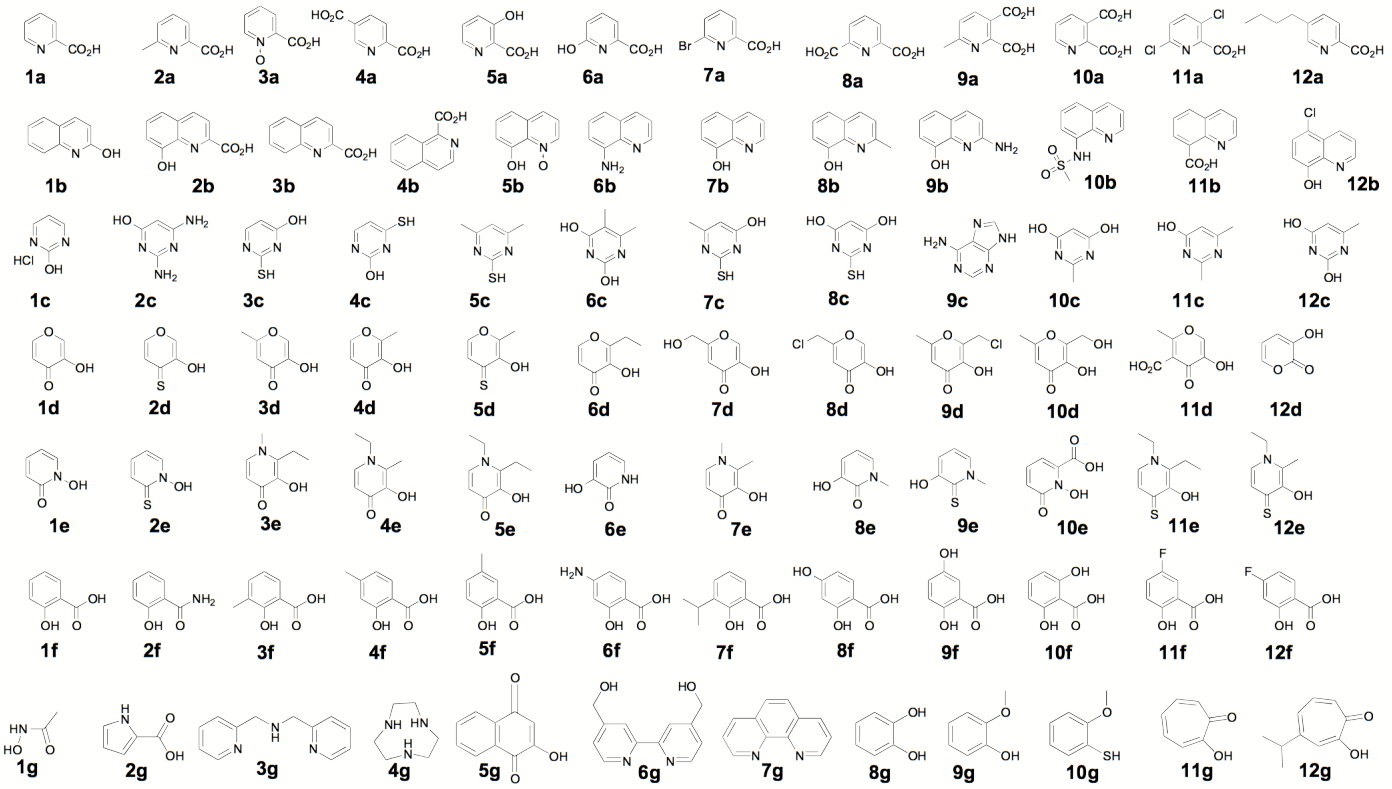

Figure 2.1 Structures of the compounds in CFL-1.1, the library is organized by MBG. Picolinic acids (**1a-12a)**, quinolines (**1b-12b**), pyrimidines (**1c-12c**), hydroxyprones (**1d-12d**), hydroxypyridinones (**1e-12e**), and salicylic acids (**1d-12f**). The remaining compounds **1g-12g** and **1h-12h** are classified as miscellaneous chelators.

2. B. Design and Evaluation of CFL-1.1

Initial designs for the library consisted of fragments with low molecular weights, (<200 amu) that possessed 2-4 nitrogen, oxygen, and/or sulfur donor atoms.[12] This chelator fragment library (CFL-1, not shown) was amended, to the current version, CFL-1.1 (Figure 2.1). While the overall structure and design of the two libraries remains constant, 5 compounds (**6b**, **10b**, **7e**, **7f**, and **2h**) were switched out to form CFL-1.1. These alterations were primarily to correct for solubility and stability issues observed in the CFL-1 compounds.[137] CFL-1.1 contains a total of 96 fragments representing six metal-binding classes including picolinic acids, quinolines, pyrimidines, hydroxypyrones, hydroxypyridinones, salicylic acids, and 24 miscellaneous compounds. All the fragments are soluble up to 50 mM in dimethyl sulfoxide (DMSO) and are commercially available or readily synthesized.[38,46,138-142]

CFL-1.1 was initially screened against MMP-1, MMP-2, MMP-3, MMP-8, MMP-9, anthrax lethal factor (LF), 5-lipoxygenase (5-LO), mushroom tyrosinsase (TY), and nitric oxide synthase (iNOS) to identify potent fragments against each enzyme. Later, two metalloforms of *E. coli* methionine aminopeptidase type 1 (*Ec*MetAP-1 metalated with Co(II) and Mn(II)) were investigated to determine if fragments had a preference towards a specific metal ion under identical enzymatic conditions. The screenings consisted of treating the enzymes with 1 mM (50 μM in *Ec*MetAP-1) of each fragment and monitoring the percent enzymatic activity to determine inhibition. Results of the screenings are depicted in heat plots representing the percent inhibition of the fragments against the respective metalloenzyme (Figure 2.2, Figure 2.8, and Figure 2.9). Hits were arbitrarily defined as fragments that inhibit a specific enzyme activity by greater than

50% of enzyme activity at 1 mM of fragment. After the initial screening, IC_{50} values of certain hits were determined (for MMP-2, LF, 5-LO, and TY) and the corresponding LEs were calculated (Table 2.1).

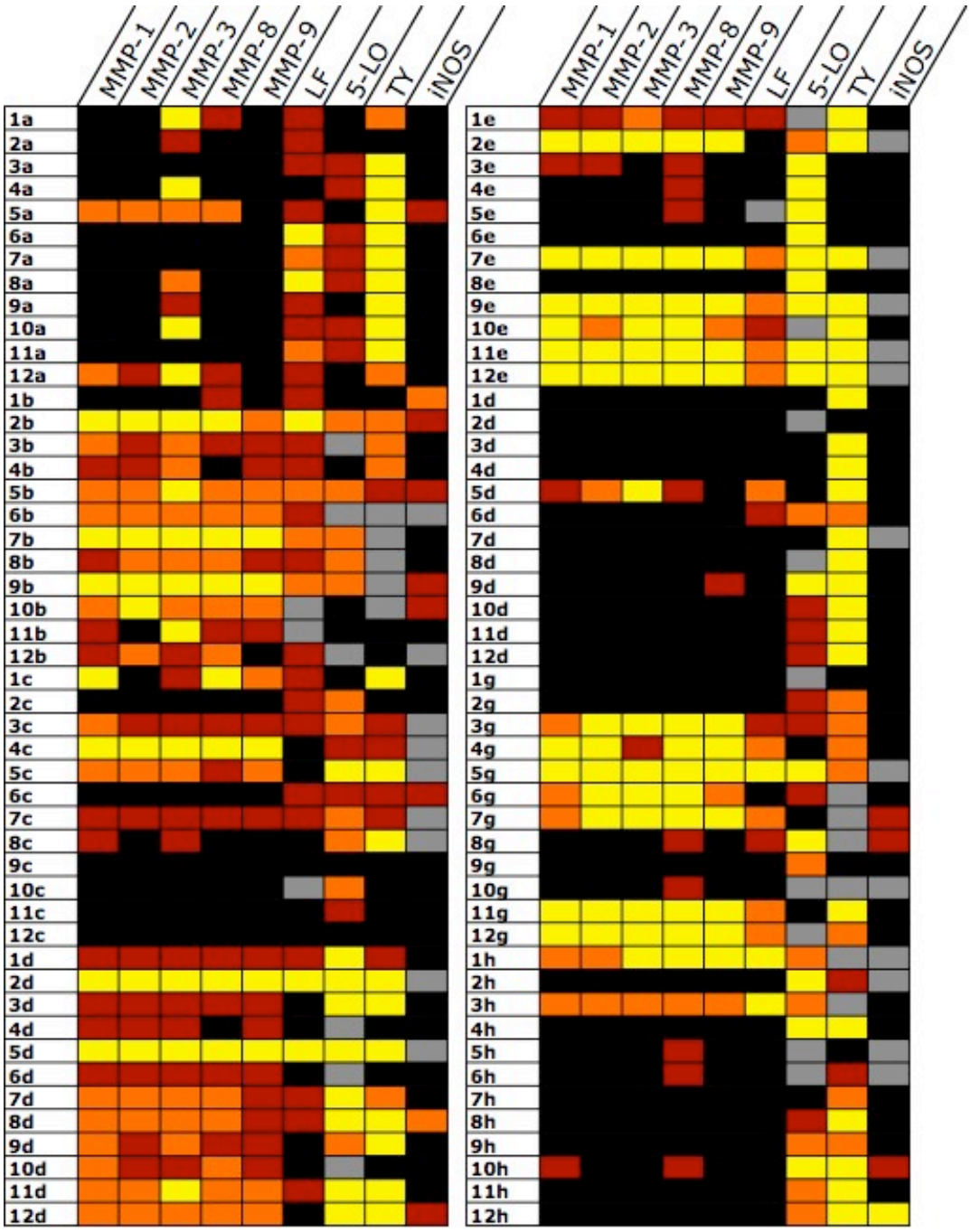

Figure 2.2 Heat plot representing the results from the screens of CFL-1.1 against the listed metalloenzymes. Cells are color-coded by percent inhibition: black (0-25%), red (25-50%), orange (51-75%), and yellow (76-100%). Gray cells indicate compounds that interfered with the assay and were not used for data analysis.

2. C. 1. CFL-1.1 Results Against MMPs

CFL-1.1 produced a significant number of hits against MMP-1, MMP-2, MMP-3, MMP-8, and MMP-9 (Figure 2.2). The percent of fragments identified as hits (hit rate) ranged from 29-43% for the various MMPs. The 3-hydroxypicolinic acids decreased the activity of MMP-1, MMP-2, MMP-3, and MMP-8 by approximately 50%. Derivatives of 8-hydroxyquinoline (**2b**, **7b**, **8b**, and **9b**) strongly inhibited all five MMPs. In particular, 8-hydroxyquinoline (**7b**) was found to have an IC_{50} value of 130 μM against MMP-2. Two other quinolines stood out as MMP hits: 8-hydroxyquinoline–*N*-oxide (**5b**) and the sulfonamide quinoline (**10b**).

Two pyrimidines (**4c** and **5c**) were broad-spectrum MMP hits, with compound **4c** having an IC_{50} value of 121 μM against MMP-2. The sulfur-containing hydroxypyrothiones (**2d** and **5d**) completely inhibited all MMPs tested, while most of the hydroxypyrones (**1d**, **7d-11d**) showed approximately 50% inhibition. The IC_{50} value of hydroxypyrothione **2d** against MMP-2 was found to be 76 μM. The sulfur-containing hydroxypyridinethiones (**2e, 7e, 9e, 11e** and **12e**) also completely inhibit all the MMPs screened. Among the hydroxypyridinones only **1e** and **10e**, both of which are based on a 1,2-hydroxypyridinone core, exhibit an inhibition of greater than 50%. Within the miscellaneous fragment group two, tropolone fragments, **11g** and **12g**, were identified as hits. The remainder of the library did not produce any hits against the MMPs.

By comparing the inhibition of MMPs across a chelator class, information about binding mode can be inferred. The most potent quinolines (**2b**, **7b-9b**) are all substituted with a hydroxyl group at the 8-position. The similarities in structures and activities of these compounds support a conserved binding mode with the quinoline nitrogen and the

hydroxyl oxygen atoms chelating to the Zn(II) ion. Consistent with prior reports, ligands with O,S donor atoms (**2d**, **5d**, **2e**, **7e,** and **9e**) are more potent against MMPs than their structural analogs with O,O donor atoms (**1d**, **4d**, **1e,** and **8e**).[12,34,38,136] This can partially be attributed to the hard-soft acid-base interactions between the metal and the ligands.[143] For example, when compared with a harder Lewis acid metal, like Mg(II) in of HIV-1 IN (discussed in Chapter 3), the Zn(II) ion is a comparatively softer Lewis acid and hence prefers softer donor atoms like sulfur. As illustrated in Figure 2.2, compounds **1d** and **8e** (both contain O,O donor atoms) are weaker inhibitors of MMPs compared to their softer O,S donor ligand analogs (**2d** and **9e** respectively).

Overall the library did not produce any highly specific hits for a given MMP; fragments found a hit for one MMP were typically potent against all the MMPs tested. One notable exception was the activity of some picolinic acids against MMP-3. In general, the picolinic acids were not very active against the MMPs with the exception of MMP-3. MMP-3 was inhibited by six picolinic acids (**1a, 4a, 5a, 8a, 9a, 10a** and **12a**), and of these only **5a** and **12a** were found to show any significant activity against other MMPs. It should be noted that the enzymatic activity of MMP-3 is optimal at pH 6, where as most other MMPs, operate best at pH 7.4. This change in pH may be one factor that contributes to the difference in potency of the picolinic acids against this particular MMP. Compound **1a**, which does not come up as a hit against MMP-1, MMP-2, MMP-8, or MMP-9, was previously reported to have an IC_{50} value of 181 μM against MMP-3.[34] The identification of this isoform-specific MBG has potential to be developed into a selective inhibitor for MMP-3 antagonism. MMP-3 targeted compounds could be used as chemical probes to aid in elucidating the role MMP-3 plays in various illnesses, as well

as a potent therapeutic, possibly with fewer side-effects that are implicated for broad-rage MMPi.

As noted, most compounds found to be a hit against one MMP isoform tended to inhibit all of the MMPs tested (Figure 2.2). For small fragments this is not surprising, as the active site around the Zn(II) ion is highly conserved within the MMP family. Thus a small fragment with good binding affinity to the Zn(II) cofactor would not be likely to show selectivity for one MMP over another. Upon lead optimization of these fragments MMP specificity might be obtained.[46]

Table 2.1 Calculated IC_{50} values, heavy atom count, and ligand efficiency (LE) values for select hits from CFL-1.1.

Enzyme	Compound	IC_{50} Value (μM)	HAC	LE (kcal/mol)
MMP-2 [a]	**7b**	130±28	11	0.50
	4c	121±37	8	0.70
	2d	76±1	8	0.73
	1g	15,000	5	0.52
	11g	146±71	9	0.61
	3h	389±134	11	0.44
LF [b]	**2d**	204 [67]	8	0.63
	1g	11,400 [67]	5	0.53
5-LO [b]	**5d**	11±2	9	0.75
	9f	75±5	11	0.51
TY [b]	**6a**	159±28	10	0.52
	5d	3.8±0.5	9	0.82
	1f	100±9	10	0.55
	11g	0.4 [96]	9	0.97

[a] Ligand efficiency calculated at 37 °C; [b] Ligand efficiency calculated at 25 °C.

2. C. 2. Hits Against Other Metalloenzymes

CFL-1.1 was screened against several other metalloenzymes; these enzymes were chosen for their structural and functional diversity, as well as for their biomedical importance. The results are summarized in Figure 2.2, which indicate that there are enzyme-specific scaffolds from which it would be possible to develop metalloenzyme-specific inhibitors.

Screening of CFL-1.1, at a fragment concentration of 1 mM, against LF yielded 22 hits, giving a hit rate of 24%. In contrast to the MMPs, several of the picolinic acid fragments (**1a-3a**, **5a, 9a-11a**) inhibited LF activity ~50%. Three picolonic acids (**6a-8a**) inhibited LF >70%, all of which are substituted at the 6-position. Because both MMPs and LF contain Zn(II) in their active site, the picolinic acid hits further illustrates that a MBG can be specific to a given metalloenzyme even if they contain the same active site metal ion. Quinoline compounds **2b**, **5b**, **7b**, and **9b** were hits against LF. The hydroxypyrothiones (**2d** and **5d**) completely inhibit LF at 1 mM, while the hydroxypyridinethiones (**7e**, **9e**, **11e** and **12e**) inhibit LF activity ~50%. Fragment **2d** was previously reported to have an IC_{50} value of 204 μM against LF, consistent with the screening results obtained here.[67]

The hit rate of CFL-1.1 against the non-heme iron protein 5-LO was 49%. Again, the 8-hydroxyquinoline fragments (**2b, 7b-9b**) including 8-hydroxyquinoline-*N*-oxide (**5b**) hit against 5-LO. The calculated IC_{50} values of **5d** and **9f** were 11 and ~75 μM respectively. Unlike the Zn(II)-dependent enzymes (LF and MMPs) a number of pyrimidine, hydroxypyrone and hydroxypyridinone derivatives showed significant inhibition against 5-LO. Only some of these compounds contain a thiol at the 2-position.

5-LO was inhibited by both O,O and O,S chelators. 5-LO shows no preference between the two donor atom sets, reflecting Fe(III) resting oxidation state of 5-LO. The hard Lewis acid Fe(III) ion is also strongly inhibited by other hard Lewis base fragments such as catechols derivatives **8g** and **4h**.[143]

CFL-1.1 has a very high hit rate of 60% against Cu-dependent TY. One factor that may account for the indiscriminate potency of the chelators against TY is the dinuclear active site of this metalloenzyme.[144] MBG fragments may find more coordination modes that result in effective enzyme inhibition when two metal ions are available for binding. Several of the chelators identified from the screening of CFL-1.1 have been previously reported as inhibitors of TY including kojic acid (**7d**, IC_{50} 23 μM)[96] 1,2-hydroxypyridinone (**7e**, IC_{50} 1.2 μM)[145] and L-mimosine, an amino acid derivative of 3,4-hydroxypyridinones (**3e**-**5e**).[144] The IC_{50} values of maltol (**4d**) and several other hydroxypyridinones against TY have also been reported.[146] These reported compounds serve as internal standards for CFL-1.1. Confirmation of these fragments as hits against TY validates CFL-1.1 as a tool for the identification of potent MBGs of target enzymes. Interesting new chelator hits included some thiopyrones (**2d** and **5d**) and thiopyridinones (**2e**, **7e**, **9e**, **11e** and **12e**). Compound **5d** was found to have an IC_{50} value of ~4 μM against TY. Similar to the MMPs, the pyrones and pyridinones with O,S donor atoms are more potent against TY than the corresponding compounds with O,O donor atoms. However, like 5-LO, many O,O donor atom chelators did exhibit some inhibition against TY.

Finally, the screening of CFL-1.1 against the heme-iron protein iNOS yielded the lowest hit rate, 4% (only 3 out of 73 fragments). Several compounds had to be excluded

due to insolubility in the assay buffer. There are only 6 compounds that inhibit iNOS greater than 40% and these fragments cover nearly all the metal-binding classes represented in CFL-1.1. Overall, CFL-1.1 did not reveal specific patterns or new insight into the types of fragments that would hit against iNOS. A slight preference for oxygen containing binders was observed.

2. D. 1. 8-Hydroxyquinoline Sublibrary: Synthesis and Screening

In order to demonstrate: a) an ability to optimize and develop novel hits from CFL-1.1, and b) the versatility offered by new chelator scaffolds, a sublibrary of fragments was developed based on a single hit from CFL-1.1. The 8-hydroxyquinoline fragment **7b**, was selected as a MBG scaffold for the development of a small sublibrary in an effort to increase potency against MMP-2 (Figure 2.2). To the best of our knowledge, hydroxyquinolines have not been previously reported for use as a MBG in MMP inhibitors.[35,136,147] A focused library of 16 fragments based on 8-hydroxyquinoline was prepared by derivatizing this scaffold around the ring at positions 2-, 4-, 5-, and 7-. These four positions were selected in order to place substituents around the entire ring system, as well as for the synthetic accessibility of these particular sites. At each of the four positions an amine group was installed that was coupled with one of four different sulfonyl chlorides to generate sulfonamide derivatives (Figure 2.3). Substituents were loosely selected based on efficacy of previously reported MMP inhibitors.[6,148] The structure of one fragment (**72b**) was verified by X-ray crystallography (Figure 2.4 Table 2.2).

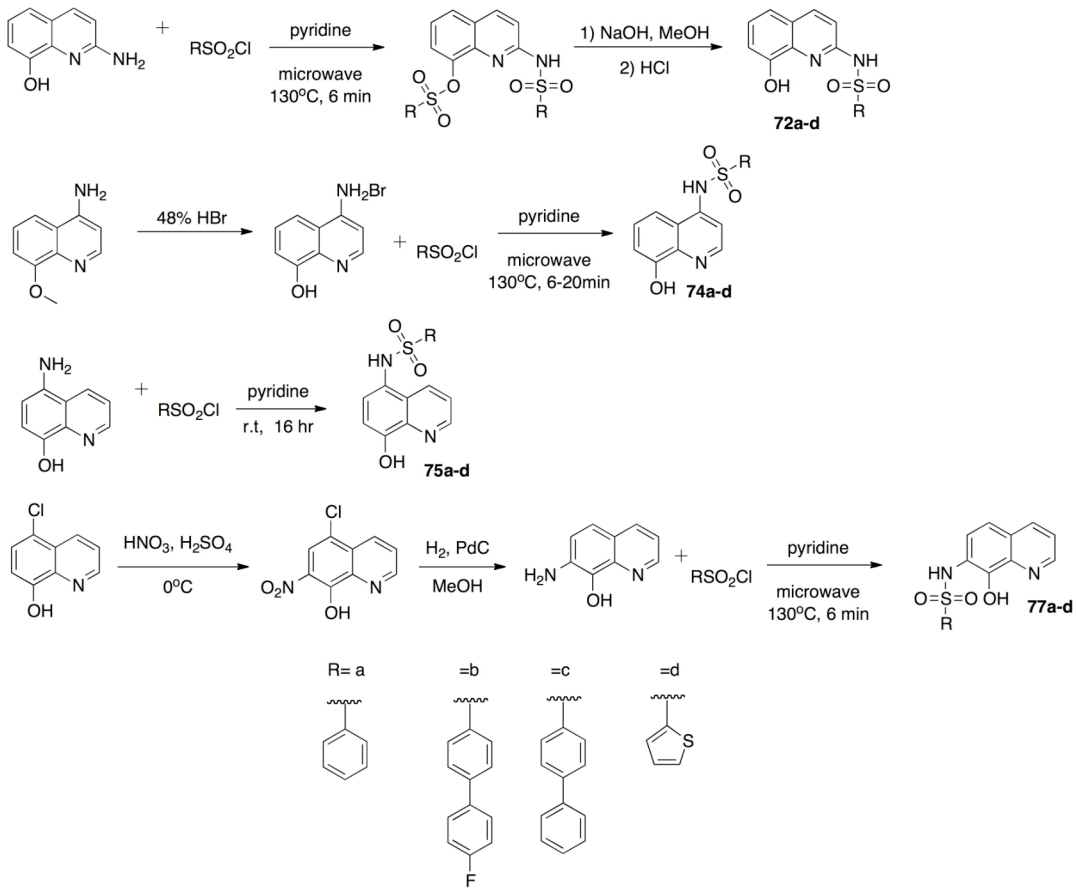

Figure 2.3 Synthesis of the 8-hydroxyquinoline sublibrary. Substituents were appended to four different positions (2-, 4-, 5-, and 7-positions) around the hydroxyquinoline ring. Phenyl (a), p-fluorophenyl (b), biphenyl (c), and thiophene (d) backbones were examined for a total of 16 fragments.

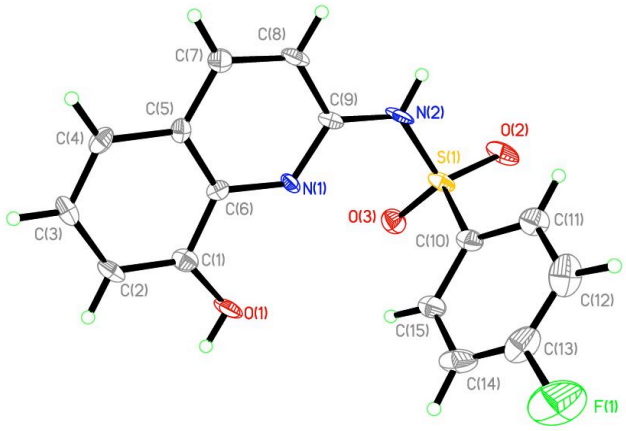

Figure 2.4 Crystal structure of 4-fluoro-N-(8-hydroxyquinolin-2-yl)benzenesulfonamide **(72b).**

Table 2.2 Crystal data and structure refinement for 4-fluoro-N-(8-hydroxyquinolin-2-yl)benzenesulfonamide **(72b)** crystal.

Empirical Formula	$C_{16}H_{19}NO_5S$	**Crystal Size**	0.5 x 0.3 x 0.1mm^3
Temperature	100 K	**Theta range for data collection**	1.47 to 25.84°
Crystal System	Triclinic	**Reflections collected**	11303
Space Group	P-1	**Independent reflections**	3071
Unit Cell Dimensions	a = 7.506 Å b = 7.910 Å c = 13.911 Å α = 86.552° β = 88.865° γ = 79.661°	**Data/restraints/parameters**	3071 / 3 / 220
		Goodness of fit on F2	1.044
		Final R indiceies I > 2	R1 = 0.0545 wR2 = 0.1395
Volume	811.0 Å^3	**R indicies (all data)**	R1 = 0.0598 wR2 = 0.1453
Z	2	**Largest diff peak and hole**	0.545 and -0.649 e Å-3
Density (calculated)	1.382 mg/m^3		

The 8-hydroxyquinoline focused sublibrary was initially screened against MMP-2 (as a representative metalloprotein target) at a concentration of 25 μM. The assay results

clearly show that the derivatives substituted at the 2- and 4-positions (**72a-d** and **74a-d)** are ineffective against MMP-2 (only **72c** has an IC_{50} value of ~48 μM). In contrast, the compounds substituted at the 5- and 7-positions (**75a-d** and **77a-d**) all showed greater than 65% inhibition of MMP-2, regardless of the specific R-group (Figure 2.5). The IC_{50} values of these compounds against MMP-2 were found to be in the low micromolar range. The best hit from this sub-library, **77b**, has an IC_{50} value of approximately 3 μM, representing a greater than 40-fold improvement over fragment **7b** (Table 2.3). This improvement clearly demonstrates that hits from CFL-1.1 can be readily developed by derivatization into more lead-like compounds. In addition, it is important to note that effective inhibition in this focused library is highly dependent on the position of the substituent, identifying at least two positions for substitution and hence two possible subclasses of lead structures. Furthermore, the position of the substituent appears to be more important than the nature of the substituent at this stage of fragment growth; i.e. none of the backbone substituents results in effective MMP-2 inhibition at all positions on the hydroxyquinoline ring. This shows both the versatility and promise presented by identifying new chelator leads from a fragment library – one hit fragment can generate more than one subsequent focused fragment (in this case both **75a-d** and **77a-d** fragments).

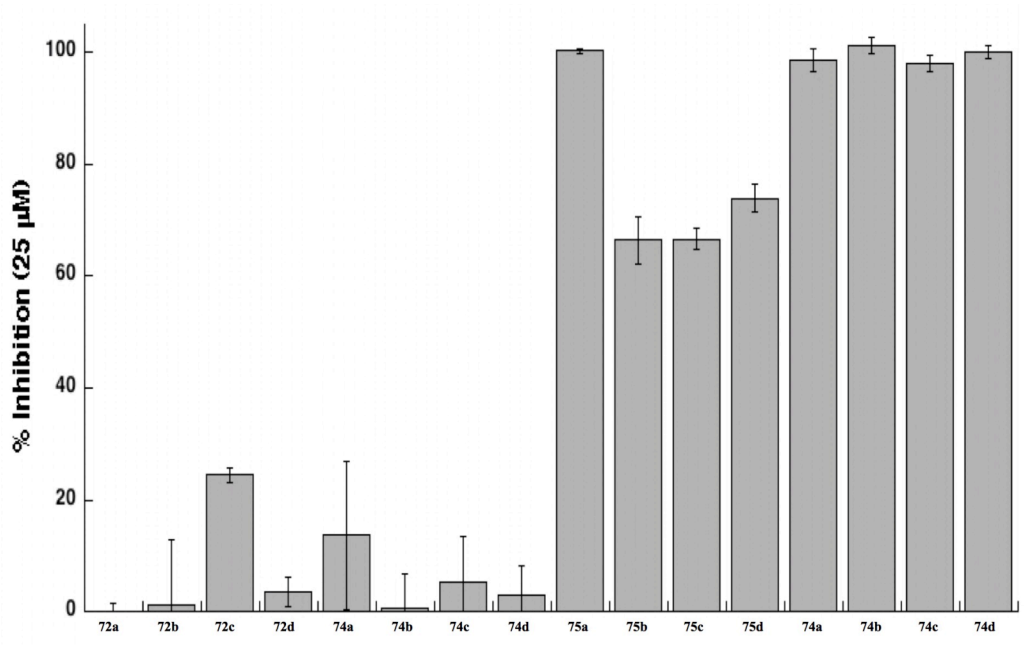

Figure 2.5 Results of 8-hydroxyquinoline sublibrary screening against MMP-2 at 25 μM. Only compounds with substituents at the 5- and 7-positions gave significant inhibition activity.

Table 2.3 IC_{50} values, heavy atom count (HAC), and ligand efficiency (LE) for **75a-d** and **77a-d** fragments. All LE values were calculated at 37 ºC.

Compound	IC_{50} Value (mM)	HAC	LE (kcal/mol)
75a	8.8±0.6	21	0.34
75b	7.2±1.0	22	0.33
75c	10.8±0.4	27	0.26
75d	8.4±0.3	20	0.36
77a	5.6±1.9	21	0.36
77b	3.0±0.5	22	0.36
77c	3.9±0.4	27	0.28
77d	4.3±0.2	20	0.38

2. D. 2. Docking Studies of Sublibrary Hits

To elucidate the mode of binding for the hydroxyquinoline derivatives, ligand-receptor docking studies and pK_a calculations were conducted. Docking studies were performed on fragments **72b** and **77b**, for which the 4-fluorophenyl backbone of each compound is directly adjacent to one of the metal coordinating atoms. The 2-position substituted compound results in a non-hit while the 7-postion substituted compound is a potent fragment. The 4- and 5-postion compounds were omitted from this study to simplify the comparisons being made. Both the 4- and 5-postion compounds yielded numerous sets of binding modes to the Zn(II) as well as varied positions of the 4-fluorophenyl backbone (not shown). Comparison of the 2-and 7-position coffered the opportunity to directly compare two structural isomers that appear to contribute identical protein-ligand interactions, yet experimentally are shown to be drastically different in respective potencies. All calculations were preformed using a molecular modeling suite from Schrödinger (Maestro v9.0; Schrödinger, Inc.). Fragment **72b** generated a pose for MMP-2 (PDB: 1QIB) with an acceptable coordination geometry at the Zn(II) ion and the 4-fluorobenzyl group resting in the S1' pocket (Figure 2.6). This low energy pose gave a Glide XP score of -11.12 kcal/mol. Fragment **77b** also generated a satisfactory pose with coordination to the Zn(II) ion. The 4-fluorobenzyl group of **77b** also enters the S1' pocket (Figure 2.5) gave a docking score of -10.63 kcal/mol. The docked structures of both **72b** and **77b** Zn-O and Zn-N bond distances are ≤2.1 Å and ≤1.9 Å, respectively. Only two notable differences are observed between the docked structures of **72b** and **77b**: a) the orientations of the ZBG in the active site are flipped ~180° relative to one another, so that with each fragment the backbone group can interact with the S1' pocket, and b) the

sulfonamide linking group in **77b** makes hydrogen bonding contacts with residues L154 and A165, which is not observed with **72b**.

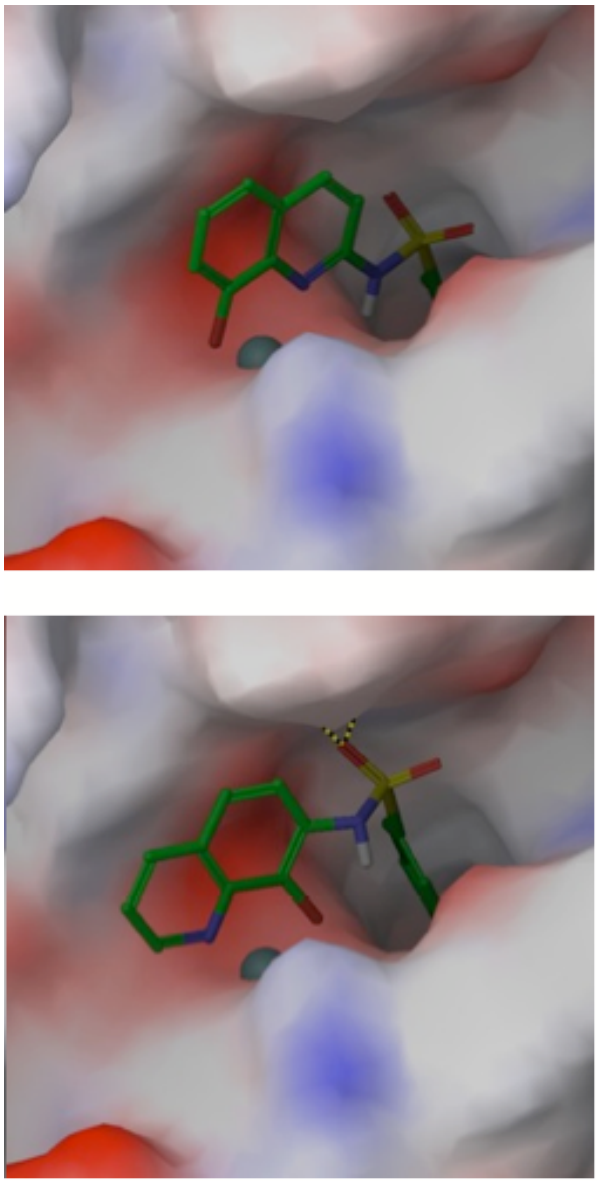

Figure 2.6 Docking results of **72b** (top) and **77b** (bottom) in the active site of MMP-2 (PDB: 1QIB). The Zn(II) ion is shown in cyan, the fragments are represented as the green colored rods. In both cases the 4-fluorobenzyl group is buried in the S1' pocket. Hydrogen bonding depicted as dashed lines between **77b** and residues L154 and A165 can be seen in the bottom figure.

Initial inspection of the docked structures of **72b** and **77b** does not explain the notable difference in potency observed for these two fragments; therefore, additional parameters were examined in order to provide a possible explanation for the disparity in observed activity. Indeed, the metal-binding ability of the fragments appears to be the key factor that discriminates between the two structural isomers. A 'metal state penalty' was calculated for each fragment, which accounts for the energetic cost of ionizing the fragment (in this case the 8-hydroxy proton) in order to bind to the Zn(II) ion. The calculated metal state penalties for **72b** and **77b** were +2.46 kcal/mol and +0.66 kcal/mol, respectively. When the penalty for each fragment is used to adjust the calculated Glide docking score, **72b** has a final value of -8.66 kcal/mol, while **77b** has a final value of -9.97 kcal/mol. The greater potency of **77b** over **72b** is consistent with this 1.3 kcal/mol difference in the adjusted docking score.

To confirm that the metal state penalty was the likely origin of the difference in activity between the 2- and 7-substituted hydroxyquinoline derivatives, quantum mechanical calculations were conducted using Jaguar (Jaguar pK_a v7.6; Schrödinger, Inc.) to determine the pK_a of each isomer. The metal state penalty used in the docking procedure is essentially the energetic cost associated with deprotonation (ionizing) of the ligand and hence should be reflected in the pK_a value of each isomer. Indeed, the calculated pK_a value for the hydroxyl group on the **72b** fragment is approximately 10.0, versus a value of 8.4 for the **77b** isomer. Under the conditions of the assay (50 mM HEPES, pH 7.5) the **77b** fragments would be more readily deprotonated than the **72b** fragments, resulting in better inhibition of the metalloenzyme under these conditions. In summary, the results found by both the docking and pK_a calculations indicated that the

77b fragment is a better hit when compared to fragment **72b** due to an appropriate p*K*a value for metal binding at physiological pH.

2. E. Screening CFL-1.1 Against Different Metalloforms: Methionine Aminopeptidase (MetAP)

The screening of CFL-1.1 against a metalloenzyme panel demonstrated the use of the fragment library as a tool to seek out new scaffolds for metalloenzyme inhibitors. While a majority of the enzymes screened contain Zn(II) metal ions, the iron and copper containing metalloenzymes have illustrated that the metal ion can dictate a preference for a type of metal-binding scaffold. It is difficult to make a direct comparison between metal ions when each is in a different and unique enzyme environment. Methionine aminopeptidase (MetAP) is a metalloenzyme capable of being reconstituted in an active form by a number of metal ions.[111] Screening of CFL-1.1 against various metalloforms of this enzyme allows for an investigation into the preferences of each metal ion in identical protein environments.

The ability of an enzyme to be activated by numerous metals poses both a challenge as well as a unique chance to utilize the chelator fragment library. Evidence suggests that there are minimal conformational changes to the active site with respect to the varied metalloforms.[111,115] Thus, there is an opportunity to screen the chelators in a protein environment where the only significant change occurring is the metal they bind to. CFL-1.1 was screened against Type I MetAP (*Ec*MetAP-1) using a fluorescence-based assay adapted from a literature procedure.[114] Two metalloforms, Co(II) and Mn(II), have been screened to date. The results of these assays are illustrated in the heat plots below (Figures 2.8, 2.9).

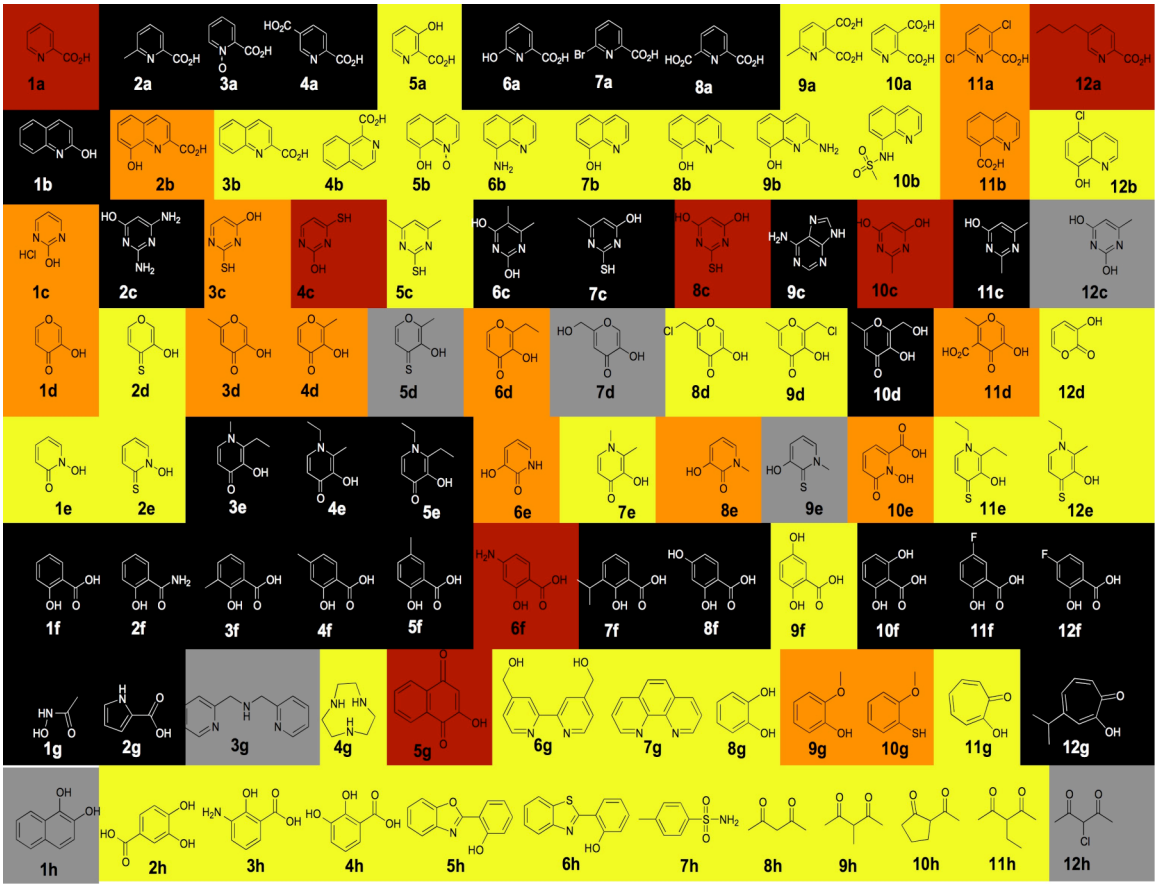

Figure 2.8 Heatplot representing results of CFL-1.1 screened at 50 μM against Co(II) *Ec*MetAP-1. Fragments are color-coded by percent inhibition: black (0-25%), red (26-50%), orange (51-75%) and yellow (76-100%). Gray indicates a fragment that gave inconsistent results due to interference with the assay.

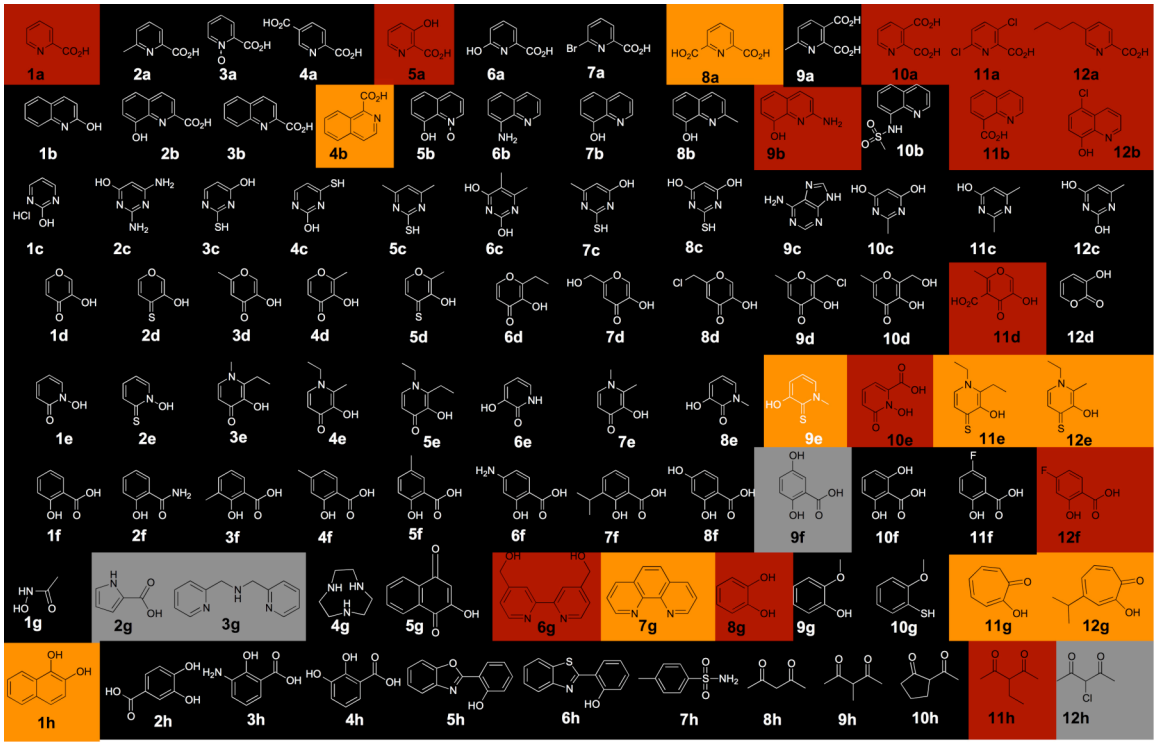

Figure 2.9 Heatplot representing results of CFL-1.1 screened at 50 µM against Mn(II) *Ec*MetAP-1. Fragments are color-coded by percent inhibition: black (0-25%), red (26-50%), orange (51-75%) and yellow (76-100%). Gray indicates a fragment that gave inconsistent results due to interference with the assay.

The screening of Co(II)-loaded EcMetAP-1 against CFL-1.1 showed more than half of the library inhibited the enzyme by >50% (Figure 2-8). Overall a majority of the quinoline-based compounds, particularly those containing an 8-hydroxyquinoline motif appear to have strong MetAP inhibitory activity. The pyrimidines (**1c-12c**) and salicylic acids (**1f-12f**) preformed the worst overall. Some notable comparisons can be made between select hydroxypyridnones. The thione containing compounds **11e** and **12e** exhibit strong inhibitory activity, where as their oxygen analogs (**4e** and **5e**) show little to

no inhibition. The difference in activity between hydroxypyrone analogues **1d** and **2d**, also shows a preference for the thione containing chelator. In contrast to the Co(II) metalloform, Mn(II)-reconstituted *Ec*MetAP-1 resulted in a lower overall hit rate when screened against CFL-1.1, with roughly only one-third of the library resulting in hits (inhibition >50%). Again the 8-hydroxyquinolines preformed moderately well, as well as a select few hydroxypyrones. With respect to the hydroxypyrones it should be noted that this metalloform appears to have a slight preference for the fragments containing O,O donor atoms sets as opposed the thione fragments (Figure 2.9). Future studies will focus on screening CFL-1.1 against two additional metalloforms of ECMetAP-1 (Ni(II) and Fe(II)).

2. F. Conclusions

This work describes the development and evaluation of a fragment library based on metal chelators. A diverse collection of ligands is presented in order to offer alternatives to the common metal-binding motifs found in most metalloenzyme inhibitors. CFL-1.1 produced high hit rates against MMPs, LF, 5-LO, TY and *Ec*MetAP-1 Co(II) but not against the heme-dependent iNOS and *Ec*MetAP-1 Mn(II). Many of the chelators identified as new MBGs have the potential to be elaborated at multiple positions, as demonstrated by the preparation of a small, focused sublibrary based on an 8-hydroxyquinoline fragment for MMP-2 inhibition. This focused library showed that substitution at either the 5- or 7-positions of the 8-hydroxyquinoline gave potent leads against MMP-2, while derivatives at the 2- and 4-positions did not. The ability to elaborate these MBG fragments into more advanced hits and eventually lead compounds is essential for inhibitor development. Unlike hydroxamic acids, many of the chelators

from CFL-1.1 may be modified at more than one position due to their cyclic structures. Having multiple sites of substitution demonstrates that one hit from CFL-1.1 can actually produce multiple sublibraries and advanced hits of different connectivity. Sublibraries can also be developed with fragments bearing more than one substituent on these cycle scaffolds. Computational studies indicate that differences in ligand acidity may contribute significantly to the range of activity observed for these focused fragment sublibraries. Overall this study shows the value of chelator libraries as a tool in FBLD against metalloprotein targets, and should open up a wide-variety of new scaffolds from which new inhibitors can be devised.

2. G. Experimental

Unless otherwise noted, starting materials were purchased from commercial suppliers (Sigma-Aldrich, ChemBridge, Acros Organics) and were used without further purification. Flash silica gel chromatography was performed using Merck silica gel 40-63 μm mesh. ^{1}H NMR spectra were recorded on one of several Varian FT-NMR spectrometers, property of the Department of Chemistry and Biochemistry, University of California San Diego. Mass spectrometry was performed at the Small Molecule Mass Spectrometry Facility in the Department of Chemistry and Biochemistry, University of California San Diego. Microwave reactions were performed in 10 mL vials using a CEM Discover S-class microwave reactor. For all assays, IC_{50} values were obtained for select fragments that showed ≥50% inhibition. IC_{50} values of hits were obtained by preparing serial dilutions of DMSO stock solutions for each compound. IC_{50} values were calculated from the plotted dose response curve using GraphPad Prism 5 software.

Chelator Fragment Library 1 (CFL-1.1) – Synthesis and Characterization

CFL-1.1 was assembled from 76 commercially available compounds the remaining of the fragments were synthesized: 13 compounds (**10b, 1d-3d**, **5d**, **8d-12d**, **8e-10e** and **6g**) were prepared according to literature precedent. Compounds **3e-5e, 7e, 11e** and **12e** were prepared according to the general procedure illustrated below with the respective starting materials of maltol (**4d**), thiomaltol (**5d**) and ethylmaltol (**6d**) and thioethylmaltol – synthesis also listed below when reacted with methylamine and ethylamine. Compounds were stored as solids or in DMSO stock solutions at a concentration of 50 mM.

Fragment 10b *N*-(quinolin-8-yl)methanesulfonamide: To a solution of 8-aminoquinoline (200 mg, 1.39 mmol) in 3 mL of pyridine, was added methanesulfonyl chloride (162 μL, 2.08 mmol). The solution was irradiated in a microwave synthesizer for 3 min at 130 °C at maximum power.[149] The reaction mixture was poured over 10 mL of cold H_2O. The resulting precipitate was isolated by vacuum filtration. The product was purified by recrystallization in EtOH, the precipitated product filtered and collected to yield 210 mg, 945 mmol. Yield: (68%). ^{1}H NMR (500 MHz, DMSO-d_6): δ 9.34 (s, br, 1H), 8.90 (dd, J = 4.0, 1.7 Hz, 1H), 8.40 (dd, J = 8.6, 1.7 Hz, 1H), 7.70 (m, 2H), 7.62 (q, J = 4 Hz, 1H), 7.57 (t, J = 8 Hz, 1H), 3.12 (s, 3H). ESI-MS(+): *m/z* 223.22 $[M+H]^+$. ^{13}C NMR (125 MHz, DMSO-d_6): δ 149.9, 139.3, 137.1, 134.7, 128.7, 127.3, 123.3, 122.9, 117.2.

Thioethylmaltol (precursor for the preparation of **11d)**: To a solution of Ethylmaltol (2.5 g, 17.8 mmol) in 100 mL toluene, was added P_4S_{10} (1.43 g, 3.2 mmol) and hexamethyldisiloxane (HMDO) (4.8 g, 30.4 mmol). The solution was heated to reflux at 100 °C overnight under nitrogen. The solution was cooled to room temperature and filtered and the filtrate was concentrated in vacuo to yield a brown oil. The oil was purified via flash silica chromatography using 1:1 CH_2Cl_2 to hexane as an eluent to yield product as a solid (2.28 g, 14.6 mmol). Yield = 82%. ^{1}H NMR (400 MHz, $CDCl_3$): δ 1.28 (t, J = 7.2 Hz, 3H), 2.83 (q, J = 7.2 Hz, 2H), 7.32 (d, 5.2 Hz, 1H; ArH), 7.61 (d, J = 4.8 Hz, 1H; ArH), 7.79 (s, 1H; ArOH). APCI-MS(-): m/z 155.00 $[M-H]^-$.

General synthesis of **3e, 4e, 5e, 7e, 11e** and **12e**: To a solution of the starting pyrone (500 mg, 3-4 mmol) in 5 mL dilute HCl (0.38 M), 2.2 equivalents of the appropriate amine was added. The solution was irradiated in a microwave synthesizer at

165 °C for 1-10 minutes. The solvent was evaporated and the crude was purified by silica column chromatography using 0-6% MeOH in CH_2Cl_2 as an eluent. The product was collected and concentrated down in vacuo to yield a solid.

3e (2-ethyl-3-hydroxy-1-methylpyridin-4(1*H*)-one): 3e was synthesized according to the above procedure starting from ethylmaltol (**6d**, 500 mg, 3.57 mmol) and methylamine (244 mg, 7.85 mmol). The product was purified by silica chromatography on silica using 0-3% MeOH in CH_2Cl_2 as the eluent to yield the product as a solid (114 mg, 0.75 mmol). Yield: 20%. ^{1}H NMR (400 MHz, DMSO-d_6): δ 7.53 (d, J = 7.6 Hz, 1H; ArH), 6.08 (d, J = 7.6 Hz, 1H; ArH), 3.67 (s, 3H), 2.70 (q, J = 7.2 Hz, 2H), 1.11 (t, J = 7.2 Hz, 3H). ESI-MS(+): m/z 154.28 $[M+H]^+$.

4e 1-ethyl-3-hydroxy-2-methylpyridin-4(1*H*)-one: 4e was synthesized according to the above procedure starting from maltol (**4d,** 500 mg, 3.97 mmol) and methylamine (393 mg, 8.72 mmol). The precipitate was filtered, rinsed with water, and dried under vacuum. The product was purified via silica column chromatography using 0-5% MeOH in CH_2Cl_2 an eluent to yield product as a solid (42 mg, 0.281 mmol). Yield = 7.1%. ^{1}H NMR (400 MHz, $CDCl_3$-d_1): δ 7.23 (d, J = 6.4 Hz, 1H), 6.39 (d, J = 7.6 Hz, 1H), 4.75-4.25 (br, 1H), 3.95-3.89 (q, J = 7.6 Hz, 2H), 2.39 (s, 3H), 1.38 (t, J = 7.6 Hz, 3H). ESI-MS(+): m/z 154.2 $[M+H]^+$.

5e (1,2-diethyl-3-hydroxypyridin-4(1*H*)-one): 5e was synthesized according to the above procedure starting from ethylmaltol (**6d**, 500 mg, 3.57 mmol) and ethylamine (354 mg, 7.85 mmol). The precipitate was filtered, rinsed with water, and dried under vacuum. The product was purified via silica column chromatography using 0-3% MeOH in CH_2Cl_2 an eluent to yield product as a solid (95 mg, 0.571 mmol). Yield: 16%. ^{1}H

NMR (400 MHz, $CDCl_3$): δ 7.22 (d, J = 7.6 Hz, 1H), 6.40 (d, J = 6.4 Hz, 1H), 4.75 (s, br, 1H), 3.93 (q, J = 7.2 Hz, 2H), 2.79 (q, J = 7.2 Hz, 2H), 1.41 (t, J =7.2 Hz, 3H), 1.23 (t, J = 7.2 Hz, 3H). ESI-MS(+): m/z 168.20 $[M+H]^+$.

7e (3-hydroxy-1,2-dimethylpyridine-4(1*H*)-thione): 7e was synthesized according to the above procedure starting from thiomaltol (**5d**, 500 mg, 3.53 mmol) and methylamine (241 mg, 7.8 mmol). The precipitate was filtered, rinsed with water, and dried under vacuum. The product was purified via silica column chromatography using 0-6% MeOH in CH_2Cl_2 an eluent to yield product as a solid (503 mg, 3.24 mmol). Yield: 92%. ^{1}H NMR (400 MHz, $CDCl_3$-d_1): δ 8.74 (s, 1H), 7.45 (d, J = 6.4 Hz, 1H), 7.11 (d, J = 6.8 Hz, 1H), 3.78 (s, 3H), 2.49 (s, 3H). ESI-MS(+): m/z 156.21 $[M+H]^+$.

11e (1,2-diethyl-3-hydroxypyridine-4(1H)-thione): 11e was synthesized according to the above procedure starting from thioethylmaltol (400 mg, 2.56 mmol) and ethylamine (254 mg, 5.63 mmol). The precipitate was filtered, rinsed with water, and dried under vacuum. The product was purified via silica column chromatography using 0-3% MeOH in CH_2Cl_2 an eluent to yield product as a solid (173 mg, 0.947 mmol). Yield: 37%. ^{1}H NMR (400 MHz, $CDCl_3$): δ 8.75 (s, 1H; ArOH), 7.50 (d, J = 6.4 Hz, 1H; ArH), 7.11 (d, J = 6.8 Hz, 1H; ArH), 4.07 (q, J = 7.2 Hz, 2H), 2.81 (q, J = 7.2 Hz, 2H), 1.49 (t, J = 7.6 Hz, 3H), 1.28 (t, J = 7.2 Hz, 3H). ESI-MS(+): m/z 184.19 $[M+H]^+$.

12e (1-ethyl-3-hydroxy-2-methylpyridine-4(1*H*)-thione): 12e was synthesized according to the above procedure starting from thiomaltol (**5d**, 500 mg, 3.53 mmol) and ethylamine (350 mg, 7.8 mmol). The precipitate was filtered, rinsed with water, and dried under vacuum. The product was purified via silica column chromatography using 0-5% MeOH in CH_2Cl_2 an eluent to yield product as a solid (206 mg, 1.12 mmol). Yield: 32%.

^{1}H NMR (400 MHz, $CDCl_3$-d_1): δ 8.74 (s, 1H), 7.45 (d, J = 7.6 Hz, 1H), 7.13 (d, J = 6.8 Hz, 1H), 4.06 (q, J = 7.2 Hz, 2H), 2.49 (s, 3H) 1.45 (t, J = 7.2 Hz, 3H). ESI-MS(+): m/z 170.16 $[M+H]^+$.

Hydroxyquinoline Sublibrary Synthesis and Charazterization

***N*-(8-Hydroxyquinolin-2-yl)benzenesulfonamide (72a):** 2-Amino-8-hydroxyquinoline (100 mg, 0.624 mmol) and benzenesulfonyl chloride (236 μL, 1.87 mmol) were dissolved in 3 mL of pyridine. The reaction mixture was irradiated in a microwave synthesizer at 130 °C for 6 min. The reaction was quenched with 10 mL of water and then extracted with 10 mL of CH_2Cl_2. The organic layer was dried over $MgSO_4$, filtered, and dried to yield a white powder. This white powder is the intermediate 2-(phenylsulfonamido)quinolin-8-yl benzenesulfonate, which contains a sulfonamide moiety at the 2-position as well as a sulfonate ester group at the 8-position of the ring. To remove the sulfonate ester, the intermediate was dissolved in 3 mL of MeOH, followed by addition of 3 mL of 2 M NaOH drop-wise, after which the mixture was heated to reflux for 5 h under nitrogen. After heating, the solution was allowed to cool to room temperature and the MeOH was removed under vacuum. To the aqueous solution was added 1M HCl drop-wise until a precipitate formed. The precipitate was filtered, rinsed with water, and purified by flash chromatography on silica with 0-3% MeOH in CH_2Cl_2 as the eluent. The solid was isolated. Yield: 40 mg (21%). ^{1}H NMR (400 MHz, DMSO-d_6): δ 12.12 (s, br, 1H), 11.04 (s, br, 1H), 8.18 (d, J = 9.2 Hz, 1H), 7.89 (s, br, 2H), 7.59-7.53 (m, 3H), 7.29-7.22 (m, 2H), 7.12 (d, J = 6.4 Hz, 1H), 7.06 (d, J = 10 Hz, 1H). ESI-MS (+): *m/z* 301.26 $[M+H]^+$. ^{13}C NMR (125 MHz, DMSO-d_6) δ 143.3, 141.9, 132.6, 132.6, 126.3, 125.3, 118.7, 115.4.

4-Fluoro-*N*-(8-hydroxyquinolin-2-yl)benzenesulfonamide (72b): 72b was synthesized according to the procedure described for **72a** starting from 2-amino-8-hydroxyquinoline (100 mg, 0.624 mmol) and 4-fluorobenzene-1-sulfonyl chloride (364 mg, 1.87 mmol). Purification of this compound did not require column chromatography. Yield: 74 mg, 0.023 mmol, 37%. ^{1}H NMR (400 MHz, DMSO-d_6): δ 12.17 (s, br, 1H), 11.05 (s, br, 1H), 8.19 (d, J = 9.2 Hz, 1H), 7.95 (s, br, 2H), 7.38 (t, J = 8.8 Hz, 2H), 7.30-7.23 (m, 2H), 7.13 (d, J = 7.2 Hz, 1H), 7.08 (d, J = 9.6 Hz, 1H). ^{13}C NMR (125 MHz, DMSO-d_6) δ 165.3, 163.3, 129.2, 125.4, 118.7, 116.6, 116.4. ESI-MS (+): *m/z* 319.24 $[M+H]^+$. Anal. Calcd for $C_{15}H_{11}FN_2O_3S$: C, 56.60; H, 3.48; N, 8.80. Found C, 56.99; H, 3.82; N, 8.74.

***N*-(8-Hydroxyquinolin-2-yl)-[1,1'-biphenyl]-4-sulfonamide (72c): 72c** was synthesized according to the procedure described for **72a** starting from 2-amino-8-hydroxyquinoline (100 mg, 0.624 mmol) and [1,1'-biphenyl]-4-sulfonyl chloride (473 mg, 1.87 mmol). The crude material was purified using column chromatography on silica with 0-3% MeOH in CH_2Cl_2 as the eluent. The solid was isolated. Yield: 26 mg (11%). ^{1}H NMR (400 MHz, DMSO-d_6): δ 12.19 (s, br, 1H), 11.07 (s, br, 1H), 8.19 (d, J = 9.2 Hz, 1H), 7.95 (d, J = 5.6 Hz, 2H), 7.83 (d, J = 8 Hz, 2H), 7.69 (d, J = 7.6 Hz, 2H), 7.48 (t, J = 7.6 Hz, 2H), 7.41 (t, J = 6.8 Hz, 1H), 7.30-7.22 (m, 2H), 7.13 (d, J = 7.6 Hz, 1H), 7.08 (d, J = 10 Hz, 1H). ESI-MS (+): *m/z* 377.28 $[M+H]^+$. ^{13}C NMR (125 MHz, DMSO-d_6) δ 139.1, 129.5, 128.8, 127.7, 127.5, 125.3, 118.7, 118.7.

***N*-(8-Hydroxyquinolin-2-yl)thiophene-2-sulfonamide (72c): 272c** was synthesized according to the procedure described for **72a** starting from 2-amino-8-hydroxyquinoline (100 mg, 0.624 mmol) and thiophene-2-sulfonyl chloride (342 mg,

1.87 mmol). The crude material was purified using column chromatography on silica with 0-3% MeOH in CH_2Cl_2 as the eluent. The solid was isolated. Yield: 30 mg (16%). ^{1}H NMR (400 MHz, CD_3OD): δ 8.17 (d, J = 9.2 Hz, 1H), 7.72 (m, 2H), 7.29 (m, 2H), 7.15 (dd, J = 5.6, 2.8 Hz, 1H), 7.10 (m, 2H). ESI-MS (+): *m/z* 307.30 $[M+H]^+$. ^{13}C NMR (125 MHz, DMSO-d_6) δ 148.8, 142.5, 132.1, 130.7, 127.8, 125.5, 118.7, 115.7.

4-Amino-8-hydroxyquinoline•HBr: 4-Amino-8-hydroxyquinoline was prepared according to a literature procedure starting from 4-amino-8-methoxyquinoline (100 mg, 0.57 mmol). Yield: 130 mg (84%).[150] ^{1}H NMR (400 MHz, D_2O): δ 7.77 (d, J = 6.4 Hz, 1H), 7.10 (d, J = 6.4 Hz, 2H), 6.93 (dd, J = 6.8, 2.4 Hz, 1H), 6.40 (d, J = 7.2 Hz, 1H). ESI-MS(+): *m/z* 161.33 $[M+H]^+$. ^{13}C NMR (125 MHz, DMSO-d_6) δ 149.9, 139.3, 137.1, 134.7, 128.7, 127.3, 123.3, 122.9, 117.2.

***N*-(8-Hydroxyquinolin-4-yl)benzenesulfonamide (74a):** 4-Amino-8-hydroxyquinoline•HBr (50 mg, 0.21 mmol) and benzenesulfonyl chloride (29 μL, 0.23 mmol) were dissolved in 3 mL of pyridine. The reaction mixture was irradiated in a microwave synthesizer at 130 °C for 6 min. The reaction was quenched with 10 mL of water and then extracted with 10 mL of CH_2Cl_2. The product was purified by recrystallization in EtOH, the precipitated product filtered and collected. The organic layer was dried with $MgSO_4$, filtered, and dried to yield a white solid. Yield: 16 mg (25%). ^{1}H NMR (400 MHz, CD_3OD): δ 8.05 (d, J = 6 Hz, 1H), 7.98 (d, J = 8.4 Hz, 1H), 7.82 (d, J = 8.4 Hz, 2H), 7.57 (q, J = 6.4 Hz, 2H), 7.42 (t, J = 8 Hz, 2H), 7.35 (t, J = 8Hz, 1H), 6.53 (d, J = 5.6 Hz, 1H). ESI-MS(+): *m/z* 301.05 $[M+H]^+$. ^{13}C NMR (125 MHz, DMSO-d_6) δ 167.6, 163.4, 160.6, 150.4, 148.8, 134.9, 134.5, 129.7, 128.7, 122.4, 119.8, 103.4.

4-Fluoro-*N*-(8-hydroxyquinolin-4-yl)benzenesulfonamide (74b): 74b was synthesized according to the procedure described for **74a** starting from 4-amino-8-hydroxyquinoline•HBr (100 mg, 0.41 mmol) and 4-fluorobenzene-1-sulfonyl chloride (126 mg, 0.65 mmol). Synthesis of this compound required 20 min of microwave irradiation. The product was purified by recrystallization in EtOH, the precipitated product filtered and collected. A white solid was isolated. Yield: 52 mg (40%). ^{1}H NMR (400 MHz, CD_3OD) δ 8.49 (s, 1H), 8.04, (t, *J* = 9.2 Hz, 1H), 7.87-7.84 (m, 2H), 7.59 (d, *J* = 6.9 Hz, 1H), 7.40 (t, *J* = 7.4 Hz, 1H), 7.16 (t, *J* = 6.9 Hz, 2H), 6.58 (d, *J* = 3.4 Hz, 1H). ESI-MS(+): *m/z* 319.02 $[M+H]^+$. ^{13}C NMR (125 MHz, DMSO-d_6) δ 166.48, 164.46, 160.9, 131.9, 131.8, 131.8, 127.9, 127.8, 122.2, 116.7, 116.5, 114.4, 114.2, 102.9.

***N*-(8-Hydroxyquinolin-4-yl)-[1,1′-biphenyl]-4-sulfonamide (74c): 74c** was synthesized according to the procedure described for **74a** starting from 4-amino-8-hydroxyquinoline•HBr (100 mg, 0.41 mmol) and [1,1'-biphenyl]-4-sulfonyl chloride (157 mg, 0.62 mmol). Synthesis of this compound required 10 min of microwave irradiation. The product was purified by recrystallization in EtOH, the precipitated product filtered and collected. A white solid was isolated. Yield: 30 mg (20%). ^{1}H NMR (400 MHz, $CDCl_3$): δ 8.30 (s, 1H), 7.00 (d, *J* = 8.6 Hz, 2H), 7.69 (d, *J* = 6.9 Hz, 1H), 7.61 (d, *J* = 8.0 Hz, 2H), 7.55 (t, *J* = 8.5 Hz, 3H), 7.47 (t, *J* = 6.3 Hz, 2H), 7.40 (t, *J* = 7.4 Hz, 1H) 7.32 (t, *J* = 8.0 Hz, 1H), 6.49 (s, 1H). ESI-MS(+): *m/z* 377.09 $[M+H]^+$. ^{13}C NMR (125 MHz, DMSO-d_6) δ 146.2, 138.5, 134.7, 129.6, 129.4, 129.3, 128.6, 127.7, 127.6, 127.6, 127.5, 122.3, 103.3.

***N*-(8-Hydroxyquinolin-4-yl)-thiophene-2-sulfonamide (74d): 74d** was synthesized according to the procedure described for **74a** starting from 4-amino-8-

hydroxyquinoline•HBr (100 mg, 0.41 mmol) and thiophene-2-sulfonyl chloride (112 mg, 0.61 mmol). The product was purified by recrystallization in EtOH, the precipitated product filtered and collected. A white solid was isolated. Yield: 54 mg (44%). ^{1}H NMR (400 MHz, CD_3OD): δ 8.09 (d, J = 5.2 Hz, 1H), 8.01 (d, J = 8.6 Hz, 1H), 7.79 (d, J = 5.2 Hz, 1H), 7.61 (d, J = 3.4 Hz, 1H), 7.57 (d, J = 8.0 Hz, 1H), 7.38 (t, J = 8.0 Hz, 1H), 7.02 (t, J = 8.6 Hz, 1H), 6.55 (d, J = 5.8 Hz, 1H). ^{13}C NMR (125 MHz, DMSO-d_6) δ 151.6, 150.6, 144.9, 142.0, 136.4, 136.0, 134.4, 127.8, 122.5, 122.1, 121.6, 120.1, 103.0. ESI-MS(+): *m/z* 307.03 $[M+H]^+$. Anal. Calcd for $C_{13}H_{10}N_2O_3S_2$: C, 50.97; H, 3.29; N, 9.14. Found C, 50.68; H, 3.64; N, 9.10.

***N*-(8-Hydroxyquinolin-5-yl)benzenesulfonamide (75a):** 5-Amino-8-hydroxyquinoline•2HCl (100 mg, 0.429 mmol) and benzenesulfonyl chloride (81 μL, 0.644 mmol) were dissolved in 3 mL of pyridine. The reaction was allowed to stir overnight under N_2. The reaction was quenched with 10 mL of water and extracted with 10 mL of CH_2Cl_2. The organic layer was dried over $MgSO_4$ and purified by flash silica chromatography in 0-3% methanol in CH_2Cl_2. Yield: 22mg (17%). ^{1}H NMR (400 MHz, DMSO-d_6): δ 9.98 (s, 2H), 8.80 (d, J = 4 Hz, 1H), 8.26 (d, J = 8.4 Hz, 1H), 7.59 (d, J = 8 Hz, 3H), 7.51-7.45 (m, 3H), 6.94 (s, 2H). ^{13}C NMR (125 MHz, DMSO-d_6) δ 152.7, 148.2, 139.4, 138.4, 132.7, 132.1, 129.1, 126.8, 126.5, 126.4, 122.4, 121.6, 110.5. ESI-MS (+): *m/z* 301.19 $[M+H]^+$. Anal. Calcd for $C_{15}H_{12}N_2O_3S$: C, 59.99; H, 4.03; N, 9.33. Found C, 59.88; H, 4.40; N, 9.70.

4-Fluoro-*N*-(8-hydroxyquinolin-5-yl)benzenesulfonamide (75b): 75b was synthesized according to the procedure described for **75a** starting from 5-amino-8-hydroxyquinoline•2HCl (100 mg, 0.429 mmol) and 4-fluorobenzenesulfonyl chloride

(125 mg, 0.644 mmol). The product was purified by flash silica chromatography in 0-3% MeOH in CH_2Cl_2. Yield: 24 mg (21%). ^{1}H NMR (400 MHz, DMSO-d_6): δ 10.03 (s, br, 2H), 8.81 (dd, J = 4, 1.6 Hz, 1H), 8.26 (dd, J = 8.8, 1.6 Hz, 1H), 7.63 (dd, J = 8.8, 5.2 Hz, 2H), 7.49 (dd, J = 8.4, 4Hz, 1H), 7.34 (t, J = 8.8 Hz, 2H), 6.95 (s, 2H). ESI-MS (+): *m/z* 319.24 $[M+H]^+$. ^{13}C NMR (125 MHz, DMSO-d_6) δ 163.2, 152.8, 148.3, 148.3, 138.4, 135.8, 132.1, 129.9, 129.8, 126.7, 126.4, 122.2, 121.7, 116.35, 116.2, 110.5.

***N*-(8-Hydroxyquinolin-5-yl)-[1,1'-biphenyl]-4-sulfonamide (75c): 75c** was synthesized according to the procedure described for **75a** starting from 5-amino-8-hydroxyquinoline•2HCl (100 mg, 0.429 mmol) and [1,1'-biphenyl]-4-sulfonyl chloride (163 mg, 0.644 mmol). The product was purified by recrystallization in EtOH, the precipitated product filtered and collected. Yield: 60 mg (37%). ^{1}H NMR (400 MHz, DMSO-d_6): δ 10.03 (s, br, 1H), 9.99 (s, br, 1H), 8.79 (dd, J = 4, 1.6Hz, 1H), 8.31 (dd, J = 8.4, 1.2 Hz, 1H), 7.79 (d, J = 8.4 Hz, 2H), 7.68 (dd, J = 13.2, 7.2 Hz, 4H), 7.50-7.43 (m, 4H), 6.98 (q, J = 8 Hz, 2H). ^{13}C NMR (125 MHz, DMSO-d_6) δ 152.7, 148.2, 144.0, 138.4, 138.3, 132.2, 129.1, 128.6, 127.5, 127.2, 127.0, 126.5, 126.4, 122.4, 122.4, 121.6, 110.5. ESI-MS (+): *m/z* 377.16 $[M+H]^+$. Anal. Calcd for $C_{21}H_{16}N_2O_3S$: C, 67.00; H, 4.28; N, 7.45. Found C, 66.77; H, 4.66; N, 7.45.

***N*-(8-Hydroxyquinolin-5-yl)thiophene-2-sulfonamide (75d): 75d** was synthesized according to the procedure described for **75a** starting from 5-amino-8-hydroxyquinoline•2HCl (100 mg, 0.429 mmol) and thiophene-2-sulfonyl chloride (118 mg, 0.644 mmol). The product was purified by flash silica chromatography in 0-3% MeOH in CH_2Cl_2 followed by recrystallization in EtOH, the precipitated product filtered and collected. Yield: 21 mg (16%). ^{1}H NMR (400 MHz, CD_3OD): δ 8.77 (dd, J = 4, 1.6

Hz, 1H), 8.33 (dd, *J* = 8.4, 1.6 Hz, 1H), 7.71 (dd, *J* = 4.8, 1.6 Hz, 1H), 7.43 (dd, *J* = 8.4, 4 Hz, 1H), 7.33 (dd, *J* = 4, 1.6 Hz, 1H), 7.10 (d, *J* = 8.4 Hz, 1H), 7.03 (dd, *J* = 5.2, 3.6 Hz, 1H), 6.98 (d, *J* = 8 Hz, 1H). ^{13}C NMR (125 MHz, DMSO-d_6) δ 153.3, 148.7, 140.3, 138.8, 133.7, 132.8, 132.4, 128.1, 127.2, 126.9, 122.6, 122.2, 110.9. ESI-MS (+): *m/z* 307.21 $[M+H]^+$. Anal. Calcd for $C_{13}H_{10}N_2O_3S_2$: C, 50.97; H, 3.29; N, 9.14. Found C, 50.82; H, 3.60; N, 9.48.

5-Chloro-8-hydroxy-7-nitroquinoline: 5-Chloro-8-hydroxy-7-nitroquinoline was prepared according to a literature procedure. Yield: 1.6 g (66%).[151] ^{1}H NMR (400 MHz, DMSO-d_6): δ 9.10 (d, *J* = 4.4 Hz, 1H), 8.61 (d, *J* = 9.2 Hz, 1H), 8.21 (s, 1H), 7.95 (dd, *J* = 8.4, 4.4 Hz, 1H). ESI-MS(-): *m/z* 223.35 $[M-H]^-$. ^{13}C NMR (125 MHz, DMSO-d_6) δ 150.9, 150.5, 140.4, 134.2, 132.8, 129.0, 126.4, 122.4, 118.4.

7-Amino-8-hydroxyquinoline: 7-Amino-8-hydroxyquinoline was prepared according to a literature procedure. Yield: 406 mg (95%).[151] ^{1}H NMR (300 MHz, DMSO-d_6): δ 10.16 (s, br, 1H), 8.77 (d, *J* = 7.5 Hz, 1H), 8.71 (d, *J* = 5.7 Hz, 1H), 8.34 (d, *J* = 3Hz, 1H), 7.66 (d, *J* = 8.7 Hz, 1H), 7.48 (t, *J* = 5.4 Hz, 1H), 7.39 (d, *J* = 8.7 Hz, 1H). ESI-MS(+): *m/z* 161.32 $[M+H]^+$. ^{13}C NMR (125 MHz, DMSO-d_6) δ 145.3, 142.7, 131.0, 123.2, 122.5, 122.2, 121.2, 117.1, 115.8.

***N*-(8-Hydroxyquinolin-7-yl)benzenesulfonamide (77a): 77a** was synthesized according to the procedure described for **74a** starting from 7-amino-8-hydroxyquinoline (100 mg, 0.625 mmol) and benzenesulfonyl chloride (78 μL, 0.618 mmol). The product was purified by flash silica chromatography in 0-3% MeOH in CH_2Cl_2 followed by recrystallization in EtOH. Yield: 11 mg (6%). ^{1}H NMR (400 MHz, DMSO-d_6): δ 9.81 (s, br, 2H), 8.76 (s, 1H), 8.24 (d, *J* = 8.4 Hz, 1H), 7.74 (d, *J* = 6.8 Hz, 2H), 7.56-7.51 (m,

1H), 7.47 (d, *J* = 7.6 Hz, 4H), 7.31 (dd, *J* = 8.8, 2.8 Hz, 1H). ESI-MS (+): *m/z* 301.19 $[M+H]^+$. ^{13}C NMR (125 MHz, DMSO-d_6) δ 148.9, 146.2, 141.2, 138.8, 136.5, 133.0, 129.4, 127.0, 126.8, 125.2, 121.8, 121.1, 117.5.

4-Fluoro-*N*-(8-hydroxyquinolin-7-yl)benzenesulfonamide (77b): 77b was synthesized according to the procedure described for **77a** starting from 7-amino-8-hydroxyquinoline (100 mg, 0.625 mmol) and 4-fluorobenzene-1-sulfonyl chloride (120 mg, 0.618 mmol). The product was purified by recrystallization in EtOH, the precipitated product filtered and collected. Yield: 52 mg (26%). ^1H NMR (300 MHz, DMSO-d_6): δ 9.84 (s, br, 1H), 8.78 (dd, *J* = 3.6, 0.9 Hz, 1H), 8.27 (dd, *J* = 8.4, 1.8 Hz, 1H), 7.77 (dd, *J* = 9, 5.7 Hz, 2H), 7.51-7.46 (m, 2H), 7.36-7.28 (m, 3H). ESI-MS (+): *m/z* 319.03 $[M+H]^+$. ^{13}C NMR (125 MHz, DMSO-d_6) δ 148.9, 146.7, 138.8, 137.5, 136.5, 130.1, 130.0, 127.0, 125.9, 121.9, 120.8, 117.6, 116.6, 116.4.

***N*-(8-Hydroxyquinolin-7-yl)-[1,1'-biphenyl]-4-sulfonamide (77c): 77c** was synthesized according to the procedure described for **77a** starting from 7-amino-8-hydroxyquinoline (100 mg, 0.625 mmol) and [1,1'-biphenyl]-4-sulfonyl chloride (156 mg, 0.618 mmol). The product was purified by flash silica chromatography in 0-3% MeOH in CH_2Cl_2. Yield: 30 mg (13%). ^1H NMR (400 MHz, DMSO-d_6): δ 9.93 (s, br, 2H), 8.81 (m, 1H), 8.29 (dd, *J* = 8.4, 2 Hz, 1H), 7.83 (q, *J* = 8 Hz, 4H), 7.71 (d, *J* = 6.4 Hz, 2H), 7.57 (dd, *J* = 8.8, 3.6 Hz, 1H), 7.51-7.47 (m, 3H), 7.44 (dd, *J* = 8, 3.2 Hz, 1H), 7.38 (dd, *J* = 8.8, 3.2 Hz, 1H). ^{13}C NMR (125 MHz, DMSO-d_6) δ 148.5, 145.7, 143.9, 139.6, 138.4, 138.3, 136.0, 129.1, 128.5, 127.3, 127.1, 127.0, 126.3, 124.8, 121.3, 120.7, 117.1. ESI-MS (+): *m/z* 377.10 $[M+H]^+$. Anal. Calcd for $C_{21}H_{16}N_2O_3S$: C, 67.00; H, 4.28; N, 7.45. Found C, 66.78; H, 4.68; N, 7.28.

***N*-(8-Hydroxyquinolin-7-yl)thiophene-2-sulfonamide (77d): 77d** was synthesized according to the procedure described for **77a** starting from 7-amino-8-hydroxyquinoline (100 mg, 0.625 mmol) and thiophene-2-sulfonyl chloride (113 mg, 0.618 mmol). The product was purified by flash silica chromatography in 0-3% MeOH in CH_2Cl_2 followed by recrystallization in EtOH. Yield: 27 mg (14%). ^{1}H NMR (400 MHz, DMSO-d_6): δ 9.97 (s, br, 1H), 8.80 (d, J = 4.4 Hz, 1H), 8.28 (d, J = 8 Hz, 1H), 7.83 (d, J = 3.6 Hz, 1H), 7.49 (d, J = 9.2 Hz, 4H), 7.35 (d, J = 8.8 Hz, 1H), 7.06 (t, J = 4.4 Hz, 1H). ESI-MS (+): m/z 306.98 $[M+H]^+$. ^{13}C NMR (125 MHz, DMSO-d_6) δ 148.5, 146.5, 141.1, 138.4, 136.1, 132.9, 131.8, 127.4, 126.6, 125.4, 121.5, 120.2, 117.1.

Procedures for in vitro assays

Fluorometric Screening against MMPs. CFL-1.1 was screened against MMP-1, -2, -3, -8, and -9 at a concentration of 1 mM for each fragment. The assay was carried out in white NUNC 96-well plates as previously described.[152] Each well contained a total volume of 90 μL including buffer (50 mM HEPES, 10 mM $CaCl_2$, 0.05% Brij-35, pH 7.5), human recombinant MMP (ENZO Life Sciences); 15.3 U MMP-1, 1.16 U MMP-2, 2 U MMP-3, 1.84 U MMP-8, or 0.9 U MMP-9), and the fragment solution (1 mM final concentration). After a 30 min incubation period at 37 °C, the reaction was initiated by the addition of 10 μL of the fluorogenic MMP substrate (4 μM final concentration, Mca-Pro-Leu-Gly-Leu-Dpa-Ala-Arg-NH_2·AcOH, ENZO Life Sciences). Fluorescence measurements were recorded using a Bio-Tek Flx 800 fluorescence plate reader every minute for 20 min with excitation and emission wavelengths at 320 and 400 nm, respectively. The rate of fluorescence increase was compared for samples versus negative controls (no inhibitor, arbitrarily set as 100% activity). Eighteen compounds from CFL-

1.1 were omitted from the screening due to excessive background fluorescence that interfered with the assay readings. A separate buffer (50 mM MES, 10 mM $CaCl_2$, 0.05% Brij-35, pH 6.0) was used for all experiments with MMP-3. The 8-hydroxyquinoline sublibrary was screened against MMP-2 using the procedure described above with a final fragment concentration in each well of 25 μM.

Colorimetric Screening against MMPs. Due to excessive background fluorescence, 18 compounds from CFL-1.1 were screened in a colorimetric assay against MMP-1, -2, -3, -8, and -9 at a concentration of 1mM for each fragment. The assay was carried out in clear Costar® 96-well, half area, flat bottom assay plates. Each well contained a total volume of 90 μL including buffer (50 mM HEPES, 10 mM $CaCl_2$, 0.05% Brij-35, 1 mM DTNB, pH 7.5), human recombinant MMP (ENZO Life Sciences), and the fragment solution (1 mM final concentration). After a 30 min incubation period at 37 °C, the reaction was initiated by the addition of 10 μL chromogenic MMP substrate (500 μM final concentration, Ac-Pro-Leu-Gly-[2-mercapto-4-methyl-pentanoyl]-Leu-Gly-OC_2H_5, BIOMOL International). Absorbance was monitored at 405 nm using a Bio-Tek FLx 808 colorimetric plate reader and measurements were recorded every minute for 20 min. The rate of absorbance increase was compared for samples versus negative controls (no inhibitor, arbitrarily set as 100% activity). A separate buffer (50 mM MES, 10 mM $CaCl_2$, 0.05% Brij-35, 1 mM DNTB, pH 6.0) was used for all experiments with MMP-3.

Screening against LF. CFL-1.1 was screened against LF at a concentration of 1mM for each fragment. The assay was carried out in white NUNC 96-well plates as previously described.[12] Each well contained a volume of 90 μL including buffer (20 mM

HEPES, pH 7.4), recombinant LF (10 nM final concentration, List Biological Laboratories), and the fragment solution (1 mM final concentration). After a 20 min incubation period at 25 °C, the reaction was initiated by the addition of 10 μL fluorogenic LF substrate (2 μM final concentration, MAPKKide DABCYL/FITC, List Biological Laboratories). Fluorescence measurements were recorded using a Bio-Tek Flx 800 fluorescence plate reader every minute for 20 min with excitation and emission wavelengths at 485 and 528 nm, respectively. The rate of fluorescence increase was compared for samples versus negative controls (no inhibitor, arbitrarily set as 100% activity). During this screen four compounds (**10b**, **11b**, **10c** and **5e**) and/or their results were excluded from the assay due to either precipitation, excessive fluorescence, presence of functional groups known to react with assay components or the compound significantly increased the fluorescence of the assay relative to the control with no inhibitor.

Screening against 5-LO. CFL-1.1 was screened against 5-LO at a concentration of 1 mM for each fragment. The assay was performed according to a literature procedure at room temperature.[153] Each well contained a volume of 80 μL including buffer (50 mM Tris, 2 mM EDTA, 2 mM $CaCl_2$, pH 7.5), human recombinant 5-LO (0.2 U, Cayman Chemicals), reporter dye (2',7'-dichlorofluorescin diacetate; H2DCFDA, 10 μM, Invitrogen), fragment solution (1 mM), arachidonic acid (AA, 3 μM, Fischer Scientific), and adenosine triphosphate (ATP, 10 μM, Sigma-Aldrich). H2DCFDA and 5-LO were incubated for 5 min prior to the addition of the fragment solution. This was followed by a second incubation for 10 min. The reaction was initiated by the addition of a substrate solution containing AA and ATP. The reaction was monitored using a Bio-Tek Flx 800

fluorescence plate reader. Fluorescence measurements were recorded every minute for 20 min with excitation and emission wavelengths at 485 and 528 nm, respectively. The rate of fluorescence increase was compared for samples versus negative controls (no inhibitor, arbitrarily set as 100% activity). The 5-LO screen of CFL-1.1 resulted in nine compounds (**3b**, **4d**, **6d**, **10d**, **10e**, **8f**, **1g**, **10g** and **12g**) that significantly increased the fluorescence of the assay relative to the control with no inhibitor. The origin of this interference was not identified and these compounds were excluded from further examination with respect to 5-LO.

Screening against TY. CFL-1.1 was screened against TY at a concentration of 1mM for each fragment. The assay was performed according to a literature procedure at room temperature.[96] Each well contained a volume of 100 μL including buffer (50 mM phosphate, pH 6.8), mushroom TY (30 U, Sigma-Aldrich), fragment solution (1 mM), and L-dopamine (0.5 mM, Sigma-Aldrich). Mushroom TY and the fragment solution were incubated for 10 min. A background absorbance reading at 475 nm was recorded using a Bio-Tek FLx 808 colorimetric plate reader. L-Dopamine was added to initiate the reaction, which was allowed to proceed for 10 min before a second absorbance reading at 475 nm was taken. After subtracting the background absorbance, the remaining absorbance of the negative controls (no inhibitor) was arbitrarily set as 100% activity. The ratio of absorbance between inhibitor and control wells was defined as percent TY activity. Several compounds from CFL-1.1 (**6b-10b**, **6g-9g** and **3h**) interfered with the TY assay, resulting in an increase in absorbance relative to the negative control. The origin of this interference was not identified and these compounds were excluded from further examination with respect to TY.

Screening against iNOS. CFL-1.1 was screened against iNOS at a concentration of 1 mM for each fragment. iNOS assays were performed at 37 °C using a commercially available colorimetric assay kit purchased from Calbiochem. Murine recombinant iNOS protein (0.1 U, Calbiochem), substrate L-arginine (80 μmol, Sigma-Aldrich), and inhibitor fragments (80 μmol) were incubated in assay buffer (Calbiochem, Catalog No. 482702) at a total volume of 60 μL for 5 min. A nitrate reductase solution (prepared as directed by supplier) was added (10 μL) followed by 10 μL of a freshly made stock of 1mM NADPH to initiate the reaction. After 40 min incubation the reaction was stopped by heat inactivation of the iNOS (incubation for 30 s in boiling water). In order to destroy excess NADPH, 10 μL of a lactate dehydrogenase (LDH) solution and 10 μL of an LDH cofactor solution were added followed by 20 min incubation. Following this incubation, a background reading of absorbance was taken at 540 nm using a Bio-Tek ELx 808 colorimetric plate reader. Griess Reagent 1 (1% sulfanilamide in 5% phosphoric acid) was added (50 μL) to each well followed by 50 μL of Griess Reagent 2 (0.1% *N*-(1-Naphthyl)ethylenediamine•2HCL in water). The reagents were allowed to develop for 10 min prior to collecting a second absorbance measurement at 540 nm. After subtracting the background absorbance, the remaining absorbance of the negative controls (no inhibitor) was arbitrarily set as 100% activity. The ratio of absorbance between inhibitor and control wells was defined as percent iNOS activity.

Screening against MetAP. This procedure has been adapted from a previously reported assay.[114] Unless otherwise stated all solutions are diluted into the buffer (50 mM MOPs at 7.5 pH). In a 96-well polystyrene plate, each well is plated with 10 μL of apo-MetAP at 12.5 μM. To this 60 μL of 50 mM MOPS buffer at pH 7.5 is added. Lastly, 10

μL of 200 μM metal solution is added. The wells are allowed to incubate for 20 min at room temperature. The metal solution is dependent to the metalloform being investigated ($CoCl_2$, $MnCl_2$, etc.). Afterwards, 10 μL of the chelator fragments at a final concentration of 50 μM was added to the wells. Again the plate is set aside to incubate at room temperature for 10 minutes. The reaction was initiated by the addition of 10 μL of Met-AMC substrate (Enzo Life Sciences) at 1 mM. Fluorescence measurements were recorded using a Bio-Tek Flx 800 fluorescence plate reader every minute for 40 min with excitation and emission wavelengths at 360 and 460 nm, respectively. As the enzyme proceeds to cleave the methionine it releases 7-amido-4-mentylcoumarin (AMC), which can be monitored at room temperature by fluorescence. In total each well contained a final volume of 100 μL including: MOPS buffer 50 mM, EcMetAP1 1.25 μM, metal solution 20 μM (8-times excess relative to enzyme), 50 μM fragment solution and Met-AMC 100 μM (all final concentrations). The rate of fluorescence increase was compared for sample verses a negative control (no inhibitor, set as 100% activity).

Computational Studies

The coordinates for the X-ray crystal structure of MMP-2 were taken from the RCSB Protein Data Bank (entry 1QIB) and prepared using the Protein Preparation Wizard, which is part of the Maestro software package (Maestro v9.1; Schrodinger, Inc.). The Protein Preparation Wizard was used to add bond order assignments and formal charges for heterogroups (amino acid residues, metal-ligand bonds) and hydrogen atoms to the system. To optimize the hydrogen bonding network, histidine tautomers and ionization states were predicted, and manual corrections were made when necessary to ensure correct coordination with the Zn(II) ion. Proper assignment of Asn and Gln

sidechains (due to ambiguity of electron density between oxygen and nitrogen) was assessed by rotating 180° around the terminal χ angle of these residues while adding hydrogen atoms to sample the hydrogen bonding network around the residues; to determine if the oxygen and nitrogen atoms were assigned properly. All water molecules in the structure were removed.

The 3-dimensional structures of fragments **72b** and **77b** in the appropriate ionization state (i.e. deprotonated 8-hydroxyl group) were prepared using LigPrep v2.3. (LigPrep v2.3; Schrödinger, Inc.) This was achieved using 'add metal binding states' option during the ligand preparation. This option generates different ionization states of the ligand that might be suitable for metal ion binding; only select ionization states were then used for docking (i.e. where the 2-hydroxyl group was deprotonated giving the ligands an overall -1 charge). Additionally, it is in this step that the metal binding penalty is calculated. Ligand-receptor docking of **72b** and **77b** was performed using Glide XP v5.5 (Glide v5.5; Schrödinger, Inc.), with a maximum of ten scoring poses saved for each fragment. The top scoring poses for each fragment were assessed for their distance and positioning of the ZBG relative to the active site zinc(II) ion. The top scoring poses for each fragment were found to possess the expected binding mode (e.g. bidentate not monodentate ligation) with reasonable metal-ligand bond distances based on crystallographically characterized zinc-hydroxyquinoline complexes. Of the final poses, those with the best overall scores were examined and compared. The final docking score was a combination of the Glide XP score and the Metal State Penalty obtained during preparation of the ligand, the latter of which accounts for the energy required to obtain the correct protonation state of the chelator.

In order to verify the metal state penalty from the docking experiments, quantum mechanical pK_a calculations were conducted on truncated versions of **72b** and **77b** (where the 4-fluorobenzyl group was replaced with a methyl group) using Jaguar v7.6 (Jaguar pK_a v7.6; Schrödinger, Inc.; B3LYP/6-31G* for geometry optimization; B3LYP/cc-pVTZ(+) for single-point energies at each optimized geometry).

2. H. Acknowledgements

Text, figures, and schemes in this chapter, in part, are reprints of the material published in the following paper: Jessica L. Fullagar, Jennifer A. Jacobsen, Melissa T. Miller, and Seth M. Cohen. "Identifying Chelators for Metalloprotein Inhibitors Using a Fragment-Based Approach" *J. Med. Chem*. **2011** *54*, 591-602. The dissertation author was a primary contributing author on the paper included. The co-authors listed in this publication also participated in the research. The permission to reproduce this paper was granted by American Chemical Society, copyright 2011.

2. I. References

(1) Lu, Y. *Inorg. Chem.* **2006**, *45*, 9930-9940.

(2) Biou, V.; Dumas, R.; Cohen-Addad, C.; Douce, R.; Job, D.; Pebay-Peyroula, E. *EMBO J.* **1997**, *16*, 3405-3415.

(3) Hou, C.-X.; Dirk, L. M. A.; Goodman, J. P.; Williams, M. A. *Weed Sci.* **2006**, *54*, 246-254.

(4) Parvez, S.; Kang, M.; Chung, H.-S.; Bae, H. *Phytother. Res.* **2007**, *21*, 805-816.

(5) Seffernick, J. L.; McTavish, H.; Osborne, J. P.; de Souza, M. L.; Sadowsky, M. J.; Wackett, L. P. *Biochemistry* **2002**, *41*, 14430-14437.

(6) Smit, N.; Vicanova, J.; Pavel, S. *Int. J. Mol. Sci.* **2009**, *10*, 5326-5349.

(7) Burnett, J. C.; Henchal, E. A.; Schmaljohn, A. L.; Bavari, S. *Nat. Rev. Drug Discov.* **2005**, *4*, 281-297.

(8) Coussens, L. M.; Fingleton, B.; Matrisian, L. M. *Science* **2002**, *295*, 2387-2392.

(9) Cristalli, G.; Costanzi, S.; Lambertucci, C.; Lupidi, G.; Vittori, S.; Volpini, R.; Camaioni, E. *Med. Res. Rev.* **2001**, *21*, 105-128.

(10) Dive, V.; Chang, C.-F.; Yiotakis, A.; Sturrock, E. D. *Curr. Pharm. Des.* **2009**, *15*, 3606-3621.

(11) Dubey, S.; Satyanarayana, Y. D.; Lavania, H. *Eur. J. Med. Chem.* **2007**, *42*, 1159-1168.

(12) Dunkel, P.; Gelain, A.; Barlocco, D.; Haider, N.; Gyires, K.; Sperlagh, B.; Magyar, K.; Maccioni, E.; Fadda, A.; Matyus, P. *Curr. Med. Chem.* **2008**, *15*, 1827-1839.

(13) Hernick, M.; Fierke, C. A. *Arch. Biochem. Biophys.* **2005**, *433*, 71-84.

(14) Ma, X.; Ezzeldin, H. H.; Diasio, R. B. *Drugs* **2009**, *69*, 1911-1934.

(15) Moss, M. L.; Sklair-Tavron, L.; Nudelman, R. *Nat. Clin. Pract. Rheumatol.* **2008**, *4*, 300-309.

(16) Shao, J.; Zhou, B.; Chu, B.; Yen, Y. *Curr. Cancer Drug Targets* **2006**, *6*, 409-431.

(17) Sousa, S. F.; Fernandes, P. A.; Ramos, M. J. *Curr. Med. Chem.* **2008**, *15*, 1478-1492.

(18) Villain-Guillot, P.; Bastide, L.; Gualtieri, M.; Leonetti, J.-P. *Drug Discov. Today* **2007**, *12*, 200-208.

(19) Jacobsen, F. E.; Lewis, J. A.; Cohen, S. M. *J. Am. Chem. Soc.* **2006**, *128*, 3156-3157.

(20) Agrawal, A.; Romero-Perez, D.; Jacobsen, J. A.; Villarreal, F. J.; Cohen, S. M. *ChemMedChem* **2008**, *3*, 812-820.

(21) Jacobsen, F. E.; Buczynski, M. W.; Dennis, E. A.; Cohen, S. M. *ChemBioChem* **2008**, *9*, 2087-2095.

(22) Puerta, D. T.; Mongan, J.; Tran, B. L.; McCammon, J. A.; Cohen, S. M. *J. Am. Chem. Soc.* **2005** *127*, 14148-14149.

(23) Hopkins, A. L.; Groom, C. R.; Alex, A. *Drug Discov.Today* **2004**, *9*, 430-431.

(24) Agrawal, A.; Johnson, S. L.; Jacobsen, J. A.; Miller, M. T.; Chen, L.-H.; Pellecchia, M.; Cohen, S. M. *ChemMedChem* **2010**, *5*, 195-199.

(25) Suzuki, T.; Miyata, N. *Mini. Rev. Med. Chem.* **2006**, *6*, 515-526.

(26) Winum, J.-Y.; Scozzafava, A.; Montero, J.-L.; Supuran, C. T. *Curr. Pharm. Des.* **2008**, *14*, 615-621.

(27) Congreve, M.; Chessari, G.; Tisi, D.; Woodhead, A. J. *J. Med. Chem.* **2008**, *51*, 3661-3680.

(28) Puerta, D. T.; Cohen, S. M. *Inorg. Chem.* **2002**, *41*, 5075-5082.

(29) Puerta, D. T.; Cohen, S. M. *Inorg. Chem.* **2003**, *42*, 3423-3430.

(30) Puerta, D. T.; Cohen, S. M. *Curr. Top. Med. Chem.* **2004**, *4*, 1551-1573.

(31) Puerta, D. T.; Schames, J. R.; Henchman, R. H.; McCammon, J. A.; Cohen, S. M. *Angew. Chem. Int. Ed.* **2003**, *42*, 3772-3774.

(32) Jacobsen, J. A.; Fullager, J. L.; Miller, M. T.; Cohen, S. M. *J. Med. Chem.* **2011**, *54*, 590-602.

(33) Liu, Z. D.; Khodr, H. H.; Liu, D. Y.; Lu, S. L.; Hider, R. C. *J. Med. Chem.* **1999**, *42*, 4814-4823.

(34) Liu, Z. D.; Piyamongkol, S.; Liu, D. Y.; Khodr, H. H.; Lu, S. L.; Hider, R. C. *Bioorg. Med. Chem.* **2001**, *9*, 563-573.

(35) Yan, Y.-L.; Cohen, S. M. *Org. Lett.* **2007**, *9*, 2517-2520.

(36) Lewis, J. A.; Cohen, S. M. *Inorg. Chem.* **2004**, *43*, 6534-6536.

(37) Wiley, R. H.; Jarboe, C. H. *J. Am. Chem. Soc.* **1956**, *78*, 2398-2401.

(38) Ho, T.-L. *Chem. Rev.* **1975**, *75*, 1-20.

(39) Lewis, J. A.; Mongan, J.; McCammon, J. A.; Cohen, S. M. *ChemMedChem* **2006**, *1*, 694-697.

(40) Liu, J.; Yi, W.; Wan, Y.; Ma, L.; Song, H. *Bioorg. Med. Chem.* **2008**, *16*, 1096-1102.

(41) Jimenez, M.; Garcia-Carmona, F. *J. Agric. Food Chem.* **1997**, *45*, 2061-2065.

(42) Peyroux, E.; Ghattas, W.; Hardre, R.; Giorgi, M.; Faure, B.; Simaan, A. J.; Belle, C.; Reglier, M. *Inorg. Chem.* **2009**, *48*, 10874-10876.

(43) Hider, R. C.; Lerch, K. *Biochem. J.* **1989**, *257*, 289-290.

(44) Jacobsen, J. A.; Jourden, J. L. M.; Miller, M. T.; Cohen, S. M. *Biochim. Biophys. Acta* **2010**, *1803*, 72-94.

(45) Whittaker, M.; Floyd, C. D.; Brown, P.; Gearing, A. J. H. *Chem. Rev.* **1999**, *99*, 2735-2776.

(46) Hajduk, P. J.; Sheppard, G.; Nettesheim, D. G.; Olejniczak, E. T.; Shuker, S. B.; Meadows, R. P.; Steinman, D. H.; Carrera Jr., G. M.; Marcotte, P. A.; J, S.; Walter, K.; Smith, H.; Gubbins, E.; Simmer, R.; Holzman, T. F.; Morgan, D. W.; Davidsen, S. K.; Summers, J. B.; Fesik, S. W. *J. Am. Chem. Soc.* **1997**, *119*, 5818-5827.

(47) Rouffet, M.; de Oliveira, C. A. F.; Udi, Y.; Agrawal, A.; Sagi, I.; McCammon, J. A.; Cohen, S. M. *J. Am. Chem. Soc.* **2010**, *132*, 8232-8233.

(48) Lowther, W. T.; Matthews, B. W. *Biochim. Biophys. Acta* **2000**, *1477*, 157-167.

(49) Wang, W.-L.; Chai, S. C.; Huang, M.; He, H.-Z.; Hurley, T. D.; Ye, Q.-Z. *J. Med. Chem.* **2008**, *51*, 6110-6120.

(50) Li, J.-Y.; Chen, L.-L.; Cui, Y.-M.; Luo, Q.-L.; Li, J.; Nan, F.-J.; Ye, Q.-Z. *Biochem. Biophys. Res. Commun.* **2003**, *307*, 172-179.

(51) Rouffet, M.; de Oliveira, C. A. F.; Udi, Y.; Agrawal, A.; Sagi, I.; McCammon, J. A.; Cohen, S. M. *J. Am. Chem. Soc.* **2010**, *132*, 8232-8233.

(52) Milbank, J. B. J.; Stevenson, R. J.; Ware, D. C.; Chang, J. Y. C.; Tercel, M.; Ahn, G.-O.; Wilson, W. R.; Denny, W. A. *J. Med. Chem.* **2009**, *52*, 6822-6834.

(53) Musser, J. H.; Jones, H.; Sciortino, S.; Bailery, K.; Coutts, S. M.; Khandwala, A.; Sonnino-Goldman, P.; Leibowitz, M.; Wolf, P.; Neiss, E. S. *J. Med. Chem.* **1985**, *28*, 1255-1259.

(54) Puerta, D. T.; Griffin, M. O.; Lewis, J. A.; Romero-Perez, D.; Garcia, R.; Villarreal, F. J.; Cohen, S. M. *J. Biol. Inorg. Chem.* **2006**, *11*, 131-138.

(55) Pufahl, R. A.; Kasten, T. P.; Hills, R.; Gierse, J. K.; Reiz, B. A.; Weinberg, R. A.; Masferrer, J. L. *Anal. Biochem.* **2007**, *364*, 204-212.

3 Probing Chelation Motifs in HIV-1 Integrase Inhibitors

3. A. Introduction

Human Immunodeficiency Virus-1 (HIV-1) as discussed in Chapter 1, is a retrovirus that causes the disease known as Acquired Immunodeficiency Syndrome (AIDS).[154,155] While no cure for HIV/AIDS has been discovered, significant advancements have been made in treatment and management, greatly improving the quality and longevity of the lives of those with the disease.[156] Without a cure or vaccine new HIV infections continue to occur, and as such HIV/AIDS is still considered a major health problem with the disease classified as a pandemic by the World Health Organization (WHO).[157]

As discussed in Chapter 1, HIV-1 Integrase (HIV-1 IN) is one of the components vital to HIV replication, representing the 'point of no return' in infection. HIV-1 IN culminates in the insertion and integration of the viral DNA into that of the host. This irreversible infection via insertion is carried out in two steps. First is 3'-processing (3P), where HIV-1 IN generates reactive CpA 3′-hydroxyl ends (cytosine–adenosine "sticky ends") by cleaving two nucleotides from the viral DNA. A second event, termed strand transfer (ST), involves the translocation to the nucleus, where HIV-1 IN uses the hydroxyl ends to integrate the viral DNA into the host genome.[158,159]

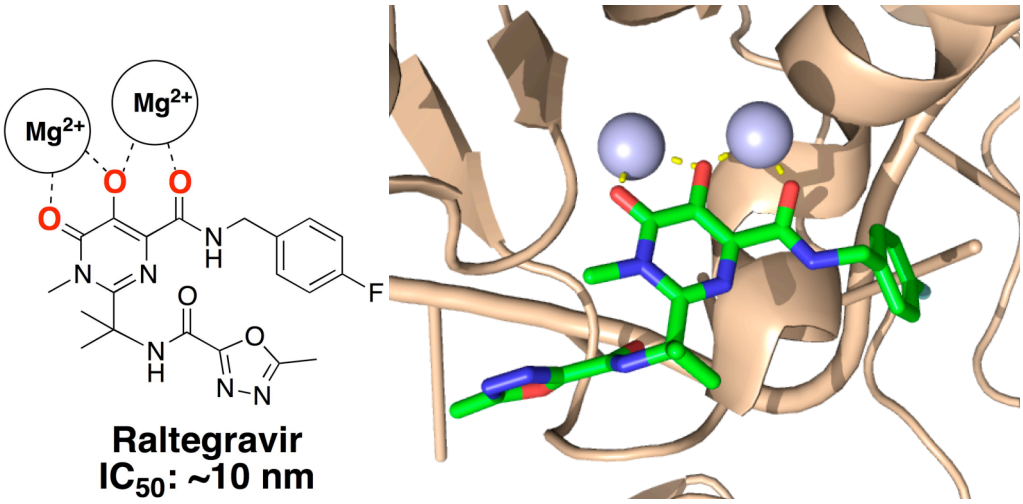

Figure 3.1 Schematic representation of FDA-approved drug raltegravir bound to the Mg(II) metal ions of the HIV-1 IN (left). Structure of PFV-IN (PDB 3OYA) complex with raltegravir. The tan ribbon represents the protein and viral DNA, grey spheres represent the Mg(II) ions and raltegravir is shown as the green rods (right).

Raltegravir is a small molecule inhibitor of HIV-1 IN via disruption of the strand transfer process, but mutational resistance has already been reported (Figure 3.1).[108,160,161] Since the approval of raltegravir in 2007, new strains of the virus have begun to develop resistance.[105,108,162] As such there is an ever present need to further understand the key interactions necessary for an effective and potent HIV-1 IN inhibition. The concepts of fragment-based lead discovery (FBLD) can be used to gain a better understanding of the essential metal-ligand interactions involved in competitive HIV-1 IN inhibition. In this Chapter a series of compounds based on the structure of raltegravir (raltegravir chelator derivatives = RCDs) were synthesized and evaluated. RCD compounds were screened against HIV-1 IN to determine which metal-binding groups (MBGs) produced inhibitors with comparable or better activity than an abbreviated raltegravir derivative (**RCD-1**). As

discussed in Chapter 1 (Figure 1.14), many HIV-1 IN inhibitors in development employ different MBGs, this study sought to systematically examine these groups while the remainder of the inhibitor structure is left unaltered.[163] The results show that several RCDs have comparable ST inhibitory activity to **RCD-1** and two derivatives, containing a hydroxypyrone MBG, were more effective at inhibiting strand transfer. Computational docking studies of RCDs in the active site of the analog enzyme prototype foamy virus integrase (PFV-IN) have been performed to shed light on the key features required to achieve effective metal chelation to the HIV-1 IN active site.

3. B. 1. Design and Synthesis

Raltegravir is noticeably similar to many previously reported metalloenzyme inhibitors prepared in our laboratory (Figure 3.2).[12,46,65] These small molecule inhibitors contain MBGs found in the chelator fragment library (CFL-1.1) discussed in Chapter 2. All the RCD compounds are identical to a core portion of raltegravir and vary only in the nature of the MBG (Figure 3.3); all contain a MBG scaffold attached to an amide-linked *p*-fluorobenzyl group backbone.[108,164]

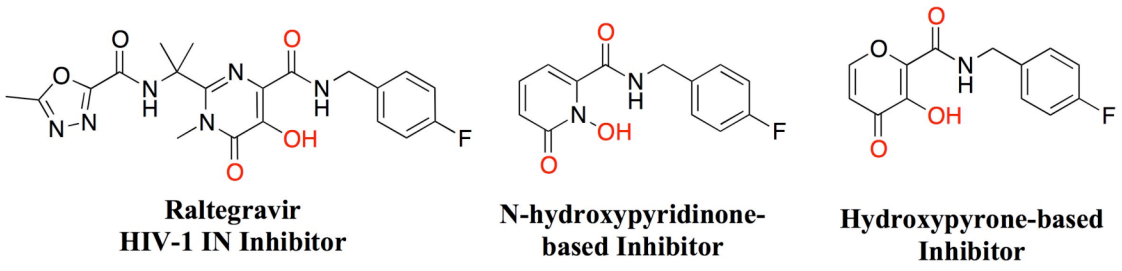

Figure 3.2 Comparison of the structural similarities between raltegravir and two metalloenzyme inhibitors previously designed in our lab. The three compounds have identical *p*-fluorophenyl backbones appended to varying MBG scaffolds. In addition, all of the compounds share identical metal-binding donor atom triads to chelate to the catalytic metal ions (highlighted in red).

As discussed in Chapter 1, the size of a fragment is generally proportional to its binding affinity. These larger lead-like RCD compounds should be more potent than un-decorated MBGs. Ideally the enhanced binding afforded by the *p*-fluorobenzyl group will highlight successful MBG-protein interactions. Additionally, the structural similarity of the RCD compounds to raltegravir will allow for more direct comparisons to be drawn between the screened compounds and the FDA approved drug. The oxodiazole substituent of raltegravir was not maintained in the RCD compounds to simplify the synthesis of the RCD compounds and so that differences in potency could be directly attributed to metal binding.[161]

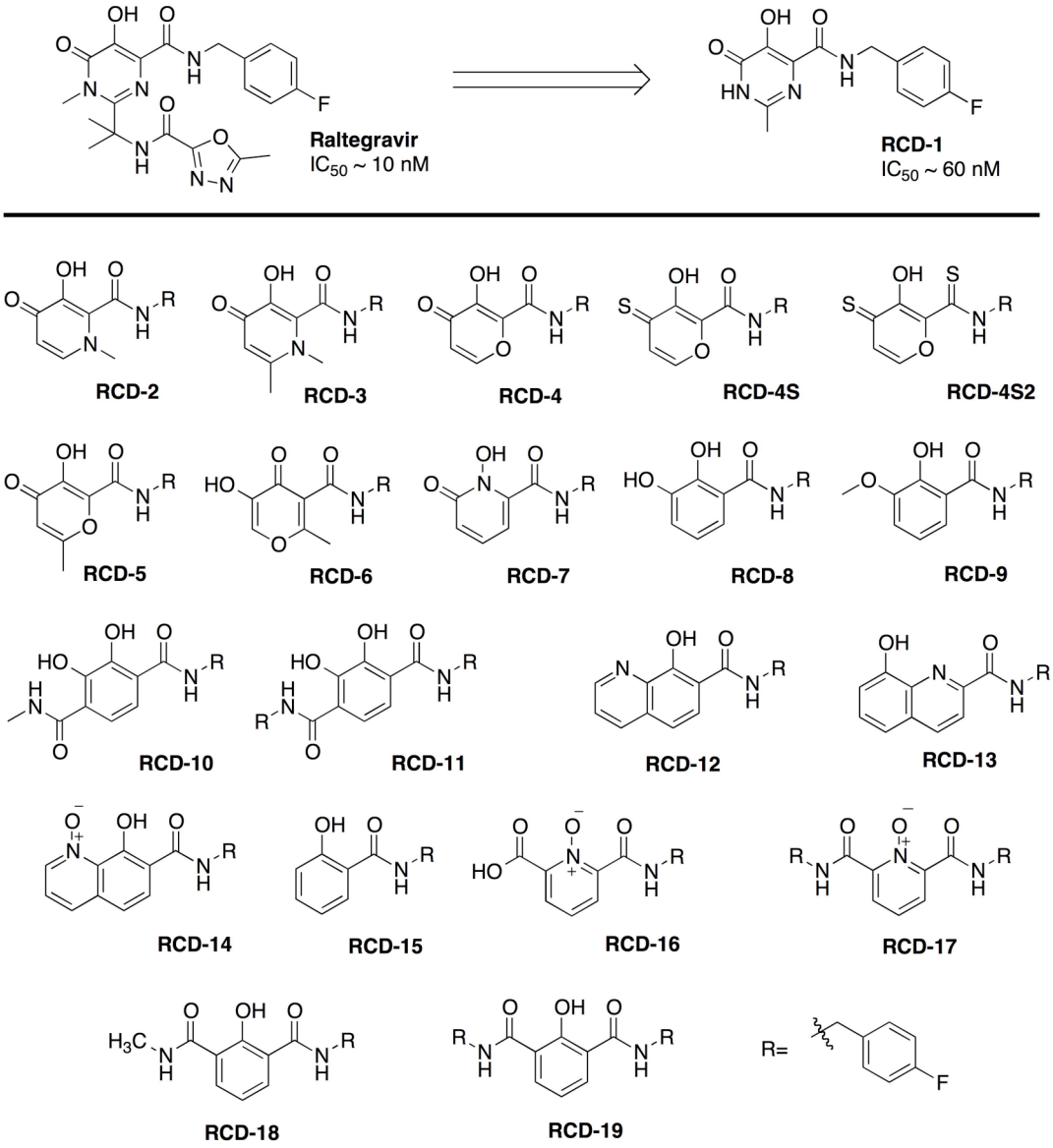

Figure 3.3 List of RCD compounds and parent compound raltegravir.

The MBGs utilized in the RCD compounds cover a wide range of chemical space, including hydroxypyridinones (**RCD-2**, **RCD-3**, **RCD-7**), hydroxypyrones (**RCD-4**, **RCD-5**, **RCD-6**), catechols (**RCD-8, RCD-9**), *p*-dicarboxycatechols (**RCD-10**, **RCD-11**), hydroxyquinolines (**RCD-12**, **RCD-13**, **RCD-14**), and several others. A total of 21 initial RCDs were prepared, each with a unique MBG, covering approximately ten chemically distinct chelating motifs. In order to provide a suitable benchmark for comparison for these RCD compounds, the reported raltegravir derivative **RCD-1** was prepared.[165] As with the other RCD compounds, **RCD-1** is an abbreviated raltegravir derivative that lacks the oxodiazole substituent, but still shows good activity against HIV-1 IN (IC_{50} value ~60 nM against the strand transfer reaction of HIV-1 IN, Figure 3.3 Table 3.1).[165] The reduced activity of **RCD-1** when compared to raltegravir is attributed to the loss of π-π stacking interaction between the omitted oxadiazole substituent and the Tyr143 active site residue.[110,162,166]

3. B. 2. RCD Activity Screening

Most HIV-1 IN inhibitors, including raltegravir, target the ST reaction of HIV-1 IN.[159] All 21 RCD compounds were screened for inhibition activity against the 3P and ST reactions using published protocols.[108,110] Compounds were initially screened for activity at higher concentrations (100-300 μM) and compounds that showed any significant ST inhibition were then further examined to determine an IC_{50} value. The results of the assays with the RCD fragments are listed in (Table 3.1).

Table 3.1 Results of RCD compounds against 3P and ST processes of HIV-1 IN. Information also listed include inhibition of viral replication and the size of the rings formed during chelation to the Mg(II) ions based off their proposed modes of binding, for clarity, the metal ions were arbitrarily labeled Mg_A and Mg_B.

Compound	Chelate Ring (Mg_A, Mg_B)	3'-Processing IC_{50} (μM)	Strand Transfer IC_{50} (μM)	Antiviral Activity IC_{50} (μM)
RCD-1	5-,6-	>100	1.0 ±0.3	1.5
RCD-2	5-,6-	>100	>100	ND
RCD-3	5-,6-	>100	>100	ND
RCD-4	5-,6-	>100	0.96±0.3	ND
RCD-4S	5-,6-	>100	11.5 ±0.9	ND
RCD-4S2	5-,6-	64 ±6	7.3 ±0.6	ND
RCD-5	5-,6-	59.5 ±1.4	0.55 ±0.1	1.0
RCD-6	5-,6-	>100	56.0 ±7.0	ND
RCD-7	5-,6-	>100	19.7 ±1.6	ND
RCD-8	5-,6-	>100	39.4 ±4.0	ND
RCD-9	5-,6-	>100	>100	ND
RCD-10	5-,6-	>200	1.5 ±0.2	4.0
RCD-11	5-,6-	>300	1.7 ±0.2	ND
RCD-12	5-,6-	>100	14.5 ±2.2	2.3*
RCD-13	5-,6-	>100	>100	>100
RCD-14	6-,6-	40.5 ±2.0	3.8 ±0.3	0.5*
RCD-15	6-,NA	>100	>100	ND
RCD-16	6-,6-	21.4 ±3.0	9.2 ±1.3	ND
RCD-17	6-,6-	>300	>100	>100
RCD-18	6-,6-	>300	>300	>100
RCD-19	6-,6-	>300	>300	ND

NA not applicable; ND not determined. *Compounds showed cytotoxicity above 10 μM.

As predicted, **RCD-1** shows effective activity against the ST reaction, with an IC_{50} value of ~1 μM. This value is higher than the reported value of 60 nM[165]; however, under our assay conditions raltegravir also produces a higher IC_{50} value of ~50 nM.[164] Compound **RCD-1** also shows selectivity for the ST versus 3P reaction, consistent with previous findings.[108] Indeed, examination of the in vitro assay results immediately reveals that all of the RCD compounds, with a few exceptions (**RCD-14**, **RCD-16**), are highly selective for ST versus 3P, suggesting a common mode of action.

Of the compounds prepared, four RCD inhibitors showed activity comparable or better than **RCD-1**. These include **RCD-4**, **RCD-5**, **RCD-10**, and **RCD-11**, with ST inhibition IC_{50} values of 0.96, 0.55, 1.5, and 1.7 μM, respectively. Importantly, these compounds fall into only two distinct classes of MBG chelators: compounds **RCD-4** and **RCD-5** contain hydroxypyrone chelators, while **RCD-10** and **RCD-11** are modified 2,3-dihydroxyterephthalic acids. This similar grouping clearly highlights the role of the MBG in inhibitor efficacy, whereby only two of at least ten distinct MBGs results in good ST inhibition activity. Other compounds showed modest activity, including **RCD-4S**, **RCD-4S2**, **RCD-7**, **RCD-12**, **RCD-14**, and **RCD-16** with IC_{50} values in the 4-20 μM range. Finally, two compounds, **RCD-6** and **RCD-8**, showed lower activity with IC_{50} values less than 40 μM. All of the remaining RCD compounds showed poor inhibition, with little or no activity at concentrations >100 μM.

In conjunction with vitro assay screenings, six RCD compounds were examined in cell-based HIV-1 IN infection screening (Table 3.1).[165] An assortment of RCD compounds, with different MBGs that were active (**RCD-1**, **RCD-5**, **RCD-10**, **RCD-12**, **RCD-14**) or inactive (**RCD-13**) in vitro, were examined. Infected P4R5 cells were treated

with the selected RCDs,[165] after which infectivity was assessed and percent neutralization was calculated (percent neutralization = [(1 – no. of infected cells with inhibitor) / (no. of infected cells without inhibitor)] × 100). A direct correlation between ST activity and P4R5 infection was observed. As listed in Table 3.1, **RCD-1**, **RCD-5**, **RCD-10**, **RCD-12** and **RCD-14**, all of which have ST IC_{50} values below 15 μM, were shown to have P4R5 infection IC_{50} values of greater than 4.0 μM. In contrast, **RCD-1**, which performs poorly in vitro (ST IC_{50} >100 μM), also showed weak activity in the cell-based infection assay (IC_{50} ~120 μM). In summary, the cell-based infectivity assay is wholly consistent with the in vitro ST activity, suggesting that the mechanism of action for the RCD compounds in HIV-1 IN inhibition.

3. B. 3. Computational Docking Studies

To elucidate the binding modes of the various RCD compounds, ligand-receptor docking studies were conducted. As previously described, the structure of the PFV-IN in complex with raltegravir shows that the O,O,O donor triad binds to the active site Mg(II) ions, with the central oxygen atom acting as a bridge between the two metal centers (Figure 3.1). The coordinates for PFV-IN (PDB: 3OYA) were used for computational docking of RCD compounds.[167,168] As a test of our docking procedure raltegravir was docked into the PFV-IN structure, resulting in a pose consistent to that seen in the crystal structure complex (not shown, RMSD 0.19 Å). **RCD-1** was docked into PFV-IN using the same procedure and gave a binding pose identical to that found for raltegravir (RMSD 0.25 Å, Figure 3.4).

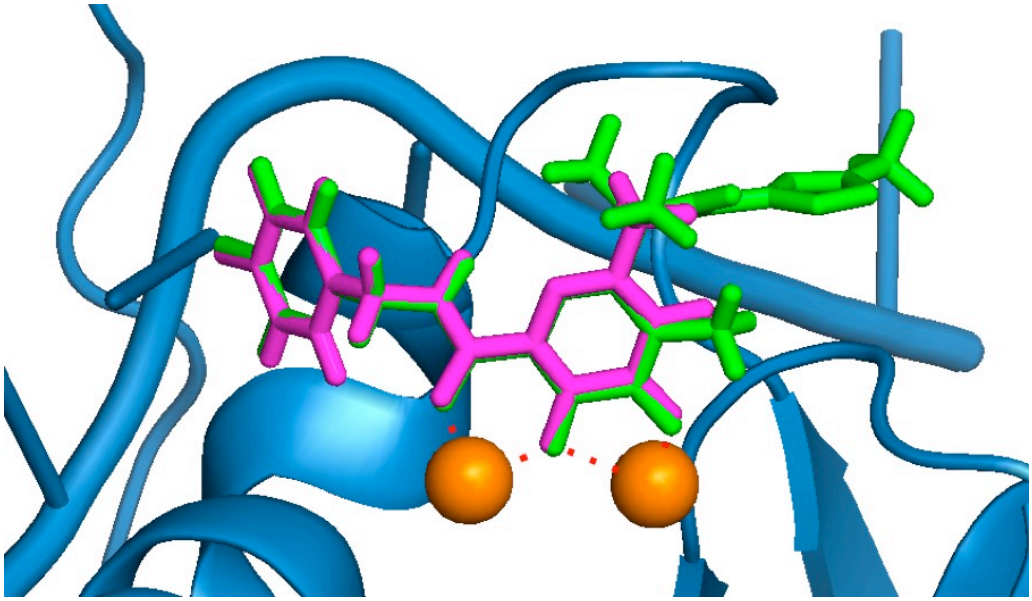

Figure 3.4 Comparison of the computational docking of **RCD-1** (pink) versus the reported crystal structure of raltegravir (green) bound in the PFV IN (blue) (PDB: 3OYA). The Root-Mean Square Difference (RMSD) between the inhibitors is 0.25 Å.

The O,O,O donor atom triad of raltegravir and **RCD-1** bind to the Mg(II) ions forming 6- and 5-membered chelate rings (Figure 3.5). The hydroxyl oxygen and the amide-linked carbonyl oxygen together form the 6-membered ring while the same hydroxyl oxygen and the exocyclic carbonyl oxygen atom of the MBG make up the 5-membered ring. In both compounds, the deprotonated, anionic hydroxyl oxygen atom binds in a bridging fashion between the two metal ions in the active site.

The *p*-fluorobenzyl substituent of raltegravir and **RCD-1** both rest in an identical pocket. It has been proposed that this pocket is formed by an induced fit mechanism upon displacement of an adenine residue (A17) from the nucleic acid substrate. The displacement of this nucleotide and the resulting pocket allow the *p*-fluorobenzyl group

to tightly fit inside and interact with bases from the invariant CA dinucleotide, guanine 4 as well as a highly conserved proline residue (P214). The placement of this group is pivotal to the impairment of HIV-1 IN activity as it causes the viral DNA to be displaced from the active site.[162] This docking exercise with raltegravir and **RCD-1** validated our assumption that the only difference in binding between these compounds is the omitted oxadiazole moiety, and that the omission of this group has little or no effect on the binding of the MBG or placement of the *p*-fluorobenzyl component of the compound.

Satisfied with the validity of the docking procedure and parameters, the remaining RCD compounds were docked in a similar manner. Docking experiments showed that the other RCD compounds formed one of several chelate ring patterns (Figure 3.5): i) a 6-membered chelate ring with Mg_B and a 5-membered chelate ring with Mg_A (**RCD-1** to **RCD-12**); ii) two 5-membered chelate rings (**RCD-13**); iii) two 6-membered chelate rings (**RCD-14**, **RCD-16**, **RCD-17**, **RCD-18**, **RCD-19**), or iv) only a single 6-membered chelate ring with Mg_A (**RCD-15**). In addition, for all RCD compounds, the *p*-fluorobenzyl substituent was bound in the same pocket as described for the raltegravir and **RCD-1**.

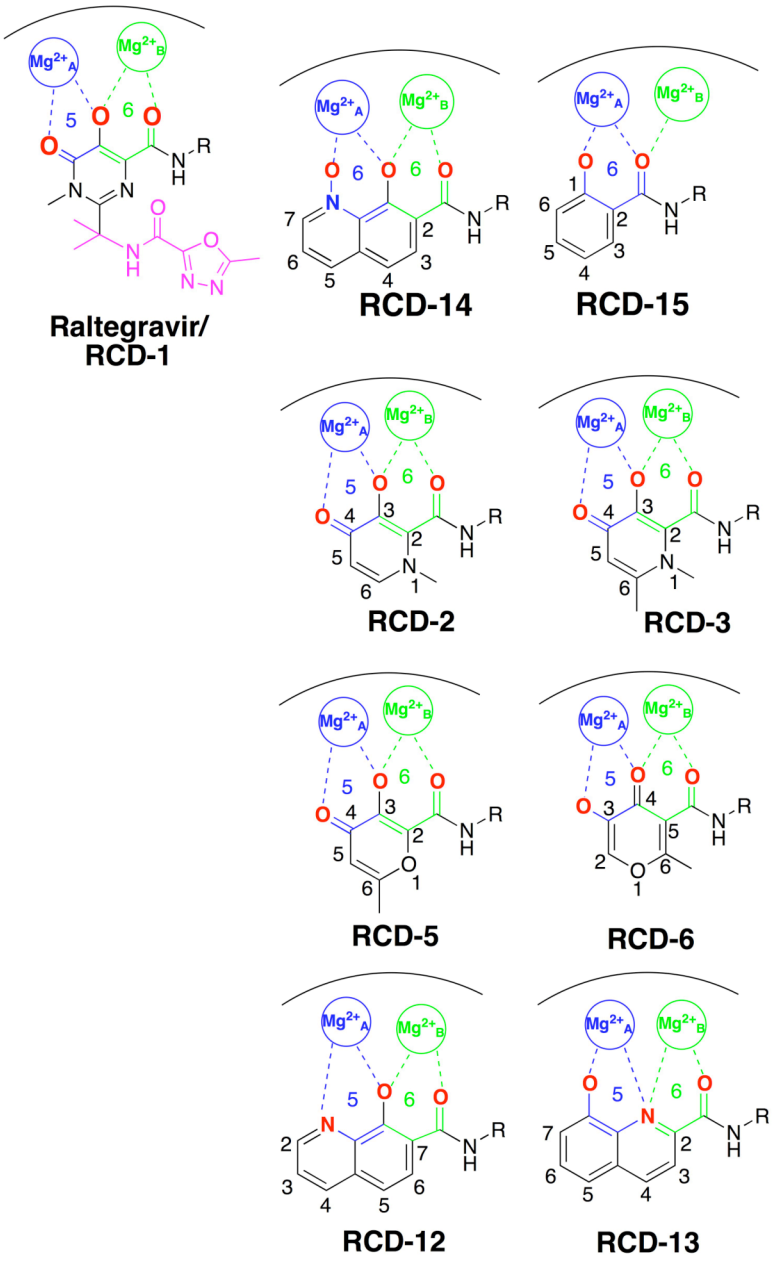

Figure 3.5 MBG numbering system and modes of metal binding for raltegravir and RCD compounds: heteroatoms in red are contributing to the coordination to the Mg(II) ions in the active site. For clarity the metal ions were arbitrarily labeled Mg_A and Mg_B; their respective chelate rings and size are colored blue and green. Raltegravir and RCD-1 are identical, except that RCD-1 lacks the oxadiazole substituent (shown in pink).

3. C. 1. Unique Features of MBG Motifs

Inspection of the in vitro ST inhibition data in conjunction with the computational docking experiments reveals several interesting trends about the MBG requirements for this series of HIV-1 IN inhibitors. One feature that is clearly important is the size of the chelate rings formed upon binding of the inhibitor (Figure 3.5). Most of the active compounds form a 6-membered chelate ring with Mg_B and a 5-membered chelate ring with Mg_A (**RCD-1**, **RCD-4**, **RCD-5**, **RCD-6**, **RCD-7**, **RCD-8**, **RCD-10**, **RCD-11**, **RCD-12**). Compounds that form two, 5-membered chelate rings (**RCD-13**), two 6-membered chelate rings (**RCD-17**, **RCD-18**, **RCD-19**), or only a single chelate ring (**RCD-15**) were generally inactive (Figure 3.6). **RCD-14** and **RCD-16** appear to be exceptions to this trend, as they both form two 6-membered chelate rings upon binding (Figure 3.7) and still exhibit moderate inhibition. These compounds both possess highly Lewis acidic *N*-oxide donors and form dianionic chelators upon metal binding, which would result in a strong electrostatic attraction between the inhibitors and active site Mg(II) ions. These features may explain the enhanced activity of **RCD-14** and **RCD-16** despite what appears to be a non-optimal coordination arrangement. The preferred 6-,5-membered chelate ring binding arrangement found for most of the active RCD compounds is also formed by raltegravir upon binding, and is also possible for compound GSK364735.[162] However elvitegravir appears to utilize a 6-,4-membered chelate ring arrangement indicating that other productive binding modes are possible (Figure 3.8).

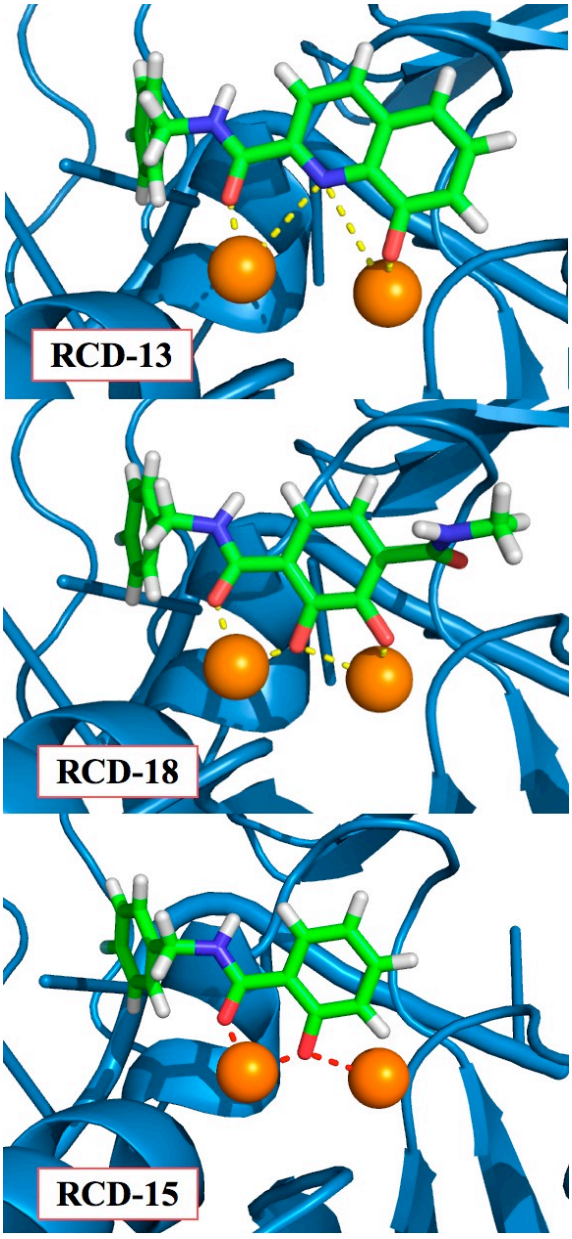

Figure 3.6 Computational docking results of atypical chelate ring patterns for RCD compounds. Compounds **RCD-13, RCD-18** and **RCD-15**. Compound **RCD-13** forms two 5-membered chelate rings, **RCD-18** forms two 6-membered chelate rings, and **RCD-15** is a case where only a single ring forms. The inhibitor is shown in sticks (colored by atom), the enzyme as a blue ribbon, and the Mg(II) ions as orange spheres.

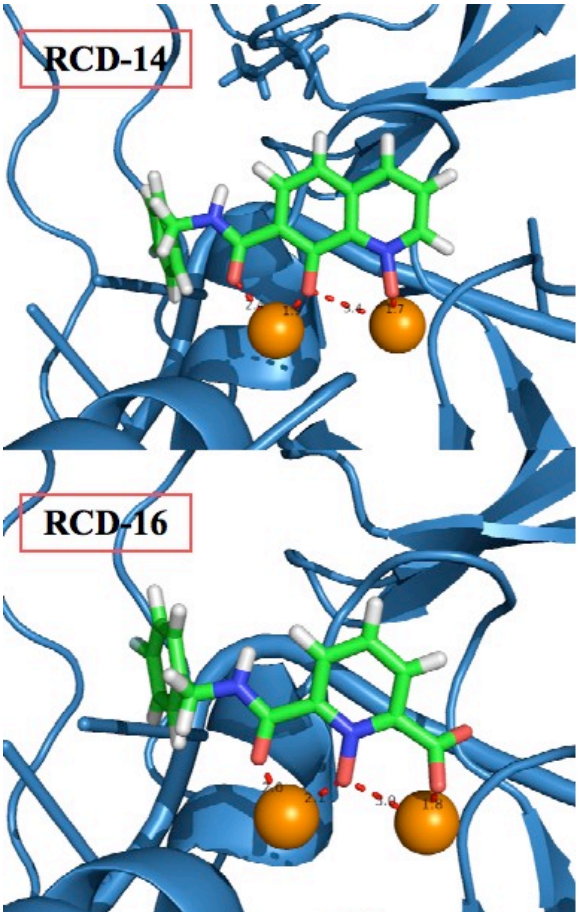

Figure 3.7 Computational docking results of atypical chelate ring patterns for RCD compounds. Compounds **RCD-14** and **RCD-16** form two 6-membered chelate rings. Unlike the compounds in Figure 3.6, these compounds show moderate inhibition (~40 μM and ~20 μM respectively). The inhibitor is shown in sticks (colored by atom), the enzyme as a blue ribbon, and the Mg(II) ions shown as orange spheres

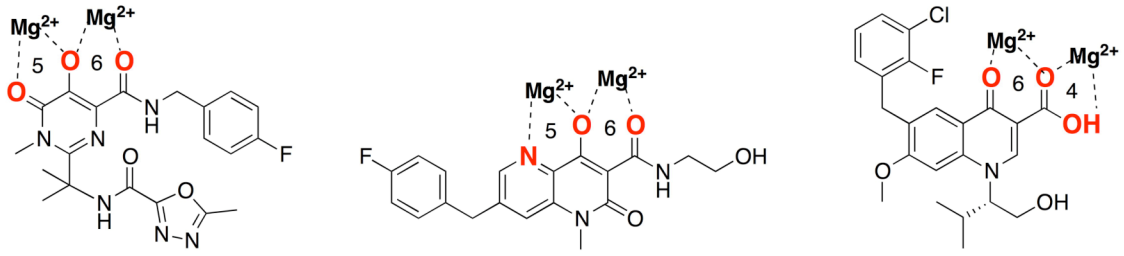

Figure 3.8 Structures of Raltegravir and other select potent HIV-1 IN inhibitors. The donor atoms highlighted in red comprise the MBG of each compound. The binding modes, IC_{50} values, and chelate ring sizes for each inhibitor are shown.

The bridging donor atom for **RCD-5** is the 3-hydroxyl oxygen. In contrast, for **RCD-6** the bridging atom is the 4-carbonyl oxygen (Figure 3.9). This subtle change in the donor atom triad arrangement contributes to the notable loss in activity between **RCD-5** and **RCD-6**. The anionic hydroxyl group is a stronger Lewis base donor than the neutral carbonyl and will serve as a stronger bridging donor atom between the Mg(II) ions.[169] This argument is supported by the activity of **RCD-4** (Figure 3.10), which also contains a hydroxypyrone MBG with a *p*-fluorobenzyl group on the 2-position of the ring (it lacks a 6-methyl group found in **RCD-5** and **RCD-6**). Like **RCD-5**, **RCD-4** presents the anionic hydroxyl atom as the bridging donor atom and similarly shows good ST inhibition.

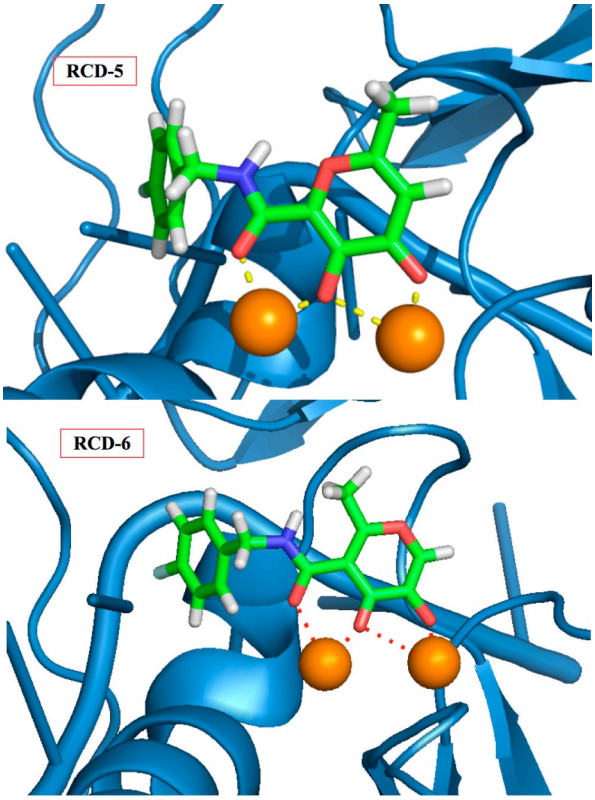

Figure 3.9 Computational docking results of compounds **RCD-5** and **RCD-6**. The location of the *p*-fluorobenzyl group was calculated to have a RMSD of ~0.3 Å difference between the two compounds. Discrepancies in potency can be attributed to the p-fluoro-benzyl group's position relative to the MBG. The inhibitor is shown in sticks (colored by atom), the enzyme as a blue ribbon, and the Mg(II) ions as orange spheres.

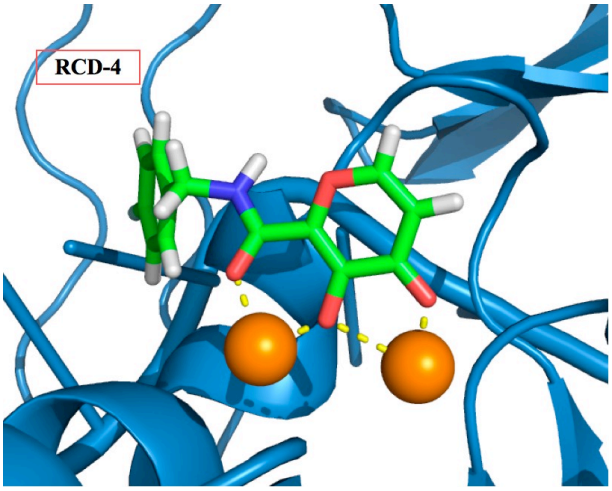

Figure 3.10 Computational docking results of **RCD-4** in PVF (PDB: 3OYA). **RCD-4** lacks the methyl group present in **RCD-5** and **RCD-6 (**Figure 3.9). The inhibitor is shown in sticks (colored by atom), the enzyme as a blue ribbon, and the Mg(II) ions as orange spheres.

Compounds **RCD-5** and **RCD-6** both contain methyl groups at the 6-postion of the MBG rings (Figure 3.5). In addition to the change in the arrangement of the donor atom triads discussed above, the difference in the position of the amide-linked *p*-fluorobenzyl group results in these methyl groups occupying different locations in the protein active site. The orientation of the methyl group upon docking of **RCD-5** in PFV-IN does not result in any significant contacts with the protein. In contrast, the same methyl group, upon docking of **RCD-6**, results in a steric clash with Pro124 in the PFV-IN active site (Figure 3.9). Binding site residue Pro124 is one of the few conserved residues in the IN active site loop that is directly involved in separating the viral DNA strands, and both raltegravir and elvitegravir make intimate Van der Waals interactions with this residue.[162] Therefore, the steric clash between Pro124 and the methyl group of

RCD-6 also likely contributes to the loss of activity for this compound. In addition to the steric clash with Pro124, the methyl group in **RCD-6** lies adjacent to the amide-linked *p*-fluorobenzyl substituent, resulting in a slight torsion of the *p*-fluorobenzyl group when compared to other RCD compounds like **RCD-5** and **RCD-4**. This intramoleular torsion results in an energetically unfavorable internal strain of **RCD-6** that is ~2 kcal/mol higher than that found for **RCD-5**, and may further contribute to its lowered activity relative to **RCD-5** and **RCD-4**.

The potential problems posed by the 6-methyl group in **RCD-6** are further supported by the poor activity of hydroxypyridinones **RCD-2** and **RCD-3**. The *N*-methyl group protruding from the MBGs in **RCD-2** and **RCD-3** is located in the same position as the 6-methyl group in **RCD-6** (Figure 3.5). Indeed, docking experiments confirm a steric clash with Pro124 and intramolecular strain, as observed for **RCD-6**. Importantly, unlike **RCD-6**, **RCD-2** and **RCD-3** contain the preferred bridging hydroxyl group found in **RCD-4** and **RCD-5**, suggesting that the steric problems posed by the methyl substituent may be the more significant factor when considering the loss in activity of **RCD-2**, **RCD-3**, and **RCD-6**. The comparisons between these compounds suggest that a combination of both the ordering of the donor triad as well as steric interactions (intra- or inter-molecular) can have a drastic affect of the potency of these inhibitors.

The dependence on the position of the amide *p*-fluorobenzyl substituent is also observed when comparing **RCD-12** and **RCD-13**, both of which contain an 8-hydroxyquinoline MBG with identical O,O,N donor atom sets (Figure 3.11). **RCD-13**, which contains the amide group at the 2-position, is essentially inactive at ~100 μM while **RCD-12**, containing the amide substituent attached at the 7-position, shows good

activity with an IC_{50} value of ~14 μM. As with **RCD-5** and **RCD-6**, **RCD-12** and **RCD-13** have the same molecular formula, overall composition, and MBG that provides an identical donor atom set (one hydroxyl oxygen atom O, one amide oxygen atom O, and one quinoline nitrogen atom N). Conversely, the position of the *p*-fluorobenzyl affects the overall arrangement of the donor atoms upon binding to the active site metal ions. As confirmed by docking studies, the position of the substituent in **RCD-12** versus **RCD-13** is a result of a significant change in the arrangement of the donor atom triad for these two compounds. As shown in Figure 3.11, for **RCD-13** the donor set will be arranged as O,N,O while for **RCD-12** the arrangement will be O,O,N. As alluded to earlier, the donor atom arrangement for **RCD-12** results in the formation of 6-membered and 5-membered chelate rings, with a bridging hydroxyl atom with the same arrangement that is found in raltegravir and the other active RCD compounds identified here.

In contrast, when the *p*-fluorobenzyl amide group is attached to the 2-postion of the scaffold as in **RCD-13**, the chelator is forced to adopt two 5-membered chelate rings, with the quinoline nitrogen atom serving as the bridging ligand. As is well-established in structural inorganic chemistry, such endocyclic nitrogen atoms do not readily engage in bridging modes of metal ion coordination;[167] furthermore, the quinoline nitrogen atom is positioned too far from the Mg(II) ions (> 3.7 Å) to form strong interactions. Despite the similar arrangement of the donor triad in **RCD-12**, this compound is still less potent than **RCD-4** and **RCD-5**, which is likely due to the preference of the hard Mg(II) ions for the harder oxygen atom donor set found in the hydroxypyrone compounds. Hard Lewis base donors such as anionic oxygen atoms are classically characterized by their small size, high charge state, and weak polarizability.[169] Comparing these compounds clearly shows

that a heteroatom triad is not sufficient for good inhibition, the correct or optimal atom arrangement of the triads is essential along with the optimal matching of the Lewis acid character of the donor atoms.

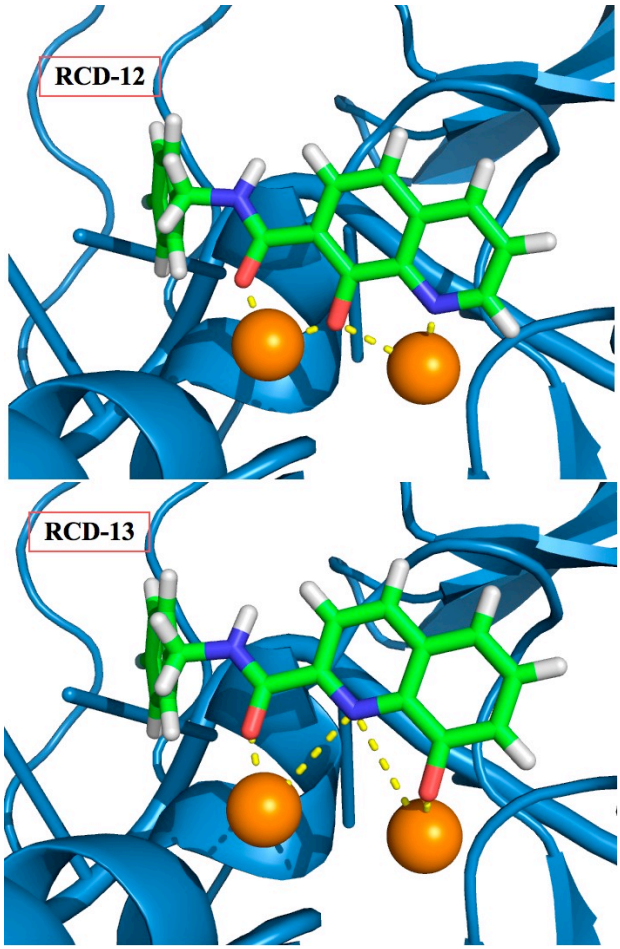

Figure 3.11 Computational docking results of **RCD-12** (top) and **RCD-13** (bottom). The inhibitor is shown in sticks (colored by atom), the enzyme as a blue ribbon, and the Mg(II) ions as orange spheres.

The comparison between **RCD-4**/**RCD-5** and **RCD-12** highlights another trend related to the nature of the MBG donor atoms. The preference for certain donor atoms

was explored by converting the O,O,O donor **RCD-4** to two different sulfur analogs. As stated above, the catalytic Mg(II) ions are hard Lewis acids and hence should bind more tightly to harder Lewis base donor atoms. The introduction of softer, more polarizable Lewis base sulfur atoms to the donor triad were expected to lower the efficacy of the compounds. Isostructural hydroxypyrothione analogs, termed **RCD-4S** and **RCD-4S2** (Figure 3.3) provide O,O,S and S,O,S donor atom sets, respectively. Both **RCD-4S** and **RCD-4S2** show a significant loss in activity when compared to **RCD-4**. The weaker ST inhibition by **RCD-4S** and **RCD-4S2** is likely due to a hard-soft mismatch between the hard Lewis acid Mg(II) ions and the soft Lewis base sulfur donor atoms. This conclusion is consistent with the improved performance of sulfur compounds like **RCD-4S2** against metalloenzymes that are dependent on the relatively softer Lewis acids like the Zn(II) ion, such as Lethal Factor (LF) discussed in Chapter 2. In the case of LF, **RCD-4S2** is a better inhibitor than **RCD-4**, due to the soft Lewis base nature of the sulfur.[170,171] In order to design an effective HIV-1 IN inhibitor the MBG must contain the appropriate Lewis acid characteristics. Hence careful selection in the use of the donor atoms is critical for obtaining optimal inhibition of HIV-1 IN.

3. C. 2. MBG Scaffolds Novel to HIV-1 IN

In this body of work, we identified two novel MBG types that appear to be promising new scaffolds for the development of HIV-1 IN inhibitors. The first MBG is the hydroxypyrone group found in **RCD-4** and **RCD-5**, shows good in vitro activity and **RCD-5** also displays good cell-based activity. The hydroxypyrone MBGs found in these compounds derive from the FDA-approved food additive maltol (3-hydroxy-2-methyl-

4H-pyran-4-one), studied extensively, which may facilitate the preparation of even more potent inhibitors based on this scaffold.[172-174]

The second class of compounds that warrants additional investigation are those based on the 2,3-dichydroxyterephthalic acid MBG (**RCD-10** and **RCD-11**). Four compounds were examined that are nominally based on a catechol MBG: **RCD-8**, **RCD-9**, **RCD-10**, and **RCD-11**. **RCD-8** contains a catecholamide MBG and shows modest ST inhibition with an IC_{50} value of 39 μM. Not surprisingly, **RCD-9** shows a complete loss of activity due to methylation of one of the phenol groups resulting in reduced donor ability. In contrast, the addition of a second carboxyamide group in **RCD-10** and **RCD-11** produces a significant improvement (greater than 20-fold) in activity with IC_{50} values less than 2 μM. One possible explanation for the improved activity of **RCD-10** and **RCD-11** over **RCD-8** would be additional interactions between the protein active site and the added carboxyamide substituents; however, **RCD-10** and **RCD-11** have very different substituents (methyl versus *p*-fluorobenzyl, Figure 3.3), and essentially identical ST inhibition IC_{50} values (1.5 and 1.7 μM, respectively). With this observation in mind, we attribute the origin of the improved activity of **RCD-10** and **RCD-11** over **RCD-8** to the reduced pK_a of the MBG. In order to obtain optimal binding to the Mg(II) ions, the MBGs should be deprotonated. Catechol is a strong, hard Lewis donor, but it is also quite basic (pK_{a1} = 9.2, pK_{a2} ~13)[175] making deprotonation under physiological conditions more difficult.

Addition of electron-withdrawing groups, such as the carboxyamide groups used in the RCD compounds described here, are known to significantly reduce the pK_a of the catechol ligand.[175] Therefore, the addition of a second carboxyamide group will result in

an inhibitor that more readily achieves deprotontion of both phenolic groups in the catechol ligand, producing a dianionic (2-) ligand with a strong electrostatic attraction between the MBG and the active site metal ions. Further evidence for electron-withdrawing groups having a potency-enhancing effect on catechol-containing HIV-1 IN inhibitors can be seen in the compounds discovered by Zhao and coworkers.[176,177] This study revolves around 2,3-dihydro-6,7-dihydroxy-1*H*-isoindol-1-one-based compounds (Figure 3.12). This warhead, similar to **RCD-8**, utilizes an identical set of donor O, O, O atoms including a catechol moiety in the MBG. The design of compound **3.a** resulted from attempts to take a HIV-1 IN inhibitor showing poor cellular activity against the target and achieve cell-based efficacy. Compound **3.a1** was reported to have a 3P IC_{50} value of greater than 200 μM and a ST IC_{50} value of ~10 μM. Through SAR a 4-fluoro,3-chlorobenzyl appendage (**3.a1**) was found to be the most potent (IC_{50} value ~0.16 μM).[177] The addition of electron-withdrawing sulfonamides (**3.a2**) lowered potency by an order of magnitude (IC_{50} value ~0.05 μM).[176] As mentioned above, due to the conditions of the assay used to screen the RCD library resulting in higher than previously reported values[178] it is difficult to compare the relative potency between the RCDs and 2,3-dihydro-6,7-dihydroxy-1*H*-isoindol-1-one analogs (no comparison was made to raltegravir). It is clear within each study that the addition of electron withdrawing groups benefits the potency of catechol containing HIV-1 IN inhibitors.

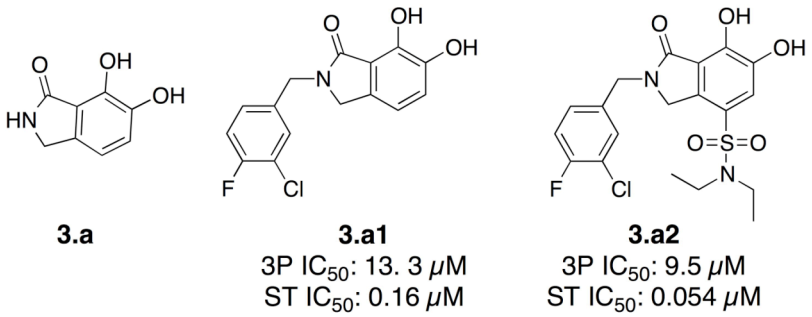

Figure 3.12 Structures and IC_{50} values of 2,3-dihydro-6,7-dihydroxy-1*H*-isoindol-1-one-based HIV-1 IN inhibitors.

We are currently testing this hypothesis by preparing other, more acidic catechol-derived inhibitors to determine if they also show efficacy against HIV-1 IN. A limited series of catechol ligands were synthesized to explore the effects of appending electron-withdrawing groups to the MBG scaffold of **RCD-8** (Figure 3.13 and Table 3.2). The addition of the small halogens makes the catechol moiety more acidic, thereby facilitating deprotonation and the ability of the chelator to bind the active site Mg(II) ions at physiological pH. Bromination at the 3-position effectively lowers the IC_{50}, but the potency is still within the same order of magnitude as the parent compound **RCD-8**. The combined effect of two bromine atoms at the 3- and 4-positions (**RCD-Br2**) drastically improves potency, comparable to **RCD-10** and **RCD-11** (Table 3.2). Similar trends can be seen with both the chloro- and nitro-derivatives (**RCD-8Cl** and **RCD-8NO_2** respectively). Because the potency of **RCD-10** and **RCD-11** was still competitive, it is possible that the larger amide bound substituent is tolerated in the active site and that a combination of the dibromo compound and **RCD-10** would cooperatively work together to produce an even more potent molecule.

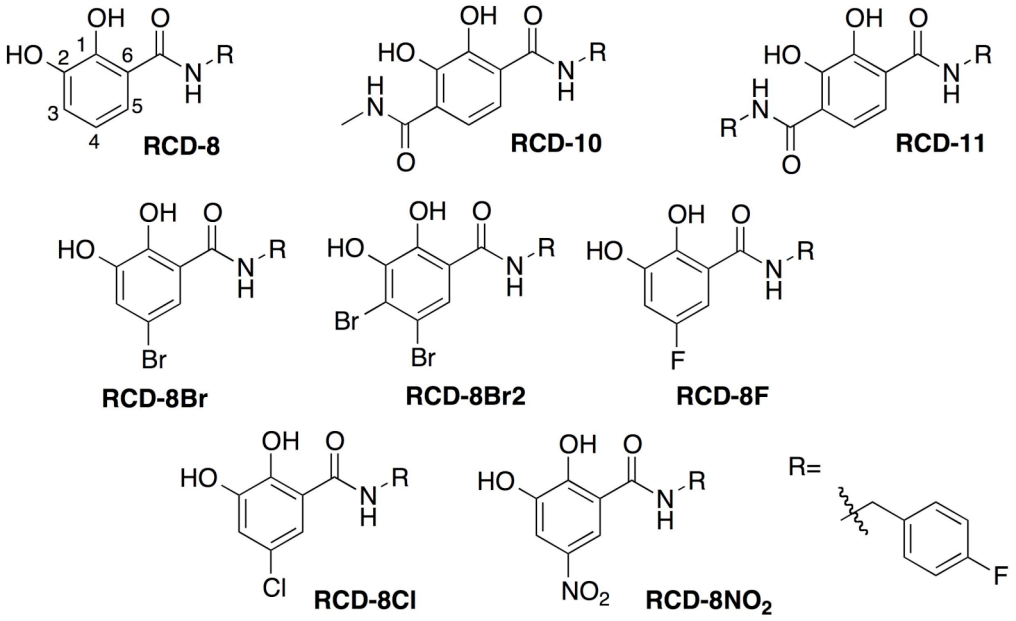

Figure 3.13 Structures of compound **RCD-8** analog sublibrary. Compounds **RCD-8, RCD-10** and **RCD-11** included (top) for reference.

Table 3.2 Assay results for **RCD-8** analog sublibrary against 3P and ST reactions of HIV-1 IN. The chelate ring sizes formed upon metal biding also included. **RCD-8, RCD-10** and **RCD-11** included for reference.

Compound	Chelate Ring Size (Mg_A, Mg_B)	3'-Processing IC_{50} (mM)	Strand Transfer IC_{50} (mM)
RCD-8	5-, 6-	>100	39.4 ±4.0
RCD-10	5-, 6-	>200	1.5 ±0.2
RCD-11	5-, 6-	>300	1.7 ±0.2
RCD-8Br	5-, 6-	>100	25±5.0
RCD-8Br2	5-, 6-	6.4±0.5	1.3±0.2
RCD-8F	5-, 6-	>100	16±4.0
RCD-8Cl	5-, 6-	>300	45±12.0
RCD-8NO_2	5-, 6-	>100	4.3±1.0

Further work needs to be conducted to validate this claim, but there is perhaps potential that future HIV-1 IN inhibitors will display antagonism to both processes. This dual action is a result at least in part, to the extra bromine in the 3-position. Additional compounds are needed to further investigate the electron-withdrawing effects on catechol MBGs. To identify the affect of multiple sites of halogenation it will be necessary to make both the doubly substituted chloro and fluoro compounds. Increased potency appears to generally follow increased electronegativity, based off of this small sample. In light of the work conducted by Zhao and coworkers, sulfonamide analogs of **RCD-8** could potentially be very strong inhibitors.[176,177]

3. D. Conclusions

This direct assessment of different MBGs on the activity of HIV-1 IN inhibitors was an evaluation of how MBGs affect inhibitor potency. While numerous inhibitors have been prepared and studied few to none have systematically dissected and evaluated the contribution and structure-activity relationship around the MBGs in these compounds.[108,159,179,180] By preparing and evaluating the RCD compounds reported here, we have identified a number of important features of the MBG for use in HIV-1 IN, including: a) the heteroatom triad should consist of hard Lewis base donor atoms to match the hard Lewis acid character of the active site Mg(II) ions; b) the triad should possess a geometry that results in the formation of adjacent 6- (Mg_B) and 5- (Mg_A) membered chelate rings; and c) the hardest, anionic donor atom should be located in the middle of the triad to provide a sufficiently electron-donating ligand in the m-bridging position between the metal ions.[181]

These experiments also lead to the identification of at least two new and distinct MBGs, hydroxypyrones (**RCD-4** and **RCD-5**) and 2,3-dihydroxyterephthalic acids (**RCD-10** and **RCD-11**) that may prove to be promising scaffolds for next-generation HIV-1 IN inhibitors. Furthermore, data on the catechol MBG suggests it may be possible to tune inhibitor activity by optimizing the pK_a of the chelator. Overall, these studies provide direct evidence that subtle variations in the MBG can substantially affect the activity of an HIV-1 IN inhibitor. This suggests that by identifying rational approaches to strengthen the metal-ligand interactions potent inhibitors can be identified that help mitigate the need for other active site interactions and hence overcome rising resistance against raltegravir.

3. E. Experimental

General. Starting materials were purchased from commercial suppliers (Sigma-Aldrich, ChemBridge, Acros Organics, TCI America) and were used without further purification. Chromatography was preformed using a CombiFlash Rf 200 from TeledyneISCO. ^{1}H NMR were recorded on one of several Varian FT-NMR spectrometers, property of the Department of Chemistry and Biochemistry, University of California San Diego. Mass spectrometry was performed at the Small Molecule Spectrometry Facility in the Department of Chemistry and Biochemistry, University of California San Diego. Compounds **RCD-2**, **RCD-3**, **RCD-4**, **RCD-4S**, **RCD-4S2**, **RCD-5**, **RCD-7**, 15a and 14a were all synthesized as previously described.[65,182,183]

Methyl 5-hydroxy-2-methyl-6-oxo-1,6-dihydropyrimidine-4-carboxylate: Synthesis adapted from literature procedure.[184] To a solution of (E)-N'-hydroxyacetimidamide (500 mg, 6.75 mmol) in 8 mL of MeOH, was added 900 μL dimethyl but-2-ynedioate (DMAD**)**. After 1 h at room temperature, 6 mL of xylenes was added and the MeOH was removed in vacuo. The solution was then refluxed at 135 °C for 16 h. The solution was cooled to 60 °C, and 3 mL of MeOH was added with stirring. After 30 minutes, 8 mL of methyl t-butyl ether (MTBE) was added drop wise and the solution was kept at 0 °C for 16 h. The black precipitate was filtered off, rinsed with cold 10% MeOH/MTBE and collected. Yield = 44%. ^{1}H NMR (400 MHz, $CDCl_3$, 25 °C): δ = 2.51 (s, 3H), 4.04 (s, 3H), 10.73 (br, 1H; N*H*). ESI-MS(+) *m/z* 184.9 $[M+H]^+$.

***N*-(4-Fluorobenzyl)-5-hydroxy-2-methyl-6-oxo-1,6-dihydropyrimidine-4-carboxamide (RCD-1):** Synthesis adapted from literature procedure.[185] A solution of 5,6-Dihydroxy-2-methyl-pyrimidine-4-carboxylic acid methyl ester (100 mg, 0.54 mmol)

and (4-fluorophenyl)methanamine (FPMA 124 μL, 1.1 mmol) in 3 mL DMF, was refluxed at 90 °C for 16 h. The reaction was then cooled to room temperature, and 1M HCl was added until precipitate formed. The solution was cooled further to 0 °C for 30 minutes. The resulting precipitate was filtered and rinsed with ether and collected to yield product as a dark brown solid (57 mg, 0.205 mmol). Yield= 38%. ^{1}H NMR (400 MHz, d_6-DMSO, 25 °C): δ = 2.23 (s, 3H), 4.42 (d, *J*= 4.0 Hz, 2H), 7.13 (t, *J*=8.0 Hz, 2H; ArH), 7.35 (t, *J*=6.0 Hz, 2H; ArH), 9.33 (brt, *J*=8.0 Hz, 1H; N*H*). ESI-MS(+) *m/z* 278.0 $[M+H]^+$. Anal. Calcd for $C_{13}H_{12}FN_3O_3$: C, 56.32; H, 4.36; N, 15.16. Found: C, 56.31; H, 4.38; N, 15.11.

5-hydroxy-2-methyl-4-oxo-4H-pyran-3-carboxylic acid: To a solution of ethyl 5-hydroxy-2-methyl-4-oxo-4H-pyran-3-carboxylate (250 mg, 1.26 mmol) in 5 mL of H_2O, was added 3 mL of a 6M NaOH solution. The mixture was stirred for 3 hr at room temperature under nitrogen. The reaction was evaporated in vacuo and the acid product 5-hydroxy-2-methyl-4-oxo-4H-pyran-3-carboxylic acid was extracted with CH_2Cl_2 and 6 M HCl. The organic phase was collected, dried over anhydrous $MgSO_4$, and concentrated in vacuo to yield product as a mustard yellow solid (150 mg, 0.88 mmol). Yield = 70%. ^{1}H NMR (400 MHz, DMSO-d_6, 25 °C): δ = 2.29 (s, 2H; CH_3), 8.05 (s, 1H; ArH), 9.36 (s, 1H; ArOH). ESI-MS(-) *m/z* 169.22 $[M-H]^-$.

4-fluorobenzyl 5-hydroxy-2-methyl-4-oxo-4H-pyran-3-carboxylate (RCD-6): To a solution of 5-hydroxy-2-methyl-4-oxo-4H-pyran-3-carboxylic acid (60 mg, 0.35 mmol) in 10 mL of dry CH_2Cl_2, was added, 1-ethyl-3-(3-dimethylaminoptopyl) carbodiimide (EDCI 81 mg, 0.42 mmol), hydroxybenzotriazole (HOBt 57 mg, 0.42 mmol) and FPMA (48 μL, 0.42 mmol). The mixture was stirred overnight at room

temperature under nitrogen. The reaction mixture was extracted with 1M HCl and CH_2Cl_2. The organic phase was collected, dried over anhydrous $MgSO_4$, and concentrated in vacuo to a yellow solid. The crude solid was purified via silica column chromatography using 0-5% MeOH/CH_2Cl_2 as an eluent to yield product as a yellow solid of **RCD-6** (28 mg, 0.10 mmol). Yield = 29%. ^{1}H NMR (500 MHz, DMSO-d_6, 25 °C): δ = 2.31 (s, 3H; CH_3), 5.64 (d, J = 2.8 Hz, 2H; CH_2), 7.08 (dd, J = 9.2, 2.8 Hz, 2H; ArH), 7.35 – 7.37 (m, 2H; ArH), 7.99 (s, 1H; ArH), 7.20 (brt, 1H; CONHCH$_2$). ESI-MS(-) *m/z* 276.25 [M-H]$^-$. Anal. Calcd for $C_{14}H_{12}FNO_4$: C, 60.65; H, 4.36; N, 5.05. Found: C, 61.04; H, 4.76; N, 5.13.

2,3-Bis(benzyloxy)benzoic acid: To a solution of dihydroxybenzoic acid (500 mg, 3.24 mmol) in 30 mL of DMF, was added benzyl chloride (1.33 mL, 11.6 mmol) and K_2CO_3 (1.71 g, 12.4 mmol). The mixture was then heated to reflux at 120 ˚C and stirred overnight under nitrogen. The resulting mixture was filtered and the filtrate was evaporated in vacuo to obtain a brown oil. The crude oil was purified via a silica plug in CH_2Cl_2 as an eluent to yield product as a clear oil (1.36 g, 3.12 mmol). Yield = 96%. To a solution of this oil (1.32 g, 3.11 mmol) in 10 mL of MeOH, was added 6 mL of a 6M NaOH solution. The mixture was stirred overnight at room temperature under nitrogen. The reaction solution was evaporated in vacuo and the pure acid product was extracted into CH_2Cl_2 and 6M HCl. The organic phase was collected, dried over anhydrous $MgSO_4$, and evaporated in vacuo to yield a pure white solid (1.03 g, 3.11mmol). Yield = 100%. ^{1}H NMR (400 MHz, $CDCl_3$-d_1, 25 °C): δ = 5.20 (s, 2H; CH_2), 5.27 (s, 2H; CH_2), 7.17 (t, J = 8.0 Hz, 1H; ArH), 7.27 - 7.50 (m, 10H; ArH), 7.73 (dd, J = 7.6, 1.6 Hz, 1H; ArH). ESI-MS(-) *m/z* 332.92 [M-H]$^-$.

2,3-Bis(benzyloxy)-N-(4-fluorobenzyl)benzamide: To a solution of 2,3-bis(benzyloxy)benzoic acid (500 mg, 1.49 mmol) in 15 mL of dry CH_2Cl_2, was added EDCI (343 mg, 1.79 mmol), HOBt (242 mg, 1.79 mmol) and FPMA (204 μL, 1.79 mmol). The mixture was stirred overnight at room temperature under nitrogen. The reaction mixture was extracted with 1M HCl and CH_2Cl_2. The organic phase was collected, dried over anhydrous $MgSO_4$ and concentrated in vacuo to a brown oil. The oil was purified via silica column chromatography using 0-1% MeOH/CH_2Cl_2 as an eluent to yield the product as a white solid (381 mg, 0.864 mmol). Yield = 58%. ^{1}H NMR (400 MHz, $CDCl_3$-d_1, 25 °C): δ = 4.42 (d, J = 5.6 Hz, 2H; NHCH_2), 4.99 (s, 2H; CH_2), 5.09 (s, 2H; CH_2), 6.93 (t, J = 8.6 Hz, 2H; ArH), 7.14 - 7.18 (m, 5H; ArH), 7.23 (d, J = 7.0 Hz, 2H; ArH), 7.27 (d, J =7.6 Hz, 1H; ArH), 7.31 (t, J = 7.4 Hz, 2H; ArH), 7.37 – 7.43 (m, 2H; ArH), 7.47 (d, J = 7.6 Hz, 2H; ArH), 7.81 (dd, J = 6.0, 3.2 Hz, 1H; ArH), 8.42 (t, J = 5.4 Hz, 1H; CONHCH$_2$). ESI-MS(+) *m/z* 441.91 $[M+H]^+$, 464.01 $[M+Na]^+$.

N-(4-Fluorobenzyl)-2,3-dihydroxybenzamide (RCD-8): 2,3-bis(benzyloxy)-N-(4-fluorobenzyl)benzamide (372 mg, 0.84 mmmol) was stirred in 25 mL of a 1:1 solution of HCl:HOAc at room temperature for three days under ambient conditions. The resulting turbid mixture was filtered under and the formed precipitate was collected and dried under vacuum to yield product, **RCD-8** as a white solid (186 mg, 0.71 mmol). Yield = 85%. ^{1}H NMR (400 MHz, DMSO-d_6, 25 °C): δ 4.45 (d, J = 6.0 Hz, 2H; NHCH_2), 6.65 (t, J = 8.0 Hz, 1H; ArH), 6.89 (d, J = 7.6 Hz, 1H; ArH), 7.12 (t, J = 8.8, Hz, 2H; ArH), 7.29 (d, J = 8.4 Hz, 1H; ArH), 7.33 (dd, J = 8.4, 2.8 Hz, 2H; ArH), 9.31 (t, J = 6.0 Hz, 1H; CONHCH$_2$). APCI-MS(+) *m/z* 262.11 $[M+H]^+$. Anal. Calcd for $C_{14}H_{12}FNO_3$•0.5 H_2O: C, 62.22; H, 4.85; N, 5.18. Found: C, 62.36; H, 5.09; N, 5.23.

2-(Benzyloxy)-3-methoxybenzoic acid: To a solution of 3-methoxysalicylic acid (500 mg, 2.97 mmol) in 10 mL of DMF, was added, benzyl chloride (880 µL, 7.63 mmol) and K_2CO_3 (1.16 g, 8.41 mmol). The mixture was heated to reflux at 120 ˚C and stirred overnight under nitrogen. The reaction was vacuum filtered and the filtrate was concentrated to a dark brown oil. The crude oil was purified via a silica plug in CH_2Cl_2 as an eluent to yield an off-white oil (763 mg, 2.19 mmol). Yield = 74%. To a solution of the oil (763 mg, 2.19 mmol) in 5 mL of MeOH, was added 3 mL of a 6M NaOH solution. The mixture was stirred overnight at room temperature under nitrogen. The reaction was evaporated in vacuo and the acid product was extracted with CH_2Cl_2 and 6M HCl. The organic phase was collected, dried over anhydrous $MgSO_4$ and concentrated in vacuo to yield product as an off-white solid (566 mg, 2.19 mmol). Yield = 100%. ^{1}H NMR (300 MHz, $CDCl_3$-*d*$_1$, 25 °C): δ = 3.97 (s, 3H; OC*H*$_3$), 5.27 (s, 2H; C*H*$_2$), 7.19 (d, *J* = 3.6 Hz, 1H; ArH), 7.36 - 7.41 (m, 5H; ArH), 7.43 (d, *J* = 2.1 Hz, 1H; ArH), 7.68 (dd, *J* = 6.3, 3.0 Hz, 1H; ArH). ESI-MS(+) *m/z* 259.11 $[M+H]^+$, 276.10 $[M+NH_4]^+$.

2,3-Bis(benzyloxy)-N-(4-fluorobenzyl)benzamide: To a solution of 2-(Benzyloxy)-3-methoxybenzoic acid (566 mg, 2.19 mmol) in 15 mL of dry CH_2Cl_2, was added EDCI (504 mg, 2.63 mmol), HOBt (335 mg, 2.63 mmol) and FPMA (301 µL, 2.63 mmol). The mixture was stirred overnight at room temperature under nitrogen. The reaction was extracted with 1M HCl and CH_2Cl_2. The organic phase was collected, dried over anhydrous $MgSO_4$ and concentrated in vacuo to a yellow oil. The crude oil was purified via silica column chromatography using 0-2% MeOH/CH_2Cl_2 as an eluent to yield product as an off-white solid (383 mg, 1.05 mmol). Yield = 48%. ^{1}H NMR (400 MHz, $CDCl_3$-*d*$_1$, 25 °C): δ = 3.92 (s, 3H; OC*H*$_3$), 4.41 (d, *J* = 5.6 Hz, 2H; NHC*H*$_2$), 4.99

(s, 2H; C*H*$_2$), 6.91 (t, *J* = 8.8 Hz, 2H; ArH), 7.07 (dd, *J* = 8.0, 1.6 Hz, 1H; ArH), 7.11 (dd, *J* = 8.4, 5.2 Hz, 2H; ArH), 7.16 (t, *J* = 8.2 Hz, 1H; ArH), 7.22 (dd, *J* = 7.2, 1.6 Hz, 2H; ArH), 7.29 - 7.37 (m, 3H; ArH), 7.74 (dd, *J* = 7.6, 1.6, Hz, 1H; ArH), 8.31 (brs, 1H; CON*H*CH$_2$). ESI-MS(+) *m/z* 366.27 $[M+H]^+$, 388.25 $[M+Na]^+$.

N-(4-Fluorobenzyl)-2-hydroxy-3-methoxybenzamide (RCD-9): 2,3-Bis(benzyloxy)-N-(4-fluorobenzyl)benzamide (300 mg, 0.82 mmol), was stirred in 10 mL of a 1:1 solution of HCl:HOAc at room temperature for 5 days under ambient conditions. The reaction was evaporated to dryness in vacuo and the residue was co-evaporated with 3x5 mL MeOH. The resulting solid was dried overnight under vacuum to yield product, **RCD-9** as a light yellow solid (163 mg, 0.59 mmol). Yield = 72%. ^{1}H NMR (500 MHz, DMSO-*d*$_6$, 25 °C): δ = 3.74 (s, 3H; OC*H*$_3$), 4.43 (d, *J* = 6.3 Hz, 2H; NHC*H*$_2$), 6.78 (t, *J* = 8.0 Hz, 1H; ArH), 7.07 (d, *J* = 7.4 Hz, 1H; ArH), 7.11 (t, *J* = 8.9, Hz, 2H; ArH), 7.31 (dd, *J* = 8.6, 3.4 Hz, 2H; ArH), 7.41 (dd, *J* = 8.0, 1.1 Hz, 2H; ArH), 9.32 (t, *J* = 6.0 Hz, 1H; CON*H*CH$_2$). ^{13}C NMR (125 MHz, DMSO-*d*$_6$, 25 °C): 42.1 (CH_2), 56.2 (OCH_3), 115.5 (ArC), 115.6 (ArC), 115.9 (ArC), 118.4 (ArC), 119.1 (ArC), 129.7 (ArC), 129.8 (ArC), 135.5 (ArC), 148.9 (ArC), 151.2 (ArC), 169.8 (C=O). ESI-MS(+) *m/z* 276.20 $[M+H]^+$. Anal. Calcd for $C_{15}H_{14}FNO_3$: C, 65.45; H, 5.13; N, 5.09. Found: C, 65.76; H, 5.51; N, 5.12.

Dimethyl 2,3-bis(benzyloxy)terephthalate: To a solution of dimethyl 2,3-dihydroxyterephthalate (1 g, 4.4 mmol) in 20 mL, DMF was added K_2CO_3 (2.43 mg, 17.6 mmol) and benzyl bromide (120 μL, 10 mmol). The mixture was refluxed for 10 h at 85 °C under nitrogen. The insoluble salts were filtered off via vacuum filtration. To the filtrate, approximately 10 mL of cold H_2O was added. The resulting off-white precipitate

was collected and dried under vacuum to yield product (1.06 g, 3.96 mmol). Yield = 90%. ^{1}H NMR (400 MHz, $CDCl_3$, 25 °C): δ = 4.49 (d, *J*=8.0 Hz, 4H), 6.86 (t, *J*= 8.0 Hz, 4H; ArH), 7.16 (t, *J*=6.0 Hz, 4H; ArH), 7.99 (t, *J*=8.0 Hz, 1H; ArH), 8.32 (d, *J*=8.0 Hz, 2H; ArH), 8.37 (brt, *J*=8.0 Hz, 2H; N*H*). ESI-MS(+) *m/z* 381.99 $[M+H]^+$.

2,3-Bis(benzyloxy)terephthalic acid: To a solution of Dimethyl 2,3-bis(benzyloxy)terephthalate (1.1 g, 2.7 mmol) in 60 mL THF was added, 20 mL of 4% KOH/H_2O. The solution was stirred for 4 h at room temperature under nitrogen. The reaction was quenched with 40 mL of cold H_2O. The reaction mixture was washed with EtOAc. The aqueous phase was acidified with 6M HCl until precipitate formed. The solid was filtered and collected and dried over night under vacuum to yield product as a white solid (928 mg, 2.45 mmol)**.** Yield = 91%. ^{1}H NMR (400 MHz, d_6-DMSO, 25 °C): δ = 5.02 (s, 4H), 7.33 (m, 6H; ArH), 7.39 (m, 4H; ArH), 7.48 (s, 2H; ArH). ESI-MS(-) *m/z* 376.83 $[M-H]^-$.

(2,3-Bis(benzyloxy)-1,4-phenylene)bis((2-thioxothiazolidin-3-yl)methanone): Synthesis adapted from literature procedure.[186] Starting from 2,3-bis(benzyloxy)terephthalic (800 mg, 2.11 mmol) and producing a yellow solid product (1.08 g, 1.87 mmol). Yield = 89%. ^{1}H NMR (400 MHz, $CDCl_3$, 25 °C): δ = 2.95 (t, *J*=8.0 Hz, 4H), 4.31 (t, *J*= 8.0 Hz, 4H), 5.07 (s, 4H), 7.20 (s, 2H; ArH), 7.35 (m, 10H; ArH). ESI-MS(+) *m/z* 580.74 $[M+H]^+$.

2,3-Bis(benzyloxy)-N1-(4-fluorobenzyl)-N4-methylterephthalamide: To a solution of 2,3-Bis(benzyloxy)-1,4-phenylene)bis((2-thioxothiazolidin-3-yl)methanone) in 120 μL of CH_2CL_2, was added FPMA (80 μL, 0.7 mmol). The mixture was stirred for 3 h under nitrogen. The reaction mixture was evaporated to dryness in vacuo. The

resulting residue was partially purified via silica plug using 5% MeOH/CH_2CL_2 as an eluent. To a solution of this material in 12 mL of CH_2Cl_2, was added 800 mL of CH_3NH_2 (40% aqueous solution). The reaction was stirred for 30 minutes under nitrogen. The reaction mixture was evaporated to dryness under vacuo. The residue was purified via silica column chromatography using 0-5% MeOH/CH_2CL_2 as eluent to yield product as a white solid (343 mg, 0.69 mmol). Yield = 98%. ^{1}H NMR (400 MHz, $CDCl_3$, 25 °C): δ = 2.82 (d, *J*=4.0 Hz, 3H), 4.44 (d, *J*= 8.0 Hz, 2H), 5.08 (d, *J*=4.0 Hz, 4H), 6.93 (t, *J*=8.0 Hz, 2H; ArH), 7.20 (m, 12H; ArH), 7.66 (brt, *J*=8.0 Hz, 1H; N*H*), 7.93 (q, *J*=8.0 Hz, 2H; ArH), 8.10 (brt, *J*=8.0 Hz, 1H; N*H*). ESI-MS(+) *m/z* 498.90 $[M+H]^+$.

N1-(4-Fluorobenzyl)-2,3-dihydroxy-N4-methylterephthalamide (RCD-10): 2,3-Bis(benzyloxy)-N1-(4-fluorobenzyl)-N4-methylterephthalamide (340 mg, 0.68 mmol) was stirred in 18 mL of a 1:1 solution of HCl:HOAc at room temperature for 3 days under ambient conditions to obtain a turbid mixture. Addition of 8 mL of cold H_2O resulted in precipitation of a white solid. The solid was isolated by filtration, washed with water and dried under vacuum to yield product **RCD-10**, as a white solid (159 mg, 0.5 mmol). Yield = 73%. ^{1}H NMR (400 MHz, d_6-DMSO, 25 °C): δ = 2.80 (d, *J*=4.0 Hz, 3H), 4.47 (d, *J*=8.0 Hz, 2H), 7.15 (t, *J*= 8.0 Hz, 2H; ArH), 7.33 (d, *J*=8.0 Hz, 2H; ArH), 7.36 (t, *J*=8.0 Hz, 2H; ArH), 8.87 (brt, *J*=4.0 Hz, 1H; N*H*), 9.36 (brt, *J*=4.0 Hz, 1H; N*H*). ESI-MS(+) *m/z* 318.96 $[M+H]^+$. Anal. Calcd for ($C_{16}H_{15}FN_2O_4$): C, 63.39; H, 4.91; N, 5.69. Found: C, 62.54; H, 4.79; N, 5.89.

2,3-Bis(benzyloxy)-N1,N4-bis(4-fluorobenzyl)terephthalamide: To a solution of dimethyl 2,3-bis(benzyloxy)terephthalate (300 mg, 0.79 mmol) in 100 mL, was added FPMA (108 μL, 0.95 mmol). The reaction was stirred at room temperature overnight

under nitrogen. The solvent was removed in vacuo. The crude product was purified via silica column chromatography using CH_2Cl_2 as an eluent to yield product as a white solid (252 mg, 0.427 mmol). Yield = 54%. ^{1}H NMR (400 MHz, $CDCl_3$, 25 °C): δ = 4.42 (d, *J*=10.0 Hz, 4H), 5.05 (s, 4H), 6.95 (t, *J*= 8.0 Hz, 4H; ArH), 7.14 (m, 10H; ArH), 7.29 (t, *J*=8.0 Hz, 4H; ArH), 7.35 (s, 2H; ArH), 8.06 (brt, *J*=8.0 Hz, 2H; N*H*). ESI-MS(+) *m/z* 592.95 $[M+H]^+$.

N1,N4-Bis(4-fluorobenzyl)-2,3-dihydroxyterephthalamide (RCD-11): 2,3-Bis(benzyloxy)-N1,N4-bis(4-fluorobenzyl)terephthalamide (250 mg, 0.42 mmol) was stirred in 16 mL of a 1:1 solution of HCl:HOAc at room temperature for 3 days under ambient conditions, to obtain a turbid mixture. Addition of 6 mL H_2O resulted in precipitation of a white solid. The solid was isolated by filtration, washed with water and dried under vacuum to yield product **RCD-11**, as a white solid (143 mg, 0.35 mmol). Yield = 83%. ^{1}H NMR (400 MHz, $CDCl_3$, 25 °C): δ = 4.62 (d, *J*=4.0 Hz, 4H), 7.05 (t, *J*= 8.0 Hz, 4H; ArH), 7.14 (s, 2H; ArH), 7.20 (brt, *J*=6.0 Hz, 2H; N*H*), 7.33 (t, *J*=6.0 Hz, 4H; ArH), 10.74 (brs, 2H, O*H*). ESI-MS(+) *m/z* 412.96 $[M-H]^+$. Anal. Calcd for ($C_{22}H_{18}F_2N_2O_4$): C, 72.69; H, 5.10; N, 4.73. Found: C, 73.17; H, 5.45; N, 4.89.

8-(Benzyloxy)quinoline-7-carboxylic acid: To a solution of 8-hydroxyquinoline-7-carboxylic acid (500 mg, 2.64 mmol) in 10 mL of DMF, was added, benzyl chloride (782 μL, 6.78 mmol) and K_2CO_3 (1.03 g, 7.47 mmol). The reaction mixture was heated to reflux at 120 ˚C stirred overnight under nitrogen. The reaction was filtered and the filtrate was concentrated in vacuo to a reddish-brown oil. The crude oil was purified via a silica plug in CH_2Cl_2 as an eluent to yield product as an orange oil (585 mg, 1.58 mmol). Yield = 60%. To a solution of this oil (585 mg, 1.58 mmol) in 5 mL of MeOH, was added 3 mL

of a 6M NaOH solution. The solution was stirred overnight at room temperature under nitrogen. The solvent was removed in vacuo and the acid product was extracted with CH_2Cl_2 and 6M HCl. The organic phase collected, dried over anhydrous $MgSO_4$, and concentrated in vacuo to yield product as a yellow solid (444 mg, 1.58 mmol). Yield = 100%. ^{1}H NMR (400 MHz, DMSO-d_6, 25 °C): δ = 5.43 (s, 2H; CH_2), 7.33 (d, J = 7.2 Hz, 2H; ArH), 7.37 (t, J = 7.2 Hz, 2H; ArH), 7.58 (d, J = 6.8 Hz, 2H; ArH), 7.63 (dd, J = 8.4, 4.4 Hz, 1H; ArH), 7.77 (d, J = 2.4 Hz, 1H; ArH), 8.42 (dd, J = 8.4, 1.4 Hz, 1H; ArH), 9.01 (dd, J = 4.4, 2.0 Hz, 1H; ArH). ESI-MS(-) *m/z* 278.32 $[M-H]^-$.

8-(Benzyloxy)-N-(4-fluorobenzyl)quinoline-7-carboxamide: To a solution of 8-(Benzyloxy)quinoline-7-carboxylic acid (400 mg, 1.43 mmol) in 15 mL of dry CH_2Cl_2, was added EDCI (329 mg, 1.72 mmol), HOBt (232 mg, 1.72 mmol) and FPMA (197 µL, 1.72 mmol). The mixture was stirred overnight at room temperature under nitrogen. The reaction was extracted with 1M HCl and CH_2Cl_2. The organic phase was collected, dried over anhydrous $MgSO_4$ and concentrated in vacuo to a yellow oil. The crude oil was purified via silica column chromatography using 0-2% MeOH/CH_2Cl_2 as an eluent to yield product as a yellow solid (171 mg, 0.44 mmol). Yield = 31%. ^{1}H NMR (400 MHz, $CDCl_3$-d_1, 25 °C): δ = 4.43 (d, J = 5.6 Hz, 2H; NHCH_2), 5.51 (s, 2H; CH_2), 6.92 (t, J = 8.8 Hz, 2H; ArH), 7.13 (dd, J = 6.4, 3.0 Hz, 2H; ArH), 7.32 (d, J = 5.2 Hz, 5H; ArH), 7.48 (dd, J = 8.4, 4.0 Hz, 1H; ArH), 7.64 (d, J = 8.4 Hz, 1H; ArH), 8.18 (dd, J = 8.4, 2.0, Hz, 1H; ArH), 8.28 (d, J = 8.8 Hz, 1H; ArH), 8.60 (brt, 1H; CONHCH$_2$), 8.99 (dd, J = 4.0, 1.6 Hz, 1H; ArH). ESI-MS(+) *m/z* 387.11 $[M+H]^+$.

7-((4-fluorobenzyl)amino)quinolin-8-ol (RCD-12): 8-(Benzyloxy)-N-(4-fluorobenzyl)quinoline-7-carboxamide (154 mg, 0.40 mmmol) was stirred in 10 mL of a

1:1 solution of HCl:HOAc at room temperature for 5 days under ambient conditions. The solution was evaporated to dryness in vacuo and the resulting residue was co-evaporated with 3x5 mL of MeOH. The resulting solid was dried overnight under vacuum to yield product **RCD-12,** as a yellow solid (101 mg, 0.34 mmol). Yield = 85%. ^{1}H NMR (500 MHz, DMSO-d_6, 25 °C): δ = 4.54 (d, J = 4.6 Hz, 2H; NHCH_2), 7.13 (t, J = 8.6 Hz, 2H; ArH), 7.38 (t, J = 6.0 Hz, 2H; ArH), 7.57 (d, J = 9.1, Hz, 1H; ArH), 7.85 (brt, 1H; ArH), 8.17 (d, J = 8.6 Hz, 1H; ArH), 8.67 (d, J = 8.0 Hz, 1H; ArH), 9.00 (brs, 1H; ArH), 9.75 (brt, 1H; CONHCH$_2$. ^{13}C NMR (125 MHz, DMSO-d_6, 25 °C): 42.4 (CH_2), 113.6 (ArC), 115.5 (ArC), 115.7 (ArC), 117.7 (ArC), 124.4 (ArC), 126.1 (ArC), 130.0 (ArC), 131.4 (ArC), 135.4 (ArC), 148.2 (ArC), 155.9 (ArC), 160.7 (ArC), 162.7 (ArC), 168.8 (C=O). ESI-MS(+) m/z 297.12 $[M+H]^+$. Anal. Calcd for $C_{17}H_{13}FN_2O_2$•2.25 H_2O: C, 60.62; H, 5.24; N, 8.32. Found: C, 60.53; H, 4.83; N, 8.33.

2-((4-fluorobenzyl)amino)quinolin-8-ol (RCD-13): To a solution of 8-hydroxyquinoline-2-carboxylic acid, (400 mg, 2.1 mmol) in 20 mL of CH_2Cl_2, was added EDCI (487 mg, 2.5 mmol), HOBt (343 mg, 2.5 mmol), and FPMA (290 μL, 2.5 mmol). The resulting mixture was stirred at room temperature for 16 h under nitrogen. The mixture was washed with 1M HCl and brine. The organic phase was collected, dried over anhydrous $MgSO_4$ and concentrated in vacuo to a crude product. The crude solid was purified via silica column chromatography in using 0-5% MeOH/CH_2Cl_2 as an eluent to yield product **RCD-13**, as a pale yellow solid (383 mg 1.3 mmol) Yield = 61%. ^{1}H NMR (400 MHz, d_6-DMSO, 25 °C): δ = 4.59 (d, J=8.0 Hz, 2H), 7.17 (t, J= 8.0 Hz, 2H; ArH), 7.19 (d, J=8.0 Hz, 1H; ArH), 7.40 (t, J=4.0 Hz, 2H; ArH), 7.46 (d, J=8.0 Hz, 1H; ArH), 7.55 (t, J=8.0 Hz, 1H; ArH), 8.15 (d, J=8.0 Hz, 1H; ArH), 8.49 (d, J=8.0 Hz, 1H; ArH),

10.14 (brt, *J*=8.0 Hz, 1H; N*H*). ESI-MS(+) *m/z* 297.09 $[M+H]^+$. Anal. Calcd for ($C_{17}H_{13}FN_2O_2$): C, 68.91; H, 4.42; N, 9.45. Found: C, 68.96; H, 4.79, N, 5.91.

7-((4-Fluorobenzyl)carbamoyl)-8-hydroxyquinoline 1-oxide (RCD-14): This compound was prepared from 7-((4-fluorobenzyl)amino)quinolin-8-ol from an adapted literature procedure.[65] To a mixture of 1.8 mL TFA and 230 µL of 30% H_2O_2 was added to 7-((4-fluorobenzyl)amino)quinolin-8-ol (183 mg, 0.5 mmol). The solution was refluxed at 80 °C for 16 h. The reaction was cooled to room temperature. Approximately 9 mL of water was added and the resulting brown precipitate was isolated via filtration. The solid was dried under vacuum to yield product **RCD-14** as a light brown solid (55 mg, 0.175 mmol).Yield = 35%. ^{1}H NMR (400 MHz, $CDCl_3$, 25 °C): δ = 4.72 (d, *J*=8.0 Hz, 2H), 7.05 (t, *J*= 8.0 Hz, 2H; ArH), 7.39 (m, 3H; ArH), 7.61 (dd, *J*=8.0 Hz, *J*=4.0 Hz, 1H; ArH), 8.17 (d, *J*=8.0 Hz, 1H; ArH), 8.24 (d, *J*=8.0 Hz, 1H), 8.27 (br, 1H; N*H*), 8.89 (d, *J*=4.0 Hz, 1H). ESI-MS(+) *m/z* 296.97 $[M-O-]^+$. Anal. Calcd for ($C_{17}H_{13}FN_2O_3$): C, 65.38; H, 4.20; N:8.97. Found: C, 63.42; H, 4.85; N, 8.17.

N-(4-Fluorobenzyl)-2-hydroxybenzamide (RCD-15): To a solution of 2-hydroxybenzoic acid (500 mg, 3.6 mmol) in 20 mL of CH_2Cl_2, was added EDCI (833 mg, 4.3 mmol), HOBt (585 mg, 4.3 mmol), and FPMA (495 µL, 4.3 mmol). The mixture was stirred at room temperature for 16 h under nitrogen. The reaction was rinsed with 1M HCl and brine. The organic phase was collected, dried over anhydrous $MgSO_4$ and concentrated in vacuo to a solid residue. The crude product was purified via flash silica column chromatography in CH_2Cl_2 as an eluent to yield product **RCD-15**, as a white solid (302 mg, 1.2 mmol). Yield = 34%. ^{1}H NMR (400 MHz, d_6-DMSO, 25 °C): δ = 4.48 (d, *J*=4.0 Hz, 2H), 6.88 (t, *J*= 8.0 Hz, 2H; ArH), 7.13 (t, *J*=8.0 Hz, 2H; ArH), 7.38 (m,

3H; ArH), 7.86 (d, *J*=8.0 Hz, 1H; ArH), 9.34 (brt, *J*=8.0 Hz, 1H; N*H*). ESI-MS(+) *m/z* 245.99 $[M+H]^+$. Anal. Calcd for ($C_{14}H_{12}FNO_2$): C, 68.56; H, 4.93; N, 5.71. Found: C, 68.18; H, 5.35; N, 5.87.

6-((Benzyloxy)carbonyl)picolinic acid: To a solution of pyridine-2,6-dicarboxylic acid **(**2.0 g, 12 mmol) in 40mL DMF, was added $NaHCO_3$ (1.18 g, 14.4 mmol) and benzyl bromide (1.7 mL, 14.4 mmol). The reaction mixture was heated to 60 °C for 16 h under nitrogen. The solution was cooled to room temperature. To the reaction mixture, 40 mL cold H_2O was added. The aqueous solution was acidified to pH 3 with 1M HCl. The solution was extracted with EtOAc, the organic phase was collected, dried over anhydrous $MgSO_4$, and concentrated in vacuo to yield product as a white solid (493 mg, 1.75mmol). Yield = 16%. ^{1}H NMR (400 MHz, d_6-DMSO, 25 °C): δ = 5.41 (s, 2H), 7.45 (m, 5H; ArH), 8.22 (m, 3H; ArH). ESI-MS(-) *m/z* 255.92 $[M-H]^-$.

***N*-(4-Fluorobenzyl)-6-(2-phenylacetyl)picolinamide:** To a solution of 6-((Benzyloxy)carbonyl)picolinic acid (400 mg, 1.56 mmol) in 15 mL of dry CH_2Cl_2, was added EDCI (347 mg, 1.80 mmol), HOBt (240 mg, 1.80 mmol) and FPMA (205 μL, 1.80 mmol). The mixture was stirred overnight at room temperature under nitrogen. The reaction mixture was extracted with 1M HCl and CH_2Cl_2. The organic phase was collected, dried over anhydrous $MgSO_4$ and concentrated in vacuo to a brown oil. The oil was purified via silica column chromatography using 0-1% MeOH/CH_2Cl_2 as an eluent to yield the product as a white solid (54 mg, 0.157 mmol). Yield = 10%. ^{1}H NMR (400 MHz, $CDCl_3$, 25 °C): δ = 4.65 (d, *J*=8.0 Hz, 2H), 5.43 (s, 2H), 7.02 (t, *J*= 8.0 Hz, 2H; ArH), 7.36 (m, 7H; ArH), 8.01 (t, *J*=8.0 Hz, 1H; ArH), 8.22 (d, *J*=8.0 Hz, 1H; ArH), 8.40 (d, *J*=8.0 Hz, 1H; ArH), 8.54 (brt, *J*=8.0 Hz, 1H; N*H*). ESI-MS(+) *m/z* 364.90 $[M+H]^+$.

6-((4-fluorobenzyl)carbamoyl)picolinic acid: To a solution of *N*-(4-Fluorobenzyl)-6-(2-phenylacetyl)picolinamide (300 mg, 0.82 mmol) in 20 mL MeOH, was added KOH (157 mg, 2.8 mmol). The reaction mixture was heated to 85 °C for 4 h under nitrogen. The reaction was neutralized with HCl. Solvent was removed in vacuo and the resulting solid was dissolved in 5% MeOH/DCM. Insoluble particles were hot filtered and the solution was dried in vacuo to yield product as a white solid (202 mg, 0.73 mmol). Yield= 90%. ^{1}H NMR (400 MHz, $CDCl_3$, 25 °C): δ= 4.32 (d, *J*=4.0 Hz, 2H), 6.72 (t, J= 8.0 Hz, 2H; ArH), 7.01 (t, *J*=6.0 Hz, 2H; ArH), 7.54 (brt, *J*=6.0 Hz, 1H; N*H*), 7.87 (d, *J*=8.0 Hz, 1H; ArH), 7.95 (d, *J*=4.0 Hz, 1H), 8.82 (brt, *J*=6.0 Hz, 1H; N*H*). ESI-MS(-) *m/z* 272.90 $[M-H]^-$.

2-Carboxy-6-((4-fluorobenzyl)carbamoyl)pyridine 1-oxide (RCD-16): Synthesis adapted from literature procedure.[65] To a mixture of 1.5 mL TFA and 220 μL of 30% H_2O_2 was added to 6-((4-fluorobenzyl)carbamoyl)picolinic acid (100 mg, 0.55 mmol). The solution was refluxed at 80 °C for 16 h. The reaction was cooled to room temperature. Approximately 7 mL of water was added and the resulting brown precipitate was isolated via filtration. The solid was dried under vacuum to yield product **RCD-16** as a light brown solid (30 mg, 0.104 mmol). Yield = 19%. ^{1}H NMR (400 MHz, $CDCl_3$, 25 °C): δ = 4.67 (d, *J*=4.0 Hz, 2H), 7.06 (t, *J*= 8.0 Hz, 2H; ArH), 7.35 (t, *J*=6.0 Hz, 2H; ArH), 7.82 (t, *J*=8.0 Hz, 1H; ArH), 8.60 (dd, *J*=8.0 Hz, *J*=4.0 Hz, 1H; ArH), 8.74 (dd, *J*=8.0 Hz, *J*=4.0 Hz, 1H; ArH), 10.29 (brt, *J*=8.0 Hz, 1H; N*H*). ESI-MS(-) *m/z* 288.65 $[M-H]^-$. Anal. Calcd for ($C_{14}H_{11}FN_2O_4$): C, 57.93; H, 3.82; N, 9.65. Found: C, 58.19; H, 4.10; N, 9.37.

N2,N6-Bis(4-fluorobenzyl)pyridine-2,6-dicarboxamide: To a solution of pyridine-2,6-dicarboxylic acid (400 mg, 2.4 mmol) in 15 mL of CH_2Cl_2**,** was added EDC (1 g, 5.3 mmol), HOBt (712 mg, 5.3 mmol), and FPMA (620 μL, 5.3 mmol). The mixture was stirred at room temperature for 16 h under nitrogen. The reaction was then washed with 1M HCl and brine. The organic phase was collected, dried over anhydrous $MgSO_4$ and concentrated in vacuo to a crude reside. The crude product was purified via silica column chromatography in 0-5% MeOH/CH_2Cl_2 as an eluent to yield the product as a beige solid (594 mg, 1.50 mmol). Yield = 65%. ^{1}H NMR (400 MHz, $CDCl_3$, 25 °C): δ = 4.49 (d, *J*=8.0 Hz, 4H), 6.86 (t, *J*= 8.0 Hz, 4H; ArH), 7.16 (t, *J*=6.0 Hz, 4H; ArH), 7.99 (t, *J*=8.0 Hz, 1H; ArH), 8.32 (d, *J*=8.0 Hz, 2H; ArH), 8.37 (brt, *J*=8.0 Hz, 2H; N*H*). ESI-MS(+) *m/z* 381.99 $[M+H]^+$.

2,6-Bis((4-fluorobenzyl)carbamoyl)pyridine 1-oxide (RCD-17): Synthesis adapted from literature procedure.[65] To a mixture of 3.2 mL TFA and 450 μL of 30% H_2O_2 was added to N2,N6-Bis(4-fluorobenzyl)pyridine-2,6-dicarboxamide (580 mg, 1.5 mmol). The solution was refluxed at 80 °C for 16 h. The reaction was cooled to room temperature. Approximately 9 mL of cold H_2O was added and the resulting in a crude brown precipitate. The crude product was isolated via filtration and purified via silica column chromatography using 0-5% MeOH/CH_2Cl_2 as an eluent to yield product **RCD-17** as a light brown solid (59 mg, 0.15 mmol). Yield: 10%. ^{1}H NMR (300 MHz, $CDCl_3$, 25 °C): δ = 4.63 (d, *J*=6.0 Hz, 4H), 7.03 (t, *J*= 9.0 Hz, 4H; ArH), 7.33 (t, *J*=7.5 Hz, 4H; ArH), 7.62 (t, *J*=6.0 Hz, 1H; ArH), 8.60 (d, *J*=6.0 Hz, 2H; ArH), 10.93 (br, 2H; N*H*). ESI-MS(+) *m/z* 397.98 $[M+H]^+$. Anal. Calcd for ($C_{21}H_{17}F_2N_3O_3$): C, 63.47; H, 4.31; N, 10.57. Found: C, 63.10; H, 4.40; N, 10.72.

(2-Methoxy-1,3-phenylene)bis((2-thioxothiazolidin-3-yl)methanone):

Synthesis adapted from literature procedure.[186] To a solution of 2-methoxyisophthalic acid (2.7 g, 13.8 mmol) in 120 mL of DCM, was added Thiazolidine-2-thione (3.3 g, 28 mmol), a catalytic amount of DMAP, and N,N-Dicyclohexylcarbodiimide (DCC) (5.7 g, 28 mmol). The mixture was stirred for 5 h at room temperature under nitrogen. The solution was filtered and the solvent was removed from the filtrate in vacuo. The compound was purified via silica column chromatography in CH_2Cl_2 as an eluent to yield product as a bright yellow solid (1.6 g, 3.9 mmol). Yield = 29%. ^{1}H NMR (400 MHz, $CDCl_3$, 25 °C): δ = 3.42 (t, *J*=8.0 Hz, 4H), 3.90 (s, 3H), 4.60 (t, *J*=8.0 Hz, 4H), 7.14 (t, *J*=8.0 Hz, 1H; ArH), 7.43 (d, *J*=4.0 Hz, 2H; ArH). ESI-MS(+) *m/z* 398.67 $[M+H]^+$.

***N*-(4-Fluorobenzyl)-2-methoxy-3-(2-thioxothiazolidine-3-carbonyl)benzamide:** Synthesis adapted from literature procedure.[187] To a solution of (2-Methoxy-1,3-phenylene)bis((2-thioxothiazolidin-3-yl)methanone) (300 mg, 0.73 mmol) in 100 mL of DCM, was added FPMA (29 μL, 0.24 mmol). The reaction mixture was stirred overnight at room temperature under nitrogen. The solvent was then removed in vacuo and the resulting crude compound was purified via silica column chromatography in CH_2Cl_2 as an eluent to yield product as a bright yellow solid (259 mg, 0.642 mmol). Yield = 88%. ^{1}H NMR (400 MHz, $CDCl_3$, 25 °C): δ = 3.43 (t, *J*=6.0 Hz, 2H), 3.75 (s, 3H), 4.60 (d, *J*=4.0 Hz, 2H), 4.65 (t, *J*= 8.0 Hz, 2H), 7.02 (t, *J*=8.0 Hz, 2H; ArH), 7.21 (t, *J*=8.0 Hz, 1H; ArH), 7.25 (t, *J*=4.0 Hz, 2H; ArH), 7.33 (d, *J*=8.0 Hz, 1H; ArH), 7.80 (brt, *J*=8.0 Hz, 1H; N*H*), 8.15 (d, *J*=8.0 Hz, 1H; ArH). ESI-MS(+) *m/z* 404.81 $[M+H]^+$.

N1-(4-Fluorobenzyl)-2-methoxy-N3-methylisophthalamide: To a solution of *N*-(4-Fluorobenzyl)-2-methoxy-3-(2-thioxothiazolidine-3-carbonyl)benzamide (150 mg, 0.37 mmol) in 4 mL, DCM was added 230 μL of 40% aq. CH_3NH_2. The solution mixture was stirred vigorously for 30 minutes at room temperature under nitrogen. The solution was washed with water. The organic phase was collected, dried over anhydrous $MgSO_4$ and concentrated in vacuo to crude residue. The crude product was purified via silica column chromatography using 0-10% MeOH/CH_2Cl_2 as an eluent to yield product as yellow solid (89 mg, 0.281 mmol). Yield = 76%. ^{1}H NMR (400 MHz, $CDCl_3$, 25 °C): δ = 2.93 (d, *J*=4.0 Hz, 3H), 3.69 (s, 3H), 4.55 (d, *J*= 4.0 Hz, 2H), 6.99 (t, *J*=8.0 Hz, 2H; ArH), 7.22 (t, *J*=8.0 Hz, 1H; ArH), 7.29 (t, *J*=8.0 Hz, 2H; ArH), 7.75 (brt, *J*=8.0 Hz, 1H; N*H*), 7.94 (d, *J*=8.0 Hz, 1H; ArH), 7.98 (d, *J*=9.0 Hz, 1H; ArH). ESI-MS(+) *m/z* 317.0 $[M+H]^+$.

N1-(4-fluorobenzyl)-2-hydroxy-N3-methylisophthalamide (RCD-18): To a solution of N1-(4-Fluorobenzyl)-2-methoxy-N3-methylisophthalamide (85 mg, 0.26 mmol) in 15 mL DCM was added, BBr_3 (140 μL, 0.21 mmol) under nitrogen at 0 °C. The mixture was allowed to warm to room temperature and was stirred for 3 days under nitrogen. The reaction was quenched with 8 mL MeOH and diluted with 10 mL of water. The solution was boiled until the yellow color dissipated and water volume was reduced by half. The solution was cooled to room temperature and MeOH was added to induce precipitation. The precipitate was isolated via filtration and dried under vacuum to yield product as a white solid (30.6 mg, 010 mmol) Yield = 36%. ^{1}H NMR (400 MHz, $CDCl_3$, 25 °C): δ = 3.01 (d, *J*=4.0 Hz, 3H), 4.61 (d, *J*= 4.0 Hz, 2H), 6.87 (t, *J*=8.0 Hz, 1H; ArH), 7.01 (t, *J*=8.0 Hz, 2H; ArH), 7.30 (t, *J*=6.0 Hz, 2H; ArH), 7.61 (br, 1H; N*H*), 7.90 (d,

j=8.0 Hz, 1H), 8.05 (d, *J*=8.0 Hz, 1H; ArH), 8.29 (br, 1H; N*H*). ESI-MS(+) *m/z* 302.95 $[M+H]^+$. Anal. Calcd for ($C_{16}H_{14}FNO_4$): C, 63.57; H, 5.00; N, 9.27. Found: C, 63.32; H, 5.10; N, 9.28.

N1,N3-Bis(4-fluorobenzyl)-2-methoxyisophthalamide: To a solution of (2-Methoxy-1,3-phenylene)bis((2-thioxothiazolidin-3-yl)methanone) (300 mg, 0.75 mmol) in 100 mL DCM was added, FPMA (215 μL, 1.87 mmol). The reaction was stirred at room temperature overnight under nitrogen. The solvent was removed in vacuo. The crude product was purified via flash silica column chromatography using CH_2Cl_2 as an eluent to yield product as a bright yellow solid (71 mg, 0.172 mmol). Yield = 23%. ^{1}H NMR (400 MHz, $CDCl_3$, 25 °C): δ = 3.43 (t, *J*=6.0 Hz, 2H), 3.75 (s, 3H), 4.60 (d, *J*= 8.0 Hz, 2H), 4.64 (t, *J*=6.0 Hz, 2H), 7.03 (t, *J*=8.0 Hz, 2H; ArH), 7.24 (t, *J*=8.0 Hz, 1H; ArH), 7.31 (t, *J*=8.0 Hz, 2 H; ArH), 7.41 (d, *J*=8.0 Hz, 1H; ArH), 7.76 (brt, *J*=8.0 Hz, 1H; N*H*), 8.16 (d, *J*=8.0 Hz, 1H; ArH). ESI-MS(+) *m/z* 404.79 $[M+H]^+$.

N1,N3-Bis(4-fluorobenzyl)-2-hydroxyisophthalamide (RCD-19): To a solution of N1,N3-Bis(4-fluorobenzyl)-2-methoxyisophthalamide (70 mg, 0.17 mmol) in 15 mL DCM was added, BBr_3 (142 μL, 0.23 mmol) under nitrogen at 0 °C. The mixture was allowed to warm to room temperature and was stirred for 3 days under nitrogen. The reaction was quenched with 8 mL MeOH and diluted with 10 mL of water. The solution was boiled until the yellow color dissipated and water volume was reduced by half. The solution was cooled to room temperature and MeOH was added to induce precipitation. The precipitate was isolated via filtration and dried under vacuum to yield product as white solid (14 mg, 0.035 mmol). Yield = 21%. ^{1}H NMR (400 MHz, $CDCl_3$, 25 °C): δ = 4.64 (d, *J*=4.0 Hz, 4H), 6.97 (t, *J*= 8.0 Hz, 1H; ArH), 7.04 (t, *J*=8.0 Hz, 4H; ArH), 7.33

(t, *J*=6.0 Hz, 4H; ArH), 7.70 (br, 2H; N*H*), 7.97 (d, *J*=8.0 Hz, 2H). ESI-MS(+) *m/z* 396.93 $[M+H]^+$. Anal. Cacld for ($C_{22}H_{18}F_2N_2O_3$): C, 66.66; H, 4.58; N, 7.07. Found: C, 66.54; H, 4.98; N, 6.86.

Computational Docking Studies: The coordinates for the X-ray crystal structure of PFV-IN were taken from the RCSB Protein Data Bank (entry: 3OYA) and prepared using the Protein Preparation Wizard, which is a part of the Maestro software package (Maestro v9.1; Schrodinger, Inc.). The Protein Preparation Wizard was used to add bond order assignments and formal charges for heterogroups (amino acid residues, metal-ligand bonds) and hydrogen atoms to the system. To optimize the hydrogen bonding network histidine tautomers and ionization states were predicted, and manual corrections were made when necessary to ensure correct coordination with the two Mg(II) ions. Proper assignment of Asn and Gln side chains was assessed by rotating 180º around the terminal χ angle of these residues while adding hydrogen atoms to sample the hydrogen bonding network around the residues; to determine if the oxygen and nitrogen atoms were properly assigned. All water molecules in the structure were removed.

Three-dimensional structures of the RCD fragments and raltegravir were prepared using LigPrep (LigPrep v2.4 Schrodinger, Inc.) with Epik (Epik v2.1 Schrodinger, Inc.) to generate multiple protonation and tautomeric states for the ligands at pH values of 7.0±2.0. The metal binding state (i.e. deprotonated hydroxyl groups) of the RCD compounds were docked flexibly into the active site of the prepared PFV-IN structure. Docking was performed with Glide 5.5 (Glide v5.5; Schrodinger, Inc.) with the standard precision scoring function to estimate protein-ligand binding affinities. A maximum of ten scoring poses were saved for each fragment. The top scoring poses for each fragment

were found to possess the most reasonable and expected binding modes with reasonable metal-ligand bond distances based on the 3OYA crystal complex.

To calculate the RMSD of the various compounds, the superposition tool within Maestro was used. The two compounds in question would be selected and an RMSD property would be created upon manually selecting the atom pairs to be compared. The calculations were conducted using the ‘in place’ option, which omits a post-docking minimization of the compounds, which is designed to move the structures in order get the lowest possible RMS difference between the two superimposed fragments.

3. F. Acknowledgments

Text, figures, and schemes in this chapter, in part, are reprints of the material published in the following paper: Arpita Agrawal, Jamie DeSoto, Jessica L. Fullagar, Kasthuraiah Maddali, Shahrzad Rostami, Douglas D. Richman, Yves Pommier, and Seth M. Cohen, "Probing Chelation Motifs in HIV Integrase Inhibitors" *Prod. Natl. Acad. Sci. USA* **2012** *109*, 2251-2256. The dissertation author was a primary contributing author on the paper included. The co-authors listed in this publication also participated in the research. The permission to reproduce this paper was granted by the National Academy of the Sciences, copyright 2012.

3. G. References

(1) Barre-Sinoussi, F.; Chermann, J. C.; Rey, F.; Nugeyre, M. T.; Chamaret, S.; Gruest, J.; Dauguet, C.; Axlerblin, C.; Vezinetbrun, F.; Rouzioux, C.; Rozenbaum, W.; Montagnier, L. *Science* **1983**, *220*, 868-871.

(2) Schupbach, J.; Popovic, M.; Gilden, R. V.; Gonda, M. A.; Sarngadharan, M. G.; Gallo, R. C. *Science* **1984**, *224*, 503-505.

(3) Mehellou, Y.; De Clercq, E. *J. Med. Chem.* **2010**, *53*, 521-538.

(4) Perryman, A. L.; Forli, S.; Morris, G. M.; Burt, C.; Cheng, Y.; Palmer, M. J.; Whitby, K.; McCammon, J. A.; Phillips, C.; Olson, A. J. *J. Mol. Biol.* **2010**, *397*, 600-615.

(5) Li, Y. Y.; Feldman, A. M.; Sun, Y.; McTiernan, C. F. *Circulation* **1998**, *98*, 1728-1734.

(6) Pommier, Y.; Johnson, A. A.; Marchand, C. *Nat. Rev. Drug Discov.* **2005**, *4*, 236-248.

(7) Iwamoto, M.; Wenning, L. A.; Petry, A. S.; Laethem, M.; De Smet, M.; Kost, J. T.; Merschman, S. A.; Strohmaier, K. M.; Ramael, S.; Lasseter, K. C.; Stone, J. A.; Gottesdiener, K. M.; Wagner, J. A. *Clin. Pharmacol. Ther.* **2008**, *83*, 293-299.

(8) Marchand, C.; Maddali, K.; Métifiot, M.; Pommier, Y. *Curr. Top. Med. Chem.* **2009**, *9*, 1016-1037.

(9) Summa, V.; Petrocchi, A.; Bonelli, F.; Crescenzi, B.; Donghi, M.; Ferrara, M.; Fiore, F.; Gardelli, C.; Paz, O. G.; Hazuda, D. J.; Jones, P.; Kinzel, O.; Laufer, R.; Monteagudo, E.; Muraglia, E.; Nizi, E.; Orvieto, F.; Pace, P.; Pescatore, G.; Scarpelli, R.; Stillmock, K.; Witmer, M. V.; Rowley, M. *J. Med. Chem.* **2008**, *51*, 5843-5855.

(10) Hare, S.; Gupta, S. S.; Valkov, E.; Engelman, A.; Cherepanov, P. *Nature* **2010**, *464*, 232-237.

(11) Hare, S.; Vos, A. M.; Clayton, R. F.; Thuring, J. W.; Cummings, M. D.; Cherepanov, P. *Proc. Natl. Acad. Sci. USA* **2010**, *107*, 20057-20062.

(12) Bacchi, A.; Carcelli, M.; Compari, C.; Fisicaro, E.; Pala, N.; Rispoli, G.; Rogolino, D.; Sanchez, T. W.; Sechi, M.; Sinisi, V.; Neamati, N. *J. Med. Chem.* **2001** *54*, 8407-8420.

(13) Agrawal, A.; de Oliveira, C. A. F.; Cheng, Y.; Jacobsen, J. A.; McCammon, J. A.; Cohen, S. M. *J. Med. Chem.* **2009**, *52*, 1063-1074.

(14) Agrawal, A.; Johnson, S. L.; Jacobsen, J. A.; Miller, M. T.; Chen, L.-H.; Pellecchia, M.; Cohen, S. M. *ChemMedChem* **2010**, *5*, 195-199.

(15) Agrawal, A.; Romero-Perez, D.; Jacobsen, J. A.; Villarreal, F. J.; Cohen, S. M. *ChemMedChem* **2008**, *3*, 812-820.

(16) Marinello, J.; Marchand, C.; Mott, B. T.; Bain, A.; Thomas, C. J.; Pommier, Y. *Biochemistry* **2008**, *47*, 9345-9354.

(17) Pace, P.; Di Francesco, M. E.; Gardelli, C.; Harper, S.; Muraglia, E.; Nizi, E.; Orvieto, F.; Petrocchi, A.; Poma, M.; Rowley, M.; Scarpelli, R.; Laufer, R.; Paz, O. G.; Monteagudo, E.; Bonelli, F.; Hazuda, D.; Stillmock, K. A.; Summa, V. *J. Med. Chem.* **2007**, *50*, 2225-2239.

(18) Metifiot, M.; Maddali, K.; Naumova, A.; Zhang, X. M.; Marchand, C.; Pommier, Y. *Biochemistry* **2010**, *49*, 3715-3722.

(19) Metifiot, M.; Marchand, C.; Maddali, K.; Pommier, Y. *Viruses* **2010**, *2*, 1347-1366.

(20) Kaes, C.; Katz, A.; Hosseini, M. W. *Chem. Rev.* **2000**, *100*, 3553-3590.

(21) Krishnan, L.; Li, X.; Naraharisetty, H. L.; Hare, S.; Cherepanov, P.; Engelman, A. *Proc. Natl. Acad. Sci. USA* **2001** *107*, 15910-15915.

(22) Ho, T.-L. *Chem. Rev.* **1975**, *75*, 1-20.

(23) Agrawal, A.; de Oliveira, C. A. F.; Cheng, Y.; Jacobsen, J. A.; McCammon, J. A.; Cohen, S. M. *J. Med. Chem.* **2009**, *52*, 1063-1074.

(24) Lewis, J. A.; Mongan, J.; McCammon, J. A.; Cohen, S. M. *ChemMedChem* **2006**, *1*, 694-697.

(25) Finnegan, M. M.; Rettig, S. J.; Orvig, S. J. *J. Am. Chem. Soc.* **1986**, *108*, 5033-5035.

(26) Puerta, D. T.; Mongan, J.; Tran, B. L.; McCammon, J. A.; Cohen, S. M. *J. Am. Chem. Soc.* **2005**, *127*, 14148-14149.

(27) Schugar, H.; Green, D. E.; Bowen, M. L.; Scott, L. E.; Storr, T.; Bohmerle, K.; Thomas, F.; Allen, D. D.; Lockman, P. R.; Merkel, M.; Thompson, K. H.; Orvig, C. *Angew. Chem. Int. Ed.* **2007**, *46*, 1716-1718.

(28) Gorden, A. E. V.; Xu, J.; Raymond, K. N.; Durbin, P. *Chem. Rev.* **2003**, *103*, 4207-4282.

(29) Zhao, X. Z.; Maddali, K.; Smith, S. J.; Metifiot, M.; Johnson, B. C.; Marchand, C.; Hughes, S. H.; Pommier, Y.; Burke Jr, T. R. *Bioorg. Med. Chem. Lett.* **2012**, *22*, 7309-7313.

(30) Zhao, X. Z.; Semenova, E. A.; Vu, B. C.; Maddali, K.; Marchand, C.; Hughes, S. H.; Pommier, Y.; Burke, T. R. *J. Med. Chem.* **2008**, *51*, 251-259.

(31) Pace, P.; Di Francesco, M. E.; Gardelli, C.; Harper, S.; Muraglia, E.; Nizi, E.; Orvieto, F.; Petrocchi, A.; Poma, M.; Rowley, M.; Scarpelli, R.; Laufer, R.; Gonzalez Paz, O.; Monteagudo, E.; Bonelli, F.; Hazuda, D.; Stillmock, K. A.; Summa, V. *J. Med. Chem.* **2007**, *50*, 2225-2239.

(32) Serrao, E.; Odde, S.; Ramkumar, , N. *Retrovirology* **2009**, *6*, 25-39.

(33) Jin, H.; Cai, R. Z.; Schacherer, L.; Jabri, S.; Tsiang, M.; Fardis, M.; Chen, X.; Chen, J. M.; Kim, C. U. *Bioorg. Med. Chem. Lett.* **2006**, *16*, 4-4.

(34) Kirschberg, T.; Parrish, J. *Curr. Opin. Drug Dis. Dev.* **2007**, *10*, 460-472.

(35) Tanabe, K. K.; Allen, C. A.; Cohen, S. M. *Angew. Chem. Int. Ed.* **2010**, *49*, 9730-9733.

(36) Agrawal, A.; Romero-Perez, D.; Jacobsen, J. A.; Villarreal, F. J.; Cohen, S. M. *ChemMedChem* **2008**, *3*, 812-820.

(37) Belyk, K. M.; Morrison, H. G.; Jones, P.; Summa, V. 2006, p 52 pp.

(38) Summa, V.; Petrocchi, A.; Matassa, V. G.; Gardelli, C.; Muraglia, E.; Rowley, M.; Paz, O. G.; Laufer, R.; Monteagudo, E.; Pace, P. *J. Med. Chem.* **2006**, *49*, 6646-6649.

(39) Cohen, S. M.; Petoud, S. p.; Raymond, K. N. *Inorg. Chem.* **1999**, *38*, 4522-4529.

(40) Cohen, S. M.; Petoud, S.; Raymond, K. N. *Inorg. Chem.* **1999**, *38*, 4522-4529.

4 Antagonism of *P. aeruginosa* Elastase Using Unique Metal-Chelating Scaffolds

4. A. Introduction

Pseudomonas aeruginosa elastase (LasB), is a Zn(II) dependent enzyme responsible for degradation of a wide variety of substrates including elastin, fibrin, immunoglobulins, complement factors and cytokines.[71,188] As discussed in Chapter 1, LasB is a virulence factor of *P. aeruginosa*, a pathogenic bacterium that is of concern due to acquired drug resistance.[188] Infections in immunocompromised patients result in the degradation of damaged tissues and can be fatal when vital organs such as the lungs and kidneys become colonized. This opportunistic bacteria is responsible for nearly 15% of all hospital-acquired infections including respiratory tract, eye, urinary and gastrointestinal tract infections.[69,189] The emergence of antibiotic resistance to nearly all-available antimicrobial agents is a real threat to public health. Therefore, there is a need to develop alternative antibacterial approaches. One approach is to target pathogenic virulence factors. This relatively new tactic has been regarded as a "second generation" antibiotic approach.[190-192] While the merit of investigating such targets remains to be seen, inhibitors that interfere with toxin function and delivery, and thus regulate virulence factor expression, have been reported with promising in vivo effects.[191,192] From an inhibitor design standpoint, the presence of the Zn(II) cofactor in LasB is an attractive tethering point for interactions between the enzyme and potential inhibitors.

An overriding theme of the work presented thus far has been the investigation of interactions of small molecule inhibitors against metalloproteases, with the goal of designing specifically tailored and potent therapeutics. Explored in Chapters 2, fragment libraries have been designed as tools to effectively identify novel metal-binding groups (MBGs) for inhibitors of therapeutic targets such as: matrix metalloproteinases

(MMPs),[193,194] anthrax lethal factor (LF),[171] HIV-1 integrase (HIV-1 IN)[195] and others.[137,196] Historically, LasB inhibitor development has generally focused on peptide-based molecules and to date there is a lack of effective, non-peptidic small molecule inhibitors.[77,78,80] Currently no studies have successfully attempted to systematically identify small molecule inhibitors via metal chelation specific to LasB.[197-199] In this Chapter the chelator fragment library (CFL-1.1) and subsequent sublibraries were used for the identification of chelating scaffolds for the development of novel, potent and selective LasB inhibitors.

4. B. Discovery and Design of LasB Inhibitors Via CFL-1.1 Screening

In a previous study, a library of over 300 hydroxamic acid containing compounds were screened using an established fluorescence assay based on a LasB-cleavable FRET peptide substrate.[80] Of this set of compounds, eight hits showed ~100% inhibition at a concentration of 50 μM. Importantly, only two of these eight compounds inhibited LasB in a dose-dependent fashion, compounds **1** and **2**, which had IC_{50} values of 13.6 μM and 16.4 μM, respectively. Live cultures of *P. aeruginosa* were then exposed to the compounds **1** and **2** in order to determine if either would display antagonistic activity towards LasB, both compounds failed, showing no in vivo activity against LasB. Thus, in a screening of >300 hydroxamic acid small molecules, not one compound resulted in a lead that was effective against the pathogen (Figure 4.1).

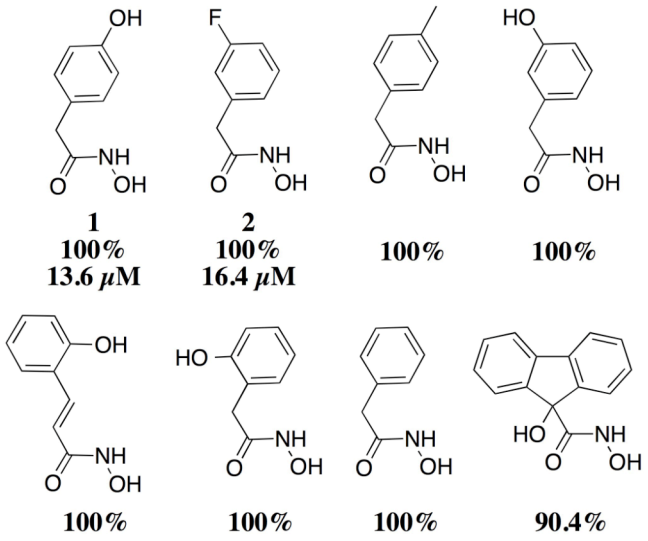

Figure 4.1 Structures and select in vitro IC_{50} values for hydroxamic acid containing small molecules against LasB. Percent inhibition when screened at 50 μM.

The majority of initial investigations for the inhibition of Zn(II) metalloenzymes often begin and end with hydroxamic acids. As noted earlier, this motif has been implicated in various unwanted side effects and exhibit poor oral viability. Additionally, under physiological conditions, the hydroxamate moiety is known to be unstable and will readily hydrolyze generally rendering the MBG weakened or ineffective.[57,200] In order to identify better MBGs, and hence better leads for LasB inhibition, CFL-1.1 was screened and was found to yield several dose-dependent fragment hits (Figure 4.2).

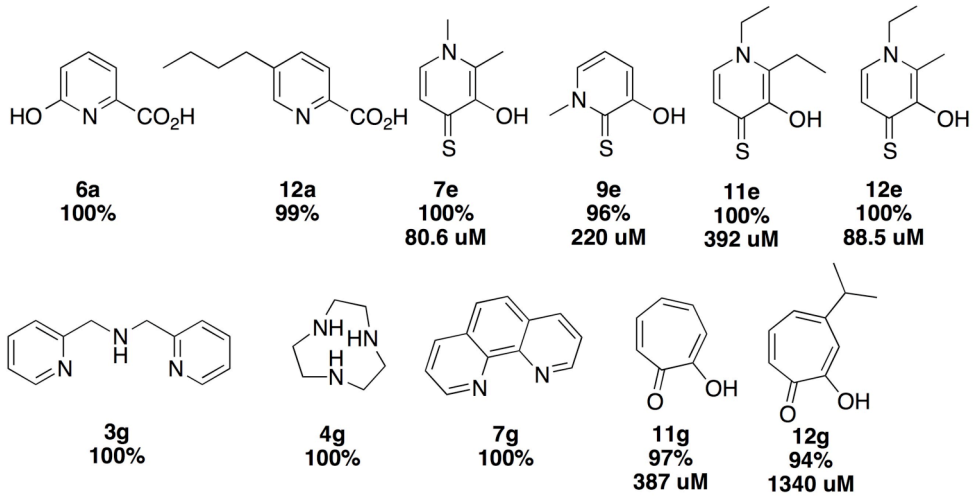

Figure 4.2 Fragment hits from screening of CFL-1.1 at 1 mM against LasB. Percent inhibition and select IC_{50} values are shown.

In this group of fragments, two sets of chelating scaffolds, the 3,4-HOPTO and tropolone moieties (**7e, 11e, 12e** and **11g**, **12g** respectively), were of particular interest. Factors in deciding to further explore these specific fragments stem from their potential to be readily functionalized and thus perform exhaustive structure activity relationship (SAR) studies in the development of a hit to a lead. Moreover, compounds based off of **11g** (tropolone) have the potential to generate novel LasB inhibitors. Tropolone has not been previously explored as a LasB inhibitor scaffold.[201] The work described herein is to date the first example of non-peptidic small molecule antagonists of LasB.[78]

4. C. 1. 3-Hydroxy-1-alkyl-2-methylpyridine-4(1*H*)-thione Inhibitors

The first set of fragments explored contained a MBG consisting of an O,S donor atom pair. Compounds **7e, 11e** and **12e**, all of which contain the 3-hydroxy-1-alkyl-2-methylpyridine-4(1*H*)-thione (3,4-HOPTO) scaffold, have been identified as inhibitors of other Zn(II) metalloproteases.[137,202,203] A sublibrary of 3,4-HOPTO compounds, initially

designed for use in the development of LF inhibitors,[170] was screened for in vitro LasB antagonism (Figure 4.3).

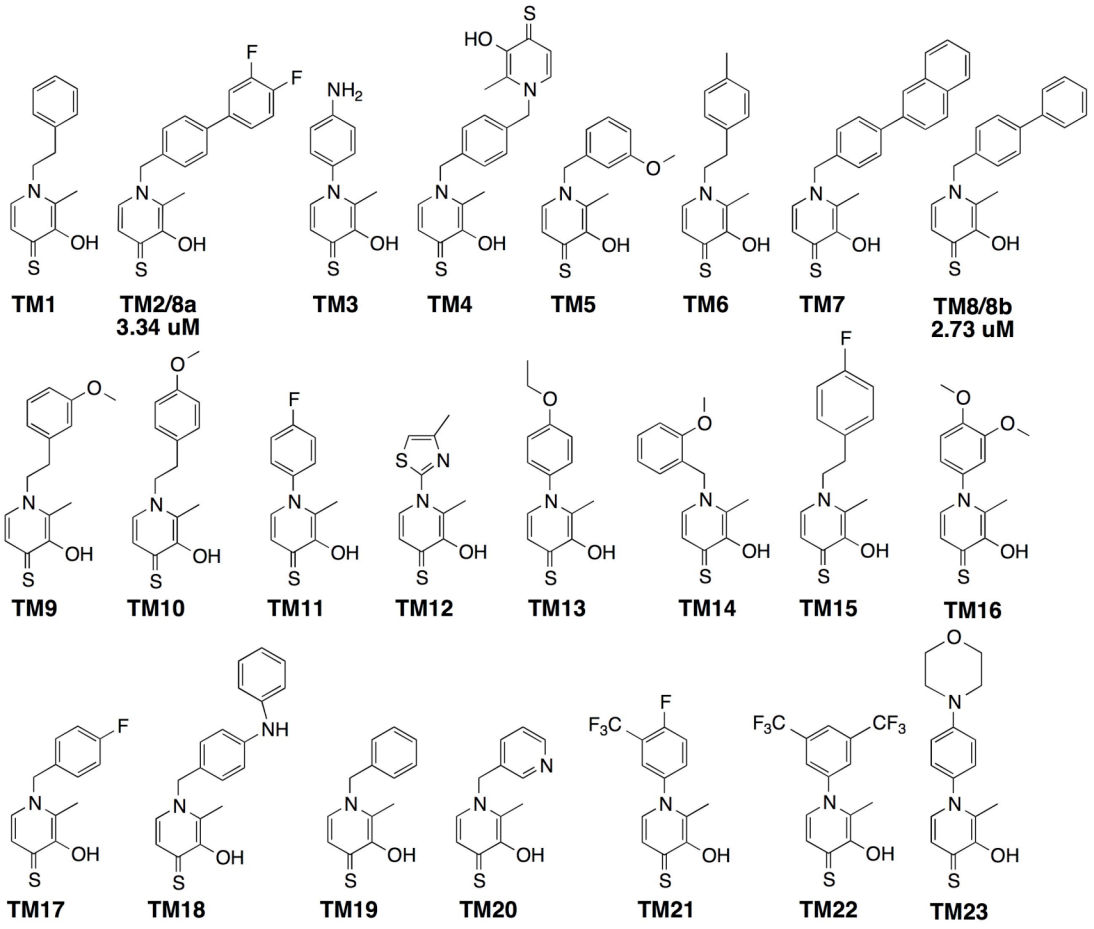

Figure 4.3 3,4-HOPTO sublibrary screened against LasB with select compounds IC_{50} values given.

From this sublibrary screen, only 4 compounds (**TM2/8a**, **TM4**, **TM7**, and **TM8/8b**) showed any significant increase in potency when compared to the CFL-1.1 fragments initially screened. In the most potent compounds, the varied substituents on the 3,4-HOPTO scaffold contained biphenyl or napthyl groups. The most potent of these 3,4-HOPTO compounds, **TM2/8a** and **TM8/8b** (both containing biphenyl groups), showed

approximately a 30-fold increase in potency over the parent fragments from CFL-1.1 (**7e, 11e, 12e**).

In an attempt to further develop these two fragments into a potent lead compound, decoration of the biphenyl backbone ring was undertaken. The types of functional groups appended on to the backbone were varied; unfortunately none of the compounds designed resulted in increased potency (Figure 4.4). This may be due to the positioning of the biphenyl functional group when inside the active site. It is plausible to suggest that the MBG is dictating a specific binding mode, and thus the biphenyl can only point in one direction towards the substrate binding pocket. As such, steric clashing with the protein wall will not tolerate further development upon the biphenyl ring.

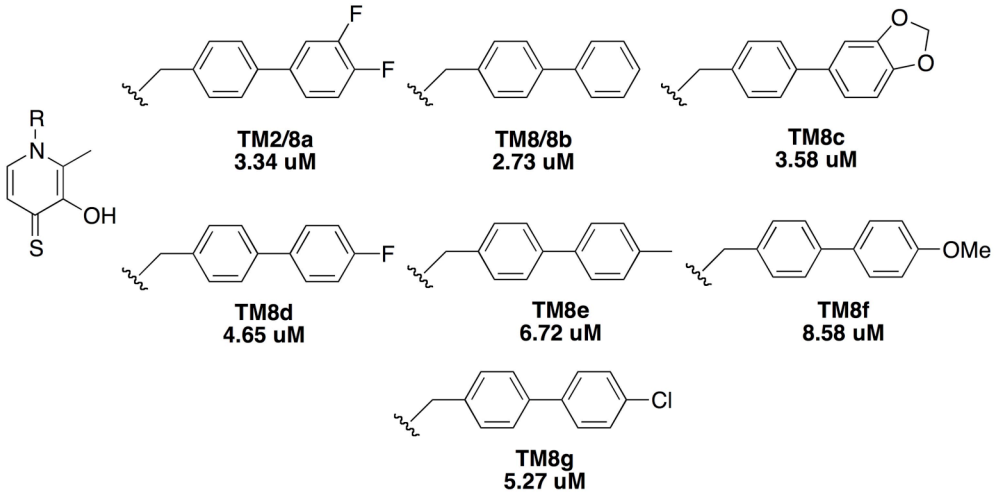

Figure 4.4 Structures and corresponding IC_{50} values for analogs of 3,4-HOPTO hit **TM8/8b**.

With two potent in vitro leads **TM2/8a** and **TM8/8b**, it was necessary to determine whether these compounds would be active in a cell-based assay. It is at this

juncture, that all of the hydroxamic acid-based hits failed to progress. None of the previously studied hydroxamate compounds were capable of showing antagonism against LasB when studied in *P. aeruginosa.* The achievement of such a compound would go beyond confirming a new scaffold in LasB inhibitor design; it would further validate the use of CFL-1.1 as a tool for the identification of significant scaffolds for metalloenzyme inhibitor design via systematic exploration of MBGs.

As described in Chapter 1, LasB is a virulence factor associated with swarming and biofilm formation. Both of these functions are known to contribute to bacterial resistance to antibiotics.[204] Studies have shown that knockout mutants of LasB cause severe defects in the formation of these biofilms and thus the ability of *P. aeruginosa* to swarm. It has been proposed that a study of a swarming ability can be used as a model for examining antibiotic resistance from biofilm formation.[204]

As shown in Figure 4.5, the swarming motility of *P. aeruginosa* was investigated under control and inhibitor conditions. Figure 4.5a depicts the swarming of *P. aeruginosa* in the presence of 25 μM DMSO (control), the dendritic swarming pattern typically seen in normal *P. aeruginosa* is observed. Conversely, Figure 4.5b shows the same strain of *P. aeruginosa* treated with **TM8/8b** (left) and **TM2/8a** (right), in which the ability of the bacteria to swarm has drastically decreased. The results clearly illustrate swarming antagonism by compounds **TM2/8a** and **TM8/8b**. This experiment successfully demonstrates that the small molecule inhibitors **TM2/8a** and **TM8/8b** are capable of showing efficacy against LasB not only in vitro, but in vivo environments as well.

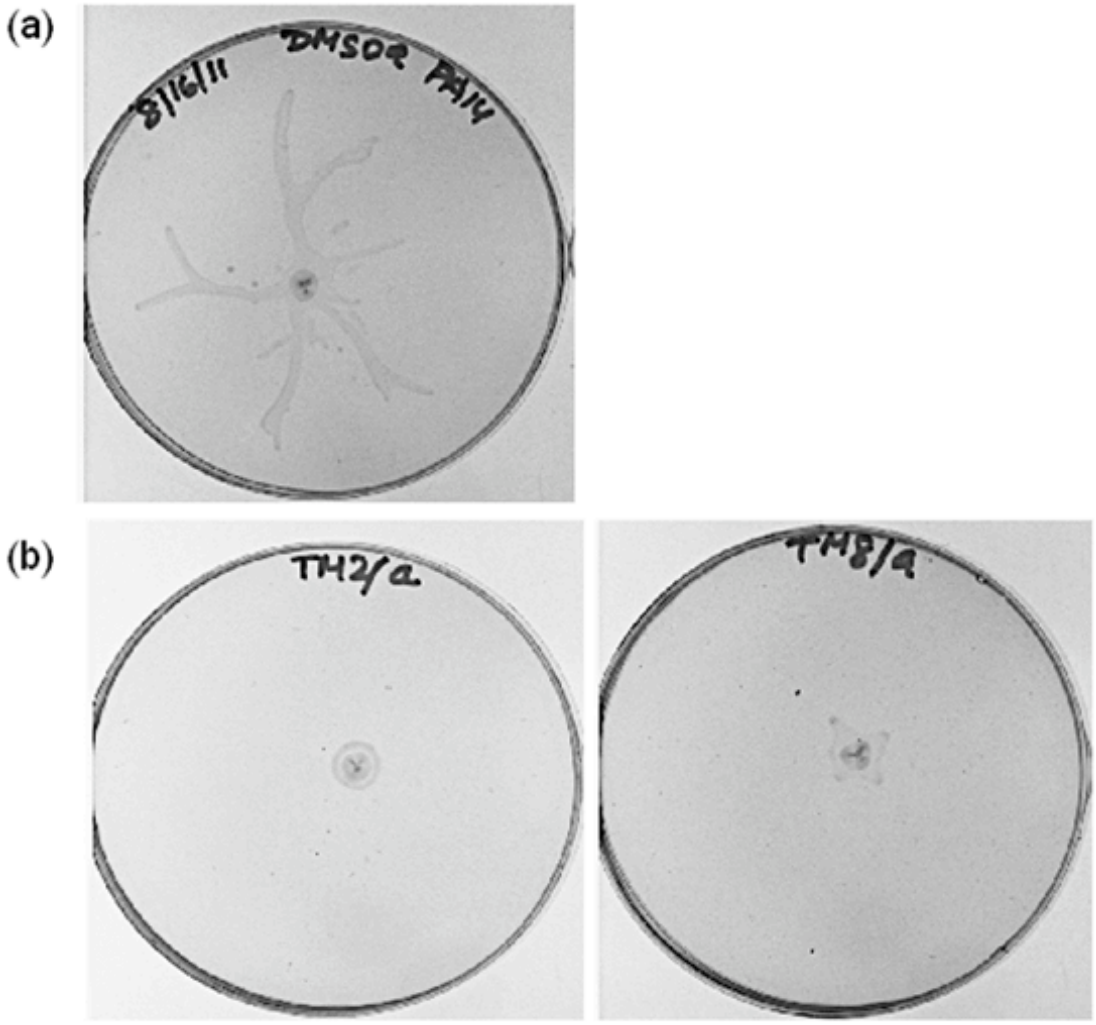

Figure 4.5 Swarming of *P. aeruginosa* strain PA14 in the presence of 25 μM of each of the following: a) DMSO; b) **TM8/8b** (left) **TM2/8a** (right).

4. C. 2. 5-Amino-2-hydroxycyclohepta-2,4,6-trienone-based Inhibitors

When CFL-1.1 was screened against LasB, numerous fragments were identified as MBGs of interest (Figure 4.2). In addition to the 3,4-HOPTO-based compounds, the small molecule 2-hydroxycyclohepta-2,4,6-trienone (tropolone, **11g**) was also identified as a potent fragment. Investigations into the ability of tropolone to chelate to Zn(II) has

been shown in model complexes mimicking the active site metal in MMPs.[40,136] Although further development of tropolone compounds did not yield more potent MMP inhibitors, this work did help to establish tropolone as a potential MBG for metalloenzyme inhibition.

Tropolone and its related natural products are a unique class of compounds with a distinctive seven-member aromatic ring. In 1942, British scientists isolated a compound they referred to as stipitatic acid containing eight carbon atoms, six hydrogen atoms, and five oxygen atoms. The structure of this new fungal metabolite eluded researchers for years. It was not until Michael Dewar proposed an entirely novel type of non-benzene-based aromatic configuration that the structure of stipitatic acid would be solved.[205,206] The ring of seven carbons, which displayed aromatic properties similar to benzene, would be known as tropolone. Dewar's accomplishments broke ground for new theories and fundamental principals about aromaticity. While tropolone itself does not occur naturally, there are numerous natural products that contain this distinctive structure.[201] It was only recently the biosynthetic pathway from which fungi produce tropolone was elucidated.[207]

Over the past half-century, tropolone-based compounds have been the core of numerous therapeutics, particularly antifungal and antimicrobial treatments.[208] It is proposed that some plant troponoids, such as those found in the essential oils of the Cupressaceous tree are a part of the natural defenses this tree uses against invading fungus.[201,209] Historically, some of the most sought after tropolone-based therapeutics have been the α, β, and γ-thujaplicins, such as puberulic acid, a promising antimalarial.[207,210] Examples of α-hydroxytropolones as effective therapeutics can be seen in the recent developments towards an α-hydroxytropolone-based inhibitor of HIV-

1 IN.[211] One area of interest, particularly with regard to this work, is the ability of tropolone to bind metals. Studies have shown that this class of compounds, particularly β-thujaplicn, can inhibit numerous metalloenzymes.[201] In addition, this tropolone-based compound has been shown to have a cytoprotective role by promoting the production of metallothionein, a protein responsible for zinc homeostasis and heavy metal detoxification.[212] Few drug candidates have resulted from a direct tropolone scaffold; this may be due in part to the desire to seek out natural product candidates rather than a true lack of activity of tropolone.[201]

The inhibitory abilities of tropolone are perhaps most widely known in connection with tyrosinase (TY). Chapters 1 and 2 highlight how potent this small molecule is against the dinuclear copper enzyme. Recently, a study out of the Netherlands was able to produce a co-crystal structure of mushroom TY with tropolone.[213-215] The structure shows that tropolone is bound to the protein wall via Van der Waals interactions and is not bound to the active site metal ions. However, the crystal structure is of the deoxy-tyrosinase isoform of the enzyme. As discussed in Chapter 1, TY can exist as three different isoforms *met*-, *oxy*-, and deoxy-tyrosinase. Only the *oxy*-tyrosinase form, where both Cu(II) ions are bound to a bridging dioxygen, is inhibited by tropolone.[215]

In the initial screening of CFL-1.1, tropolone (**11g**) and a tropolone-based natural product, β-thujaplicin (**12g**) showed moderate potency against LasB (Figure 4.2 and Figure 4.6). The potential to develop a simple tropolone-scaffold inhibitor for a Zn(II) dependent metalloenzyme was intriguing.[216]

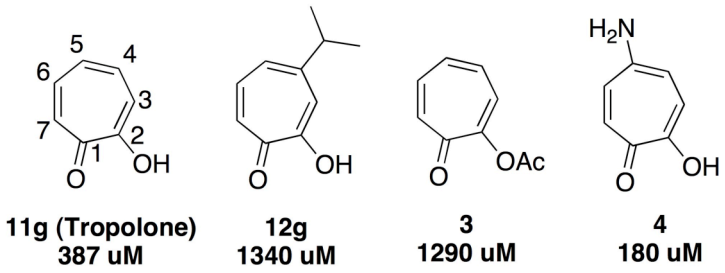

Figure 4.6 List of tropolone and tropolone-like fragments with corresponding IC_{50} values against LasB.

Before progressing with fragment development, a simple proof of concept compound (**3**) was designed to illustrate the vital contribution the MBG makes to the potency of the molecule. Shown in Figure 4.6, when compared to tropolone, compound **3** is significantly less potent. The acetylated phenolic oxygen located on C2 blocks the metal-binding ability of the MBG, and thus affects binding and inhibition. It is understood that the carbonyl and hydroxyl groups in the scaffold are crucial to metal binding.[217] Studies of other metalloenzyme interactions with tropolone and ß-thujaplicin have indicated that at least a portion of the ability of these compounds to inhibit stem from metal chelation between the hydroxyl and carbonyl groups.[218] The decrease in activity between **11g** and **3** highlights the significance of the interactions between the metal cofactor and the small molecule.

5-Amino-2-hydroxycyclohepta-2,4,6-trienone (5-aminotropolone), compound **4** (Figure 4.6), was an appealing starting scaffold for hit development. It offered a functional handle for further synthetic chemistry to be explored. The lower IC_{50} value of **4** compared to **11g** indicated that not only would functionalization in this direction be tolerated but that there was the possibility of protein-ligand hydrogen bonding from the amine. A library of tropolone compounds was made via one-step condensation with

isocyanates under microwave irradiation. From this sublibrary (Figure 4.7, Table 4.1), nine compounds were discovered to be at least as potent as the 3,4-HOPTO small molecule inhibitors **TM2/8a** and **TM8/8b**. The most potent tropolone compound (**4.a)** exhibited an IC_{50} value of 1.16 μM. In addition, using Michaelis-Menten kinetics **4.a** was found to be a competitive inhibitor of LasB with a K_i of ~336 nM (Figure 4.8).

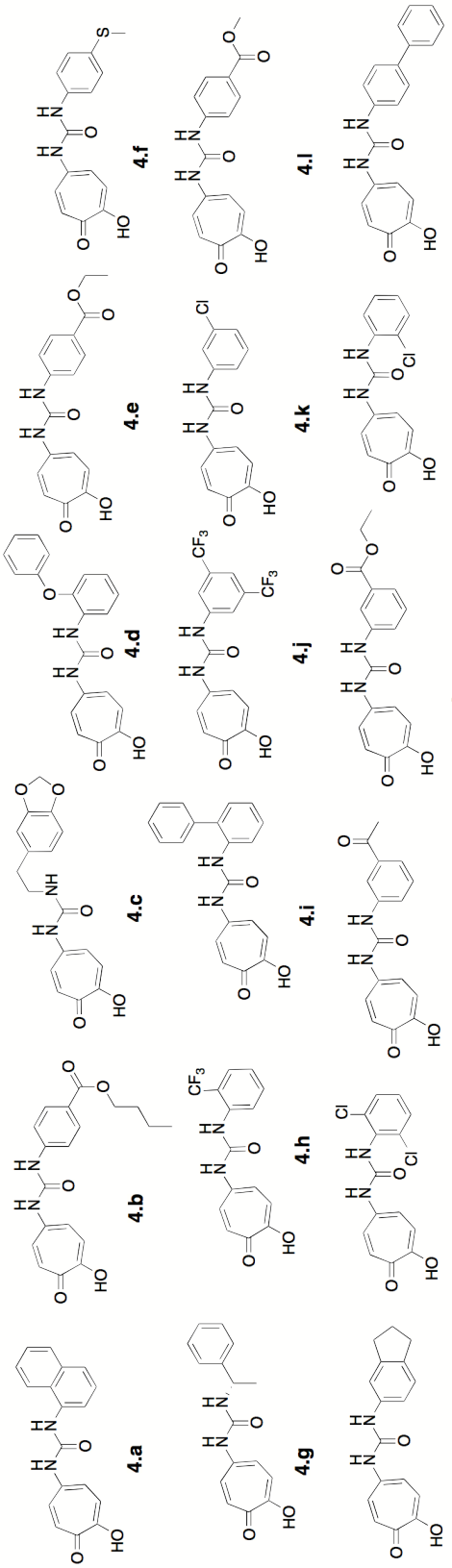

Figure 4.7 List of tropolone sublibrary compounds and controls. Compounds are arranged in decreasing order of potency against LasB.

Table 4.1 Table of tropolone sublibrary IC_{50} values against LasB.

Compound	IC_{50}	Compound	IC_{50}
4.a	1.16 ± 0.06 μM	**4.s**	7.80 ± 0.32 μM
4.b	1.28 ± 0.04 μM	**4.t**	8.73 ± 0.04 μM
4.c	1.64 ± 0.03 μM	**4.u**	9.00 ± 0.14 μM
4.d	1.73 ± 0.01 μM	**4.v**	9.56 ± 0.03 μM
4.e	1.90 ± 0.10 μM	**4.w**	11.0 ± 0.03 μM
4.f	2.30± 0.25 μM	**4.x**	14.1 ± 0.08 μM
4.g	2.40 ± 0.21 μM	**4.y**	14.8 ± 0.06 μM
4.h	2.51 ± 0.03 μM	**4.z**	19.0 ± 0.05 μM
4.i	2.60 ± 0.01 μM	**4.aa**	20.4 ± 0.15 μM
4.j	3.09 ± 0.10 μM	**4.ab**	24.1 ± 0.08 μM
4.k	3.15 ± 0.04 μM	**4.ac**	31.7 ± 0.19 μM
4.l	4.00 ± 0.08 μM	**4.ad**	43.6 ± 0.14 μM
4.m	4.03 ± 0.07 μM	**4.ae**	45.3 ± 0.36 μM
4.n	4.10 ± 0.18 μM	**4.af**	46.7 ± 0.53 μM
4.o	4.60 ± 0.13 μM	**5**	9.86 ± 0.13 μM
4.p	5.30 ± 0.08 μM	**6**	56.3 ± 0.10 μM
4.q	5.40 ± 0.01 μM	**7**	58.4 ± 0.90 μM
4.r	7.65 ± 0.08 μM		

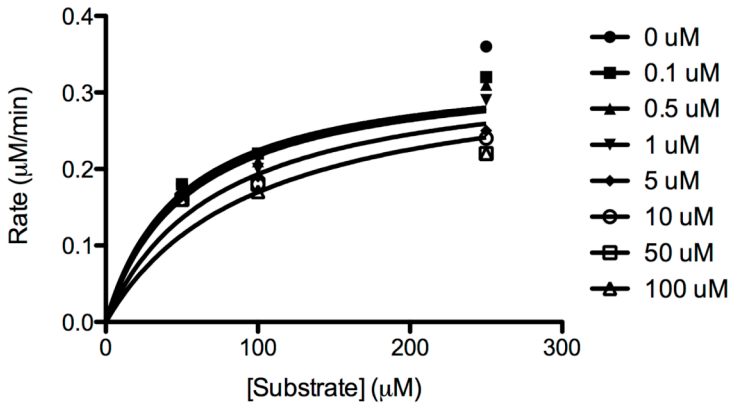

Figure 4.8 Competitive inhibition curve to determine K_i of **4.a** to be 336 ± 24 nM.

The compounds of the tropolone sublibrary (Figure 4.7) all contain a urea group that acts as a linker between the MBG and the backbone. This functionality contains two potential hydrogen bond donors. Control compounds **5** and **6**, both of which contain an amide linkage were synthesized to determine the importance of this urea linker. A significant loss in activity is observed in both control compounds. Compound **5** is an exact analog of the most potent compound, **4.a**, but one of the amides has been eliminated. Control compound **5** is a weaker inhibitor when compared to **4.a** by nearly an order of magnitude. Compound **6** is also missing the urea and the linker length was shortened. The reduction in activity for this compound (IC_{50} value ~56 μM) suggests the spacing between the napthyl group and the MBG, in addition to the urea linkage, contributes to the potency of the compound. An unrelated control compound, **7**, is an acetylated version of **4.a**. Identical to the results seen between **11g** and **3** (Figure 4.7 and Table 4.1), the acetylated MBG results in ~50-fold loss of potency; further suggesting that coordination to the metal cofactor is critical to the activity of these tropolone-based inhibitors.

In vitro, the tropolone compounds preformed as well as the 3,4-HOPTO-based inhibitors. Identical to the procedure used for the 3,4-HOPTO compounds, *P. aeruginosa* was grown on agar plates in the presence of either DMSO or **4.a** (Figure 4.9). The inhibitory activity of compound **4.a** was verified in the cellular assay. To further prove the necessity for an inhibitor with a MBG, compound **7** was also plated with *P. aeruginosa* in the same manner as described above (Figure 4.9). The acetylated compound showed a decrease in antagonism towards *P. aeruginosa* swarming. Compound **7** still showed some reduction in swarming when compared with the DMSO control sample (Figure 4.9a). This observation is attributed to hydrolysis of **7** to the potent unprotected **4.a** compound.

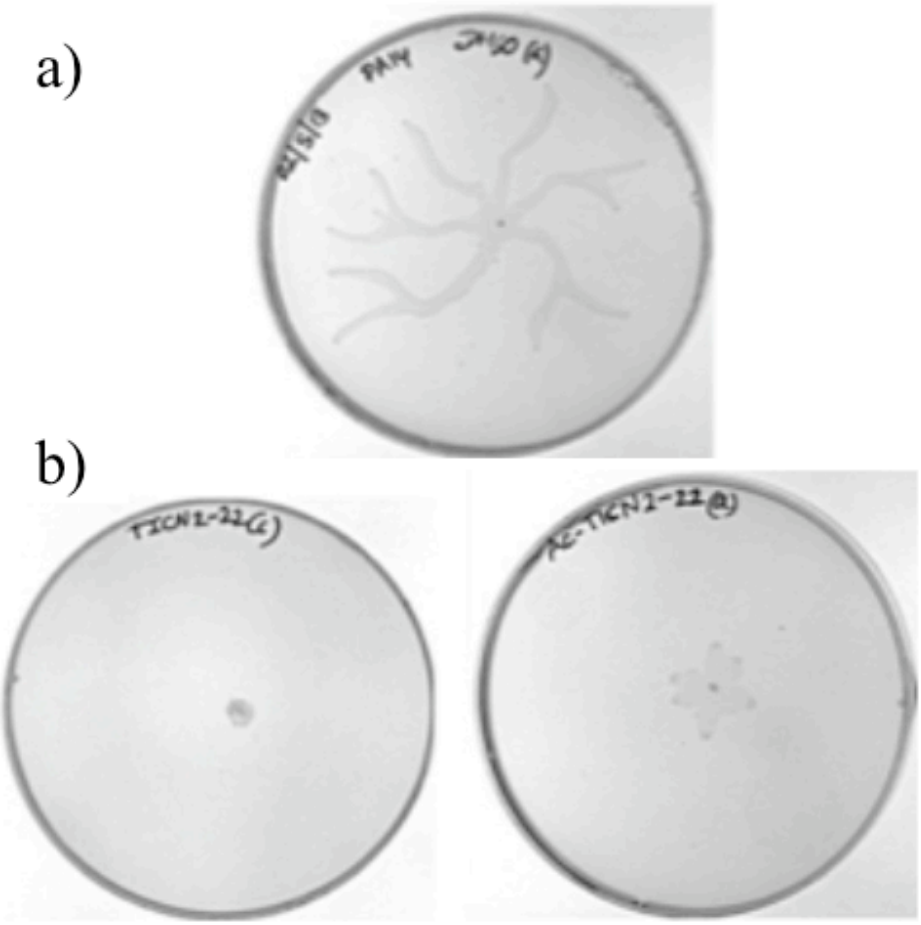

Figure 4.9 Swarming of *P. aeruginosa* strain PA14 in the presence of 25 μM a) DMSO or b) **4.a** (left) **7** (right).

4. D. Comparison of Small Molecule LasB Inhibitors: Cross-Inhibition Screen

All of the lead inhibitors of LasB identified in this Chapter (**TM2/8a**, **TM8/8b**, **4.a)** have comparable activity (1.16 μM - 3.34 μM). However, the 3,4-HOPTO motif is known to inhibit numerous Zn(II) metalloenzymes.[137,170,202] Indeed, the sublibrary of compounds screened (Figure 4.3) were adapted from previous studies against other Zn(II)-dependent targets.[170,202] In order to determine if either of the MBG scaffolds could

improve selectivity, 3,4-HOPTO compound **TM8/8b** and tropolone compound **4.a** were tested against a panel of metalloenzymes.

The primary focus of this cross-inhibition study was to illustrate selectivity for an enzyme with a specific Zn(II) cofactor. As such, three Zn(II) mediated enzymes (MMP-2, MMP-9 and human carbonic anhydrase II (hCAII)) and one Cu-dependent enzyme, mushroom TY, were selected. The last enzyme in the panel was selected specifically for the tropolone-based compounds as TY is strongly inhibited by troplone.[219] In order to validate the selectivity of these advanced fragments, certain criteria need to be met. First, a highly selective compound will discriminate against other enzymes that utilize the same metal ion cofactor as the target. Secondly, any advanced compound containing a fragment known to be potent to an enzyme other than the target needs to diminish in efficacy with respect to the off-target protein. The selectivity screening was conducted via a series of in vitro assays. Each enzyme was treated with 50 μM of either **TM8/8b** or **4.a** and monitored for percent enzyme activity (Figure 4.10).

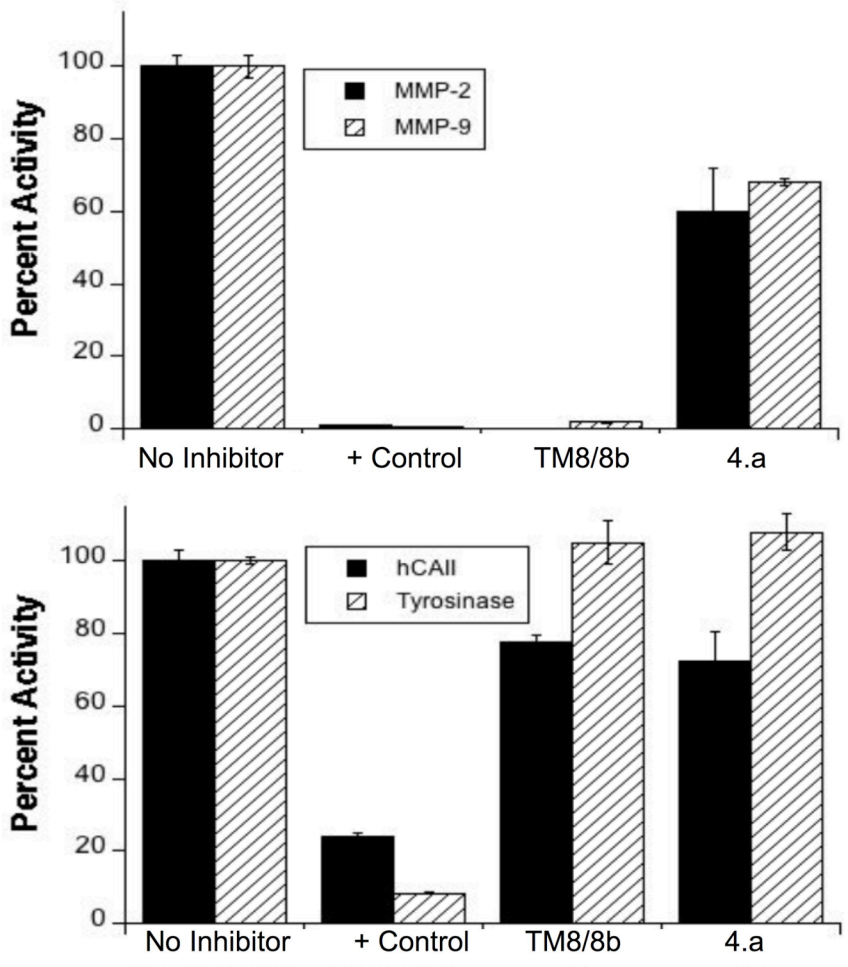

Figure 4.10 Cross-inhibition screening results of **TM8/8b** and **4.a** against MMPs -2, -9, hCAII and TY at 50 μM. Positive control for MMP-2 and MMP-9 was CGS 27023A (IC_{50} values 20 and 8 nM respectively)[220], for hCAII was acetazolamide (IC_{50} value 12 nM)[221] and for tyrosinase was tropolone (**11g**, IC_{50} value 400 nM).[95]

It is important to note that the cross-inhibitory screen was conducted at a relatively high concentration (50 μM); as such non-specific, off-target inhibition should be observed. The results of the MMP enzymes indicate that **TM8/8b** is a strong inhibitor of these Zn(II) endopeptidases, as previously reported.[170,202] The 3,4-HOPTO compound

TM8/8b completely inhibited MMP activity, whereas **4.a** reduced MMP activity by < 50%. Both **TM8/8b** and **4.a** showed some activity against hCAII, but overall neither compound gave considerable inhibition. Lastly, neither compound demonstrated substantial antagonism towards TY (Figure 4.10). What is significant about this result is the lack of efficacy in the tropolone-based compound (**4.a**). It would appear that the hit optimization of the tropolone parent fragment has altered the inherent affinity of the tropolone MBG for TY, thus allowing **4.a** to be selective for LasB. These results are quite significant. The cross-inhibitory screen illustrates that by developing tropolone towards a lead compound, a highly selective inhibitor can be obtained. The tropolone-base compound is no longer potent towards TY or any of the other metalloenzymes screened. This is unlike the results seen with the HOPTO-based compounds that remain promiscuous to many other Zn(II) dependent enzymes even after hit development. This study gives further evidence that target-specific metalloenzyme inhibitors can be achieved through a FBLD approach.

4. E. Conclusions

In conclusion, this study successfully identified the first, non-peptidic inhibitors of LasB that showed activity in a pathogen-based assay.[78] Using MBG fragments, with hit optimization, resulted in the discovery of potent small molecule inhibitors of LasB, with evidence for Zn(II) ion cofactor chelation. The tropolone-based compounds, in particular **4.a,** illustrate not only potency against the target enzyme but also selectivity against a panel of similar metalloenzymes. Through the use of cell-based assays, these compounds were shown to have anti-swarming activity. It is important to note that traditionally swarming antagonism has only been studied with general virulence factor

expression and bacterial adhesion inhibitors; as such, these compounds are also the first targeted compounds to show direct swarming antagonism.[57,213,222,223] These selective compounds will be incredibly valuable for gaining a greater knowledge regarding the part LasB has in contributing to antibiotic resistance in *P. aeruginosa* swarms. There is potential for further investigations into the use of these novel small molecule LasB inhibitors in *P. aeruginosa* infection models to study the influence this virulence factor has in promoting bacterial potency. Ultimately, it may be possible to use a combination of a LasB inhibitor with traditional antibiotics as a new treatment for multi-drug resistant *P. aeruginosa*.

The wider scope of this study illustrates two key concepts. The discovery and study of these small molecule virulence factor inhibitors will help evaluate the impact of targeting bacterial virulence factors as a viable approach for the development of new antibiotics. Secondly, the use of fragment libraries and sublibraries swiftly identified the key functional features required for potency and more importantly selectivity. The use of CFL-1.1 to identify not one, but two potential leads is further validation that a FBLD approach to the identification and design of metalloenzyme inhibitors is effective.

4. F. Experimental

General. Reactions were carried out under standard atmospheric conditions. Yields refer to purified, isolated compounds, unless otherwise stated. All reactions were conducted in a CEM Discover® Microwave Reactor and were monitored by thin-layer chromatography (TLC) carried out on silica gel plates using UV-light (254 nm). THF was dried and stored over molecular sieves. Flash chromatography separations were performed using a CombiFlash® Rf automated chromatography system by Teledyne Isco. All compounds were confirmed to have ≥95% purity by HPLC (254 or 280 nm). NMR spectra were recorded on a Bruker or Varian 300 or 400 MHz spectrometers at 25 °C and calibrated using a solvent peak as an internal reference. The following abbreviations are used to indicate the multiplicities: s, singlet; d, doublet; t, triplet; q, quartet; m, multiplet; br, broad.

Data measurement and analysis: All fluorescence readings were measured in black 96-well microtiter plates with clear bottoms (Corning Costar) on a SpectraMax M2e Microplate Reader (Molecular Devices). GraphPad Prism version 5.0a for Mac OS X (GraphPad Software, www.graphpad.com) was used for all IC_{50} and K_i analyses.

Materials: LasB was purchased from Elastin Products Company and used as received. The LasB pro-fluorescent substrate, Abz-Ala-Gly-Leu-Ala-p-Nitro-Benzyl-Amide (SAG-3905-PI), was purchased from Peptides International and used as received. Molecular biology grade DMF and DMSO were purchased from Sigma Aldrich and used as received.

Synthesis and Characterization for 3,4-HOPTO Compounds

General. 3-Hydroxy-2-methyl-4*H*-pyran-4-thione (thiomaltol,) (1.0 equiv) and amine (2.0 equiv) were added to a round-bottom flask and dissolved in toluene (0.8 M). The resulting mixture was heated to 110–115 °C to boil off all solvent. After ~5 min of additional heating, the contents were cooled to 25 °C and dissolved in a minimal amount of EtOAc. Compounds **TM1-TM23** and **TM8a-TM8g** were then obtained via recrystallization from EtOAc and hexanes or silica column chromatography to yield yellow powders. Compounds **TM1-TM23** were from previously reported compounds.[170,202] Compounds **TM8a, and TM8c-TM8g** are reported below.

1-((3',4'-Difluoro-[1,1'-biphenyl]-4-yl)methyl)-3-hydroxy-2-methylpyridine-4(1*H*)-thione (TM8/8a): The pure product was obtained via silica column chromatography using 0-4% MeOH in DMC as an eluent to yield product as a beige solid (82 mg, 0.239 mmol). Yield: 67%. ^{1}H NMR (400 MHz, DMSO, 25 °C): δ 2.34 (s, 3H), 5.51 (s, 2H), 7.23 (d, *J* = 8.1 Hz, 2H), 7.42 (d, *J* = 6.6 Hz, 1H), 7.46 (dd, *J* = 8.4, 6.3 Hz, 2H), 7.73 (d, *J* = 8.2 Hz, 2H), 7.78 (t, *J* = 5.9 Hz, 1H), 7.88 (d, *J* = 6.7 Hz, 1H), 8.76 (s, 1H). ^{13}C NMR (400 MHz, DMSO, 25 °C): δ 13.25, 57.90, 116.32, 116.50, 118.56, 118.73, 124.07, 124.17, 125.59, 127.86, 128.10, 128.95, 134.25, 135.93, 138.34, 153.36, 170.34. ESI-MS(+) *m/z* 344.09$[M+H]^{+}$.

1-(4-(Benzo[*d*][1,3]dioxol-5-yl)phenethyl)-3-hydroxy-2-methylpyridine-4(1*H*)-thione (TM8c): The pure product was obtained via silica column chromatography using 0-3% MeOH in DMC as an eluent to yield product as a brown solid (103 mg, 0.282 mmol). Yield: 63%. ^{1}H NMR (400 MHz, DMSO, 25 °C): δ 2.35 (s, 3H), 5.48 (s, 2H),

6.05 (s, 2H), 6.99 (d, *J* = 8.1 Hz, 1H), 7.13 (dd, *J* = 8.1, 1.6 Hz, 1H), 7.18 (d, *J* = 8.1 Hz, 2H), 7.24 (d, *J* = 1.4 Hz, 1H), 7.41 (d, *J* = 6.6 Hz, 1H), 7.63 (d, *J* = 8.2 Hz, 2H), 7.87 (d, *J* = 6.7 Hz, 1H), 8.76 (s, 1H). ^{13}C NMR (400 MHz, DMSO, 25 °C): δ 13.26, 57.96, 101.86, 107.74, 109.37, 120.96, 125.56, 127.71, 127.74, 128.97, 134.22, 134.30, 134.77, 140.31, 147.69, 148.67, 153.34, 170.24. ESI-MS(+) *m/z* 352.01$[M+H]^+$.

1-(2-(4'-Fluoro-[1,1'-biphenyl]-4-yl)ethyl)-3-hydroxy-2-methylpyridine-4(1*H*)-thione (TM8d): The pure product was obtained via silica column chromatography using 0-3% MeOH in DMC as an eluent to yield product as a dark brown solid (45 mg, 0.132 mmol). Yield: 39%. ^{1}H NMR (400 MHz, DMSO, 25 °C): δ 2.34 (s, 3H), 5.51 (s, 2H), 7.23 (d, *J* = 8.1 Hz, 2H), 7.42 (d, *J* = 6.6 Hz, 1H), 7.52 (d, *J* = 4.1 Hz, 2H), 7.72 (d, *J* = 8.2 Hz, 2H), 7.77 (d, *J* = 4.8 Hz, 1H), 7.88 (d, *J* = 8.3 Hz, 2H). ^{13}C NMR (400 MHz, DMSO, 25 °C): δ 13.25, 54.76, 103.48, 112.40, 135.09, 137.49, 139.99, 142.97, 143.59, 140.31, 147.69, 148.69, 153.65, 170.24, 172.11. ESI-MS(+) *m/z* 325.34$[M+H]^+$.

3-Hydroxy-2-methyl-1-(2-(4'-methyl-[1,1'-biphenyl]-4-yl)ethyl)pyridine-4(1*H*)-thione (TM8e): The pure product was obtained via recrystalization from 1:2 EtOAc/Hexanes, the precipitate isolated via vacuum filtration. The product was dried under vacuum to yield a beige solid (82 mg, 0.244 mmol). Yield: 67%. ^{1}H NMR (400 MHz, $CDCl_3$, 25 °C): δ 7.60 (m, 4H), 7.48 (d, 2H, *J* = 7.0 Hz), 7.23 (m, 2H), 7.08 (d, 2H, *J* = 7.0 Hz), 5.25 (s, 2H), 2.48 (s, 3H), 2.42 (s, 3H). HRMS (ESI-TOF) *m/z* calcd for $C_{20}H_{19}NOS$ $[M+H]^+$ 322.1260, found 322.1254.

3-Hydroxy-1-(2-(4'-methoxy-[1,1'-biphenyl]-4-yl)ethyl)-2-methylpyridine-4(1*H*)-thione (TM8f): The pure product was obtained via silica column chromatography using 0-6% MeOH in DMC as an eluent to yield product as a brown solid (91 mg, 0.259

mmol). Yield: 88%. ^{1}H NMR (400 MHz, $CDCl_3$, 25 °C): δ 7.60 (m, 4H), 7.48 (d, 2H, *J* = 7.0 Hz), 7.23 (m, 2H), 7.08 (d, 2H, *J* = 7.0 Hz), 5.25 (s, 2H), 2.48 (s, 3H), 2.42 (s, 3H). HRMS (ESI-TOF) *m/z* calcd for $C_{20}H_{19}NOS$ $[M+H]^+$ 322.1260, found 322.1254.

1-(2-(4'-Chloro-[1,1'-biphenyl]-4-yl)ethyl)-3-hydroxy-2-methylpyridine-4(1*H*)-thione (TM8g): The pure product was obtained via recrystalization from 1:2 EtOAc/Hexanes, the precipitate isolated via vacuum filtration. The product was dried under vacuum to yield a dark solid (59 mg, 0.166 mmol). Yield: 60%. ^{1}H NMR (400 MHz, $CDCl_3$, 25 °C): δ 7.57 (d, 2H, *J* = 7.0 Hz), 7.55 (d, 2H, *J* = 7.0 Hz), 7.48 (d, 1H, *J* = 6.8 Hz), 7.23 (d, 1H, *J* = 6.8 Hz), 7.08 (d, 2H, *J* = 7.0 Hz), 6.96 (d, 2H, *J* = 7.0 Hz), 5.25 (s, 2H), 3.81 (s, 3H), 2.42 (s, 3H). HRMS (ESI-TOF) *m/z* calcd for $C_{20}H_{19}NO_2S$ $[M+H]^+$ 338.1209, found 338.1214.

Synthesis and Characterization for Tropolone Compounds

7-Oxocyclohepta-1,3,5-trien-1-yl acetate (3): To a solution of tropolone (**11g**, 300 mg, 2.45 mmol) in 5 mL acetic anhydride, was added 4 drops of concentrated sulfuric acid. The reaction was left to stir for 4 h at room temperature under nitrogen. The reaction mixture was quenched with 30 mL of ice. Excess acetic anhydride was evaporated in vacuo. The crude mixture was dissolved in DCM and extracted with water. The organic fractions were collected, dried over anhydrous MgSO4 and concentrated in vacuo to a crude residue. The crude solid was purified via silica column chromatography using 0–7% MeOH in DCM as an eluent to yield product **3,** as a white solid (125 mg, 0.726 mmol). Yield: 31%. ^{1}H NMR (400 MHz, DMSO-d_6): δ 7.31–7.23 (m, 5H), 2.26 (s, 3H). ^{13}C NMR (200 MHz, DMSO-d_6): δ 175.5, 161.5, 148.1, 139.7, 138.4, 131.0, 128.1, 124.2, 30.1. ESI-MS(-) *m/z* 163.12, found for $C_9H_7O_3$ $[M-H]^-$.

2-Hydroxy-5-nitrosocyclohepta-2,4,6-trienone: To a solution of tropolone (5.0 g, 41 mmol) in 14.5 mL H_2O, was added an acetic acid (12 mL, 210 mmol) and sodium nitrite (3.1 g, 45 mmol) mixture. The reaction solution was then stirred at room temperature for 3 h under nitrogen. The resulting brown solid was isolated via filtration over a frit and washed with 50 ml of cool water. The solid was collected and dried under vacuum to yield 5-nitrosotropolone as a light brown solid (3.8 g, 25.16 mmol). Yield: 62%. ^{1}H NMR (400 MHz, DMSO-d_6): δ 8.85 (d, J = 40.0 Hz, 2H), 7.58 (dd, J = 12.2, 1.5 Hz, 2H). ^{13}C NMR (200 MHz, DMSO-d_6): δ 185.7, 184.2, 152.3, 139.7, 130.3, 128.1, 124.2. ESI-MS(-) *m/z* 150.12, found for $C_7H_4NO_3$ $[M-H]^-$.

5-Amino-2-hydroxycyclohepta-2,4,6-trienone (**4**): The synthesis of **4** was adapted from previous procedures.[224225] In a large Parr bottle, to a solution of 2-hydroxy-5-nitrosocyclohepta-2,4,6-trienone (2.2 g, 14.6 mmol) in 100 mL of ethanol, was added palladium on carbon (10%, 0.029 g, 0.028 mmol). The bottle was placed in a hydrogenator and purged three times with hydrogen gas before being set to shake for 18 h at 22 psi. The reaction mixture was filtered over celite and the filtrate was collected and evaporated to dryness in vacuo. The resulting dark orange residue was dissolved in 50 mL of boiling ethyl acetate, and the turbid mixture was hot filtered. The filtrate was reduced in volume to 35 mL, and allowed to cool. The resulting golden precipitate was isolated via filtration. The solid was collected and dried under vacuum to yield product 4, as a golden solid (1.66 g, 12.11 mmol) Yield: 83% yield. ^{1}H NMR (400 MHz, DMSO-d_6): δ 7.11 (d, J = 12.1 Hz, 2H), 6.72 (d, J = 12.1 Hz, 2H), 6.27 (s, 2H). ^{13}C NMR (200 MHz, DMSO-d_6): δ 185.7, 184.2, 161.1, 139.7, 156.5, 120.1, 124.2. ESI-MS(-) *m/z* 136.11, found for $C_7H_6NO_2$ $[M-H]^-$.

General procedure for aminotropolone derivatives. To a solution of 5-Aminotropolone (**4,** 100 mg, 0.73 mmol) in THF (4 mL), was added an isocyanate (1.1 mmol, 1.5 equiv). The reaction mixture irradiated on the microwave synthesizer for 120 minutes at 95 °C with the following settings: maximum pressure 250 psi, 300 watts, and medium stirring. The mixture was transferred to a round-bottomed flask and concentrated in vacuo. Compounds (**4.a-4.af**) were purified via hot filtration with boiling MeOH and recrystallization or via silica column chromatography using 0–8% MeOH in DCM as an eluent to yield solid product.

1-(4-Hydroxy-5-oxocyclohepta-1,3,6-trien-1-yl)-3-(naphthalen-1-yl)urea (4.a): The pure product was obtained via silica column chromatography using 0-6% MeOH in DMC as an eluent to yield product as a white solid (96 mg, 0.313 mmol). Yield: 31%. ^{1}H NMR (400 MHz, DMSO-d_6): δ 9.26 (s, 1H), 8.88 (s, 1H), 8.12 (d, J = 8.4 Hz, 1H), 7.95 (t, J = 7.5 Hz, 2H), 7.69–7.65 (m, 3H), 7.61–7.56 (m, 2H), 7.50 (d, J = 7.6 Hz, 1H), 7.27 (dd, J = 12.2, 0.9 Hz, 2H). ^{13}C NMR (200 MHz, DMSO-d_6): δ 173.9, 173.9, 153.7, 144.9, 140.6, 137.9, 136.9, 133.2, 128.3, 126.1, 126.0, 125.2, 124.4, 121.6, 119.8, 118.8, 108.1, 106.2. ESI-MS(-) *m/z* 304.94, found for $C_{18}H_{13}N_2O_3$ $[M-H]^-$.

Butyl 4-(3-(4-hydroxy-5-oxocyclohepta-1,3,6-trien-1-yl)ureido)benzoate (4.b): The pure product was obtained via silica column chromatography using 0-4% MeOH in DMC as an eluent to yield product as a gray solid (39 mg, 0.109 mmol). Yield: 14 %. ^{1}H NMR (400 MHz, DMSO-d_6): δ 9.23 (s, 1H), 9.01 (s, 1H), 7.89 (d, J = 8.6 Hz, 2H), 7.58 (dd, J = 10.6, 4.3 Hz, 4H), 7.23 (d, J = 12.2 Hz, 2H), 4.24 (t, J = 6.5 Hz, 2H), 1.67 (dd, J = 14.4, 6.6 Hz, 2H), 1.42 (dd, J = 15.0, 7.3 Hz, 2H), 0.93 (t, J = 7.4 Hz, 3H). ^{13}C NMR

(200 MHz, DMSO-d_6): δ 169.7, 166.0, 153.0, 144.6, 139.9, 131.0, 128.8, 125.6, 123.7, 118.2, 61.0, 50.9, 14.9. ESI-MS(+) *m/z* 357.39, found for $C_{19}H_{21}N_2O_5$ $[M+H]^+$.

1-(2-(Benzo[*d*][1,3]dioxol-5-yl)ethyl)-3-(4-hydroxy-5-oxocyclohepta-1,3,6-trien-1-yl)urea (4.c): The pure product was obtained via recrystalization from EtOAc, the precipitate isolated via vacuum filtration. The product was dried under vacuum to yield a brown solid (103 mg, 0.134 mmol). Yield: 32%. ^{1}H NMR (300 MHz, DMSO-d_6): δ 9.22 (s, 1H), 8.99 (s, 1H), 7.89 (s, 1H), 7.56 (dd, *J* = 10.7, 4.3 Hz, 4H), 7.21 (d, *J* = 12.1 Hz, 2H), 4.22 (t, *J* = 6.5 Hz, 2H), 1.66 (dt, *J* = 14.1, 6.9 Hz, 2H), 1.40 (dd, *J* = 15.0, 7.3 Hz, 2H). ^{13}C NMR (150 MHz, DMSO-d_6): δ 174.7, 172.9, 154.9, 150.9, 148.4, 146.7, 137.8, 136.4, 131.3, 121.5, 120.7, 119.7, 110.0, 109.1, 108.0, 51.1, 49.1. ESI-MS(+) *m/z* 328.98, found for $C_{17}H_{17}N_2O_5$ $[M+H]^+$.

1-(4-Hydroxy-5-oxocyclohepta-1,3,6-trien-1-yl)-3-(2-phenoxyphenyl)urea (4.d): The pure product was obtained via silica column chromatography using 0-3% MeOH in DMC as an eluent to yield product as a beige solid (64 mg, 0.184 mmol). Yield: 24%. ^{1}H NMR (400 MHz, DMSO-d_6): δ 9.47 (s, 1H), 8.56 (s, 1H), 8.25 (d, *J* = 8.2 Hz, 1H), 7.59 (d, *J* = 12.3 Hz, 2H), 7.43 (t, *J* = 8.0 Hz, 2H), 7.24 (d, *J* = 12.2 Hz, 2H), 7.18 (td, *J* = 7.4, 1.1 Hz, 1H), 7.15–7.10 (m, 1H), 7.07 (dd, *J* = 7.7, 1.0 Hz, 2H), 7.01–6.97 (m, 1H), 6.85 (dd, *J* = 8.1, 1.2 Hz, 1H). ^{13}C NMR (200 MHz, DMSO-d_6): δ 169.0, 156.8, 152.5, 145.4, 139.8, 131.0, 127.5, 125.3, 124.1, 123.8, 122.8, 120.0, 118.5. ESI-MS(+) *m/z* 348.88, found for $C_{20}H_{17}N_2O_4$ $[M+H]^+$.

Ethyl 4-(3-(4-hydroxy-5-oxocyclohepta-1,3,6-trien-1-yl)ureido)benzoate (4.e): The pure product was obtained via silica column chromatography using 0-6% MeOH in DMC as an eluent to yield product as a pale yellow solid (81 mg, 0.247 mmol). Yield:

34%. ^{1}H NMR (400 MHz, DMSO-d_6): δ 9.08 (s, 1H), 8.92 (s, 1H), 8.16 (t, J = 1.9 Hz, 1H), 7.65 (d, J = 8.1 Hz, 1H), 7.58 (d, J = 12.2 Hz, 3H), 7.43 (t, J = 7.9 Hz, 1H), 7.24–7.21 (m, 2H), 4.31 (q, J = 7.1 Hz, 2H), 1.32 (t, J = 7.1 Hz, 3H). ^{13}C NMR (200 MHz, DMSO-d_6): δ 169.7, 166.0, 153.0, 144.6, 139.9, 131.0, 128.8, 125.6, 123.7, 118.2, 61.0, 14.9. ESI-MS(-) *m/z* 326.99, found for $C_{17}H_{15}N_2O_5$ $[M-H]^-$.

1-(4-Hydroxy-5-oxocyclohepta-1,3,6-trien-1-yl)-3-(4-(methylthio)phenyl)urea (4.f): The pure product was obtained via silica column chromatography using 0-5% MeOH in DMC as an eluent to yield product as a white solid (76 mg, 0.251 mmol). Yield: 34%. ^{1}H NMR (400 MHz, DMSO-d_6): δ 8.89 (s, 1H), 8.82 (s, 1H), 7.57 (dd, J = 11.0, 1.3 Hz, 2H), 7.44–7.41 (m, 2H), 7.24–7.21 (m, 4H), 2.44 (s, 3H). ^{13}C NMR (400 MHz, DMSO-d_6): δ 169.4, 153.2, 140.4, 137.6, 131.1, 128.4, 128.2, 125.7, 119.9, 16.5. ESI-MS(-) *m/z* 300.87, found for $C_{15}H_{13}N_2O_3S$ $[M-H]^-$.

(*S*)-1-(4-hydroxy-5-oxocyclohepta-1,3,6-trien-1-yl)-3-(1-phenylethyl)urea (4.g): The pure product was obtained via silica column chromatography using 0-3% MeOH in DMC as an eluent to yield product as a beige solid (101 mg, 0.355 mmol). Yield: 36%. ^{1}H NMR (400 MHz, DMSO-d_6): δ 8.67 (s, 1H), 7.53 (d, J = 12.3 Hz, 2H), 7.34 (d, J = 4.4 Hz, 4H), 7.24 (q, J = 4.4 Hz, 1H), 7.17 (d, J = 12.3 Hz, 2H), 6.80 (d, J = 7.8 Hz, 1H), 4.80 (t, J = 7.3 Hz, 1H), 1.39 (d, J = 6.9 Hz, 3H). ^{13}C NMR (400 MHz, DMSO-d_6): δ 169.0, 154.9, 145.5, 141.4, 129.0, 128.3, 127.4, 126.5, 126.0, 121.3, 49.5, 23.6. ESI-MS(-) *m/z* 283.05, found for $C_{16}H_{15}N_2O_3$ $[M-H]^-$.

1-(4-Hydroxy-5-oxocyclohepta-1,3,6-trien-1-yl)-3-(2-(trifluoromethyl)phenyl)urea (4.h): The pure product was obtained via silica column chromatography using 0-4% MeOH in DMC as an eluent to yield product as a white solid

41 mg, 0.126 mmol). Yield: 17%. ^{1}H NMR (400 MHz, DMSO-d_6): δ 9.19 (d, J = 0.5 Hz, 1H), 9.03 (s, 1H), 8.01 (s, 1H), 7.59–7.50 (m, 4H), 7.33 (d, J = 7.7 Hz, 1H), 7.23 (d, J = 10.8 Hz, 2H). ^{13}C NMR (200 MHz, DMSO-d_6): δ 174.8, 171.3, 166.5, 137.6, 134.6, 133.9, 130.1, 129.0, 128.2, 127.5, 125.7, 123.6, 120.3, 119.9. ESI-MS(+) *m/z* 324.96, found for $C_{15}H_{12}F_3N_2O_3$ $[M+H]^+$.

1-([1,1'-Biphenyl]-2-yl)-3-(4-hydroxy-5-oxocyclohepta-1,3,6-trien-1-yl)urea (4.i): The pure product was obtained via silica column chromatography using 0-3% MeOH in DMC as an eluent to yield product as a beige solid (59 mg, 0.117 mmol). Yield: 23%. ^{1}H NMR (400 MHz, DMSO-d_6): δ 9.21 (s, 1H), 7.88 (d, J = 8.2 Hz, 1H), 7.78 (s, 1H), 7.54-7.49 (m, 4H), 7.42 (td, J = 8.0, 1.4 Hz, 3H), 7.34 (dd, J = 8.2, 7.3 Hz, 1H), 7.24–7.15 (m, 4H). ^{13}C NMR (200 MHz, DMSO-d_6): δ 169.4, 153.4, 140.6, 139.1, 135.9, 133.8, 131.1, 129.8, 129.5, 128.5, 128.2, 128.0, 125.8, 124.4, 123.6. ESI-MS(+) *m/z* 333.76, found for $C_{20}H_{17}N_2O_3$ $[M+H]^+$.

1-(3,5-Bis(trifluoromethyl)phenyl)-3-(4-hydroxy-5-oxocyclohepta-1,3,6-trien-1-yl)urea (4.j): The pure product was obtained via recrystalization from 1:1 EtOAc/Hexanes, the precipitate isolated via vacuum filtration. The product was dried under vacuum to yield a brown solid (72 mg, 0.184 mmol). Yield: 24%. ^{1}H NMR (400 MHz, DMSO-d_6): δ 9.52 (s, 1H), 9.19 (s, 1H), 8.14 (s, 2H), 7.67 (s, 1H), 7.57 (d, J = 12.1 Hz, 2H), 7.23 (d, J = 12.0 Hz, 2H). ^{13}C NMR (200 MHz, DMSO-d_6): δ 169.5, 169.9, 153.2, 140.4, 138.5, 128.4, 127.7, 127.6, 127.5, 126.9, 126.1, 125.8, 119.4, 119.2. ESI-MS(-) *m/z* 390.92, found for $C_{16}H_9F_6N_2O_3$ $[M-H]^-$.

1-(3-Chlorophenyl)-3-(4-hydroxy-5-oxocyclohepta-1,3,6-trien-1-yl)urea (4.k): The pure product was obtained via silica column chromatography using 0-8% MeOH in

DMC as an eluent to yield product as a beige solid (65 mg, 0.224 mmol). Yield: 15%. ^{1}H NMR (400 MHz, DMSO-d_6): δ 9.05 (s, 1H), 9.00 (s, 1H), 7.71 (d, J = 2.1 Hz, 1H), 7.58 (d, J = 12.4 Hz, 2H), 7.31 (d, J = 6.9 Hz, 2H), 7.24 (d, J = 12.2 Hz, 2H), 7.06 (dd, J = 5.1, 3.6 Hz, 1H). ^{13}C NMR (200 MHz, DMSO-d_6): δ 174.0, 172.9, 145.5, 137.2, 136.2, 134.6, 131.2, 129.8, 125.7, 125.3, 124.9, 124.2, 122.0, 119.3. ESI-MS(+) *m/z* 291.03, found for $C_{14}H_{12}ClN_2O_3$ $[M+H]^+$.

Methyl 4-(3-(4-hydroxy-5-oxocyclohepta-1,3,6-trien-1-yl)ureido)benzoate (4.l): The pure product was obtained via silica column chromatography using 0-4% MeOH in DMC as an eluent to yield product as a beige solid (88 mg, 0.280 mmol). Yield: 38%. ^{1}H NMR (400 MHz, DMSO-d_6): δ 9.23 (s, 1H), 9.01 (s, 1H), 7.90 (d, J = 8.7 Hz, 2H), 7.60–7.56 (m, 4H), 7.23 (d, J = 12.3 Hz, 2H), 3.81 (s, 3H). ^{13}C NMR (200 MHz, DMSO-d_6): δ 169.7, 166.0, 153.0, 144.6, 139.9, 131.0, 128.8, 125.6, 123.7, 118.2, 52.8. ESI-MS(-) *m/z* 312.89, found for $C_{16}H_{13}N_2O_5$ $[M-H]^-$.

1-(2,3-Dihydro-1*H*-inden-5-yl)-3-(4-hydroxy-5-oxocyclohepta-1,3,6-trien-1-yl)urea (4.m): The pure product was obtained via silica column chromatography using 0-3% MeOH in DMC as an eluent to yield product as a beige solid (48 mg, 0.162 mmol). Yield: 22%. ^{1}H NMR (400 MHz, DMSO-d_6): δ 8.86 (s, 1H), 8.66 (s, 1H), 7.60–7.56 (m, 2H), 7.37 (s, 1H), 7.24–7.21 (m, 2H), 7.16–7.11 (m, 2H), 2.81 (dt, J = 14.0, 7.2 Hz, 4H), 2.00 (quintet, J = 7.4 Hz, 2H). ^{13}C NMR (200 MHz, DMSO DMSO-d_6): δ 169.7, 166.0, 153.0, 146.0, 144.6, 143.8, 139.7, 137.6, 133.3, 129.5, 124.0, 121.4, 120.4, 120.0, 43.2, 43.1, 20.1. ESI-MS(-) *m/z* 294.92, found for $C_{17}H_{15}N_2O_3$ $[M-H]^-$.

1-(2,6-Dichlorophenyl)-3-(4-hydroxy-5-oxocyclohepta-1,3,6-trien-1-yl)urea (4.n): The pure product was obtained via recrystalization from EtOAc, the precipitate

isolated via vacuum filtration. The product was dried under vacuum to yield a tan solid (109 mg, 0.336 mmol). Yield: 46%. ^{1}H NMR (400 MHz, DMSO-d_6): δ 9.20 (s, 1H), 8.38 (s, 1H), 7.57 (dd, J = 14.3, 10.3 Hz, 4H), 7.33 (t, J = 8.1 Hz, 1H), 7.22 (d, J = 12.3 Hz, 2H). ^{13}C NMR (200 MHz, DMSO-d_6): δ 169.4, 158.2, 157.3, 156.3, 140.5, 135.9, 130.6, 128.4, 125.8, 123.5, 120.9, 120.4, 118.4. ESI-MS(-) *m/z* 322.83, found for $C_{14}H_9Cl_2N_2O_4$ $[M-H]^-$.

1-(3-Acetylphenyl)-3-(4-hydroxy-5-oxocyclohepta-1,3,6-trien-1-yl)urea (4.o): The pure product was obtained via silica column chromatography using 0-5% MeOH in DMC as an eluent to yield product as a pale yellow solid (64 mg, 0.214 mmol). Yield: 29%. ^{1}H NMR (400 MHz, DMSO-d_6): δ 9.04 (s, 1H), 8.95 (s, 1H), 8.08 (s, 1H), 7.67 (dd, J = 8.0, 1.1 Hz, 1H), 7.61–7.57 (m, 3H), 7.45 (t, J = 7.9 Hz, 1H), 7.23 (d, J = 12.2 Hz, 2H), 2.56 (s, 3H). ^{13}C NMR (200 MHz, DMSO-d_6): δ 171.2, 169.0, 154.9, 149.5, 136.5, 136.0, 133.4, 129.0, 128.3, 127.4, 126.5, 126.0, 23.6. ESI-MS(-) *m/z* 296.98, found for $C_{16}H_{13}N_2O_4$ $[M-H]^-$.

Ethyl 3-(3-(4-hydroxy-5-oxocyclohepta-1,3,6-trien-1-yl)ureido)benzoate (4.p): The pure product was obtained via silica column chromatography using 0-4% MeOH in DMC as an eluent to yield product as a beige solid (81 mg, 0.247 mmol). Yield: 34%. ^{1}H NMR (400 MHz, DMSO-d_6): δ 9.08 (s, 1H), 8.92 (s, 1H), 8.16 (t, J = 1.9 Hz, 1H), 7.65 (d, J = 8.1 Hz, 1H), 7.58 (d, J = 12.2 Hz, 3H), 7.43 (t, J = 7.9 Hz, 1H), 7.24–7.21 (m, 2H), 4.31 (q, J = 7.1 Hz, 2H), 1.32 (t, J = 7.1 Hz, 3H). ^{13}C NMR (200 MHz, DMSO-d_6): δ 169.7, 166.0, 153.0, 144.6, 141.0, 139.9, 137.3, 131.0, 128.8, 125.6, 123.7, 118.2, 79.1, 31.1. ESI-MS(-) *m/z* 326.99, found for $C_{17}H_{15}N_2O_5$ $[M-H]^-$.

1-(2-Chlorophenyl)-3-(4-hydroxy-5-oxocyclohepta-1,3,6-trien-1-yl)urea (4.q): The pure product was obtained via silica column chromatography using 0-3% MeOH in DMC as an eluent to yield product as a white solid (89 mg, 0.306 mmol). Yield: 40%. ^{1}H NMR (400 MHz, DMSO-d_6): δ 9.59 (s, 1H), 8.41 (s, 1H), 8.12 (d, J = 8.4 Hz, 1H), 7.60 (d, J = 12 Hz, 2H), 7.48 (d, J = 7.9 Hz, 1H), 7.31 (t, J = 8 Hz, 1H), 7.24 (d, J = 12 Hz, 2H), 7.06 (t, J = 7.4 Hz, 1H). ^{13}C NMR (200 MHz, DMSO-d_6): δ 174.8, 171.3, 152.5, 137.6, 134.6, 132.7, 130.1, 129.0, 128.2, 127.5, 125.7, 123.6, 120.2, 119.6. ESI-MS(+) *m/z* 292.00, found for $C_{14}H_{12}ClN_2O_3$ $[M+H]^+$.

1-([1,1'-Biphenyl]-4-yl)-3-(4-hydroxy-5-oxocyclohepta-1,3,6-trien-1-yl)urea (4.r): The pure product was obtained via silica column chromatography using 0-4% MeOH in DMC as an eluent to yield product as a white solid (96 mg, 0.298 mmol). Yield: 40%. ^{1}H NMR (400 MHz, DMSO-d_6): δ 8.93 (d, J = 8.1 Hz, 2H), 7.65–7.54 (m, 8H), 7.44 (s, 2H), 7.31 (t, J = 7.4 Hz, 1H), 7.24 (d, J = 12.3 Hz, 2H). ^{13}C NMR (200 MHz, DMSO-d_6): δ 174.8, 172.9, 152.5, 145.5, 140.6, 139.4, 138.4, 137.9, 137.0, 129.2, 128.2, 127.9, 127.6, 125.8, 121.5, 119.7 (only 16 of 20 carbons found). ESI-MS(-) *m/z* 330.94, found for $C_{20}H_{15}N_2O_3$ $[M-H]^-$.

1-(4-Hydroxy-5-oxocyclohepta-1,3,6-trien-1-yl)-3-(4-phenoxyphenyl)urea (4.s): The pure product was obtained via silica column chromatography using 0-6% MeOH in DMC as an eluent to yield product as a tan solid (50 mg, 0.143 mmol). Yield: 20%. ^{1}H NMR (400 MHz, DMSO-d_6): δ 8.89 (s, 1H), 8.81 (s, 1H), 7.58 (d, J = 12.3 Hz, 2H), 7.47 (d, J = 8.9 Hz, 2H), 7.36 (d, J = 0.9 Hz, 2H), 7.23 (d, J = 12.3 Hz, 2H), 7.09 (t, J = 7.4 Hz, 1H), 6.97 (dd, J = 10.0, 8.5 Hz, 4H). ^{13}C NMR (200 MHz, DMSO-d_6): δ

169.4, 158.2, 153.3, 151.6, 140.5, 135.9, 130.6, 128.4, 125.8, 123.5, 120.9, 120.4, 118.4. ESI-MS(-) *m/z* 346.98, found for $C_{20}H_{15}N_2O_4$ $[M-H]^-$.

1-(9*H*-Fluoren-2-yl)-3-(4-hydroxy-5-oxocyclohepta-1,3,6-trien-1-yl)urea (4.t): The pure product was obtained via recrystalization from 1:1 EtOAc/Hexanes, the precipitate isolated via vacuum filtration. The product was dried under vacuum to yield a pale yellow solid (63 mg, 0.183 mmol). Yield: 25%. ^{1}H NMR (400 MHz, DMSO-d_6): δ 8.92 (d, J = 15.4 Hz, 2H), 7.80 (d, J = 8.2 Hz, 3H), 7.60 (d, J = 12.3 Hz, 2H), 7.54 (d, J = 7.4 Hz, 1H), 7.41 (dd, J = 8.2, 2.0 Hz, 1H), 7.35 (t, J = 7.3 Hz, 1H), 7.27–7.22 (m, 3H), 3.90 (s, 2H). ^{13}C NMR (200 MHz, DMSO-d_6): δ 174.7, 172.7, 154.1, 153.0, 145.5, 143.4, 143.1, 141.1, 140.0, 137.9, 135.5, 129.1, 126.8, 125.8, 121.6, 120.3, 119.9, 117.3, 115.9, 105.3, 36.5. ESI-MS(-) *m/z* 342.94, found for $C_{21}H_{15}N_2O_3$ $[M-H]^-$.

Methyl 3-(3-(4-hydroxy-5-oxocyclohepta-1,3,6-trien-1-yl)ureido)benzoate (4.u): The pure product was obtained via silica column chromatography using 0-4% MeOH in DMC as an eluent to yield product as a gray solid (88 mg, 0.280 mmol). Yield: 38%. ^{1}H NMR (400 MHz, DMSO-d_6): δ 9.09 (s, 1H), 8.94 (s, 1H), 8.21 (s, 1H), 7.63-7.56 (m, 4H), 7.44 (t, J = 7.9 Hz, 1H), 7.22 (d, J = 11.7 Hz, 2H), 3.85 (s, 3H). ^{13}C NMR (400 MHz, DMSO-d_6): δ 169.7, 166.0, 153.0, 145.8, 142.1, 138.8, 137.3, 131.0, 128.8, 125.6, 123.7, 118.2, 55.9. ESI-MS(-) *m/z* 312.93, found for $C_{16}H_{13}N_2O_5$ $[M-H]^-$.

1-(4-Hydroxy-5-oxocyclohepta-1,3,6-trien-1-yl)-3-(3-(trifluoromethyl)phenyl)urea (4.v). (67 mg, 0.206 mmol). Yield: 27%. ^{1}H NMR (400 MHz, DMSO-d_6): δ 9.53 (s, 1H), 8.18 (s, 1H), 7.89 (d, J = 8.2 Hz, 1H), 7.71–7.58 (m, 4H), 7.31 (t, J = 7.6 Hz, 1H), 7.25–7.22 (m, 2H). ^{13}C NMR (200 MHz, DMSO-d_6): δ

169.3, 133.0, 129.0, 128.7, 126.4, 126.2, 125.8, 125.6, 124.1. ESI-MS(+) *m/z* 326.01, found for $C_{15}H_{11}F_3N_2O_3$ $[M+H]^+$.

1-(4-Hydroxy-5-oxocyclohepta-1,3,6-trien-1-yl)-3-(4-methoxyphenyl)urea (4.w): The pure product was obtained via silica column chromatography using 0-5% MeOH in DMC as an eluent to yield product as a beige solid (90 mg, 0.314 mmol). Yield: 21%. ^{1}H NMR (300 MHz, DMSO-d_6): δ 8.84 (s, 1H), 8.62 (s, 1H), 7.58 (d, *J* = 12.4 Hz, 2H), 7.37-7.35 (m, 2H), 7.23 (d, *J* = 12.2 Hz, 2H), 6.90-6.87 (m, 2H), 3.72 (s, 3H). ^{13}C NMR (150 MHz, DMSO-d_6): δ 169.4, 153.2, 140.4, 137.6, 132.2, 128.4, 127.0, 125.7, 119.9, 35.7. ESI-MS(+) *m/z* calcd for $C_{15}H_{14}N_2O_4$ 287.21 $[M+H]^+$.

1-(4-Hydroxy-5-oxocyclohepta-1,3,6-trien-1-yl)-3-(*p*-tolyl)urea (4.x): The pure product was obtained via recrystalization from EtOAc, the precipitate isolated via vacuum filtration. The product was dried under vacuum to yield a brown solid (93 mg, 0.317 mmol). Yield: 47%. ^{1}H NMR (400 MHz, DMSO-d_6): δ 8.70 (s, 1H), 7.55 (dd, *J* = 12.2, 0.8 Hz, 2H), 7.19 (dd, *J* = 12.2, 0.8 Hz, 2H), 6.32 (t, *J* = 5.7 Hz, 1H), 3.04 (q, *J* = 6.5 Hz, 2H), 1.45 (dt, *J* = 14.5, 7.2 Hz, 2H), 0.87 (t, *J* = 7.4 Hz, 3H). ^{13}C NMR (200 MHz, DMSO-d_6): δ 173.3, 172.7, 151.5, 145.9, 139.9, 138.0, 136.1, 128.0, 127.0, 126.2, 121.6, 119.1, 26.1. ESI-MS(+) *m/z* 271.50, found for $C_{15}H_{15}N_2O_3$ $[M+H]^+$.

1-Benzyl-3-(4-hydroxy-5-oxocyclohepta-1,3,6-trien-1-yl)urea (4.y): The pure product was obtained via recrystalization from EtOAc, the precipitate isolated via vacuum filtration. The product was dried under vacuum to yield a white solid (30 mg, 0.111 mmol). Yield: 15%. ^{1}H NMR (400 MHz, DMSO-d_6): δ 8.84 (s, 1H), 7.57 (d, *J* = 11.9 Hz, 2H), 7.36–7.18 (m, 7H), 6.80 (t, *J* = 3.5 Hz, 1H), 4.30 (d, *J* = 5.6 Hz, 2H). ^{13}C NMR (200 MHz, DMSO-d_6): δ 173.8, 172.6, 151.3, 146.8, 143.7, 140.1, 137.9, 132.9,

128.9, 128.1, 122.0, 119.8, 44.1 (only 13 of 15 carbons found). ESI-MS(-) *m/z* 269.02, found for $C_{15}H_{13}N_2O_3$ $[M-H]^-$.

1-(4-Hydroxy-5-oxocyclohepta-1,3,6-trien-1-yl)-3-phenylurea (4.z): The pure product was obtained via silica column chromatography using 0-7% MeOH in DMC as an eluent to yield product as a yellow solid (75 mg, 0.293 mmol). Yield: 40%. ^{1}H NMR (400 MHz, DMSO-d_6): δ 8.85 (d, J = 40.0 Hz, 2H), 7.58 (dd, J = 12.2, 1.5 Hz, 2H), 7.45 (d, J = 8.1 Hz, 2H), 7.31–7.21 (m, 4H), 6.99 (t, J = 7.4 Hz, 1H). ^{13}C NMR (200 MHz, DMSO-d_6): δ 169.9, 157.8, 142.7, 127.3, 126.0, 120.3, 120.3, 120.2, 115.5, 113.9, 105.2. ESI-MS(+) *m/z* 257.22, found for $C_{14}H_{13}N_2O_3$ $[M+H]^+$.

1-Cyclohexyl-3-(4-hydroxy-5-oxocyclohepta-1,3,6-trien-1-yl)urea (4.aa): The pure product was obtained via silica column chromatography using 0-4% MeOH in DMC as an eluent to yield product as a white solid (30 mg, 0.114 mmol). Yield: 15% yield. ^{1}H NMR (400 MHz, DMSO-d_6): δ 8.56 (s, 1H), 7.52 (d, J = 12.3 Hz, 2H), 7.17 (d, J = 12.3 Hz, 2H), 6.22 (d, J = 7.8 Hz, 1H), 3.43 (dd, J = 6.8, 2.9 Hz, 1H), 1.77 (d, J = 12.1 Hz, 2H), 1.66–1.62 (m, 2H), 1.52 (d, J = 12.1 Hz, 1H), 1.30 (t, J = 11.2 Hz, 2H), 1.20–1.11 (m, 3H). ^{13}C NMR (200 MHz, DMSO-d_6): δ 168.9, 154.8, 141.7, 127.3, 126.0, 48.5, 48.5, 48.4, 33.5, 25.9, 25.0. ESI-MS(-) *m/z* 261.06, found for $C_{14}H_{17}N_2O_3$ $[M-H]^-$.

1-(4-Hydroxy-5-oxocyclohepta-1,3,6-trien-1-yl)-3-(4-nitrophenyl)urea (4.ab): The pure product was obtained via silica column chromatography using 0-5% MeOH in DMC as an eluent to yield product as a beige solid (30 mg, 0.099 mmol). Yield: 15%. ^{1}H NMR (400 MHz, DMSO-d_6): δ 9.53 (s, 1H), 9.09 (s, 1H), 8.18 (d, J = 9.2 Hz, 2H), 7.68 (d, J = 9.3 Hz, 2H), 7.55 (dd, J = 12.1, 1.1 Hz, 2H), 7.23–7.20 (m, 2H). ^{13}C NMR (200

MHz, DMSO-d_6): δ 174.2, 172.9, 154.3, 145.7, 145.3, 141.7, 137.5, 132.0, 125.8, 124.1, 121.6, 119.9. ESI-MS(-) *m/z* 299.8, found for $C_{14}H_{17}N_2O_3$ $[M-H]^-$.

1-(2,4-Dichlorophenyl)-3-(4-hydroxy-5-oxocyclohepta-1,3,6-trien-1-yl)urea (4.ac): The pure product was obtained via silica column chromatography using 0-3% MeOH in DMC as an eluent to yield product as a white solid (180 mg, 0.555 mmol). Yield: 76%. ^{1}H NMR (400 MHz, DMSO-d_6): δ 9.59 (s, 1H), 8.47 (s, 1H), 8.15 (d, *J* = 9.0 Hz, 1H), 7.63–7.57 (m, 3H), 7.39 (dd, *J* = 9.0, 2.5 Hz, 1H), 7.25–7.22 (m, 2H). ^{13}C NMR (200 MHz, DMSO-d_6): δ 169.5, 153.2, 140.4, 139.5, 134.6, 129.6, 128.4, 127.7, 127.5, 126.8, 125.8, 119.4, 119.2. ESI-MS(-) *m/z* 322.9, found for $C_{14}H_9Cl_2N_2O_3$ $[M-H]^-$.

1-(2-Bromo-4,6-difluorophenyl)-3-(4-hydroxy-5-oxocyclohepta-1,3,6-trien-1-yl)urea (4.ad): The pure product was obtained via recrystalization from EtOAc the precipitate isolated via vacuum filtration. The product was dried under vacuum to yield a yellow solid (71 mg, 0.192 mmol). Yield: 26%. ^{1}H NMR (400 MHz, DMSO-d_6): δ 9.23 (s, 1H), 8.20 (s, 1H), 7.60–7.57 (m, 3H), 7.50–7.44 (m, 1H), 7.22 (d, *J* = 12.2 Hz, 2H). ^{13}C NMR (200 MHz, DMSO-d_6): δ 174.9, 172.9, 166.6, 152.4, 145.5, 139.2, 137.9, 129.7, 125.8, 125.8, 124.5, 121.2, 116.5, 103.9. ESI-MS(-) *m/z* 368.71, found for $C_{14}H_8BrF_2N_2O_3$ $[M-H]^-$.

1-(2,6-Difluorophenyl)-3-(4-hydroxy-5-oxocyclohepta-1,3,6-trien-1-yl)urea (4.ae): The pure product was obtained via silica column chromatography using 0-3% MeOH in DMC as an eluent to yield product as a tan solid (66 mg, 0.226 mmol). Yield: 31%. ^{1}H NMR (400 MHz, DMSO-d_6): δ 9.18 (s, 1H), 8.28 (s, 1H), 7.60–7.57 (m, 2H), 7.37–7.30 (m, 1H), 7.24–7.14 (m, 4H). ^{13}C NMR (200 MHz, DMSO-d_6): δ 169.4, 158.2,

157.3, 156.3, 140.5, 135.9, 134.6, 128.4, 125.8, 124.4, 120.9, 120.4, 119.6. ESI-MS(+) *m/z* 293.10, found for $C_{14}H_{11}F_2N_2O_3$ $[M+H]^+$.

1-(4-Hydroxy-5-oxocyclohepta-1,3,6-trien-1-yl)-3-propylurea (4.af): The pure product was obtained via silica column chromatography using 0-4% MeOH in DMC as an eluent to yield product as a white solid (66 mg, 0.293 mmol). Yield: 31%. ^{1}H NMR (400 MHz, DMSO-d_6): δ 8.65 (s, 1H), 7.55 (dd, *J* = 12.2, 0.8 Hz, 2H), 7.19 (dd, *J* = 12.2, 0.8 Hz, 2H), 6.32 (t, *J* = 5.7 Hz, 1H), 3.04 (q, *J* = 6.5 Hz, 2H), 1.45 (dt, *J* = 14.5, 7.2 Hz, 2H), 0.87 (t, *J* = 7.4 Hz, 3H). ^{13}C NMR (200 MHz, DMSO-d_6): δ 169.4, 158.2, 156.3, 140.5, 135.9, 50.5, 30.2, 26.8. ESI-MS(+) *m/z* 223.70, found for $C_{11}H_{15}N_2O_3$ $[M+H]^+$.

***N*-(4-hydroxy-5-oxocyclohepta-1,3,6-trien-1-yl)-2-(naphthalen-1-yl)acetamide (5):** To a solution of **4** (250 mg, 1.8 mmol) in 20 mL of DMF, was added triethylamine (280 μL, 2.0 mmol) EDC (419 mg, 2.2 mmol), HOBt (335 mg, 2.2 mmol), and 2-(naphthalen-1-yl)acetic acid (407 mg, 2.2 mmol). The mixture was stirred for 18h at room temperature under nitrogen. The solvent was removed in vacuo and reaction was extracted with H_2O and DCM. The organic phase was collected, dried over anhydrous $MgSO_4$ and concentrated in vacuo to a pale yellow residue. The residue was purified via silica column chromatography using 0-3% MeOH in as an eluent to yield **5** as a pale yellow solid (70 mg, 0.230 mmol). Yield: 13% yield. ^{1}H NMR (400 MHz, DMSO-d_6): δ 10.48 (s, 1H), 8.14 (d, *J* = 8.1 Hz, 1H), 7.97 (d, *J* = 8.2 Hz, 1H), 7.90–7.87 (m, 1H), 7.72 (d, *J* = 12.1 Hz, 2H), 7.60–7.51 (m, 4H), 7.24 (d, *J* = 11.7 Hz, 2H), 4.19 (s, 2H). ^{13}C NMR (200 MHz, DMSO-d_6): δ 173.9, 173.9, 153.7, 144.9, 140.6, 137.9, 136.9, 133.2, 128.3, 126.1, 126.0, 125.2, 124.4, 121.6, 119.8, 118.8, 108.1, 106.2, 43.8. ESI-MS(-) *m/z* 304.08, found for $C_{19}H_{14}NO_3$ $[M-H]^-$.

***N*-(4-hydroxy-5-oxocyclohepta-1,3,6-trien-1-yl)-1-naphthamide 6:** Compound **(6)** was prepared as described for **5**, substituting 1-naphthoic acid for 2-(naphthalen-1-yl)acetic acid to yield product as a beige solid (82 mg, 0.292 mmol). Yield: 15%. ^{1}H NMR (400 MHz, DMSO-d_6): δ 8.83 (d, J = 8.4 Hz, 1H), 8.27 (dd, J = 17.3, 7.7 Hz, 2H), 8.07 (d, J = 8.0 Hz, 1H), 7.70–7.63 (m, 3H), 7.25 (d, J = 12.0 Hz, 2H), 7.08 (s, 2H). ^{13}C NMR (200 MHz, DMSO-d_6): δ 169.7, 168.2, 161.2, 153.7, 137.6, 136.4, 136.1, 134.7, 133.9, 132.7, 131.1, 130.0, 126.1, 121.6, 120.5, 120.3, 119.8, 105.8. ESI-MS(-) *m/z* 289.89, found for $C_{18}H_{12}NO_3$ $[M-H]^-$.

4-(3-(Naphthalen-1-yl)ureido)-7-oxocyclohepta-1,3,5-trien-1-yl acetate (7): To a solution of **4.a** (125 mg, 0.41 mmol) in acetic anhydride (3.0 mL, 32 mmol), was added sulfuric acid (22 μL, 0.41 mmol). The reaction was stirred for 24 h at room temperature under nitrogen. The reaction was quenched with 20 mL of ice and extracted with DCM. The organic phase was collected, dried over anhydrous $MgSO_4$ and concentrated in vacuo to a white residue. The crude product was purified via silica column chromatography using 0–7% MeOH in DCM as an eluent to yield **7** (125 mg, 0.359 mmol). Yield: 31%. ^{1}H NMR (300 MHz, DMSO-d_6): δ 9.57 (s, 1H), 8.99 (s, 1H), 8.06 (d, J = 6.3 Hz, 1H), 7.91 (t, J = 6.0 Hz, 2H), 7.67 (d, J = 6.0 Hz, 1H), 7.60–7.52 (m, 4H), 7.46 (t, J = 6.0 Hz, 1H), 7.30 (d, J = 9.0 Hz, 2H), 2.20 (s, 3H). ^{13}C NMR (150 MHz, DMSO-d_6): δ 168.7, 153.3, 145.8, 134.4, 134.1, 129.1, 127.0, 126.7, 126.6, 126.5, 124.6, 122.1, 119.2, 21.1. ESI-MS(+) *m/z* 348.98, found for $C_{20}H_{17}N_2O_4$ $[M+H]^+$.

Enzymatic Assays

Assay Protocol. Fluorescence Assay for LasB Activity, this assay was adapted from that previously reported.[80] To the wells of a 96-well microtiter plate

(Corning®Costar®; black with clear bottom), add 91 μL Buffer B, 2 μL of each inhibitor stock and 2 μL LasB solution (2 μg/mL final) (in this order). It should be noted that: 1) positive control: 2 μL DMSO in place of inhibitor and 2) negative control: 4 μL DMSO in place of LasB and inhibitor stock. The plates were incubated at 37 °C for 30 min, while incubating, the fluorescence plate reader was turned on and set up: λ_{ex} = 340 nm, λ_{em} = 415 nm, 37°C, read on kinetic setting over 30 min. After 30 min incubation at 37 °C, 5 μL of LasB substrate solution (250 μM final) was added to each well. After which the plate was directly transferred to the fluorescence plate reader and measured fluorescence. For an inhibitor, *decreased* fluorescence signal will be observed in comparison to the positive control

Assay Buffers:

A: 50 mM Tris-HCl, 2.5 mM $CaCl_2$ (pH 7)

To prepare: 25 mL Tris-HCl (1 M solution), 475 mL H_2O, 139 mg $CaCl_2$

B: 50 mM Tris-HCl, 2.5 mM $CaCl_2$, 1% DMF (pH 7)

To prepare: 25 mL Tris-HCl (1 M solution), 475 mL H_2O, 139 mg $CaCl_2$, 5 mL DMF (molecular biology grade)

Assay Stock Solutions:

LasB: 0.1 mg/mL in Buffer A

LasB substrate: 5 mM in DMF (molecular biology grade)

To prepare: 3 mg (MW: 583.64 g/mol), 1 mL DMF

Inhibitor Stock Solutions:

10 mM, 5 mM, 2.5 mM, 500 μM, 250 μM, 50 μM, 25 μM in DMSO

Note: 2 μL of each stock used in the assay

Stock	Assay Final Concentration (μM)
10 mM	200
5 mM	100
2.5 mM	50
500 μM	10
250 μM	5
50 μM	1
25 μM	0.5

Cross-Inhibition Assays

Assay for MMP-2 and MMP-9. The assay was carried out in white NUNC* 96-well opaque round-bottomed plates as previously described.[137] For the assay, each well contained a total volume of 90 μL including buffer (50 mM HEPES, 10 mM $CaCl_2$, 0.05% Brij-35, pH 7.5), human recombinant MMP (ENZO Life Sciences; 1.16 U MMP-2 and 0.9 U MMP-9), and compound **7** (50 μM final concentration). After a 30 min incubation period at 37 °C, the reaction was initiated by the addition of 10 μL of the fluorogenic MMP substrate (4 μM final concentration, Mca-Pro-Leu-Gly-Leu-Dpa-Ala-Arg-NH_2·AcOH, ENZO Life Sciences). Fluorescence measurements were recorded using a Bio-Tek Flx 800 fluorescence plate reader every minute for 20 min at excitation and emission wavelengths of 320 and 400 nm, respectively. The rate of fluorescence increase was compared for samples and negative controls (no inhibitor, arbitrarily set as 100% activity).

Assay for Mushroom Tyrosinase (TY). The assay was carried out as previously described.[219] The assay was performed in black 96-well clear flat-bottomed plates with

each well containing a total volume of 100 μL. This included buffer (50 mM phosphate, pH 6.8), mushroom TY (30 U, Sigma-Aldrich), inhibitor (50 μM), and *L*-dopamine (0.5 mM, Sigma-Aldrich). Mushroom TY and inhibitor were pre-incubated in the buffer solution at room temperature for 10 min. A background absorbance reading at 475 nm was recorded using a Bio-Tek ELx 808 colorimetric plate reader. *L*-Dopamine was added to initiate the reaction, which was allowed to proceed for 10 min before a second absorbance reading at 475 nm was taken. After subtracting the background absorbance, the remaining absorbance of the negative controls (no inhibitor) was arbitrarily set as 100% activity. The ratio of absorbance between inhibitor and control wells was defined as percent TY activity.

Assay for Human Carbonic Anhydrase II (hCAII). hCAII activity was measured in 50 mM Tris (pH 8) using an esterase activity assay with 4-nitrophenyl acetate as the substrate. Conversion of 4-nitrophenyl acetate to 4-nitrophenol by hCAII is observed as an increase in absorbance at 405 nm, which was read on a BioTek ELx808 plate reader. Protein (100 nM, final concentration, expressed as previously described[226] in was incubated with inhibitor (50 μM) for 10 min at room temperature followed by addition of substrate (in DMSO, 500 μM final concentration). The total well volume (clear, flat-bottom, 96-well plates) was 100 μL and contained 5% DMSO. Initial linear rates were compared to both negative (inhibitor-free) and positive (100% inhibition with 50 μM benzenesulfonamide)[227] controls in order to determine percent inhibition.

***P. aeruginosa* Cell-based Assays**

P. aeruginosa Swarming Assay. A swarming motility assay using *P. aeruginosa* strain PA14 was executed as previously described.[228] Overnight cultures of PA14 strain,

prepared in Tryptic soy broth (TSB) at 37 °C (250 rpm), were washed (3×) with phosphate-buffered saline buffer (pH 7.4). The washed culture was then diluted with the same buffer to an OD_{600} of ~3.0. Swarm agar medium was a modified M9 agar medium and contained: 20 mM NH_4Cl, 12 mM Na_2HPO_4, 22 mM KH_2PO_4, 8.6 mM NaCl, 1 mM $MgSO_4$, 1 mM $CaCl_2$•2 H_2O, 11 mM dextrose, 0.5% casamino acids (Difco) and Bacto-agar (Difco). The medium was autoclaved, and upon cooling was diluted with filter-sterilized $MgSO_4$ and $CaCl_2$•$2H_2O$. ~20 mL of swarm agar medium containing compound **TM2/8a**, **TM8/8b**, **4.a,** or **7** (25 μM) was poured into 100×25 mm Petri dishes housed in a laminar flow cabinet and dried for 1 h. 5 μL of the bacterial culture (OD_{600} of ~3.0) was spotted onto each plate followed by incubation at 30 °C for 18 h.

4. G. Acknowledgements

Text, figures, and schemes in this chapter, in part, are reprints of the material published in the following papers: Amanda L. Garner, Jessica L. Fullagar, Anjali K. Struss, Arpita Agrawal, Amira Y. Moreno, Seth M. Cohen, and Kim D. Janda, "3-Hydroxy-1-alkyl-2-methylpyridine-4(1*H*)-thiones: Inhibition of the *P. aeruginosa* Virulence Factor LasB" *ACS Med. Chem. Lett*. **2012**, *3*, 668-672 and Jessica L. Fullagar, Amanda L. Garner, Anjali K. Struss, Joshua A. Day, David P. Martin, Jing Yu, Xiaoqing Cai, Kim D. Janda, and Seth M. Cohen "Antagonism of a Zinc Metalloprotease Using a Unique Metal-Chelating Scaffold Tropolones as Inhibitors of *P. aeruginosa* Elastase" *Chem. Commun.* **2013** 49, 3197-3199. The dissertation author was a primary contributing author on the paper included. The co-authors listed in this publication also participated in the research. The permission to reproduce this paper was granted by the American Chemical Society, copyright 2013 and Royal Society of Chemistry, copyright 2013.

4. H. References

(1) Congreve, M.; Chessari, G.; Tisi, D.; Woodhead, A. J. *J. Med. Chem.* **2008**, *51*, 3661-3680.

(2) Leach, A. R.; Hann, M. M.; Burrows, J. N.; Griffen, E. J. *Mol. Biosyst.* **2006**, *2*, 429-446.

(3) Carr, R. A. E.; Congreve, M.; Murray, C. W.; Rees, D. C. *Drug Discov. Today* **2005**, *10*, 987-992.

(4) Maly, D. J.; Choong, I. C.; Ellman, J. A. *Proc. Natl. Acad. Sci. USA* **2000**, *97*, 2419-2424.

(5) Jencks, W. P. *Proc. Natl. Acad. Sci. USA* **1981**, *78*, 4046-4050.

(6) Hajduk, P. J.; Sheppard, G.; Nettesheim, D. G.; Olejniczak, E. T.; Shuker, S. B.; Meadows, R. P.; Steinman, D. H.; Carrera Jr., G. M.; Marcotte, P. A.; J, S.; Walter, K.; Smith, H.; Gubbins, E.; Simmer, R.; Holzman, T. F.; Morgan, D. W.; Davidsen, S. K.; Summers, J. B.; Fesik, S. W. *J. Am. Chem. Soc.* **1997**, *119*, 5818-5827.

(7) Blundell, T. L.; Jhoti, H.; Abell, C. *Nat. Rev. Drug Disocv.* **2002**, *1*, 45-54.

(8) Hann, M. M.; Leach, A. R.; Harper, G. *J. Chem. Inf. Comput. Sci.* **2001**, *41*, 856-864.

(9) Carr, R.; Jhoti, H. *Drug Discov. Today* **2002**, *7*, 522-527.

(10) Lipinski, C.; Hopkins, A. *Nature* **2004**, *432*, 855-861.

(11) Teague, S. J.; Davis, A. M.; Leeson, P. D.; Oprea, T. *Angew. Chem. Int. Ed.* **1999**, *38*, 3743-3748.

(12) Agrawal, A.; Johnson, S. L.; Jacobsen, J. A.; Miller, M. T.; Chen, L.-H.; Pellecchia, M.; Cohen, S. M. *ChemMedChem* **2010**, *5*, 195-199.

(13) Pellecchia, M.; Bertini, I.; Cowburn, D.; Dalvit, C.; Giralt, E.; Jahnke, W.; James, T. L.; Homans, S. W.; Kessler, H.; Luchinat, C.; Meyer, B.; Oschkinat, H.; Peng, J.; Schwalbe, H.; Siegal, G. *Nat. Rev. Drug Disocv.* **2008**, *7*, 738-745.

(14) Shuker, S. B.; Hajduk, P. J.; Meadows, R. P.; Fesik, S. W. *Science* **1996**, *274*, 1531-1534.

(15) Kuhn, P.; Wilson, K.; Patch, M. G.; Stevens, R. C. *Curr. Opin. Chem. Biol.* **2002**, *6*, 704-710.

(16) Nakamura, C. E.; Abeles, R. H. *Biochemistry* **1985**, *24*, 1364-1376.

(17) Lewell, X. Q.; Judd, D. B.; Watson, S. P.; Hann, M. M. *J. Chem. Inf. Comput. Sci.* **1998**, *38*, 511-522.

(18) Erlanson, D. A.; McDowell, R. S.; O'Brien, T. *J. Med. Chem.* **2004**, *47*, 3463-3482.

(19) Esposito, E. X.; Baran, K.; Kelly, K.; Madura, J. D. *J. Mol. Graphics Modell.* **2000**, *18*, 283-289.

(20) Irwin, J. J.; Raushel, F. M.; Shoichet, B. K. *Biochemistry* **2005**, *44*, 12316-12328.

(21) Menikarachchi, L. C.; Gasicn, J. A. *Curr. Top. Med. Chem.* **2009**, *10*, 46-54.

(22) Perspicace, S.; Banner, D.; Benz, J. r.; M√ºller, F.; Schlatter, D.; Huber, W. *J. Biomol. Screen.* **2009**, *14*, 337-349.

(23) Nordstroàm, H.; Gossas, T.; Haàmaàlaàinen, M.; Kaàllblad, P.; Nystroàm, S.; Wallberg, H.; Danielson, U. H. *J. Med. Chem.* **2008**, *51*, 3449-3459.

(24) Neumann, T.; Junker, H.; Schmidt, K.; Sekul, R. *Curr. Top. Med. Chem.* **2007**, *7*, 1630-1642.

(25) Schade, M.; Oschkinat, H. *Curr. Opin. Drug Discov. Devel.* **2005**, *8*, 365.

(26) Leach, A. R.; Hann, M. M.; Burrows, J. N.; Griffen, E. J. *Mol. Biosyst.* **2006**, *2*, 429-446.

(27) McGovern, S. L.; Helfand, B. T.; Feng, B.; Shoichet, B. K. *J. Med. Chem.* **2003**, *46*, 4265-4272.

(28) Bleicher, K. H.; Buhm, H.-J.; Muller, K.; Alanine, A. I. *Nat. Rev. Drug Disocv.* **2003**, *2*, 369-378.

(29) Ramstradm, O.; Lehn, J.-M. *Nat. Rev. Drug Disocv.* **2002**, *1*, 26-36.

(30) Rees, D. C.; Congreve, M.; Murray, C. W.; Carr, R. *Nat. Rev. Drug Disocv.* **2004**, *3*, 660-672.

(31) Baker, M. *Nat. Rev. Drug Disocv.* **2013**, *12*, 5-7.

(32) Bollag, G.; Hirth, P.; Tsai, J.; Zhang, J.; Ibrahim, P. N.; Cho, H.; Spevak, W.; Zhang, C.; Zhang, Y.; Habets, G.; Burton, E. A.; Wong, B.; Tsang, G.; West, B. L.; Powell, B.; Shellooe, R.; Marimuthu, A.; Nguyen, H.; Zhang, K. Y. J.; Artis, D. R.; Schlessinger, J.; Su, F.; Higgins, B.; Iyer, R.; D/'Andrea, K.; Koehler, A.; Stumm, M.; Lin, P. S.; Lee, R. J.; Grippo, J.; Puzanov, I.; Kim, K. B.; Ribas, A.; McArthur, G. A.; Sosman, J. A.; Chapman, P. B.; Flaherty, K. T.; Xu, X.; Nathanson, K. L.; Nolop, K. *Nature* **2010**, *467*, 596-599.

(33) Tsai, J.; Lee, J. T.; Wang, W.; Zhang, J.; Cho, H.; Mamo, S.; Bremer, R.; Gillette, S.; Kong, J.; Haass, N. K.; Sproesser, K.; Li, L.; Smalley, K. S. M.; Fong, D.; Zhu, Y.-L.; Marimuthu, A.; Nguyen, H.; Lam, B.; Liu, J.; Cheung, I.; Rice, J.; Suzuki, Y.; Luu, C.; Settachatgul, C.; Shellooe, R.; Cantwell, J.; Kim, S.-H.; Schlessinger, J.; Zhang, K. Y. J.; West, B. L.; Powell, B.; Habets, G.; Zhang, C.; Ibrahim, P. N.; Hirth, P.; Artis, D. R.; Herlyn, M.; Bollag, G. *Proc. Natl. Acad. Sci. USA* **2008**, *105*, 3041-3046.

(34) Jacobsen, F. E.; Lewis, J. A.; Cohen, S. M. *J. Am. Chem. Soc.* **2006**, *128*, 3156-3157.

(35) Jacobsen, J. A.; Jourden, J. L. M.; Miller, M. T.; Cohen, S. M. *Biochim. Biophys. Acta* **2010**, *1803*, 72-94.

(36) Muri, E. M. F.; Nieto, M. J.; Sindelar, R. D.; Williamson, J. S. *Curr. Med. Chem.* **2002**, *9*, 1631-1653.

(37) Puerta, D. T.; Cohen, S. M. *Inorg. Chem.* **2002**, *41*, 5075-5082.

(38) Puerta, D. T.; Cohen, S. M. *Inorg. Chem.* **2003**, *42*, 3423-3430.

(39) Puerta, D. T.; Lewis, J. A.; Cohen, S. M. *J. Am. Chem. Soc.* **2004**, *126*, 8388-8389.

(40) Lewis, J. A.; Puerta, D. T.; Cohen, S. M. **2003**, *40*, 2213-2215.

(41) Lu, Y. *Inorg. Chem.* **2006**, *45*, 9930-9940.

(42) McRae, R.; Bagchi, P.; Sumalekshmy, S.; Fahrni, C. J. *Chem. Rev.* **2009**, *109*, 4780-4827.

(43) Jarcho, S. *Am. J. Cardiol.* **1958**, *2*, 507-508.

(44) Ludwiczek, S.; Theurl, I.; Bahram, S.; Schümann, K.; Weiss, G. *J. Cell. Physiol.* **2005**, *204*, 489-499.

(45) Dive, V.; Chang, C.-F.; Yiotakis, A.; Sturrock, E. D. *Curr. Pharm. Des.* **2009**, *15*, 3606-3621.

(46) Agrawal, A.; Romero-Perez, D.; Jacobsen, J. A.; Villarreal, F. J.; Cohen, S. M. *ChemMedChem* **2008**, *3*, 812-820.

(47) Rao, B. G. *Curr. Pharm. Des.* **2005**, *11*, 295-322.

(48) Cuniasse, P.; Devel, L.; Makaritis, A.; Beau, F.; Georgiadis, D.; Matziari, M.; Yiotakis, A.; Dive, V. *Biochimie* **2005**, *87*, 393-402.

(49) Overall, C. M.; Kleifeld, O. *Br. J. Cancer* **2006**, *94*, 941-946.

(50) Coussens, L. M.; Fingleton, B.; Matrisian, L. M. *Science* **2002**, *295*, 2387-2392.

(51) Uchida, M.; Shima, M.; Shimoaka, T.; Fujieda, A.; Obara, K.; Suzuki, H.; Nagai, Y.; Ikeda, T.; Yamato, H.; Kawaguchi, H. *J. Cell. Physiol.* **2000**, *185*, 207-214.

(52) Nagase, H.; Visse, R.; Murphy, G. *Cardiovasc. Res.* **2006**, *69*, 562-573.

(53) Nuti, E.; Tuccinardi, T.; Rossello, A. *Curr. Pharm. Des.* **2007**, *13*, 2087-2100.

(54) Dollery, C. M.; McEwan, J. R.; Henney, A. M. *Circ. Res.* **1995**, *77*, 863-868.

(55) Hidalgo, M.; Eckhardt, S. G. *J. Natl. Cancer Inst.* **2001**, *93*, 178-193.

(56) Brown, P.; Giavazzi, R. *Ann. Oncol.* **1995**, *6*, 967-974.

(57) Flipo, M.; Charton, J.; Hocine, A.; Dassonneville, S.; Deprez, B.; Deprez-Poulain, R. *J. Med. Chem.* **2009**, *52*, 6790-6802.

(58) Chen, L.; Rydel, T. J.; Gu, F.; Dunaway, C. M.; Pikul, S.; Dunham, K. M.; Barnett, B. L. *J. Mol. Biol.* **1999**, *293*, 545-557.

(59) Tonello, F.; Montecucco, C. *Mol. Aspects Med.* **2009**, *30*, 431-438.

(60) Hammond, S.; Hanna, P. *Infect. Immun.* **1998**, *66*, 2374-2378.

(61) Burnett, J. C.; Henchal, E. A.; Schmaljohn, A. L.; Bavari, S. *Nat. Rev. Drug Discov.* **2005**, *4*, 281-297.

(62) Moayeri, M.; Leppla, S. H. *Curr. Opin. Microbiol.* **2004**, *7*, 19-24.

(63) Collier, R. J.; Young, J. A. *Annu. Rev. Cell Dev. Biol.* **2003**, *19*, 45-70.

(64) Abrami, L.; Reig, N.; van der Goot, F. G. *Trends Microbiol.* **2005**, *13*, 72-78.

(65) Agrawal, A.; de Oliveira, C. A. F.; Cheng, Y.; Jacobsen, J. A.; McCammon, J. A.; Cohen, S. M. *J. Med. Chem.* **2009**, *52*, 1063-1074.

(66) Johnson, S. L.; Chen, L.-H.; Barile, E.; Emdadi, A.; Sabet, M.; Yuan, H.; Wei, J.; Guiney, D.; Pellecchia, M. *Bioorg. Med. Chem.* **2009**, *17*, 3352-3368.

(67) Lewis, J. A.; Mongan, J.; McCammon, J. A.; Cohen, S. M. *ChemMedChem* **2006**, *1*, 694-697.

(68) Stover, C.; Pham, X.; Erwin, A.; Mizoguchi, S.; Warrener, P.; Hickey, M.; Brinkman, F.; Hufnagle, W.; Kowalik, D.; Lagrou, M. *Nature* **2000**, *406*, 959-964.

(69) Mesaros, N.; Nordmann, P.; Plesiat, P.; Roussel-Delvallez, M.; Van Eldere, J.; Glupczynski, Y.; Van Laethem, Y.; Lebecque, P.; Malfroot, A.; Tulkens, P. M.; Van Bambeke, F. *Clin. Microbiol. Infect.* **2007**, *13*, 560-578.

(70) Breidenstein, E. B. M.; de la Fuente-Nunez, C.; Hancock, R. E. W. *Trends Microbiol.* **2011**, *19*, 419-426.

(71) Wretlind, B.; Pavlovskis, O. R. *Rev. Infect. Dis.* **1983**, *5*, S998-S1004.

(72) Kamath, S.; Kapatral, V.; Chakrabarty, A. M. *Mol. Microbiol.* **1998**, *30*, 933-941.

(73) Overhage, J.; Bains, M.; Brazas, M. D.; Hancock, R. E. W. *J. Bacteriol.* **2008**, *190*, 2671-2679.

(74) Woods, D. E.; Cryz, S. J.; Friedman, R. L.; Iglewski, B. H. *Infect. Immun.* **1982**, *36*, 1223-1228.

(75) Felise, H. B.; Nguyen, H. V.; Pfuetzner, R. A.; Barry, K. C.; Jackson, S. R.; Blanc, M.-P.; Bronstein, P. A.; Kline, T.; Miller, S. I. *Cell Host Microbe* **2008**, *4*, 325-336.

(76) Grobelny, D.; Poncz, L.; Galardy, R. E. *Biochemistry* **1992**, *31*, 7152-7154.

(77) Cathcart, G. R.; Gilmore, B. F.; Greer, B.; Harriott, P.; Walker, B. *Bioorg. Med. Chem. Lett.* **2009**, *19*, 6230-6232.

(78) Cathcart, G. R.; Quinn, D.; Greer, B.; Harriott, P.; Lynas, J. F.; Gilmore, B. F.; Walker, B. *Antimicrob. Agents Chemother.* **2011**, *55*, 2670-2678.

(79) Kessler, E.; Israel, M.; Landshman, N.; Chechick, A.; Blumberg, S. *Infect. Immun.* **1982**, *38*, 716-723.

(80) Nishino, N.; Powers, J. C. *J. Biol. Chem.* **1980**, *255*, 3482-3486.

(81) Thayer, M. M.; Flaherty, K. M.; McKay, D. B. *J. Biol. Chem.* **1991**, *266*, 2864-2871.

(82) Werz, O.; Steinhilber, D. *Pharmacol. Ther.* **2006**, *112*, 701-718.

(83) Samuelsson, B.; Dahlen, S. E.; Lindgren, J. A.; Rouzer, C. A.; Serhan, C. N. *Science* **1987**, *237*, 1171-1176.

(84) Peters-Golden, M.; Canetti, C.; Mancuso, P.; Coffey, M. J. *J. Immunol.* **2005**, *174*, 589-594.

(85) Hite, G. A.; Mihelich, E. D.; Suarez, T.; Google Patents: 1991.

(86) Israel, E.; Cohn, J.; Dubum, L.; Drazen, J. M.; Ratner, P.; Pleskow, W.; DeGraff Jr, A.; Chervinsky, P.; Wasserman, S.; Nelson, H. *J. Am. Med. Assoc.* **1996**, *275*, 931-936.

(87) Young, R. N. *Eur. J. Med. Chem.* **1999**, *34*, 671-685.

(88) Kim, Y.-J.; Uyama, H. *Cell. Mol. Life Sci.* **2005**, *62*, 1707-1723.

(89) Sanchez-Ferrer, A.; Rodreguez-Lopez, J. N.; Garcia-Cnovas, F.; Garcia-Carmona, F. *Biochim. Biophys. Acta* **1995**, *1247*, 1-11.

(90) Kaplan, J.; De Domenico, I.; Ward, D. M. *Curr. Opin. Hematol.* **2008**, *15*, 22-29

(91) Hearing, V.; Ekel, T. *Biochem. J* **1976**, *157*, 549.

(92) Jaenicke, E.; Decker, H. *Biochem. J.* **2003**, *371*, 515-523.

(93) Lewis, E. A.; Tolman, W. B. *Chem. Rev.* **2004**, *104*, 1047-1076.

(94) Seo, S.-Y.; Sharma, V. K.; Sharma, N. *J. Agric. Food. Chem.* **2003**, *51*, 2837-2853.

(95) Espin, J. C.; Wichers, H. J. *J. Agric. Food. Chem.* **1999**, *47*, 2638-2644.

(96) Liu, J.; Yi, W.; Wan, Y.; Ma, L.; Song, H. *Bioorg. Med. Chem.* **2008**, *16*, 1096-1102.

(97) Mangili, A.; Murman, D.; Zampini, A.; Wanke, C.; Mayer, K. H. *Clin. Infet. Dis.* **2006**, *42*, 836-842.

(98) Paterson, D. L.; Swindells, S.; Mohr, J.; Brester, M.; Vergis, E. N.; Squier, C.; Wagener, M. M.; Singh, N. *Ann. Intern. Med.* **2000**, *133*, 21-30.

(99) Friedland, G. H.; Williams, A. *Aids* **1999**, *13*, S61-S72.

(100) De Cock, K. M.; Fowler, M. G.; Mercier, E.; de Vincenzi, I.; Saba, J.; Hoff, E.; Alnwick, D. J.; Rogers, M.; Shaffer, N. *J. Am. Med. Assoc.* **2000**, *283*, 1175-1182.

(101) Hazuda, D. J.; Felock, P.; Witmer, M.; Wolfe, A.; Stillmock, K.; Grobler, J. A.; Espeseth, A.; Gabryelski, L.; Schleif, W.; Blau, C. *Science* **2000**, *287*, 646-650.

(102) Craigie, R. *J Biol Chem* **2001**, *276*, 23213-23216.

(103) Chiu, T. K.; Davies, D. R. *Curr. Topics Med. Chem.* **2004**, *4*, 965-977.

(104) Leavitt, A.; Shiue, L.; Varmus, H. *J. Biol. Chem.* **1993**, *268*, 2113-2119.

(105) Hare, S.; Vos, A. M.; Clayton, R. F.; Thuring, J. W.; Cummings, M. D.; Cherepanov, P. *Proc, Natil. Acad. Sci. USA* **2010**, *107*, 20057-20062.

(106) Grobler, J. A.; Stillmock, K.; Hu, B.; Witmer, M.; Felock, P.; Espeseth, A. S.; Wolfe, A.; Egbertson, M.; Bourgeois, M.; Melamed, J. *Proc, Natil. Acad. Sci. USA* **2002**, *99*, 6661-6666.

(107) Pommier, Y.; Johnson, A. A.; Marchand, C. *Nat. Rev. Drug Discov.* **2005**, *4*, 236-248.

(108) Marchand, C.; Maddali, K.; Métifiot, M.; Pommier, Y. *Curr. Top. Med. Chem.* **2009**, *9*, 1016-1037.

(109) Christ, F.; Voet, A.; Marchand, A.; Nicolet, S.; Desimmie, B. A.; Marchand, D.; Bardiot, D. e.; Van der Veken, N. J.; Van Remoortel, B.; Strelkov, S. V. *Nat. Chem. Bio. 6*, 442-448.

(110) Metifiot, M.; Maddali, K.; Naumova, A.; Zhang, X. M.; Marchand, C.; Pommier, Y. *Biochemistry* **2010**, *49*, 3715-3722.

(111) Lowther, W. T.; Matthews, B. W. *Biochim. Biophys. Acta* **2000**, *1477*, 157-167.

(112) Vaughan, M. D.; Sampson, P. B.; Honek, J. F. *Curr. Med. Chem.* **2002**, *9*, 385-409.

(113) Bradshaw, R. A.; Brickey, W. W.; Walker, K. W. *Trends Biochem. Sci* **1998**, *23*, 263-267.

(114) Li, J.-Y.; Chen, L.-L.; Cui, Y.-M.; Luo, Q.-L.; Li, J.; Nan, F.-J.; Ye, Q.-Z. *Biochem. Biophys. Res. Commun.* **2003**, *307*, 172-179.

(115) Wang, W.-L.; Chai, S. C.; Huang, M.; He, H.-Z.; Hurley, T. D.; Ye, Q.-Z. *J. Med. Chem.* **2008**, *51*, 6110-6120.

(116) Chai, S. C.; Ye, Q.-Z. *Bioorg. Med. Chem. Lett.* **2009**, *19*, 6862-6864.

(117) Biou, V.; Dumas, R.; Cohen-Addad, C.; Douce, R.; Job, D.; Pebay-Peyroula, E. *EMBO J.* **1997**, *16*, 3405-3415.

(118) Hou, C.-X.; Dirk, L. M. A.; Goodman, J. P.; Williams, M. A. *Weed Sci.* **2006**, *54*, 246-254.

(119) Parvez, S.; Kang, M.; Chung, H.-S.; Bae, H. *Phytother. Res.* **2007**, *21*, 805-816.

(120) Seffernick, J. L.; McTavish, H.; Osborne, J. P.; de Souza, M. L.; Sadowsky, M. J.; Wackett, L. P. *Biochemistry* **2002**, *41*, 14430-14437.

(121) Smit, N.; Vicanova, J.; Pavel, S. *Int. J. Mol. Sci.* **2009**, *10*, 5326-5349.

(122) Cristalli, G.; Costanzi, S.; Lambertucci, C.; Lupidi, G.; Vittori, S.; Volpini, R.; Camaioni, E. *Med. Res. Rev.* **2001**, *21*, 105-128.

(123) Dubey, S.; Satyanarayana, Y. D.; Lavania, H. *Eur. J. Med. Chem.* **2007**, *42*, 1159-1168.

(124) Dunkel, P.; Gelain, A.; Barlocco, D.; Haider, N.; Gyires, K.; Sperlagh, B.; Magyar, K.; Maccioni, E.; Fadda, A.; Matyus, P. *Curr. Med. Chem.* **2008**, *15*, 1827-1839.

(125) Hernick, M.; Fierke, C. A. *Arch. Biochem. Biophys.* **2005**, *433*, 71-84.

(126) Ma, X.; Ezzeldin, H. H.; Diasio, R. B. *Drugs* **2009**, *69*, 1911-1934.

(127) Moss, M. L.; Sklair-Tavron, L.; Nudelman, R. *Nat. Clin. Pract. Rheumatol.* **2008**, *4*, 300-309.

(128) Shao, J.; Zhou, B.; Chu, B.; Yen, Y. *Curr. Cancer Drug Targets* **2006**, *6*, 409-431.

(129) Sousa, S. F.; Fernandes, P. A.; Ramos, M. J. *Curr. Med. Chem.* **2008**, *15*, 1478-1492.

(130) Villain-Guillot, P.; Bastide, L.; Gualtieri, M.; Leonetti, J.-P. *Drug Discov. Today* **2007**, *12*, 200-208.

(131) Jacobsen, F. E.; Buczynski, M. W.; Dennis, E. A.; Cohen, S. M. *ChemBioChem* **2008**, *9*, 2087-2095.

(132) Puerta, D. T.; Mongan, J.; Tran, B. L.; McCammon, J. A.; Cohen, S. M. *J. Am. Chem. Soc.* **2005** *127*, 14148-14149.

(133) Hopkins, A. L.; Groom, C. R.; Alex, A. *Drug Discov. Today* **2004**, *9*, 430-431.

(134) Suzuki, T.; Miyata, N. *Mini. Rev. Med. Chem.* **2006**, *6*, 515-526.

(135) Winum, J.-Y.; Scozzafava, A.; Montero, J.-L.; Supuran, C. T. *Curr. Pharm. Des.* **2008**, *14*, 615-621.

(136) Puerta, D. T.; Cohen, S. M. *Curr. Top. Med. Chem.* **2004**, *4*, 1551-1573.

(137) Jacobsen, J. A.; Fullagar, J. L.; Miller, M. T.; Cohen, S. M. *J. Med. Chem.* **2011**, *54*, 590-602.

(138) Liu, Z. D.; Khodr, H. H.; Liu, D. Y.; Lu, S. L.; Hider, R. C. *J. Med. Chem.* **1999**, *42*, 4814-4823.

(139) Liu, Z. D.; Piyamongkol, S.; Liu, D. Y.; Khodr, H. H.; Lu, S. L.; Hider, R. C. *Bioorg. Med. Chem.* **2001**, *9*, 563-573.

(140) Yan, Y.-L.; Cohen, S. M. *Org. Lett.* **2007**, *9*, 2517-2520.

(141) Lewis, J. A.; Cohen, S. M. *Inorg. Chem.* **2004**, *43*, 6534-6536.

(142) Wiley, R. H.; Jarboe, C. H. *J. Am. Chem. Soc.* **1956**, *78*, 2398-2401.

(143) Ho, T.-L. *Chem. Rev.* **1975**, *75*, 1-20.

(144) Jimenez, M.; Garcia-Carmona, F. *J. Agric. Food Chem.* **1997**, *45*, 2061-2065.

(145) Peyroux, E.; Ghattas, W.; Hardre, R.; Giorgi, M.; Faure, B.; Simaan, A. J.; Belle, C.; Reglier, M. *Inorg. Chem.* **2009**, *48*, 10874-10876.

(146) Hider, R. C.; Lerch, K. *Biochem. J.* **1989**, *257*, 289-290.

(147) Whittaker, M.; Floyd, C. D.; Brown, P.; Gearing, A. J. H. *Chem. Rev.* **1999**, *99*, 2735-2776.

(148) Rouffet, M.; de Oliveira, C. A. F.; Udi, Y.; Agrawal, A.; Sagi, I.; McCammon, J. A.; Cohen, S. M. *J. Am. Chem. Soc.* **2010**, *132*, 8232-8233.

(149) Rouffet, M.; de Oliveira, C. A. F.; Udi, Y.; Agrawal, A.; Sagi, I.; McCammon, J. A.; Cohen, S. M. *J. Am. Chem. Soc.* **2010**, *132*, 8232-8233.

(150) Milbank, J. B. J.; Stevenson, R. J.; Ware, D. C.; Chang, J. Y. C.; Tercel, M.; Ahn, G.-O.; Wilson, W. R.; Denny, W. A. *J. Med. Chem.* **2009**, *52*, 6822-6834.

(151) Musser, J. H.; Jones, H.; Sciortino, S.; Bailery, K.; Coutts, S. M.; Khandwala, A.; Sonnino-Goldman, P.; Leibowitz, M.; Wolf, P.; Neiss, E. S. *J. Med. Chem.* **1985**, *28*, 1255-1259.

(152) Puerta, D. T.; Griffin, M. O.; Lewis, J. A.; Romero-Perez, D.; Garcia, R.; Villarreal, F. J.; Cohen, S. M. *J. Biol. Inorg. Chem.* **2006**, *11*, 131-138.

(153) Pufahl, R. A.; Kasten, T. P.; Hills, R.; Gierse, J. K.; Reiz, B. A.; Weinberg, R. A.; Masferrer, J. L. *Anal. Biochem.* **2007**, *364*, 204-212.

(154) Barre-Sinoussi, F.; Chermann, J. C.; Rey, F.; Nugeyre, M. T.; Chamaret, S.; Gruest, J.; Dauguet, C.; Axlerblin, C.; Vezinetbrun, F.; Rouzioux, C.; Rozenbaum, W.; Montagnier, L. *Science* **1983**, *220*, 868-871.

(155) Schupbach, J.; Popovic, M.; Gilden, R. V.; Gonda, M. A.; Sarngadharan, M. G.; Gallo, R. C. *Science* **1984**, *224*, 503-505.

(156) Mehellou, Y.; De Clercq, E. *J. Med. Chem.* **2010**, *53*, 521-538.

(157) Perryman, A. L.; Forli, S.; Morris, G. M.; Burt, C.; Cheng, Y.; Palmer, M. J.; Whitby, K.; McCammon, J. A.; Phillips, C.; Olson, A. J. *J. Mol. Biol.* **2010**, *397*, 600-615.

(158) Li, Y. Y.; Feldman, A. M.; Sun, Y.; McTiernan, C. F. *Circulation* **1998**, *98*, 1728-1734.

(159) Pommier, Y.; Johnson, A. A.; Marchand, C. *Nat. Rev. Drug Discov.* **2005**, *4*, 236-248.

(160) Iwamoto, M.; Wenning, L. A.; Petry, A. S.; Laethem, M.; De Smet, M.; Kost, J. T.; Merschman, S. A.; Strohmaier, K. M.; Ramael, S.; Lasseter, K. C.; Stone, J. A.; Gottesdiener, K. M.; Wagner, J. A. *Clin. Pharmacol. Ther.* **2008**, *83*, 293-299.

(161) Summa, V.; Petrocchi, A.; Bonelli, F.; Crescenzi, B.; Donghi, M.; Ferrara, M.; Fiore, F.; Gardelli, C.; Paz, O. G.; Hazuda, D. J.; Jones, P.; Kinzel, O.; Laufer, R.; Monteagudo, E.; Muraglia, E.; Nizi, E.; Orvieto, F.; Pace, P.; Pescatore, G.; Scarpelli, R.; Stillmock, K.; Witmer, M. V.; Rowley, M. *J. Med. Chem.* **2008**, *51*, 5843-5855.

(162) Hare, S.; Gupta, S. S.; Valkov, E.; Engelman, A.; Cherepanov, P. *Nature* **2010**, *464*, 232-237.

(163) Bacchi, A.; Carcelli, M.; Compari, C.; Fisicaro, E.; Pala, N.; Rispoli, G.; Rogolino, D.; Sanchez, T. W.; Sechi, M.; Sinisi, V.; Neamati, N. *J. Med. Chem.*, *54*, 8407-8420.

(164) Marinello, J.; Marchand, C.; Mott, B. T.; Bain, A.; Thomas, C. J.; Pommier, Y. *Biochemistry* **2008**, *47*, 9345-9354.

(165) Pace, P.; Di Francesco, M. E.; Gardelli, C.; Harper, S.; Muraglia, E.; Nizi, E.; Orvieto, F.; Petrocchi, A.; Poma, M.; Rowley, M.; Scarpelli, R.; Laufer, R.; Paz, O. G.; Monteagudo, E.; Bonelli, F.; Hazuda, D.; Stillmock, K. A.; Summa, V. *J. Med. Chem.* **2007**, *50*, 2225-2239.

(166) Metifiot, M.; Marchand, C.; Maddali, K.; Pommier, Y. *Viruses* **2010**, *2*, 1347-1366.

(167) Kaes, C.; Katz, A.; Hosseini, M. W. *Chem. Rev.* **2000**, *100*, 3553-3590.

(168) Krishnan, L.; Li, X.; Naraharisetty, H. L.; Hare, S.; Cherepanov, P.; Engelman, A. *Proc, Natil. Acad. Sci. USA*, *107*, 15910-15915.

(169) Ho, T.-L. *Chem. Rev.* **1975**, *75*, 1-20.

(170) Agrawal, A.; de Oliveira, C. A. F.; Cheng, Y.; Jacobsen, J. A.; McCammon, J. A.; Cohen, S. M. *J. Med. Chem.* **2009**, *52*, 1063-1074.

(171) Lewis, J. A.; Mongan, J.; McCammon, J. A.; Cohen, S. M. *ChemMedChem* **2006**, *1*, 694-697.

(172) Finnegan, M. M.; Rettig, S. J.; Orvig, S. J. *J. Am. Chem. Soc.* **1986**, *108*, 5033-5035.

(173) Puerta, D. T.; Mongan, J.; Tran, B. L.; McCammon, J. A.; Cohen, S. M. *J. Am. Chem. Soc.* **2005**, *127*, 14148-14149.

(174) Schugar, H.; Green, D. E.; Bowen, M. L.; Scott, L. E.; Storr, T.; Bohmerle, K.; Thomas, F.; Allen, D. D.; Lockman, P. R.; Merkel, M.; Thompson, K. H.; Orvig, C. *Angew. Chem. Int. Ed.* **2007**, *46*, 1716-1718.

(175) Gorden, A. E. V.; Xu, J.; Raymond, K. N.; Durbin, P. *Chem. Rev.* **2003**, *103*, 4207-4282.

(176) Zhao, X. Z.; Maddali, K.; Smith, S. J.; M√©tifiot, M.; Johnson, B. C.; Marchand, C.; Hughes, S. H.; Pommier, Y.; Burke Jr, T. R. *Bioorg. Med. Chem. Lett.* **2012**, *22*, 7309-7313.

(177) Zhao, X. Z.; Semenova, E. A.; Vu, B. C.; Maddali, K.; Marchand, C.; Hughes, S. H.; Pommier, Y.; Burke, T. R. *J. Med. Chem.* **2008**, *51*, 251-259.

(178) Pace, P.; Di Francesco, M. E.; Gardelli, C.; Harper, S.; Muraglia, E.; Nizi, E.; Orvieto, F.; Petrocchi, A.; Poma, M.; Rowley, M.; Scarpelli, R.; Laufer, R.; Gonzalez Paz, O.; Monteagudo, E.; Bonelli, F.; Hazuda, D.; Stillmock, K. A.; Summa, V. *J. Med. Chem.* **2007**, *50*, 2225-2239.

(179) Serrao, E.; Odde, S.; Ramkumar, K.; Neamati, N. *Retrovirology* **2009**, *6*, 25-39.

(180) Jin, H.; Cai, R. Z.; Schacherer, L.; Jabri, S.; Tsiang, M.; Fardis, M.; Chen, X.; Chen, J. M.; Kim, C. U. *Bioorg. Med. Chem. Lett.* **2006**, *16*, 4-4.

(181) Kirschberg, T.; Parrish, J. *Curr. Opin. Drug Dis. Dev.* **2007**, *10*, 460-472.

(182) Tanabe, K. K.; Allen, C. A.; Cohen, S. M. *Angew. Chemie Intl. Ed.* **2010**, *49*, 9730-9733.

(183) Agrawal, A.; Romero-Perez, D.; Jacobsen, J. A.; Villarreal, F. J.; Cohen, S. M. *ChemMedChem* **2008**, *3*, 812-820.

(184) Belyk, K. M.; Morrison, H. G.; Jones, P.; Summa, V. 2006, p 52 pp.

(185) Summa, V.; Petrocchi, A.; Matassa, V. G.; Gardelli, C.; Muraglia, E.; Rowley, M.; Paz, O. G.; Laufer, R.; Monteagudo, E.; Pace, P. *J. Med. Chem.* **2006**, *49*, 6646-6649.

(186) Cohen, S. M.; Petoud, S. p.; Raymond, K. N. *Inorg. Chem.* **1999**, *38*, 4522-4529.

(187) Cohen, S. M.; Petoud, S.; Raymond, K. N. *Inorg. Chem.* **1999**, *38*, 4522-4529.

(188) Kipnis, E.; Sawa, T.; Wiener-Kronish, J. *Medecine et Maladies Infectieuses* **2006**, *36*, 78-91.

(189) Strateva, T.; Mitov, I. *Ann. Microbiol.* **2011**, *61*, 717-732.

(190) Travis, J.; Potempa, J. *Biochim. Biophys. Acta* **2000**, *1477*, 35-50.

(191) Clatworthy, A. E.; Pierson, E.; Hung, D. T. *Nat. Chem. Biol.* **2007**, *3*, 541-548.

(192) Barczak, A. K.; Hung, D. T. *Curr. Opin. Microbiol.* **2009**, *12*, 490-496.

(193) Puerta, D. T.; Lewis, J. A.; Cohen, S. M. *J. Am. Chem. Soc.* **2004**, *126*, 8388-8389.

(194) Jacobsen, F. E.; Lewis, J. A.; Cohen, S. M. *J. Am. Chem. Soc.* **2006**, *128*, 3156-3157.

(195) Agrawal, A.; DeSoto, J.; Fullagar, J. L.; Maddali, K.; Rostami, S.; Richman, D. D.; Pommier, Y.; Cohen, S. M. *Proc. Natl. Acad. Sci.* **2012**.

(196) Puerta, D. T.; Mongan, J.; Tran, B. L.; McCammon, J. A.; Cohen, S. M. *J. Am. Chem. Soc.* **2005**, *127*, 14148-14149.

(197) Kessler, E.; Israel, M.; Landshman, N.; Chechick, A.; Blumberg, S. *Infect. Immun.* **1982**, *38*, 716-723.

(198) Smith, K. M.; Bu, Y.; Suga, H. *Chem. Bio.* **2003**, *10*, 563-571.

(199) Mue, U.; Schuster, M.; Heim, R.; Singh, A.; Olson, E. R.; Greenberg, E. P. *Antimicrob. Agents Chemother.* **2006**, *50*, 3674-3679.

(200) Garner, A. L.; Struss, A. K.; Fullagar, J. L.; Agrawal, A.; Moreno, A. Y.; Cohen, S. M.; Janda, K. D. *Med. Chem. Lett.* **2012**, *3*, 668-672.

(201) Zhao, J. *Curr. Med. Chem.* **2007**, *14*, 2597-2621.

(202) Agrawal, A.; Johnson, S. L.; Jacobsen, J. A.; Miller, M. T.; Chen, L.; Pellecchia, M.; Cohen, S. M. *ChemMedChem* **2010**, *5*, 195-199.

(203) Johnson, S.; Barile, E.; Farina, B.; Purves, A.; Wei, J.; Chen, L.; Shiryaev, S.; Zhang, Z.; Rodionova, I.; Agrawal, A.; Cohen, S. M.; Osterman, A.; Strongin, A.; Pellecchia, M. *Chem. Biol. Drug Des.* **2011**, *78*, 211-223.

(204) Lai, S.; Tremblay, J.; Deziel, E. *Environ. Microbiol.* **2009**, *11*, 126-136.

(205) Brikinshaw, J.; Chambers, A.; Raistrick, H. *Biochem. J.* **1942**, *36*, 242-251.

(206) Dewar, M. *Nature* **1945**, 50-51.

(207) Davison, J.; al Fahad, A.; Cai, M.; Song, Z.; Yehia, S. Y.; Lazarus, C. M.; Bailey, A. M.; Simpson, T. J.; Cox, R. J. *Proc. Natl. Acad. Sci.* **2012**.

(208) Baillie, A. J.; Freeman, G. G.; Cook, J. W.; Somerville, A. R. *Nature* **1950**, *166*, 65-65.

(209) Haluk, J.; Roussel, C. *Ann. Forest Sci.* **2000**, *57*, 819.

(210) Iwatsuki, M.; Takada, S.; Mori, M.; Ishiyama, A.; Namatame, M.; Nishihara-Tsukashima, A.; Nonaka, K.; Masuma, R.; Otoguro, K.; Shiomi, K.; Omura, S. *J. Antibiot.* **2011**, *64*, 183-188.

(211) Semenova, E. A.; Johnson, A. A.; Marchand, C.; Davis, D. A.; Yarchoan, R.; Pommier, Y. *Mol. Pharmacol.* **2006**, *69*, 1454-1460.

(212) Inamori, Y.; Sakagami, Y.; Morita, Y.; Shibata, M.; Sugiura, M.; Kumeda, Y.; Okabe, T.; Tsujibo, H.; Ishida, N. *Biol. Pharm. Bull.* **2000**, *23*, 995-997.

(213) Espin, J. C.; Wichers, H. J. *J. Agric. Food. Chem.* **1999**, *47*, 2638-2644.

(214) Ismaya, W. T.; Rozeboom, H. J.; Weijn, A.; Mes, J. J.; Fusetti, F.; Wichers, H. J.; Dijkstra, B. W. *Biochemistry*, *50*, 5477-5486.

(215) Kahn, V.; Andrawis, A. *Phytochemistry* **1985**, *24*, 905-908.

(216) Angawi, R. F.; Swenson, D. C.; Gloer, J. B.; Wicklow, D. T. *Tetrahedron Lett.* **2003**, *44*, 7593-7596.

(217) Inamori, Y.; Shinohara, S.; Tsujibo, H.; Okabe, T.; Morita, Y.; Sakagami, Y.; Kumeda, Y.; Ishida, N. *Bio. Pharm. Bull.* **1999**, *22*, 990-993.

(218) Kurihara, T.; Noguchi, M.; Noguchi, T.; Wakabayashi, H.; Motohashi, N.; Sakagami, H. *In Vivo* **2006**, *20*, 385-389.

(219) Liu, J.; Yi, W.; Wan, Y.; Ma, L.; Song, H. *Biorg. Med. Chem.* **2008**, *16*, 1096-1102.

(220) MacPherson, L. J.; Bayburt, E. K.; Capparelli, M. P.; Carroll, B. J.; Goldstein, R.; Justice, M. R.; Zhu, L.; Hu, S.-i.; Melton, R. A.; Fryer, L. *Journal of Medicinal Chemistry* **1997**, *40*, 2525-2532.

(221) Supuran, C. T.; Scozzafava, A.; Casini, A. *Med. Res. Rev.* **2003**, *23*, 146-189.

(222) Lee, J.; Attila, C.; Cirillo, S. L. G.; Cirillo, J. D.; Wood, T. K. *Microb. Biotechnol.* **2009**, *2*, 75-90.

(223) Wu, H.; Lee, B.; Yang, L.; Wang, H.; Givskov, M.; Molin, S.; Hoiby, N.; Song, Z. *FEMS Immunol. Med. Microbiol.* **2011**, *62*, 49-56.

(224) Uemura, T.; Takenaka, S.; Kusabayashi, S.; Seto, S. *Mol. Cryst. Liq. Cryst.* **1983**, *95*, 287-297.

(225) Elliott, J. M.; Chipperfield, J. R.; Clark, S.; Sinn, E. *Inorg. Chem.* **2001**, *40*, 6390-6396.

(226) Monnard, F. W.; Heinisch, T.; Nogueira, E. S.; Schirmer, T.; Ward, T. R. *Chem. Commun.*, *47*, 8238-8240.

(227) Iyer, R.; Barrese III, A. A.; Parakh, S.; Parker, C. N.; Tripp, B. C. *J. Biomol. Screen.* **2006**, *11*, 782-791.

(228) Tremblay, J.; Deziel, E. *J. Basic Microbiol.* **2008**, *48*, 509-515.